GEOLOGICAL SURVEY OF CANADA
PAPER 91-15

AN INTEGRATED GEOLOGICAL, GEOCHEMICAL, AND GEOPHYSICAL INVESTIGATION OF URANIUM METALLOGENESIS IN SELECTED GRANITIC PLUTONS OF THE MIRAMICHI ANTICLINORIUM, NEW BRUNSWICK

H.H. Hassan and A.L. McAllister

1992

Energy, Mines and Resources Canada
Énergie, Mines et Ressources Canada

Canada

Natural Resources and Energy
New Brunswick

Ressources Naturelles et Énergie
Nouveau-Brunswick

Contribution to Canada-New Brunswick Mineral Development Agreement 1984-89, a subsidiary agreement under the Economic and Regional Development Agreement.
Project funded by the Geological Survey of Canada.

Contribution à l'Entente auxiliaire Canada/Nouveau-Brunswick sur l'Exploitation minérale 1984-89 faisant partie de l'entente de développement économique et régional. Ce projet a été finance par la Commission geologique du Canada.

Energy, Mines and Resources Canada

Énergie, Mines et Ressources Canada

92-07196/

GEOLOGICAL SURVEY OF CANADA
PAPER 91-15

AN INTEGRATED GEOLOGICAL, GEOCHEMICAL, AND GEOPHYSICAL INVESTIGATION OF URANIUM METALLOGENESIS IN SELECTED GRANITIC PLUTONS OF THE MIRAMICHI ANTICLINORIUM, NEW BRUNSWICK

H.H. Hassan and A.L. McAllister

1992

© Minister of Supply and Services Canada 1992

Available in Canada through authorized
bookstore agents and other bookstores

or by mail from

Canada Communication Group — Publishing
Ottawa, Canada K1A 0S9

and from

Geological Survey of Canada offices:

601 Booth Street
Ottawa, Canada K1A 0E8

3303-33rd Street N.W.,
Calgary, Alberta T2L 2A7

A deposit copy of this publication is also available for
reference in public libraries across Canada

Cat. No. M44-91/15E
ISBN 0-660-14435-2

Price subject to change without notice

Cover Description

Fall Brook: A hanging valley cut into the hornfels around the Rocky Brook Pluton at the mouth of Fall Brook where it flows into the Southwest Miramichi River (courtesy of W. Gardiner, 1986). GSC 1992-093

Critical Readers

V. Ruzicka
W.W. Gardiner
D.V. Venugopal

Authors' address

Department of Geology
University of New Brunswick
Fredericton, New Brunswick
E3B 5A3

Scientific Editor

O.E. Inglis

Original manuscript received: 1989 - 08
Final version approved for publication: 1991 - 06

CONTENTS

1 Abstract/Résumé

2 Summary/Sommaire

9 Introduction
9 Scope and objectives of the project
9 Method of investigation
9 Previous investigations
11 Acknowledgments

11 General geology of the Miramichi Anticlinorium
11 General statement
11 Tectonic setting
12 Igneous intrusions
12 Metamorphism
12 Economic potential

13 General geology of Long Lake area and the central Miramichi Anticlinorium area
13 Long Lake area
13 Overview
13 Geology of North Pole Pluton
13 Biotite granite
13 Biotite-muscovite granite
15 Quartz-feldspar porphyry
15 Age of North Pole Pluton
15 Depth of emplacement of North Pole Pluton
15 Breccia zones of the North Pole Pluton
16 Wall rock alterations
16 Mineralization related to the North Pole Pluton
16 Chronological development of the North Pole Pluton metallogeny
18 Central Miramichi Anticlinorium area
18 Overview
18 Geology of central Miramichi Anticlinorium posttectonic plutons
18 Melanocratic biotite granite
20 Porphyritic granite
20 Equigranular granite
20 Microgranite and associated aplite dykes and minor pegmatite pods
20 Age of the granitic plutons
20 Depth of emplacement of the central Miramichi granitic plutons
21 Structural control of veins and late stage dykes
21 Wall rock alterations
22 Mineralization related to the granitic plutons

22 Review of geochemical and geophysical surveys for uranium and other metals in the Long Lake area and the central Miramichi Anticlinorium area
22 Overview
22 Long Lake area
22 Geophysical surveys
22 Gravity
23 Magnetic
23 Very-low frequency electromagnetic technique (VLF)
24 Induced polarization (IP)
24 Geochemical surveys
24 Lake sediments geochemistry

25 Spring and stream sediments geochemistry
27 Soil geochemistry
28 Till geochemistry
29 Seep water geochemistry
29 Central Miramichi Anticlinorium area
29 Geophysical surveys
29 Gravity
29 Magnetic
29 Geochemical surveys
29 Spring and stream sediments geochemistry
31 Soil geochemistry
32 Till geochemistry
32 Gamma ray spectrometry surveys
32 Overview
36 Interpretation of airborne gamma ray spectrometry data
36 General statement
36 Miramichi Anticlinorium area
38 Favourability indices of the granitic plutons
40 Long Lake area
47 Central Miramichi Anticlinorium area
47 Aeroradiometric data
47 In situ gamma ray spectrometry data
50 Relationships of uranium and other metallogenic elements to the petrochemical characteristics of the granitic rocks
50 Overview
50 North Pole Pluton
50 Whole rock geochemistry
53 Variation of uranium contents with respect to alteration and mineralization
53 Uranium variation with petrochemical indices of North Pole Pluton
54 Uranium and tin specialization of the granitic rocks of the North Pole Pluton
55 Statistical relationship between uranium and other elements in the North Pole Pluton
55 Major oxides
55 Trace elements
57 Central Miramichi Anticlinorium granitic plutons
57 General statement
57 Whole rock geochemistry for the granitic plutons, general review
60 Burnthill Pluton
60 Whole rock geochemistry
62 Uranium and thorium variations with petrochemical indices of Burnthill Pluton
65 Uranium and tin specialization of the granitic rocks of the Burnthill Pluton
66 Statistical relationship between uranium and thorium and other elements in the Burnthill Pluton
66 Major oxides
68 Trace elements
69 Uranium and associated elements contents with respect to the granitic types
69 General statement
71 Granite types of the North Pole and the Burnthill plutons
72 Granite type determination of the North Pole and the Burnthill plutons by using discriminant analyses
75 Metallogenic maps and conceptual models for uranium and associated elements distribution in North Pole and central Miramichi Anticlinorium plutons
75 Metallogenic maps

75 General statement
75 Long Lake area
77 Central Miramichi Anticlinorium area
77 Conceptual models
77 General statement
77 North Pole Pluton
79 Central Miramichi Anticlinorium plutons

80 Conclusions and guidelines for future exploration
80 Conclusions
82 Guide for future exploration
82 Geological signatures
82 Geochemical signatures
82 Geophysical signatures

82 References

Appendices

87 I – Best overall analytical results for elements in different types of samples for the Long Lake area
88 II – Brief description of the mineral occurrences associated with the Burnthill, Dungarvon, Trout Brook, and Rocky Brook plutons
94 III – Element contents in spring and stream sediment samples in the Long Lake area
95 IV – Element contents in spring and stream sediment samples
109 V – Contents of U, Sn, W, and Mo in soil samples, Otter Brook area, Burnthill Pluton
110 VI – Chemical analyses and locations of till samples overlying the granitic plutons of central Miramichi Anticlinorium area
114 VII – Locations and in situ determinations of uranium, thorium and potassium contents of the granitic rocks of Burnthill, Dungarvon, Trout Brook, and Rocky Brook plutons
127 VIII – Chemical analyses, norms, and locations of the granitic rocks of the North Pole Pluton
129 IX – Chemical analyses, norms, locations, and descriptions of the granitic rocks of the central Miramichi Anticlinorium plutons
134 X – Chemical analyses of Au, Th, U, Cu, Pb, Zn, Mo, and Ag in outcrop, float, and trench samples in the Long Lake area

Figures

10 1. Geology and uranium metallogeny of Miramichi Anticlinorium, New Brunswick
12 2. Lithotectonic zones of New Brunswick
14 3. Generalized geology and uranium occurrences, Long Lake area
15 4. Q-Or-Ab ternary diagram for normative quartz, orthoclase, and albite in various phases of the North Pole Pluton
17 5. Geochronological sequence of metallogenic development in the Long Lake area
19 6. Generalized geology and uranium occurrences of the granitic plutons, central Miramichi Anticlinorium
21 7. Q-Or-Ab ternary diagram for normative quartz, orthoclase, and albite in various phases of the Burnthill Pluton
23 8. Bouguer gravity data, Long Lake area
24 9. Airborne magnetic data, Long Lake area
26 10. Contents of spring and stream sediments, Long Lake area
30 11. Bouguer gravity map of the granitic plutons, central Miramichi Anticlinorium
31 12. Airborne magnetic data of the granitic plutons, central Miramichi Anticlinorium
34 13. Uranium (ppm) content in spring and stream sediments of the granitic plutons, central Miramichi Anticlinorium
35 14. Uranium content in clay-sized (<2 μm) till samples, central Miramichi Anticlinorium, New Brunswick
37 15. eU airborne gamma ray spectrometry data, Miramichi Anticlinorium, New Brunswick
38 16. Plots of eU versus SiO_2 and eTh versus SiO_2 for selected granitic plutons in the Miramichi Anticlinorium
38 17. eU-eTh-K ternary variation diagram of the selected granitic plutons in the Miramichi Anticlinorium and for some uraniferous granites
42 18. Plot of |UPC1/UPC3| vs. |UPC2/UPC3| ratio for selected granitic plutons in the Miramichi Anticlinorium
43 19. Airborne gamma ray spectrometry data, Long Lake area
44 20. Plots of airborne eU profiles across the Long Lake area
45 21. Plots of airborne eTh profiles across the Long Lake area
46 22. Plots of airborne eU/eTh ratio profiles across the Long Lake area
48 23. Equivalent uranium aeroradiometric map of the granitic plutons, central Miramichi Anticlinorium
50 24. Equivalent uranium aeroradiometric anomalies of the granitic plutons, central Miramichi Anticlinorium
51 25. eU-eTh-K ternary variation diagram for in situ gamma ray data of U, Th, and K contents in the granitic plutons, central Miramichi Anticlinorium
53 26. The eU, eTh, and K contents in fresh, weathered, altered, and fractured rock samples of the Burnthill Pluton
53 27. The effect of alteration on uranium content in the North Pole Pluton
54 28. Plot of uranium versus SiO_2 for the rocks of the North Pole Pluton
54 29. Plot of uranium versus felsic index for the rocks of the North Pole Pluton
54 30. Plot of uranium versus degree of oxidation for the rocks of the North Pole Pluton
54 31. A Rb-Sr-Ba ternary variation diagram for the rocks of the North Pole Pluton
59 32. Plots of Factor I, II, and III loadings for major oxide contents in the rocks of the North Pole Pluton
60 33. Plots of Factor I, II, and III loadings for trace element contents in the rocks of the North Pole Pluton
61 34. Chondrite-normalized REE plot for mineralized granitic rocks of central Miramichi Anticlinorium plutons
65 35. Plot of U, Th, and Th-U ratio versus SiO_2 for the rocks of the Burnthill Pluton
65 36. Plot of U, Th, and Th-U ratio versus total alkalies for the rocks of the Burnthill Pluton
66 37. Plot of U, Th, and Th-U ratio versus La-Yb ratio for the rocks of the Burnthill Pluton
66 38. Rb-Sr-Ba ternary variation diagram for the rocks of the Burnthill Pluton

69 39. Plots of Factor I, II, and III loadings for major oxide contents in the unmineralized rocks of the Burnthill Pluton
71 40. Plots of Factor I, II, and III loadings for trace element contents in the unmineralized rocks of the Burnthill Pluton
72 41. Plot of molecular $Al_2O_3/(Na_2O + K_2O)$ versus molecular $Al_2O_3/(Na_2O + K_2O + CaO)$ for the rocks of the North Pole and Burnthill plutons
72 42. ACF plot of the granitic rocks of the North Pole and Burnthill plutons
75 43. Plot of the granitic rock samples of the North Pole Pluton on the proposed discriminant diagram used to distinguish I-, S-, and A-type granitoids
75 44. Plot of the granitic rock samples of the Burnthill Pluton on the proposed discriminant diagram used to distinguish I-, S-, and A-type granitoids
78 45. Favourability zones for uranium exploration in the Long Lake area
80 46. Proposed conceptual model for uranium and associated metals concentration in the North Pole Pluton
81 47. Proposed conceptual model for uranium and associated metals concentration in the granitic rocks of the central Miramichi Anticlinorium plutons

Tables

22 1. Various types and products of hydrothermal alterations identified in the granitic plutons of central Miramichi Anticlinorium
25 2. Means and ranges of U and other elements analyzed in the Long Lake sediments and their global averages
25 3. Correlation coefficients among elements analyzed from 439 lake sediment samples from Long Lake
27 4. Statistical abundances of elements in spring and stream sediment samples for the Long Lake area
28 5. Correlation coefficients for elements in 72 spring and stream sediment samples of Long Lake area
28 6. Mean, standard deviations, and ranges of analyzed metals in soils of the Long Lake area
29 7. Statistical abundances of metals in 173 till samples from Long Lake area
29 8. Geochemical abundances in six seep water samples from Long Lake area
32 9. Comparison between spring and stream sediment samples in terms of trace element contents for the area shown in Figure 13
33 10. Uranium and other trace element contents in spring and stream sediment samples in the Burnthill, Dungarvon, Trout Brook, and the Rocky Brook granites
34 11. Correlation coefficient between U and other elements in stream and spring sediments of the granitic plutons of the central Miramichi Anticlinorium area
35 12. Soil samples over Burnthill Pluton
36 13. Correlation coefficients among U, Sn, Mo, and W in the samples of soil over the Burnthill Pluton
38 14. Statistical abundances of metals in till samples overlying the granitic rocks of central Miramichi Anticlinorium plutons
39 15. Matrix of Spearman rank correlation coefficients for metals in 77 till samples overlying the granitic rocks of central Miramichi Anticlinorium plutons
39 16. Aeroradiometric abundances of eU, eTh, and K; silica, aluminium, and alkali contents and the amplitude of gravity anomalies for the granitic rocks of the Miramichi Anticlinorium
41 17. Uranium favourability indices for the granitic plutons in the Miramichi Anticlinorium
42 18. Statistical abundances of aeroradiometric eU, eTh, and K contents in various rock units of the Long Lake area
49 19. Means and standard deviations of U, Th, and K contents and 50 and 90 percentile contents of U measured by means of in situ and airborne gamma ray spectrometry for different rock types of the granitic plutons

51	20.	Means and standard deviations of in situ radiometric eU, eTh, and K contents in various types of dykes and pods intersecting the granitic plutons
51	21.	In situ gamma ray spectrometry values of eU, eTh, and K in the coarse grained seriate porphyritic granitic rocks that have undergone various postmagmatic processes
52	22.	Averages of major and trace elements in fresh and altered rocks of various phases of the North Pole Pluton and their comparison with normal and uraniferous granites
55	23.	Selected geochemical parameters distinguishing specialized granites from normal granites for the rocks of the North Pole Pluton
56	24.	Matrix of Spearman rank correlation coefficients for U and major oxides in fresh and mineralized rock samples of North Pole Pluton
57	25.	Matrix of Spearman rank correlation coefficients for normative composition in fresh rock samples of the North Pole Pluton
58	26.	Matrix of Spearman rank coefficients for U and other trace elements in fresh and mineralized rock samples of the North Pole Pluton
62	27.	Average U, Th, major oxides, and trace elements in fresh rock samples of the Burnthill, Dungarvon, and Trout Brook plutons and their global averages
63	28.	Average U, Th, major oxides, and trace elements in mineralized rock samples of the Burnthill, Dungarvon, Trout Brook, and Rocky Brook plutons and their global averages
64	29.	Average U, Th, major oxides, trace elements, and norms in fresh, altered, and mineralized rock samples of the Burnthill Pluton
67	30.	Matrix of Spearman rank correlation coefficients for U, Th, and major oxides in fresh and mineralized rock samples of the Burnthill Pluton
68	31.	Matrix of Spearman rank correlation coefficients for normative composition in fresh rock samples of the Burnthill Pluton
70	32.	Matrix of Spearman rank correlation coefficients for U, Th, and other trace elements in fresh and mineralized rock samples of the Burnthill Pluton
73	33.	Geological features of the North Pole and Burnthill plutons and their comparison to I-, S-, and A-type granitoids
74	34.	Average major oxides and trace element contents in the North Pole Pluton and the Burnthill Pluton and their comparison to I-, S-, and A-type granitoids
76	35.	Statistical abundances of elements in bedrock and float samples in the Long Lake area

AN INTEGRATED GEOLOGICAL, GEOCHEMICAL, AND GEOPHYSICAL INVESTIGATION OF URANIUM METALLOGENESIS IN SELECTED GRANITIC PLUTONS OF THE MIRAMICHI ANTICLINORIUM, NEW BRUNSWICK

Abstract

Integrated geological, geochemical, and geophysical data for the posttectonic granitic rocks of the North Pole, Burnthill, Dungarvon, Trout Brook, and Rocky Brook plutons and surrounding areas were examined to assess their potential for uranium mineralization. Geological, geochemical, and geophysical criteria that are thought to be useful guides for uranium exploration were also established for the host granites.

The granitic plutons were emplaced discordantly, late in the tectonomagmatic sequence and at shallow depths within the metasedimentary rocks of the Miramichi Anticlinorium. Geochemically, the host granites are highly evolved (SiO_2 > 75 wt. %), peraluminous and have strong similarities with ilmenite-series 'S-type' and 'A-type' granitoids. Uranium occurrences are spatially and perhaps temporally associated with late-phase differentiates of the plutons where elevated levels of other lithophile elements such as Sn, W, Mo, and F were also detected. Geophysically, the granitic plutons are associated with distinctively high aeroradiometric eU, eTh, and K anomalies that coincide with strong negative Bouguer anomalies and low magnetic values.

Conceptual models involving magmatic and hydrothermal processes have been adopted to explain the concentration of uranium and associated metals in the granitic plutons.

Résumé

Des données géologiques, géochimiques et géophysiques intégrées sur les roches granitiques post-tectoniques des plutons de North Pole, de Burnthill, de Dungarvon, de Trout Brook et de Rocky Brook et des zones avoisinantes ont été analysées dans le but d'évaluer leur potentiel de minéralisation en uranium. Des critères géologiques, géochimiques et géophysiques que l'on considère utiles pour l'exploration de l'uranium ont également été établis pour les granites encaissants.

Les plutons granitiques ont été mis en place en discordance, à la fin de la séquence tectono-magmatique et à faible profondeur au sein des roches métasédimentaires de l'anticlinorium de Miramichi. Géochimiquement, les granites encaissants sont très évolués (SiO_2 > 75 % poids), hyperalumineux et présentent de fortes ressemblances avec les granitoïdes de «type S» et de «type A» de la série des ilménites. Les venues d'uranium sont associées, spatialement et peut-être temporellement, aux produits de différenciation de phase tardive des plutons où des concentrations élevées d'autres éléments lithophiles, comme Sn, W, Mo et F, ont également été détectées. Du point de vue géophysique, les plutons granitiques sont associés à des anomalies aéroradiométriques nettement élevées de eU, eTh et K qui coïncident avec des anomalies de Bouguer fortement négatives et de faibles valeurs magnétiques.

Pour expliquer la concentration d'uranium et de métaux connexes dans les plutons granitiques, on a adopté des modèles conceptuels comportant des processus magmatiques et hydrothermaux.

SUMMARY

This report presents a compilation and interpretation of data relevant to exploration for uranium in the Miramichi Anticlinorium of central New Brunswick. It is a follow-up of a more regional study also carried out under the Canada-New Brunswick Mineral Development Agreement (MDA) program and completed in 1986. The initial study identified the Miramichi Anticlinorium as favourable ground for uranium prospecting, especially the areas characterized by late stage, Hercynian, granitic intrusions similar to those associated with uranium deposits in Nova Scotia and western Europe.

The Miramichi Anticlinorium contains several large massive syngenetic sulphide orebodies containing Zn, Pb, Cu, and Ag, but many smaller epigenetic deposits containing some combination of Cu, Pb, Zn, W, Mo, Sn, Sb, Ag, Au, and U also are found. Many of the epigenetic deposits are spatially, and probably genetically, associated with the granite pluton.

Much exploration work was carried out in the study area in the 1970s and early 1980s by companies, the New Brunswick Department of Natural Resources and Energy, and the Geological Survey of Canada. Data from published and available unpublished reports have been collected for areas intruded by five plutons, the North Pole Pluton (and younger quartz-feldspar dykes) in the north-central part of the Anticlinorium (the Long Lake area) and the Burnthill, Trout Brook, Dungarvon, and Rocky Brook plutons in the south-central part, all deemed to be favourable for uranium occurrences.

Thus, this report examines these granitic plutons with respect to their potential for uranium mineralization by using available integrated geological, geochemical, and geophysical data. In addition, in situ gamma ray spectrometry data for equivalent uranium (eU), equivalent thorium (eTh), and potassium (K) in rocks of plutons were collected and integrated with the compiled data.

Objectives of this project were to create a database for the status of uranium resources in the Miramichi Anticlinorium, to assess the possibility of discovering economic uranium deposits and to establish geological, geochemical, and geophysical criteria that are associated with the host granitic rocks and considered to be useful clues for uranium exploration.

The Miramichi Anticlinorium was probably developed as a result of the closure of the Iapetus (proto-Atlantic) Ocean during the Ordovician Taconic Orogeny (480 Ma) and subsequently by the Devonian Acadian Orogeny (400 Ma). It forms a sinuous northeast-trending belt of rocks including a Precambrian (?) migmatitic complex overlain by the polydeformed Cambro-Ordovician Tetagouche Group. The Tetagouche Group rocks have undergone at least six phases of deformation during the Taconic and the Acadian orogenies. The

SOMMAIRE

Le présent rapport contient une compilation et une interprétation de données ayant rapport à l'exploration de l'uranium dans l'anticlinorium de Miramichi dans le centre du Nouveau-Brunswick. Ce rapport fait suite à une étude plus régionale réalisée elle aussi dans le cadre de l'Entente Canada-Nouveau-Brunswick d'exploitation minérale (EEM) et terminée en 1986. L'étude initiale a permis d'identifier l'anticlinorium de Miramichi comme un terrain favorable à la prospection de l'uranium, en particulier dans les zones caractérisées par des intrusions granitiques hercyniennes de phase tardive, semblables à celles associées aux gisements d'uranium de Nouvelle-Écosse et d'Europe occidentale.

L'anticlinorium de Miramichi contient plusieurs grands massifs minéralisés de sulfures syngénétiques contenant Zn, Pb, Cu et Ag, mais on y trouve également de nombreux petits gisements épigénétiques contenant une combinaison de Cu, Pb, Zn, W, Mo, Sn, Sb, Ag, Au et U. Nombre des gisements épigénétiques sont spatialement et probablement génétiquement associés au pluton granitique.

La grande partie des travaux d'exploration ont été réalisés dans la zone à l'étude au cours des années 1970 et au début des années 1980 par plusieurs sociétés, le ministère des Ressources naturelles et de l'Énergie du Nouveau-Brunswick et la Commission géologique du Canada. On a tiré de rapports publiés et non publiés des données sur les zones recoupées par cinq plutons : le pluton de North Pole (et des dykes quartzo-feldspathiques plus récents) dans la partie centre-nord de l'anticlinorium (la zone du lac Long) et les plutons de Burnthill, de Trout Brook, de Dungarvon et de Rocky Brook dans le centre-sud, tous considérés susceptibles de receler des venues d'uranium.

Le présent rapport fait donc une analyse de ces plutons granitiques en fonction de leur potentiel de minéralisation en uranium en utilisant les données géologiques, géochimiques et géophysiques intégrées disponibles. En outre, on a recueilli des données gammamétriques in situ sur l'uranium équivalent (eU), le thorium équivalent (eTh) et le potassium (K) contenus dans les roches des plutons, données que l'on a intégrées aux données compilées.

Ce projet a pour objectif de créer une base de données sur la situation des ressources en uranium dans l'anticlinorium de Miramichi afin d'évaluer les possibilités d'y découvrir des gisements d'uranium de valeur commerciale et d'établir des critères géologiques, géochimiques et géophysiques associés aux roches granitiques encaissantes et considérés comme des indices utiles à l'exploration de l'uranium.

L'anticlinorium de Miramichi s'est probablement formé par suite de la fermeture de l'océan Iapetus (proto-Atlantique) durant l'orogenèse taconique à l'Ordovicien (480 Ma) et l'orogenèse acadienne au Dévonien (400 Ma). Il forme une zone de roches sinueuse à direction nord-est incluant un complexe migmatitique précambrien (?) sur lequel repose le groupe de Tétagouche, groupe cambro-ordovicien polydéformé. Les roches du groupe de Tétagouche ont subi au moins six phases de déformation durant les phases taconique et acadienne. Les plutons granitiques traités dans le présent rapport

granitic plutons covered in this report were emplaced during the waning stages of the Acadian Orogeny. The metasedimentary rocks are thermally metamorphosed, within 1 km of the granitic plutons, into the following assemblages of index minerals: chlorite, biotite, cordierite, andalusite, and sillimanite.

Generally speaking the granitic rocks of the North Pole, Burnthill, Dungarvon, Trout Brook, and Rocky Brook plutons were emplaced discordantly at shallow depths (<3 km) in the crust in a relatively seismically active zone. They are circular and relatively small in size and formed late in the tectonomagmatic sequence. They postdate the earlier (Taconic) and more recent (Acadian) tectonic activities. They are usually associated with low- to medium-grade thermal aureole metamorphism. They commonly exhibit a high variation in textures and appear to be intruded in multiple stages. Associated mineralization favours late-formed fractures, particularly those which have undergone brecciation.

The granitic rocks of the North Pole Pluton (Long Lake area) include three phases: quartz-feldspar porphyry (youngest), biotite-muscovite granite, and biotite granite (oldest). The biotite granite is the most extensive. It is generally pink and contains coarse grained, equigranular crystals of quartz, alkali feldspar, and plagioclase in equal proportion. The alkali feldspar is orthoclase perthite containing domains of microcline. The plagioclase is altered to sericite and epidote; the biotite is partly altered to chlorite.

The biotite-muscovite granite intrudes the biotite granite. It is characterized by medium grain size and is light grey to light pink. In addition to mica, it contains quartz, plagioclase, potassium feldspar, and chlorite (altered from biotite). Sphene, apatite, epidote, and opaque minerals are the main accessory minerals.

The quartz-feldspar porphyry occurs as dykes intruding the biotite granite. The dykes, located mainly in the eastern side of Long Lake, trend northwest parallel to the 120° trending joints in the biotite granite. Phenocrysts of plagioclase, quartz, orthoclase, and minor biotite constitute about 50% of the rock and are embedded in a matrix of quartzo-feldspathic material. The quartz- feldspar porphyry is extensively altered by hydrothermal solutions. The plagioclase phenocrysts are almost entirely altered to sericite. Orthoclase is partially replaced by calcite. Biotite is completely altered to chlorite. Miarolitic cavities occur in these dykes.

Geochemically, the North Pole Pluton is an evolved granite (SiO_2 >70 wt. %), and characterized by high SiO_2, K_2O, and Na_2O contents relative to normal granites, particularly the biotite-muscovite granite. The TiO_2, Fe_2O_3, FeO, MgO, and CaO contents are low relative to normal granites. The trace element composition varies, and relative to normal granites the biotite and the biotite-muscovite granites have a higher content of

ont été mis en place durant les derniers stades de l'orogenèse acadienne. Les roches métasédimentaires ont subi un métamorphisme thermique, à moins d'un kilomètre des plutons granitiques, responsable de la création des minéraux caractéristiques suivants : chlorite, biotite, cordiérite, andalousite et sillimanite.

De façon générale, les roches granitiques des plutons de North Pole, de Burnthill, de Dungarvon, de Trout Brook et de Rocky Brook ont été mises en place en discordance à faible profondeur (<3 km) dans la croûte dans une zone sismique relativement active. Circulaires et relativement peu volumineuses, elles se sont formées à la fin de la séquence tectonomagmatique. Elles sont postérieures aux événements tectoniques précoces (taconiques) et plus récents (acadiens). Elles sont habituellement associées à un métamorphisme thermique à auréole de degré faible à moyen. Leur texture varie, en général, beaucoup et les intrusions semblent les avoir recoupées en plusieurs phases. La minéralisation associée a favorisé la formation de fractures tardives, en particulier de fractures qui ont subi une bréchification.

Les roches granitiques du pluton de North Pole (zone du lac Long) comportent trois phases : un porphyre quartzo-feldspathique (récent), un granite à biotite et muscovite et un granite à biotite (ancien). Le granite à biotite est le plus étendu. Il est généralement rose et contient des cristaux grossiers isogranulaires de quartz, de feldspath alcalin et de plagioclase en égales proportions. Le feldspath alcalin est un orthoclase-perthite contenant des domaines de microcline. Le plagioclase est transformé par altération en séricite et en épidote; la biotite est en partie transformée en chlorite.

Le granite à biotite et muscovite forme une intrusion dans le granite à biotite. Il est caractérisé par un grain moyen et sa couleur varie de gris clair à rose clair. En plus du mica, il contient du quartz, du plagioclase, du feldspath potassique et de la chlorite (produit d'altération de la biotite). Le sphène, l'apatite, l'épidote et les minéraux opaques sont les principaux minéraux accessoires.

Le porphyre quartzo-feldspathique forme des dykes dans le granite à biotite. Les dykes, surtout situés dans le côté est du lac Long, sont orientés au nord-ouest parallèlement aux joints à direction de 120° dans le granite à biotite. Les phénocristaux de plagioclase, de quartz, d'orthoclase et d'une faible quantité de biotite constituent environ 50 % de la roche et sont incorporés dans une matrice quartzo-feldspathique. Le porphyre quartzo-feldspathique est très altéré par des solutions hydrothermales. Les phénocristaux de plagioclase sont presque entièrement transformés en séricite. L'orthoclase est en partie remplacé par de la calcite. La biotite est entièrement transformée en chlorite. Ces dykes contiennent des cavités microlitiques.

Du point de vue chimique, le pluton de North Pole est un granite évolué (SiO_2 > 70 % poids) et est caractérisé par des teneurs élevées en SiO_2, K_2O et Na_2O comparativement aux granites ordinaires, en particulier le granite à biotite et muscovite. Les teneurs en TiO_2, Fe_2O_3, FeO, MgO et CaO sont faibles comparativement à celles des granites ordinaires. La composition des éléments à l'état de traces varie, et, comparativement aux granites ordinaires, les granites à biotite et à

base metals. Tin abundance is high in the biotite-muscovite granites. Rubidium values are generally high in all phases of the pluton, but Sr, Zr, Ba, F, and Li contents are low.

The granitic rocks of Burnthill, Dungarvon, Trout Brook, and Rocky Brook plutons (central Miramichi Anticlinorium) are similar in mineralogy, texture, and age. They also have similar metal associations such as Sn, Mo, W, and U. Therefore, it is suggested that these plutons may have been derived from a single magmatic chamber and it is possible they join at depth as a large batholith. The four plutons, of which Burnthill Pluton is the largest, comprise two major phases: equigranular granite and porphyritic granite; and two minor phases: microgranite (with associated aplite dykes and pegmatite pods) and biotite melanocratic granite.

The melanocratic biotite granite (oldest phase) is characterized by its high biotite content (up to 20%), coarse K-feldspar phenocrysts and by few euhedral plagioclase and quartz phenocrysts.

The porphyritic granite is the largest in terms of areal extent. It consists essentially of subhedral, tabular crystals of plagioclase, embedded in an interlocking mosaic of quartz and K-feldspar anhedra. Biotite flakes are scattered throughout the rock but only accessory amounts of muscovite are present. Quartz forms irregularly shaped anhedra, of variable size, that range from unstrained to moderately strained. The plagioclase is unzoned to faintly zoned, with a composition of about An_{12}, and is partly altered to sericite. The K-feldspar is highly perthitic and fresh. Biotite crystals are irregularly shaped, deep brown, and characterized by dark, pleochroic haloes around zircon inclusions. In addition to zircon, other accessory minerals are apatite and magnetite. Sericitization and muscovitization of plagioclase, and chloritization of biotite are the major alteration processes to have effected the rocks.

The equigranular granite is composed essentially of an interlocking mosaic of quartz, plagioclase, and K-feldspar anhedra through which are scattered occasional flakes of muscovite and accessory biotite. Quartz occurs as irregularly shaped anhedra which are slightly to moderately strained. Plagioclase usually forms equidimensional anhedra and is typically unzoned An_{12}. Muscovite and zircon are the major accessory minerals.

Microgranites (with associated aplite dykes and pegmatite pods) were formed late during magmatic crystallization.

Geochemically, the granitic rocks of the central Miramichi Anticlinorium plutons are highly evolved (SiO_2 >74 wt. %). They have high SiO_2, K_2O, and Na_2O contents and low TiO_2, CaO, MgO, and P_2O_5 contents in

biotite et muscovite ont une teneur élevée en métaux communs. L'abondance en étain est élevée dans les granites à biotite et muscovite. Les teneurs en rubidium sont généralement élevées dans toutes les phases du pluton, mais les teneurs en Sr, Zr, Ba, F et Li sont faibles.

Les roches granitiques des plutons de Burnthill, de Dungarvon, de Trout Brook et de Rocky Brook (centre de l'anticlinorium de Miramichi) ont une minéralogie, une texture et un âge semblables. Les associations métalliques y sont, en outre, similaires (Sn, Mo, W et U). Par conséquent, ces plutons pourraient être issus d'une seule chambre magmatique; ils se rejoindraient en profondeur pour former un grand batholithe. Les quatre plutons dont le plus vaste est le pluton de Burnthill, comprennent deux phases principales : un granite isogranulaire et un granite porphyritique; et deux phases secondaires : un microgranite (associé à des dykes d'aplite et des lentilles de pegmatite) et un granite mélanocrate à biotite.

Le granite mélanocrate à biotite (phase la plus ancienne) est caractérisé par une haute teneur en biotite (jusqu'à 20 %) et la présence de phénocristaux grossiers de feldspath potassique et de quelques phénocristaux de plagioclase et de quartz euédriques.

Le granite porphyritique est le plus vaste en superficie. Il est composé essentiellement de cristaux tabulaires subautomorphes de plagioclase, incorporés dans une mosaïque entrecroisée de quartz et de feldspath potassique anédriques. Les lamelles de biotite sont disséminées dans la roche tandis que la muscovite n'est présente qu'en quantités accessoires. Le quartz forme des cristaux anédriques de taille variable dont la déformation varie de nulle à moyenne. Le plagioclase, dont la zonation varie elle aussi de nulle à faible, se compose d'environ An_{12} et se trouve en partie transformé par altération en séricite. Le feldspath potassique est très perthitique et non altéré. Les cristaux de biotite sont de forme irrégulière, de couleur brun foncé et caractérisés par des auréoles pléochroïques foncées autour des inclusions de zircon. Les minéraux accessoires autres que le zircon sont l'apatite et la magnétite. Les principaux processus d'altération qui ont affecté les roches sont la séricitisation et la muscovitisation du plagioclase et la chloritisation de la biotite.

Le granite isogranulaire est composé essentiellement d'une mosaïque entrecroisée de cristaux anédriques de quartz, de plagioclase et de feldspath potassique dans lesquels sont disséminées des lamelles occasionnelles de muscovite et des lamelles accessoires de biotite. Le quartz se présente sous forme de cristaux anédriques de forme irrégulière dont le taux de déformation varie de léger à moyen. Le plagioclase forme habituellement des cristaux anédriques équidimensionnels et consiste typiquement d'An_{12} non zoné. La muscovite et le zircon sont les principaux minéraux accessoires.

Les microgranites (associés aux dykes d'aplite et aux lentilles de pegmatite) se sont formés à la fin de la phase de cristallisation magmatique.

Du point de vue géochimique, les roches granitiques des plutons du centre de l'anticlinorium de Miramichi sont très évoluées (SiO_2 > 74 % poids). Leurs teneurs en SiO_2, K_2O et Na_2O sont élevées et leurs teneurs en TiO_2, CaO, MgO et P_2O_5

comparison to global averages. Furthermore, they are enriched with incompatible trace elements such as Rb, Y, and Ta and depleted of compatible trace elements such as Sr, Zr, and Ba relative to global averages. They are also impoverished in some transition elements such as Ni, Cr, Co, and V and enriched with others such as Cu and Zn. They are in general depleted in rare-earth elements (REEs) relative to global average granites. The depletion is most obvious in the uranium-mineralized rocks.

The chemical characteristics and the statistical analyses of the chemical data suggest that the North Pole and the Burnthill plutons belong to the ilmenite-series granitoids of S-type. However, an enrichment of the granites with F, Nb, Ta, and Y and their depletion of V, Ni, Co, and Cr suggest that the Burnthill Pluton especially and, to some extent the North Pole Pluton, are A-type granitoids.

Geophysically, the granitic plutons of the Long Lake area and central Miramichi Anticlinorium are associated with strong negative Bouguer gravity anomalies and low, poorly defined, magnetic anomalies – features observed in other uraniferous granites such as the Hercynian granites of Europe and Nova Scotia.

Airborne gamma ray spectrometry data outline several equivalent uranium (eU) anomalies in the study areas. These anomalies are spatially linked to the granitic plutons. In the Long Lake area, the aeroradiometric data show that eU, eTh, and K contents in the late stage biotite-muscovite granite are higher than contents in the early stage biotite granite of the North Pole Pluton. One of the prominent eU anomalous areas is located on the eastern side of Long Lake over the North Pole Pluton and coincides with anomalous uranium concentrations along highly altered and brecciated chalcedony (jasperoid)-bearing faults.

The highest equivalent uranium anomalies on the gamma ray spectrometry maps coincide with the centres of the negative Bouguer gravity anomalies and both are, in turn, associated with Sn, W, and Mo mineralization.

In the central Miramichi Anticlinorium, the strongest and broadest airborne eU anomalies are associated with the Burnthill Pluton. Most are confined to the eastern and southeastern margins of the intrusion where much of the Sn, W, and Mo mineralization has been reported. The late stage equigranular phase of the granitic plutons appears to have slightly higher uranium and thorium contents than the early stage porphyritic phase. This was also indicated by the in situ gamma ray spectrometry data, which reveal that eU was slightly depleted in weathered and altered granites relative to fresh granites.

The geochemical data (lake sediments, spring and stream sediments, soil, till, and rock samples) indicate that the granitic plutons are highly anomalous in terms of their uranium content.

sont faibles comparativement aux moyennes globales. De plus, elles sont enrichies en éléments à l'état de traces incompatibles, comme Rb, Y et Ta, et appauvries en éléments traces compatibles, comme Sr, Zr et Ba, comparativement aux moyennes globales. Elles sont également appauvries en certains éléments de transition comme Ni, Cr, Co et V mais enrichies notamment en Cu et Zn. Elles sont en général appauvries en éléments des terres rares comparativement à la moyenne globale des granites. L'appauvrissement est plus évident dans les roches minéralisées en uranium.

Les caractéristiques et les analyses statistiques des données chimiques indiquent que les plutons de North Pole et de Burnthill font partie de la famille des granitoïdes de la série des ilménites de type S. Cependant, un enrichissement des granites en F, Nb, Ta et Y et leur appauvrissement en V, Ni, Co et Cr indiquent que le pluton de Burnthill, en particulier, et dans une certaine mesure, le pluton de North Pole, sont des granitoïdes de type A.

Du point de vue géophysique, les plutons granitiques de la région du lac Long et de la partie centrale de l'anticlinorium de Miramichi sont associés à des anomalies gravimétriques de Bouguer très négatives et à de faibles anomalies magnétiques mal définies. Ces caractéristiques ont également été observées dans d'autres granites uranifères comme les granites hercyniens d'Europe et de la Nouvelle-Écosse.

Les données gammamétriques recueillies par aéronef permettent de délimiter plusieurs anomalies d'uranium équivalent (eU) dans les zones à l'étude. Ces anomalies sont spatialement liées aux plutons granitiques. Dans la région du lac Long, les données aéroradiométriques indiquent que les teneurs en eU, eTh et K dans le granite à biotite et muscovite de phase tardive sont plus élevées que dans le granite à biotite de phase précoce du pluton de North Pole. L'une des zones d'anomalies de eU dominantes est située sur le côté est du lac Long au-dessus du pluton de North Pole et coïncide avec des concentrations anormales d'uranium et des failles contenant de la calcédoine (très altérée et brèchifiée).

Les fortes anomalies en uranium équivalent que l'on observe sur les cartes gammamétriques coïncident avec le centre des anomalies gravimétriques de Bouguer négatives. Ces deux types d'anomalies sont à leur tour associées à une minéralisation en Sn, W et Mo.

Dans le centre de l'anticlinorium de Miramichi, les anomalies de eU les plus fortes et les plus étendues, telles que déterminées par les données aériennes, sont associées au pluton de Burnthill. La plupart sont confinées aux bordures est et sud-est de l'intrusion où l'on a signalé la plupart des minéralisations en Sn, W et Mo. La phase isogranulaire tardive des plutons granitiques semble contenir des teneurs légèrement plus élevées d'uranium et de thorium que la phase porphyritique précoce. Cette observation est corroborée par les données gammamétriques recueillies in situ qui révèlent que eU était légèrement plus appauvri dans les granites météorisés et altérés que dans les granites non altérés.

Les données géochimiques (sédiments lacustres, sédiments de sources et de cours d'eau, échantillons de sol, de till et de roche) indiquent que les plutons granitiques ont des teneurs en uranium anormalement élevées.

Multielement (U, Cu, Pb, Zn, Ag, Mo, and Mn) chemical analyses of 439 lake sediment samples from Long Lake reveal the presence of 17 multielement anomalies. The anomalies are in general elongated, suggesting that they may be related to metal concentrations along shear zones. They have different trends but are chiefly northeasterly or northwesterly. The northwest-trending anomalies are located in the centre of the lake and appear to be related to a major northwest-trending fault. This, along with the occurrence of mineralized vein-type float around the lake shore, suggests that vein-type mineralization may exist in the centre of the lake. With the exception of Cu and Ag, all the above elements in the lake sediment samples exceed their corresponding global abundances, particularly uranium, which exceeds its global average by an order of six. Uranium, in the lake sediment samples, has a strong positive correlation with Cu and Zn and low to moderate correlations with Ag, Pb, Mo, and Mn.

Uranium has a strong positive correlation with Ag and Cu within the spring and stream sediment samples, which were analyzed for U, Cu, Pb, Zn, Co, Ni, Mn, Fe, Mo, W, and Ag. Unexpectedly, it was found that uranium content in spring and stream sediments in the area underlain by the granitic rocks of the North Pole Pluton is, in general, not anomalous, whereas it is high in the adjacent area that is underlain by Precambrian amphibolite and Ordovician granite. It is suggested that uranium may have migrated either in solution or as particles from the area underlain by the North Pole Pluton (high topography) to areas underlain by Precambrian amphibolite and Ordovician granites (relatively low area). Alternatively, the uranium- bearing late phase quartz-feldspar porphyry dykes of North Pole Pluton which intruded the adjacent rocks may have provided the uranium and associated metals.

The 3732 soil samples from the Long Lake area (analyzed for their U, Cu, Pb, Zn, Mn, Mo, and Ag contents) reveal the presence of 54 multielement soil anomalies. The majority of these anomalies are located on the eastern side of Long Lake in an area underlain by the North Pole Pluton. These anomalies have, in general, a linear pattern with west-northwest, east, and northeast trends which could be a reflection of mineralization along linear features such as fault zones. Furthermore, two common metal associations were observed in the soil samples. The first is between Cu, Pb, Zn, Mn, and Ag in areas underlain by biotite granite. The second includes U and Mo in northwest-trending anomalies.

Till samples in the Long Lake area which were analyzed for their U, Cu, Pb, Zn, Fe, Co, Ni, W, Mo, and Au contents also outlined several U, Pb, Sn, Cu, and Mn anomalies in the area underlain by the granitic rocks of the North Pole Pluton. The anomalies appear to be related to northwest-trending fracture zones in the biotite granite.

L'analyse chimique de plusieurs éléments (U, Cu, Pb, Zn, Ag, Mo et Mn) de 439 échantillons de sédiments lacustres prélevés dans le lac Long révèle la présence de 17 anomalies liées à ces éléments. Les anomalies sont en général allongées, indiquant qu'elles pourraient être liées à des concentrations métalliques longeant les zones de cisaillement. Leurs directions diffèrent mais elles sont principalement orientées au nord-est ou au nord-ouest. Les anomalies à direction nord-ouest sont situées dans le centre du lac et semblent être liées à une importante faille à direction nord-ouest. Si l'on ajoute à cela la présence de fragments d'altération filoniens autour des rives du lac, on peut supposer la présence d'une minéralisation filonienne dans le centre du lac. À l'exception de Cu et de Ag, tous les éléments ci-haut mentionnés contenus dans les échantillons de sédiments lacustres ont une teneur dépassant leur abondance globale correspondante, en particulier l'uranium dont la teneur est de six fois supérieure à la moyenne globale. L'uranium, dans les échantillons de sédiments lacustres, présente une forte corrélation positive avec Cu et Zn et une corrélation qui varie de faible à moyenne avec Ag, Pb, Mo et Mn.

L'uranium présente une forte corrélation positive avec Ag et Cu dans les échantillons de sédiments de source et de cours d'eau pour lesquels on a analysé la teneur en U, Cu, Pb, Zn, Co, Ni, Mn, Fe, Mo, W et Ag. Contrairement aux prévisions, la teneur en uranium dans les sédiments de source et de cours d'eau dans la zone reposant sur des roches granitiques du pluton de North Pole est, en général, non anormale, tandis qu'elle est élevée dans la zone adjacente reposant sur des amphibolites précambriennes et des granites ordoviciens. L'uranium a pu migrer soit en solution ou sous forme de particules depuis la zone reposant sur le pluton de North Pole (zone élevée) vers les zones reposant sur l'amphibolite précambrienne et les granites ordoviciens (zone relativement basse). Ou bien, les dykes uranifères de porphyre quartzo-feldspathique de phase tardive du pluton de North Pole qui forment des intrusions dans les roches adjacentes ont pu produire l'uranium et les métaux connexes.

Les 3732 échantillons de sol provenant de la région du lac Long (analysés pour leur teneur en U, Cu, Pb, Zn, Mn, Mo et Ag) révèlent la présence de 54 anomalies de plusieurs éléments. La majorité de ces anomalies sont situées sur le côté est du lac Long dans une zone reposant sur le pluton de North Pole. Ces anomalies présentent, en général, une configuration linéaire à directions ouest-nord-ouest, est et nord-est qui pourrait refléter une minéralisation longeant des formes linéaires comme les zones faillées. En outre, on a observé dans les échantillons de sol deux associations métalliques courantes. La première comporte Cu, Pb, Zn, Mn et Ag dans les zones reposant sur le granite à biotite. La seconde contient U et Mo dans des anomalies à direction nord-ouest.

Les échantillons de till dans la région du lac Long ont été analysés pour leurs teneurs en U, Cu, Pb, Zn, Fe, Co, Ni, W, Mo et Au et ont permis de délimiter plusieurs anomalies de U, Pb, Sn, Cu et Mn dans la zone reposant sur les roches granitiques du pluton de North Pole. Les anomalies sembent être liées aux zones fracturées à direction nord-ouest présentes dans le granite à biotite.

In the central Miramichi Anticlinorium, the results of 344 samples of sediments from springs and streams (analyzed for U, Mo, W, Cu, Pb, Zn, Mn, and Fe contents) draining the granitic rocks of the Burnthill, Dungarvon, Trout Brook, and Rocky Brook plutons indicate highly anomalous values for U, Mo, W, and to some extent Pb relative to global averages of these elements in sediments. Uranium, tin, molybdenium, and tungsten contents of soils sampled in the central Miramichi Anticlinorium are in general anomalous in comparison with global averages. The uranium content in the soil decreases systematically upward from C-horizon to A-horizon. This pattern of uranium distribution in the soil horizons may suggest that uranium was derived from the underlying granitic rocks. Correlation coefficients calculated among U, W, Mo, and Sn contents of the soil are moderate and also suggest that all these elements have been derived from similar source rocks such as the granitic rocks of the Burnthill Pluton.

Seventy-seven till samples of two textural fractions, clay-sized (<2 μm) and clay- plus silt-sized (<63 μm) covering the granitic plutons of the central Miramichi Anticlinorium reveal the presence of several uranium anomalies coincident with areas where the bedrocks are also anomalous. This may indicate that till samples were derived locally and most probably from the underlying granitic rocks. With the exception of Cr, all other elements (U, Th, Sn, Mo, W, Sb, Au, As, Mn, Fe, Cu, Pb, Zn, Ni, and Co) analyzed in the two fractions tend to be enriched in the fine fraction rather than in the coarse fraction. This contrast in chemical composition between the two fractions is more obvious for the lithophile elements U, Mo, and W which suggests that these elements are associated with the weathering and alteration products of the rocks which are enriched in the fine fraction of till rather than with primary silicate minerals enriched in the coarse fraction. Alternatively, this may reflect the tendency of these lithophile elements to be absorbed by the clays and organic matter that are predominant in the fine fraction of till samples.

The uranium content in granitic rock samples of all five plutons is higher than the global average for normal granites.

Rocks showing effects of hydrothermal alteration show, in general, an increase in uranium content. Furthermore, it appears that uranium concentration favours rocks which have undergone low to medium temperature hydrothermal alteration such as hematitization and albitization rather than high temperature alteration such as greisenization.

Despite the amount of exploration and the favourable geological environment, only low grade concentrations of uranium have been found to date within the Miramichi Anticlinorium. These occurrences are spatially and possibly temporally associated with the Acadian granitic plutons and are frequently found along with other economically important elements, especially with Sn, W, Mo, and base metal sulphides.

Dans la partie centrale de l'anticlinorium de Miramichi, une analyse de 344 échantillons de sédiments provenant de sources et de cours d'eau (détermination de leurs teneurs en U, Mo, W, Cu, Pb, Zn, Mn et Fe) drainant les roches granitiques des plutons de Burnthill, de Dungarvon, de Trout Brook et de Rocky Brook, indique des teneurs anormalement élevées de U, Mo, W et, dans une certaine mesure, de Pb, comparativement aux teneurs moyennes globales de ces éléments dans les sédiments. Les teneurs en uranium, étain, molybdène et tungstène des sols échantillonnés dans la partie centrale de l'anticlinorium de Miramichi sont, en général, anormales comparativement aux moyennes globales. La teneur en uranium du sol diminue systématiquement vers le haut, de l'horizon C à l'horizon A. Ce profil de répartition de l'uranium dans les horizons pourrait indiquer que l'uranium provient des roches granitiques sous-jacentes. Les coefficients de corrélation calculés entre les teneurs en U, W, Mo et Sn du sol sont modérés et laissent également supposer que tous ces éléments proviennent de roches semblables comme les roches granitiques du pluton de Burnthill.

L'analyse de 77 échantillons de till de deux granulométries différentes, fraction argileuse (<2 μm) et granulométrie argileuse-silteuse (<63 μm), couvrant les plutons granitiques de la partie centrale de l'anticlinorium de Miramichi révèle la présence de plusieurs anomalies d'uranium qui coïncident avec des zones où le socle contient des teneurs anormales. Les échantillons de till pourraient donc être d'origine locale et, fort probablement, provenir des roches granitiques sous-jacentes. À l'exception de Cr, tous les autres éléments (U, Th, Sn, Mo, W, Sb, Au, As, Mn, Fe, Cu, Pb, Zn, Ni et Co) qui ont été analysés dans les deux fractions ont tendance à être enrichis dans la fraction fine plutôt que dans la fraction grossière. Cette différence de composition chimique entre les deux fractions est plus évidente dans le cas des éléments lithophiles U, Mo et W, signe que ces éléments sont associés aux produits de météorisation et d'altération des roches enrichies contenues dans la fraction fine du till plutôt qu'aux minéraux silicatés primaires enrichis de la fraction grossière. Sinon, cela pourrait refléter la tendance de ces éléments lithophiles à être absorbés par les argiles et les matières organiques qui dominent dans la fraction fine des échantillons de till.

La teneur en uranium dans les échantillons de roche granitique des cinq plutons est plus élevée que la teneur moyenne globale relevée dans les granites ordinaires.

Les roches qui affichent les signes d'une altération hydrothermale présentent, en général, une augmentation de teneur en uranium. De plus, il semble que la concentration d'uranium est plus élevée dans les roches qui ont subi une altération hydrothermale de température faible à moyenne comme une hématitisation et une albitisation, que dans les roches ayant subi une altération à température élevée comme une greisenisation.

Malgré les nombreux travaux d'exploration accomplis et un milieu géologique favorable, on n'a trouvé à ce jour dans l'anticlinorium de Miramichi, que des concentrations d'uranium à faible teneur. Ces venues sont spatialement, et peut-être temporellement, associées aux plutons granitiques acadiens et sont fréquemment associées à d'autres éléments économiquement importants, en particulier Sn, W, Mo et les sulfures de métaux communs.

The uranium deposits in the Long Lake area occur as polymetallic vein-types and are concentrated along northwest-trending chalcedony (jasperoid)-filled fractures and fault breccias which crosscut the Lower Devonian granitic rocks of the North Pole Pluton. They mostly have associated Cu, Pb, Zn, Sn, W, Mo, Bi, Ag, and Au. Pyrite, chalcopyrite, covellite, and molybdenite are the major sulphide minerals identified in the veins. Small amounts of arsenopyrite, matildite, and native bismuth were also identified. Cassiterite and autunite-torbernite have been identified in float only. Uranium also has been found in veins intersected in trenches and drill holes but no mineral identifications were made. Three styles of uranium mineralization were displayed in the float samples, (a) in discrete grains, (b) in fracture fillings, and (c) diffused within the rocks.

Uranium occurrences are associated with late phase differentiates of the granitic rocks of the Burnthill, Dungarvon, Trout Brook, and Rocky Brook plutons. In addition to uranium these granites host Sn, W, Mo, and F minerals. Anomalous levels of uranium are associated with the eastern and southeastern portion of the Burnthill Pluton, east and southern portion of the Dungarvon Pluton and eastern portion of the Rocky Brook and Trout Brook plutons. Furthermore, the uranium anomalies, more or less, are spatially associated with the equigranular granitic phases of the plutons. A significant uranium occurrence is located in the northeastern part of the Dungarvon Pluton, where uranium is associated with a quartz-fluorite breccia emplaced along a southeasterly (130°) trending shear zone.

Data are insufficient to define with confidence any one conceptual model of uranium ore genesis. The spatial relationship with the acidic intrusions, uranium enrichment in hydrothermally altered rocks, uranium association, in some cases, with other minerals of generally accepted hydrothermal origin, and uranium enrichment in late stage specialized phases are strongly suggestive of a genetic relationship with the granites. Whether or not the uranium was deposited from magmatic fluids, magma-driven convection cells, or some combination of the two has not been proven.

The secondary nature of some uranium minerals and of some alteration products are suggestive of supergene processes involving meteoric waters of an oxidizing nature in a subaerial environment. The anomalously high uranium content of the granites would contribute to the formation of such deposits.

Les gisements d'uranium dans la région du lac Long se présentent sous forme de filons polymétalliques et sont concentrés le long de fractures remplies de calcédoine à direction nord-ouest et de brèches de faille qui recoupent transversalement les roches granitiques du Dévonien inférieur du pluton de North Pole. Ils sont pour la plupart associés à Cu, Pb, Zn, Sn, W, Mo, Bi, Ag et Au. Les principaux minéraux sulfurés identifiés dans les filons sont la pyrite, la chalcopyrite, la covellite et la molybdénite. De petites quantités d'arsénopyrite, de matildite et de bismuth natif ont également été relevées. La cassitérite et l'autunite-torbernite n'étaient présentes que dans les fragments d'altération disséminés. On a également trouvé de l'uranium dans des filons recoupés par des tranchées et des trous de sondage mais aucun minéral n'a été identifié. Dans les échantillons de fragments d'altération, on distingue trois styles de minéralisation de l'uranium : a) dans des grains distincts, b) dans des remplissages de fracture et c) disséminés au sein des roches.

Les venues d'uranium sont associées à des produits de différenciation tardifs des roches granitiques des plutons de Burnthill, de Dungarvon, de Trout Brook et de Rocky Brook. Ces granites, recèlent non seulement de l'uranium mais des minéraux à Sn, W, Mo et F. Les concentrations anormales d'uranium sont associées aux parties est et sud-est du pluton de Burnthill, aux parties est et sud du pluton de Dungarvon et à la partie est des plutons de Rocky Brook et de Trout Brook. De plus, les anomalies d'uranium, sont plus ou moins spatialement associées aux phases granitiques isogranulaires des plutons. Une importante venue d'uranium est située dans la partie nord-est du pluton de Dungarvon où l'uranium est associé à une brèche de fluorite avec quartz mise en place le long d'une zone de cisaillement à direction sud-est (130°).

Faute de données suffisantes, il n'est pas possible de définir avec netteté un modèle conceptuel de la genèse de l'uranium. La relation spatiale qui existe avec les intrusions acides, un enrichissement en uranium dans les roches hydrothermalement altérées, l'association de l'uranium, dans certains cas, avec d'autres minéraux d'origine hydrothermale généralement acceptée et un enrichissement en uranium dans des phases particulières tardives incitent fortement à supposer un lien génétique avec les granites. Que l'uranium provienne ou non de fluides magmatiques, de cellules de convexion produites par le magma ou d'une combinaison des deux n'a pas été prouvé.

La nature secondaire de certains minéraux d'uranium et de certains produits d'altération laisse supposer que des processus secondaires mettant en oeuvre des eaux météoriques de nature oxydante dans un milieu subaérien ont eu lieu. La teneur anormalement élevée en uranium des granites aurait contribué à la formation de ces gisements.

INTRODUCTION

Scope and objectives of the project

This study represents a summary of part of a research project dealing with the metallogeney of uranium in the province of New Brunswick.

During previous years, 82 uranium occurrences in New Brunswick have been investigated (Hassan et al., 1987). Of the seven tectono-stratigraphic domains examined, the Gaspé Synclinorium, Aroostook-Matapedia Anticlinorium, Chaleur Bay Synclinorium, Miramichi Anticlinorium, Fredericton Trough, Avalonian Platform and the Carboniferous Basin, the Miramichi Anticlinorium (Fig. 1) was chosen for further study because several plutons within that domain represent environments found favorable for uranium occurrences in other areas such as Nova Scotia and the Massif Central of France. Attention was drawn particularly to the North Pole Pluton in the Long Lake area and the Burnthill, Dungarvon, Trout Brook and Rocky Brook plutons in the central part of the anticlinorium (Fig. 1). This report concentrates on these two areas.

The main objectives of the project are to establish a database for the status of uranium resources in these two areas in order to assess the possibility of discovering economic uranium deposits and to establish geological, geochemical, and geophysical criteria associated with the host granitic rocks that are thought to be useful guides for uranium exploration.

Method of investigation

The two areas outlined in Figure 1 are both characterized by thick glacial till, emplaced during the Pleistocene Epoch (Poole, 1963) and a dense forest. Thus, rock outcrops are fairly rare and of poor quality, particularly in the central Miramichi area, making exploration difficult for minerals in general and for uranium in particular. Uranium is expected to be depleted in the exposed surfaces of the rocks by weathering and it is difficult to detect buried uranium deposits (deeper than 50 cm) by means of gamma ray spectrometry unless some of the element or its decay products have been leaked to the overburden materials.

Despite the difficulties, a good deal of uranium exploration has been carried out in the last decade and a large amount of data (published and unpublished) was accumulated by private companies, government agencies, and universities. In this report, the data on the Long Lake and central Miramichi areas were compiled and reviewed in the context of uranium and associated elements metallogenesis. Field examinations were carried out and in some cases rock samples and in situ gamma ray spectrometry data were obtained.

Previous investigations

Active search for uranium in the study area started in 1975, following the signing of the Federal-Provincial Uranium Reconnaissance Program (URP). The initial phase of this program involved airborne gamma ray spectrometric traverses in 1976 at a five kilometre line spacing. The results of this study were released by the Geological Survey of Canada in the spring of 1977. Following this, extensive follow-up ground gamma ray spectrometric surveys (e.g., Chandra, 1981; Ford, 1982), lake and stream sediment surveys, and water sampling for geochemical analysis for uranium (e.g., Austria, 1976, 1977) were carried out.

Several other reconnaissance and detailed investigations, including geophysics, geochemistry, and borehole drilling, have been carried out by personnel of the New Brunswick Department of Natural Resources and Energy, the Geological Survey of Canada, and numerous exploration companies.

The search for uranium was substantially increased in the late 1970s and the early 1980s by several private companies especially when it was found that similar Hercynian granitic rocks in Europe, U.S.A., and Nova Scotia are associated with vein-type uranium deposits.

No uranium prospects of known economic significance have been located in these investigations. However, several favourable and subeconomic uranium occurrences were identified in the vicinity of the posttectonic granitic plutons. The most significant ones were located in and around the North Pole Pluton of the Long Lake area and the Burnthill, Dungarvon, Trout Brook, and Rocky Brook plutons of the central Miramichi area (Fig. 1). Many of these occurrences are associated with significant amounts of other ore forming elements, particularly Sn, W, and Mo.

Between 1971 and 1982 the Canadian Occidental Petroleum Company carried out several reconnaissance and detailed geological, geochemical, and geophysical surveys for uranium and base metal sulphides. A summary of best results obtained by Occidental during its surveys is shown in Appendix I.

In 1979 Western Mines Limited carried out an extensive exploration program over the eastern part of the Burnthill Pluton (Butler, 1980) as part of the New Brunswick Uranium Joint Venture Project initiated in 1979. The aim of the program was to search for intragranitic uranium vein-type deposits similar to those in the Massif Central of France. In addition to geological, geochemical, and geophysical surveys, trenching was also performed. Anomalous amounts of uranium in spring sediments — up to 2540 ppm — were detected by delayed neutron activation (D.N.A.) methods, and up to 2000 ppm by fluorimetric analysis. Anomalous amounts of uranium in water samples — up to 11.8 ppb — were detected by fluorimetric methods. Drilling of these anomalous zones by Western Resources Ltd. in 1981 revealed the presence of a 1.5 m thick uranium anomalous zone (62 ppm) within the granitic rocks (Hattie, 1981). The mineralization is associated with green clays on joints.

In 1979, 50 stream sediment samples were collected in the Little Dungarvon River and its tributaries by Beth-Canada Mining Company (Bloemraad and Reid, 1980). Samples were analyzed for Sn, W, Mo, F, Cu, Pb, Zn, and U. The results indicated highly anomalous values for U and

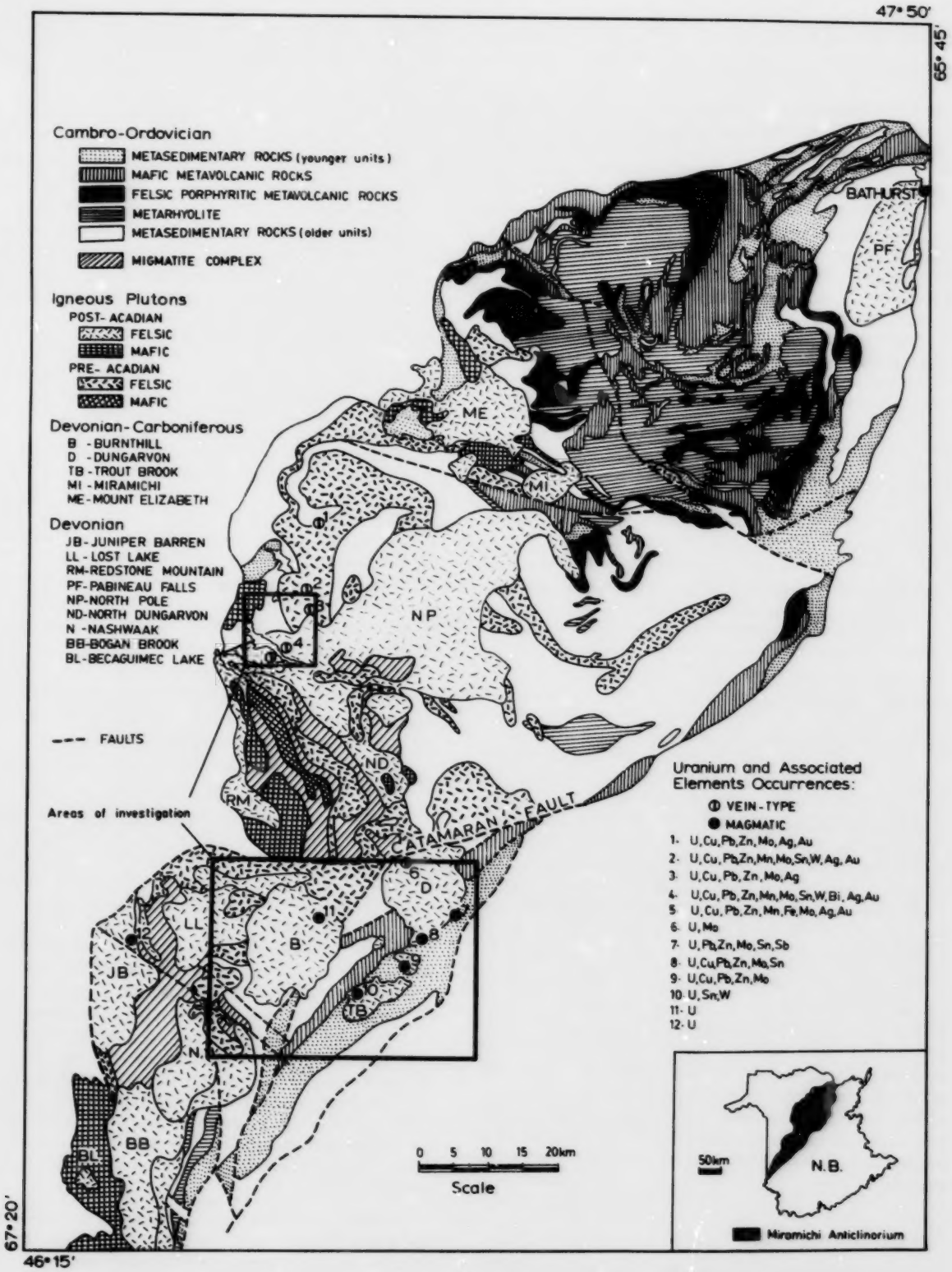

Figure 1. Geology and uranium metallogeny of Miramichi Anticlinorium, New Brunswick.

Mo. Of the 50 samples, 8 contained more than 200 ppm U, the highest being 465 ppm. The results also indicated a correlation between anomalous U and Mo values.

The Trout Brook Pluton was explored by Eldorado Nuclear Limited in 1979 (Lafontaine, 1980). Their exploration program consisted of geological mapping, systematic soil sampling, and radiometric surveying. Within the granitic rocks, it was noticed that uranium is relatively enriched with respect to thorium. However, the overall concentration of the two elements was within the normal range of felsic igneous rocks. Anomalous uranium concentrations in soil, correlated to organic-rich horizons, were located in an area characterized by the presence of abundant joints in the granite. Four other anomalous radiometric zones which were also outlined within the pluton, were associated, to some degree, with veins and pegmatite pods.

This survey was followed by a more detailed one in 1980, in order to further investigate the uranium anomalies outlined during the 1979 program. Other uranium anomalies (up to 1300 ppm) were located in soils and also correlated with high organic content in the samples. In spring and stream sediment samples, uranium anomalies of up to 590 ppm were outlined near the southeastern margin of Trout Brook Pluton. Eldorado Nuclear carried out trenching in the vicinity of these anomalies in 1981 (Brulé, 1982), revealing a complex network of northeast- and northwest-trending vertical joints enriched with uranium.

A uranium anomaly was discovered in the northeastern part of the Dungarvon Pluton by R. Shives of the Geological Survey of Canada in 1985 (Fyffe and MacLellan, 1988). This anomaly is associated with a quartz-fluorite breccia emplaced along a southeasterly (130°) trending shear zone intersecting the Middle Devonian granitic rocks of the Dungarvon Pluton. The shear zone covers an area 1 m wide and 100 m long.

Acknowledgments

This project is sponsored and funded by the Geological Survey of Canada under the Canada-New Brunswick Mineral Development Agreement 1984-89.

The authors would like to thank the late Dr. W.E. Hale of the Department of Geology, University of New Brunswick for his contribution and guidance while he supervised the senior author on the initial stage of this project before his sudden death on September 23, 1986; to his memory the authors express gratitude and respect.

The authors are very grateful to the Scientific Authority of this project, Dr. Vlad Ruzicka of the Geological Survey of Canada, for his continuous interest, support, and advice.

The authors would also like to thank those who contributed data, information, or facilities to this project particularly Ms. H.E. MacLellan of Carleton University, Mr. G.W. Crouse of New Brunswick Department of Natural Resources and Energy, and Mr. R. Crosby of Miramichi Lumber Company. Our thanks is also extended to Mr. W.W. Gardiner and Mr. D.V. Venugopal of the New Brunswick Department of Natural Resources and Energy for reviewing the manuscript and making valuable comments.

Special thanks to the Department of Geology, University of New Brunswick (particularly to the Chairman, Dr. van de Poll and to Dr. K.B.S. Burke) for providing facilities, information and advice.

The authors are also indebted to Sherri Townsend for manuscript preparation.

GENERAL GEOLOGY OF THE MIRAMICHI ANTICLINORIUM

General statement

New Brunswick has been divided into seven lithotectonic zones (Fig. 2). This study area is within the Miramichi Anticlinorium zone, which is composed of a northeast-trending belt of rocks including a Precambrian (?) migmatic complex overlain by the poly-deformed Cambro-Ordovician Tetagouche Group (Skinner, 1974). During the Acadian Orogeny the anticlinorium was pervasively intruded by large volumes of predominantly granitic magma.

The lower part of the Tetagouche Group contains a thick sequence of quartz wacke, quartzite, and slate (Fyffe, 1976). The quartzose rocks are believed to be late Precambrian (Hadrynian) to early Ordovician rift facies developed off the northern margin of the Avalonian Platform (Rast et al., 1976; Ruitenberg et al., 1977).

The upper part of the Tetagouche Group is composed of rhyolite, quartz-feldspar tuff, and pillow basalt interbedded with red and black slate and chert, iron-formation, and minor limestone (Fyffe et al., 1981). The upper Tetagouche Group is Middle Ordovician (Caradocian) in age (Nowlan, 1981).

Tectonic setting

The Cambro-Ordovician metasedimentary rocks of the Miramichi Anticlinorium have undergone at least three phases of deformation during the Taconic (480 Ma) and the Acadian (400 Ma) orogenies (Rast, 1983) or as many as six according to van Staal (1987). The Taconic Orogeny was more intense in the northern part of the anticlinorium whereas the Acadian Orogeny was uniform along the entire length (Fyffe, 1982a).

The Taconic Orogeny took place during Ordovician time as a result of the closing of the Iapetus Ocean and the destruction of the ancient continental margin of North America (i.e., continent-continent collision) (Williams, 1979).

The Acadian Orogeny took place during late Lower to Middle Devonian and produced the major anticlinoria and synclinoria in the Appalachians including the Miramichi Anticlinorium (St. Julien and Béland, 1982). McKerrow and

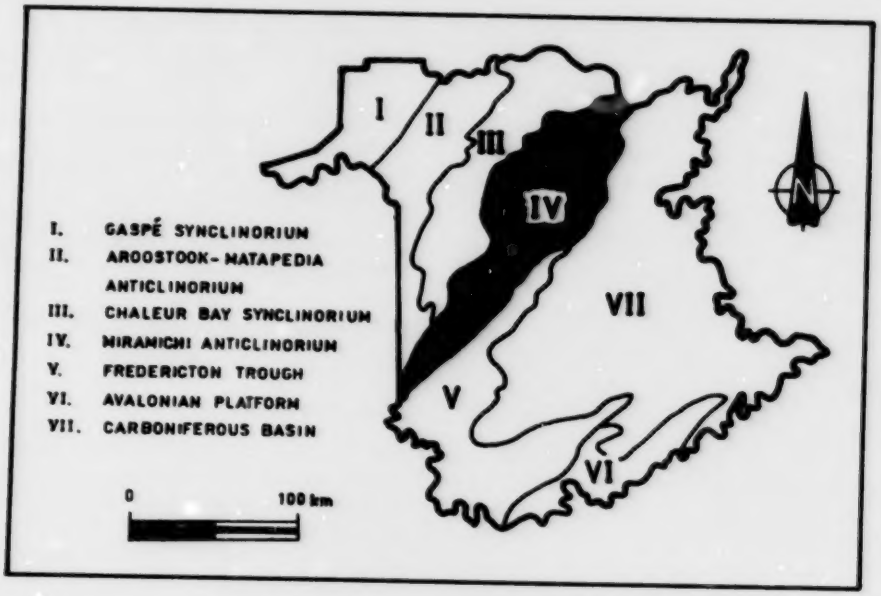

Figure 2. Lithotectonic zones of New Brunswick.

Ziegler (1971) and Keppie (1977) related the Acadian Orogeny to the final stages of the closure of the Iapetus Ocean.

Major northeast- and northwest-trending faults are common in the Miramichi Anticlinorium. The most prominent of these faults is the east-northeast trending Catamaran Fault (Fig. 1), which has a right lateral slip with an approximate displacement of 7.2 km (Anderson, 1972). The Catamaran Fault displaces a granite pluton dated at 315 ± 7 Ma (Fyffe, 1982b).

Igneous intrusions

Two groups of igneous rocks, mainly felsic, were intruded in the Miramichi Anticlinorium (Fig. 1). The first group (older granitoids) were emplaced during the Taconic Orogeny and are deformed (cataclastic). The second group (younger granitoids) were emplaced during and after the waning stages of the Acadian Orogeny and are generally undeformed.

The granitic rocks of the North Pole, Burnthill, Dungarvon, Trout Brook, and Rocky Brook plutons are younger granitoids belonging to the second group.

Metamorphism

The rocks of the Miramichi Anticlinorium have undergone both regional and thermal metamorphism. Those of Precambrian (?) age have been altered to high grade assemblages including migmatites and amphibolites. The more abundant Cambro-Ordovician sedimentary rocks of the Tetagouche Group are regionally metamorphosed to subgreenschist and amphibolite facies, in addition to the contact metamorphism near intrusions. The regional metamorphism ranges, generally from chlorite grade in the north to biotite grade in the centre, and is believed related to the Taconic Orogeny. Rocks in the southern part of the anticlinorium have undergone prehnite-pumpellyite grade metamorphism, possibly as a result of the Acadian Orogeny (Venugopal, 1979).

Within one kilometre of the igneous plutons, the country rocks were thermally metamorphosed into the following assemblages of index minerals: chlorite, biotite, cordierite, andalusite, and sillimanite.

Economic potential

The Miramichi Anticlinorium encompasses most of the important ore and potential ore deposits in New Brunswick. The anticlinorium has a high potential for undiscovered mineral resources, including uranium, because of its lithological and tectonic settings favourable for metal dissolution, transportation, and concentration in suitable sites.

Several major or significant mineral occurrences are known to exist. Among these are up to 33 massive sulphide deposits occurring within the Ordovician volcanic and sedimentary rocks of the Tetagouche Group in the northern part of the Anticlinorium (Bathurst-Newcastle Mining Camp). The largest of these is the Brunswick No. 12 orebody which contains proven reserves (as of December 1985) of 83 025 000 tonnes of 9.15% Zn, 3.73% Pb, 0.31% Cu, and 98 g/t Ag (Canadian Mines Handbook, 1986-1987). Pyrite, sphalerite, and galena are the main minerals.

In addition to these mines, several other occurrences are located in the anticlinorium and contain some combination

of Cu, Pb, Zn, W, Mo, Sn, Sb, Ag, Au, and U (Ruitenberg and Fyffe, 1982). These deposits include breccia fillings, fault controlled veins of various compositions, disseminations, greisen veins and stringers, magmatic deposits, etc. Many are associated spatially and temporally with the Acadian granitic rocks. Many have been either recently discovered or re-evaluated.

With regard to uranium deposits, only low grade occurrences are known to exist within the Miramichi Anticlinorium (Fig. 1). Most are associated with Acadian granitic plutons. The polymetallic vein-type deposits of the Long Lake area are the best known of these (Hassan and McAllister, 1988). They are related to hydrothermally altered and highly brecciated northwest-trending fractures crosscutting granites of the Lower Devonian North Pole Pluton. The uranium is commonly in chalcedony (jasperoid) veins and associated with significant amounts of other elements such as Cu, Pb, Zn, Mo, W, Sn, Ag, and Au (Fig. 1).

GENERAL GEOLOGY OF LONG LAKE AREA AND THE CENTRAL MIRAMICHI ANTICLINORIUM AREA

Long Lake Area

Overview

The Long Lake area (Fig. 3) is underlain by polydeformed Cambro-Ordovician metasedimentary rocks intruded by a pre-Acadian Ordovician felsic pluton and Acadian, Lower Devonian felsic and mafic plutons. The North Pole Pluton comprises the youngest granitic rocks in the Long Lake area.

The stratified rocks have been thermally metamorphosed in a zone up to 2 km wide around their contact with the North Pole Pluton, to an alkali feldspar-cordierite-andalusite-biotite-muscovite hornfels (Fyffe and Pronk, 1985).

The older rocks (Precambrian?) exposed in the Long Lake area belong to the Trousers Lake Complex (Fig. 3), in which two units were identified by Fyffe and Pronk (1985). The younger unit outcrops in the southwestern part of the map area and is composed in general of psammite and interbedded pelite. The older unit is located in the northeastern part of the map area and is composed of amphibolite and granitic gneiss.

The high grade metamorphic rocks of the Trousers Lake Complex are covered by lower grade Cambro-Ordovician rocks comprised of quartz sandstone intercalated with phyllite (Fyffe and Pronk, 1985). The sandstone contains 60 to 85% quartz, 15 to 40% chlorite and mica. The mica is mostly sericite with minor biotite and muscovite. The phyllite is comprised of sericite and chlorite (Crouse, 1977).

The deformed granite (Ordovician) that outcrops in the northeastern corner of the map area (Fig. 3), is concordant with the Cambro-Ordovician rocks and has a foliation parallel to their trends (i.e., northwest to north-northwest). It is mainly pink, equigranular, and medium grained. Recrystallized phases of the granite contain crystals of perthite and plagioclase up to 4 mm in diameter embedded in a finer matrix of quartz and biotite (Fyffe and Pronk, 1985). The deformed granite contains abundant roof pendants of Cambro-Ordovician rocks.

In the northwestern corner of the map area (Fig. 3), a mafic mass mapped by Fyffe and Pronk (1985) as part of the Devonian Redstone Mountain Pluton, is exposed. This mass is composed mostly of olivine gabbro (Fyffe and Pronk, 1985).

Geology of North Pole Pluton

Uranium and associated metals in the Long Lake area are spatially, temporally, and possibly genetically associated with the North Pole Pluton (Fig. 3) which is a posttectonic, peraluminous granite that intrudes the Cambro-Ordovician rocks discordantly (Fyffe and Pronk, 1985). Chemically and texturally, the North Pole Pluton is similar to the Pokiok Batholith of New Brunswick and the South Mountain Batholith of Nova Scotia (Fyffe and Pronk, 1985). The Pokiok Batholith lies adjacent to uraniferous stibnite-bearing quartz veins in the Silurian metasedimentary rocks of the Lake George antimony mine. The South Mountain Batholith hosts Sn-U deposits.

Recent mapping by Fyffe and Pronk (1985) indicates that the North Pole Pluton is divided into three phases; quartz-feldspar porphyry (youngest), biotite-muscovite granite, and biotite granite (oldest), and the following descriptions are from their paper.

Biotite granite

The biotite granite (Fig. 3) constitutes most of the pluton. It is generally pink and contains coarse grained, equigranular crystals of quartz, alkali feldspar, and plagioclase in equal proportion. Biotite forms 1 to 2% of the rock. The alkali feldspar is an orthoclase perthite containing domains of microcline. The plagioclase is altered to sericite and epidote; biotite is partly altered to chlorite.

Biotite-muscovite granite

The biotite-muscovite granite (Fig. 3) is second in areal extent and intrudes the biotite granite. The biotite and muscovite together account for 3 to 5% of the rock. The equigranular two-mica granite occurs predominantly in the western side of Long Lake and is identified by its medium grain size and light-grey to light-pink color. In addition to mica, the granite contains 25 to 35% quartz, 30% plagioclase, 15 to 20% potassium feldspar, and 5% chlorite (altered from biotite). Sphene, apatite, epidote, and opaque minerals are present as accessories.

Two-mica granites are recognized by a number of geologists for their metallogenic specialization in U, Sn, Mo, Be, Li, and F mineralization. The U-producing Hercynian granite of Massif Central, France is the best example of two-mica granites (Moreau, 1976).

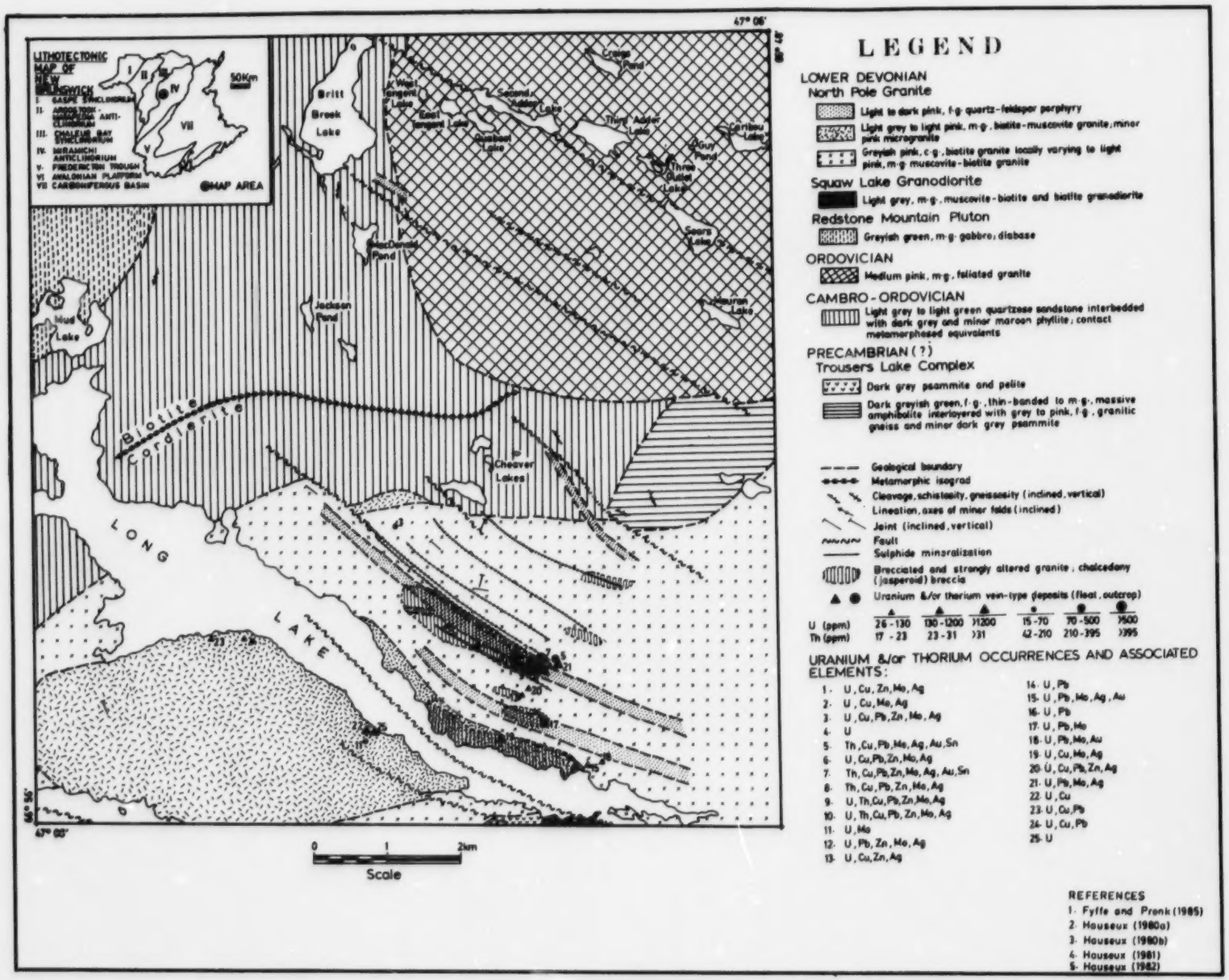
LITHOTECTONIC MAP OF NEW BRUNSWICK
I GASPE SYNCLINORIUM
II ACADIAN-MIRAMICHI ANTICLINORIUM
III CHALEUR BAY SYNCLINORIUM
IV MIRAMICHI ANTICLINORIUM
V FREDERICTON TROUGH
VI AVALONIAN PLATFORM
VII CARBONIFEROUS BASIN
50Km
MAP AREA
47° 05'
66° 55'
Britt Brook Lake
West Tetagouche Lake
East Tetagouche Lake
Second Adder Lake
Third Adder Lake
Quetbaut Lake
Three Outlet Lake
Sears Lake
Caribou Lake
Crimp Pond
Guy Pond
MacDonald Pond
Jackson Pond
Mud Lake
Jacquet Lake
Biotite
Cordierite
Cheaver Lakes
LONG
LAKE
0 1 2km
Scale
LEGEND
LOWER DEVONIAN
North Pole Granite
Light to dark pink, f-g quartz-feldspar porphyry
Light grey to light pink, m-g, biotite-muscovite granite, minor pink microgranite
Greyish pink, c-g, biotite granite locally varying to light pink, m-g muscovite-biotite granite
Squaw Lake Granodiorite
Light grey, m-g, muscovite-biotite and biotite granodiorite
Redstone Mountain Pluton
Greyish green, m-g gabbro; diabase
ORDOVICIAN
Medium pink, m-g, foliated granite
CAMBRO-ORDOVICIAN
Light grey to light green quartzose sandstone interbedded with dark grey and minor maroon phyllite; contact metamorphosed equivalents
PRECAMBRIAN (?)
Trousers Lake Complex
Dark grey psammite and pelite
Dark greyish green, f-g, thin-banded to m-g, massive amphibolite interlayered with grey to pink, f-g, granitic gneiss and minor dark grey psammite
Geological boundary
Metamorphic isograd
Cleavage, schistosity, gneissosity (inclined, vertical)
Lineation, axes of minor folds (inclined)
Joint (inclined, vertical)
Fault
Sulphide mineralization
Brecciated and strongly altered granite; chalcedony (jasperoid) breccia
Uranium &/or thorium vein-type deposits (float, outcrop)
U (ppm) 26-130 130-1200 >1200 15-70 70-500 >500
Th (ppm) 17-23 23-31 >31 42-210 210-395 >395
URANIUM &/or THORIUM OCCURRENCES AND ASSOCIATED ELEMENTS:
1. U, Cu, Zn, Mo, Ag
2. U, Cu, Mo, Ag
3. U, Cu, Pb, Zn, Mo, Ag
4. U
5. Th, Cu, Pb, Mo, Ag, Au, Sn
6. U, Cu, Pb, Zn, Mo, Ag
7. Th, Cu, Pb, Zn, Mo, Ag, Au, Sn
8. Th, Cu, Pb, Zn, Mo, Ag
9. U, Th, Cu, Pb, Zn, Mo, Ag
10. U, Th, Cu, Pb, Zn, Mo, Ag
11. U, Mo
12. U, Pb, Zn, Mo, Ag
13. U, Cu, Zn, Ag
14. U, Pb
15. U, Pb, Mo, Ag, Au
16. U, Pb
17. U, Pb, Mo
18. U, Pb, Mo, Au
19. U, Cu, Mo, Ag
20. U, Cu, Pb, Zn, Ag
21. U, Pb, Mo, Ag
22. U, Cu
23. U, Cu, Pb
24. U, Cu, Pb
25. U
REFERENCES
1. Fyffe and Pronk (1985)
2. Houseux (1980a)
3. Houseux (1980b)
4. Houseux (1981)
5. Houseux (1982)

Figure 3. Generalized geology and uranium occurrences, Long Lake area.

Quartz-feldspar porphyry

The quartz-feldspar porphyry (Fig. 3) occurs as dykes intruding the biotite granite. The dykes, located mainly in the eastern side of Long Lake, trend northwesterly, parallel to the 120° trending joints in the biotite granite. The phenocrysts consist of plagioclase, quartz, orthoclase, and minor biotite. The phenocrysts are about 2 mm in diameter, constitute about 50% of the rock and are embedded in a matrix of quartzo-feldspathic material. The plagioclase phenocrysts are almost entirely altered to sericite. Orthoclase is partially replaced by calcite. Biotite is completely altered to chlorite. Miarolitic cavities have been observed in these dykes.

The quartz-feldspar porphyry is extensively altered by hydrothermal solutions. Fresh varieties are pink whereas the altered varieties are greenish grey.

Age of North Pole Pluton

Samples taken for age determination suggest that the granitic phases have been intruded over a relatively short period of time. Rubidium-strontium ages of 378 ± 7 Ma are assigned to them by Fyffe et al. (1981). A K-Ar age determination on biotite from the granite taken from a drill hole gave an age of 391 ± 14 Ma (Hauseux, 1980b). This age agrees, within the limits of error, with the Rb-Sr age.

A K-Ar whole rock determination on the biotite-muscovite granite gave an age of 355 ± 18 Ma (Fyffe and Pronk, 1985). Fyffe and Pronk referred this age to the cooling stage of the granite. A Rb-Sr determination on muscovite granite from a drill hole yielded an age of 408 Ma (Hauseux, 1982) which Fyffe and Pronk (1985) believed to represent the age of crystallization of the granite.

A K-Ar whole rock determination on samples from the quartz-feldspar porphyry gave an age of 337 ± 17 Ma (Fyffe and Pronk, 1985). This age contradicts the Rb-Sr age determination (278 Ma, Hauseux, 1982) on mineral separates from an altered sample of the quartz-feldspar porphyry. Fyffe and Pronk (1985) related this contradiction to hydrothermal activity assumed to have operated on the granite after crystallization. It is also recognized that the quartz-feldspar porphyry may be much younger and related to a different magma source.

Depth of emplacement of North Pole Pluton

A rough estimate of the depth of emplacement for the North Pole Pluton was determined mainly from the stability fields of the mineral assemblages in the pluton and the country rocks. The first estimate was made on the basis of the presence of andalusite in the metamorphic aureole of the granite in the country rocks and indicates a depth of about 13 km below the surface (Holdaway, 1971). Recently, Fyffe (1982b) used primary muscovite for depth of emplacement estimation, using an empirical diagram given by Carmichael et al. (1974), in which a depth greater than 12 km is assumed for primary muscovite-bearing granites.

On the basis of the average normative quartz, orthoclase, and albite (Q-Or-Ab) ternary diagram of Tuttle and Bowen (1958), Fyffe and Pronk (1985) have concluded that the biotite granite crystallized at 1 kb PH_2O (Fig. 4) which suggests an emplacement at a depth of at least 3.5 km. The quartz-feldspar porphyry sample crystallized at 0.5 kb, which is equivalent to a depth of 2 km (Fig. 4). These variation in depth of emplacement between the biotite granite and the quartz-feldspar porphyry led Fyffe and Pronk (1985) to suggest that over a kilometre of overlying rocks were removed by erosion between the time of the biotite granite emplacement and the quartz-feldspar porphyry intrusion.

Geophysical modeling of the North Pole Pluton by using gravity data yields a value of 8 km as the probable thickness (Burke and Chandra, 1983). The model also reveals that the Cambro-Ordovician metasedimentary rocks covering the granite vary in thickness from 0 to 1 km.

On the basis of these studies it is suggested that the North Pole Pluton was emplaced at shallow depth in the crust (i.e., epizonal). These types of granitoids fracture easily and allow the hydrothermal fluids to escape along fracture systems to form ore deposits (Hosking, 1977).

Breccia zones of the North Pole Pluton

The most interesting structural features observed in the North Pole Pluton are the breccia zones, which were observed in several localities, particularly on the eastern side of Long Lake (Fig. 3; Hauseux, 1980a, 1982). As indicated from the map (Fig. 3) these zones are distinctly elongate in the northwest direction, near or along the northwest-trending shear zones. The majority of the polymetallic vein-type uranium mineralization zones are associated with these breccias which are characterized by their extensive hydrothermal alteration and by their content of chalcedony (usually jasperiod) veins, features typical of hydrothermal processes.

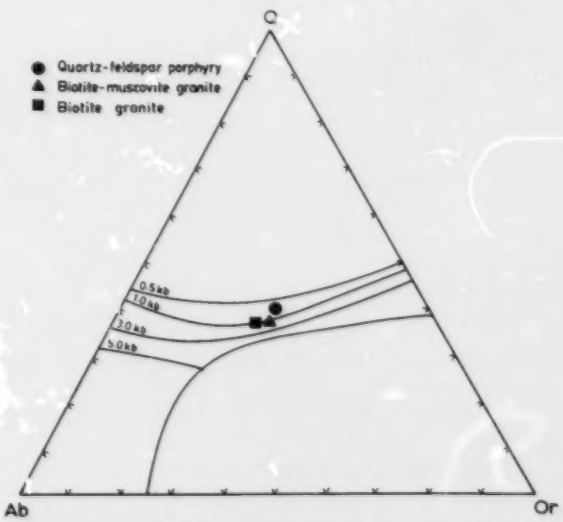

Figure 4. Q-Or-Ab ternary diagram for normative quartz, orthoclase, and albite in various phases of the North Pole Pluton (after Fyffe and Pronk, 1985).

The breccia zones of the Long Lake area contain angular granitic fragments of variable sizes (up to 1.5 cm), in which quartz, alkali feldspar and plagioclase are the essential constituents. The alkali feldspar and plagioclase fragments usually appear strongly strained and are crosscut by chalcedony filled fractures. The fine grained matrix is mostly of the same material, but also contains grains of sericite, biotite, and chlorite along with epidote grains which are sometimes associated with the chlorite.

Breccia pipes have long been considered excellent targets for mineral exploration in general and for uranium in particular (Kents, 1964; Sawkins, 1969; Fletcher, 1977; Simmons and Sawkins, 1983). In the Long Lake area both breccia faults and the host rock lithology of North Pole Pluton are possible major ore controls.

Brecciation is a characteristic feature of hydrothermal systems generated around felsic to intermediate igneous rocks emplaced at shallow depths in the crust (Sotnikov et al., 1974; Allman-Ward et al., 1982). Scherkenbach (1982) suggested that breccia occurs as a result of a sharp drop in P_{H_2O}. This sharp drop in pressure can take place when hot magmatic hydrothermal solutions at depth rise through fractures or faults to the surface. The breccias may also form by hydraulic ramming of residual fluids and magma during cooling of the granite (Lindsey and Fisher, 1985).

Another mechanism was proposed by Fisher (1976) during his study of vein-type uranium deposits in the Front Range, Colorado. There uranium is found in fault breccia systems. According to Fisher, breccia is generated whenever Laramide faulting is at a high angle to metamorphic foliation, and maximized at places where the intersection angle approaches 90°.

The mechanism responsible for the breccia generation east of Long Lake is not fully known at present. However, Fyffe and Pronk (1985) stated that brecciation may have occurred during release of silica-rich hydrothermal fluids into the fractures.

In the Long Lake area the trends of the breccia faults are parallel to the trends of the metamorphic foliation of the Cambro-Ordovician metasedimentary rocks (northwest to north-northwest), suggesting some support for the probability of the brecciation being produced more by the action of hydrothermal fluids than by the purely mechanical method described by Fisher (1976).

Wall rock alterations

Hauseux (1980a) has identified three episodes of hydrothermal and supergene alteration in the Long Lake area. The alterations are in general associated with highly fractured and brecciated zones, and are characterized by the following:

1. Sericite-chlorite-silica-pyrite
   The sericite-chlorite-silica-pyrite hydrothermal alteration is associated with northwesterly trending quartz-pyrite veining of the North Pole Pluton. This veining is believed to be the earlier of two stages of veining related to post-magmatic northwest-southeast faulting.
2. Kaolin-sericite-calcite (± fluorite)
   The kaolin-sericite-calcite hydrothermal alteration is associated with the later stage of northwesterly trending calcite-veining.
3. Fe-Mn-oxide staining
   The Fe-Mn staining occurred within the top 30 m of the weathered zone of the granite by supergene processes. It is the last episode of alteration that affected rocks in the area.

Mineralization related to the North Pole Pluton

Uranium- and sulphide-bearing silica (mostly jasperoid chalcedony) veins occur in at least four northwest-trending faults that intersect the North Pole Pluton (Fig. 3). The mineralization and associated alteration are most commonly concentrated in the fault breccia. Pyrite, chalcopyrite, sphalerite, galena, covellite, and molybdenite are the main sulphide minerals found (Hauseux, 1980a), along with small amounts of arsenopyrite, matildite, and native bismuth. Cassiterite and autunite-torbernite have been identified in float only. Uranium was also found in veins intersected in trenches and drill holes but no mineral identifications were made.

Mineralization in float samples was investigated by Gasparrini (1981), who identified uranium (a) in discrete grains, (b) in fracture fillings, and (c) diffused within the rocks.

Four phases of secondary uranium minerals were recognized by a microscope-electron microprobe study of two thin sections from medium grained muscovite granite float (Gasparrini, 1981). These phases are:

1. Uranium-phosphorous-copper:
The mineral of this compound is most abundant and identified as torbernite $Cu(PO_4)_2(UO_2)_2.8\text{-}12H_2O$. It is distributed among the rock-forming minerals of the granite.

2. Uranium-phosphorous-iron-copper compound:
The mineral of this compound was identified as iron torbernite (mixture of iron oxide and torbernite). The mineral forms platy crystals.

3. Iron-phosphorous compound with minor uranium:
The mineral of this compound was not identified. The mineral is very fine grained and it is deep red under transmitted light. It is distributed in fractures and dispersed through the rock.

4. Iron-uranium-phosphorous compound:
This unidentified mineral is less common than the above. It is opaque under transmitted light.

Chronological development of the North Pole Pluton metallogeny

Metallogenic developments of the North Pole Pluton and associated post-Precambrian geological events are illustrated in Figure 5. Sequential summary of these events is as follows:

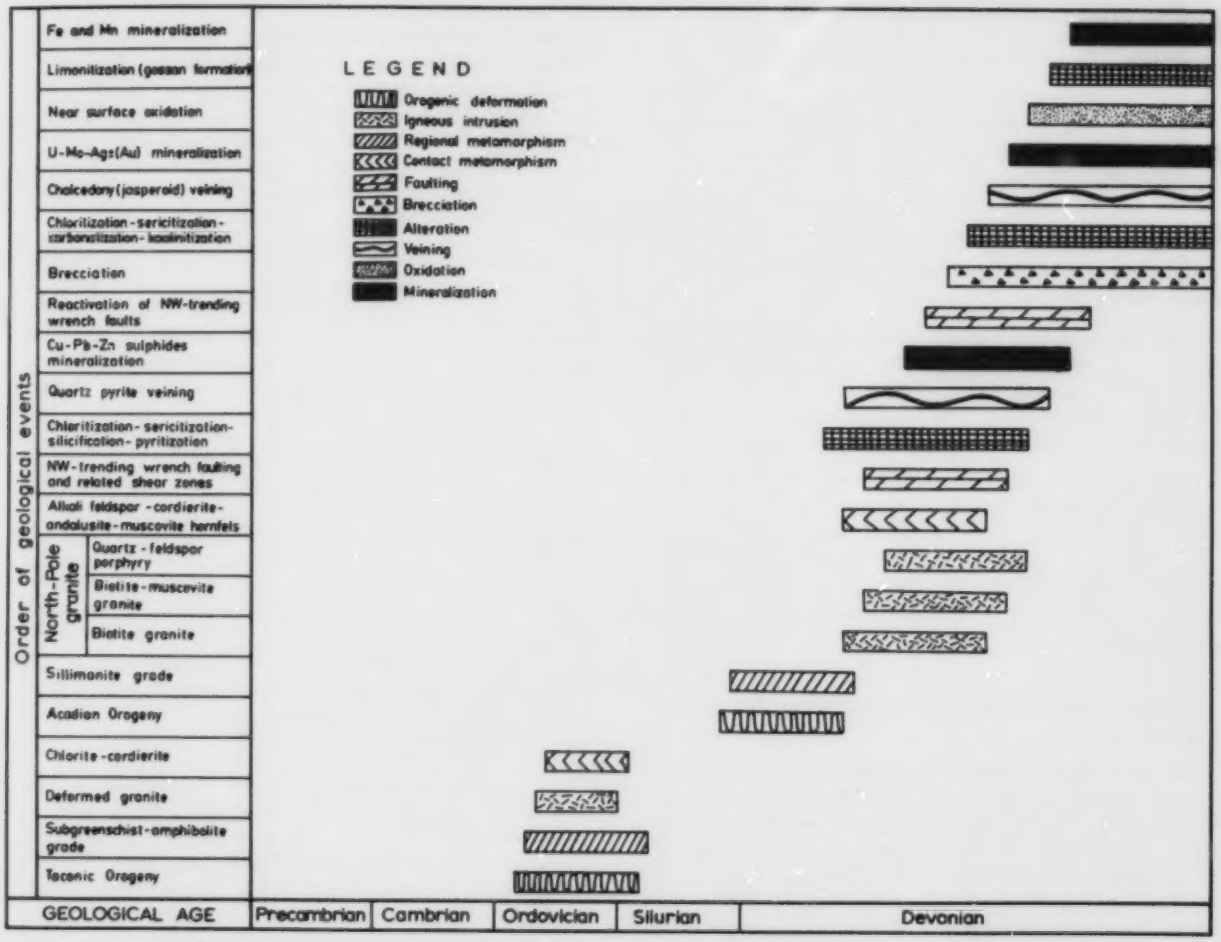

Figure 5. Geochronological sequence of metallogenic development in the Long Lake area.

1. Deposition of the Cambro-Ordovician sedimentary rocks in a paraplatformal environment.
2. During the Taconian Orogeny (480 Ma) the Cambro-Ordovician rocks were tightly folded, regionally metamorphosed (subgreenschist-amphibolite grade), intruded by granite, uplifted, and deeply eroded. Sedimentary rocks at contact with the granitic rocks were thermally metamorphosed to chlorite-cordierite grade.
3. During the Acadian Orogeny (400 Ma), the rocks underwent open-fold deformation along northeast axes.
4. North Pole Pluton was emplaced at this stage and metamorphosed the contact rocks to alkali feldspar-cordierite-andalusite-muscovite hornfels. The associated quartz-feldspar dykes are much younger but are assumed to be genetically related.
5. Northwest-trending wrench faults and associated shear zones were generated at the later stages of the Acadian Orogeny.
6. The rocks along these faults were hydrothermally metamorphosed giving rise to chloritization, sericitization, silicification, and pyritization which are the major alterations identified for this stage.
7. This process led to quartz-pyrite vein generation some of which was accompanied by Cu-Pb-Zn sulphides mineralization.
8. The northwest-trending wrench faults were reactivated and this event was accompanied by brecciation of the granitic rocks of North Pole Pluton along these faults. That brecciation was promoted by pulses of hydrothermal fluids is evidenced by the generation of a second episode of hydrothermal alteration (chloritization, sericitization, carbonatization, and kaolinitization) of the wall rocks. These events also produced chalcedony (jasperoid) veining.
9. At this stage there was further deposition of Cu-Zn-Pb sulphides; U-Mo-Ag ± (Au) minerals were added.
10. Supergene processes, aided by the action of meteoric waters near the surface, led to depletion of Fe and Mn from the rocks, and produced limonite staining.

Central Miramichi Anticlinorium area

Overview

The central Miramichi Anticlinorium area (Fig. 6) includes Cambro-Ordovician rocks of the Tetagouche Group comprising a thick sequence of metasedimentary and metavolcanic rocks which have undergone multiple deformation and metamorphism during their geological history.

The Tetagouche Group is in faulted contact with metasedimentary rocks of Silurian age in the eastern part of the map area (Fig. 6).

The stratified rocks of the central Miramichi area were intruded by both deformed (pretectonic) and undeformed (posttectonic), mainly felsic, plutons (Fig. 1). Most of the mineral occurrences in the area are spatially and perhaps genetically associated with the posttectonic granitic plutons.

The Cambro-Ordovician sedimentary rocks in the study area were regionally metamorphosed to the lower greenschist facies. At the contact with the plutons, the sedimentary rocks were thermally metamorphosed to biotite and cordierite grade (Fig. 6). The cordierite zone is about 300 to 700 m wide, whereas the biotite zone is about 1500 m to 3000 m wide.

Geology of central Miramichi Anticlinorium posttectonic plutons

Four major granitic plutons of Middle Devonian age are known to intrude rocks of the area (Fig. 6). These plutons are: Burnthill, Dungarvon, Trout Brook, and Rocky Brook. Although several investigators (i.e., Poole, 1963; Irrinki, 1979; Crouse, 1981; Taylor et al., 1987) have dealt with them as separate plutons, recent mapping by staff of the New Brunswick Department of Natural Resources and Energy (Fyffe and MacLellan, 1988) suggests that they are similar in mineralogy, texture, and perhaps geological age. They also have similar metal associations such as Sn, Mo, W, and U. Therefore, these plutons may have been derived from a single magmatic chamber and it is possible they join at depth as a large batholith (Crocco, 1975).

The granitic plutons have been ascribed to be post-orogenic (Fyffe et al., 1981). They are formed late in the tectonomagmatic sequence and are typical of high level intrusions in that they have sharp, strongly discordant contacts with the country rocks. The high level intrusion is also evidenced by their granophyric and miarolitic textures as well as their moderate to low grade metamorphic aureoles. The chemical and mineralogical variations of different phases of the plutons are characteristics of low pressure and minimum temperature melt composition (Taylor et al., 1987). The miarolitic cavities are believed to be formed as a result of late H_2O saturation of an initially undersaturated magma.

The granitic plutons are intersected by several phases of dykes and veins. The veins are thought to form as a result of fluids introduced by the plutons themselves during early postmagmatic stages (MacLellan et al., 1986).

The four plutons (Fig. 6), of which Burnthill Pluton is the largest, are high-silica granites (Gardiner and Garnett, 1986; MacLellan et al., 1986). They comprise two major phases: equigranular granite and porphyritic granite, and two minor phases: microgranite (with associated aplite dykes and pegmatite pods) and biotite melanocratic granite. Both major phases are cut by younger microgranite, aplite, and pegmatite. The contacts between the two major phases are gradational to sharp.

Despite the variation in textures, the chemical composition of the two major phases is comparable. This indicates, according to MacLellan et al. (1986) that these phases may have crystallized from a single, zoned magma chamber that has undergone a complex cooling history involving localized remobilization of the magma. Textural variation may suggest a multiple intrusion history.

It appears, as shown in Figure 6, that the porphyritic granite is predominantly in the northern part of the plutons whereas the equigranular granite is common in the southern parts. MacLellan et al. (1986) have attributed this to variation in temperatures of crystallization which decreased from north to south, and suggested that this variation in temperature and pressure between the two main textural phases led to the accumulation of a higher amount of fluids in the equigranular granite relative to the porphyritic granite at late stage crystallization. This may explain the intense hydrothermal alteration and mineralization within the equigranular granite.

The late stage microgranite and asscciated aplite dykes and pegmatite pods that are commonly found cutting all other phases of the plutons are believed to be derived from the porphyritic granite (MacLellan et al., 1986). It is also believed that they were generated by local perturbations of fluid concentrations and thermal conditions within the magma chamber. Pockets of phenocryst-bearing, late crystallizing magmas were later tapped by brittle fractures developed during cooling.

The four phases indicated above are more or less chemically, texturally, and mineralogically similar within different plutons. For this reason and for simplicity the following general descriptions of the different phases are given, from older to younger, without referring to the plutons unless there is significant variation in a phase within an individual pluton.

Melanocratic biotite granite

The melanocratic biotite granite occurs in all the plutons and forms about 10% of their total outcrop area (Fig. 6). It is characterized by its high biotite content (up to 20%), coarse K-feldspar phenocrysts and by sparsely developed euhedral plagioclase and quartz phenocrysts (Gardiner and Garnett, 1986; MacLellan et al., 1986; Taylor et al., 1987).

The porphyritic melanocratic granite is thought to be roof pendants, but the lack of a similar rock type in the country rocks may suggest that this unit is a remnant of an early magmatic phase (MacLellan et al., 1986).

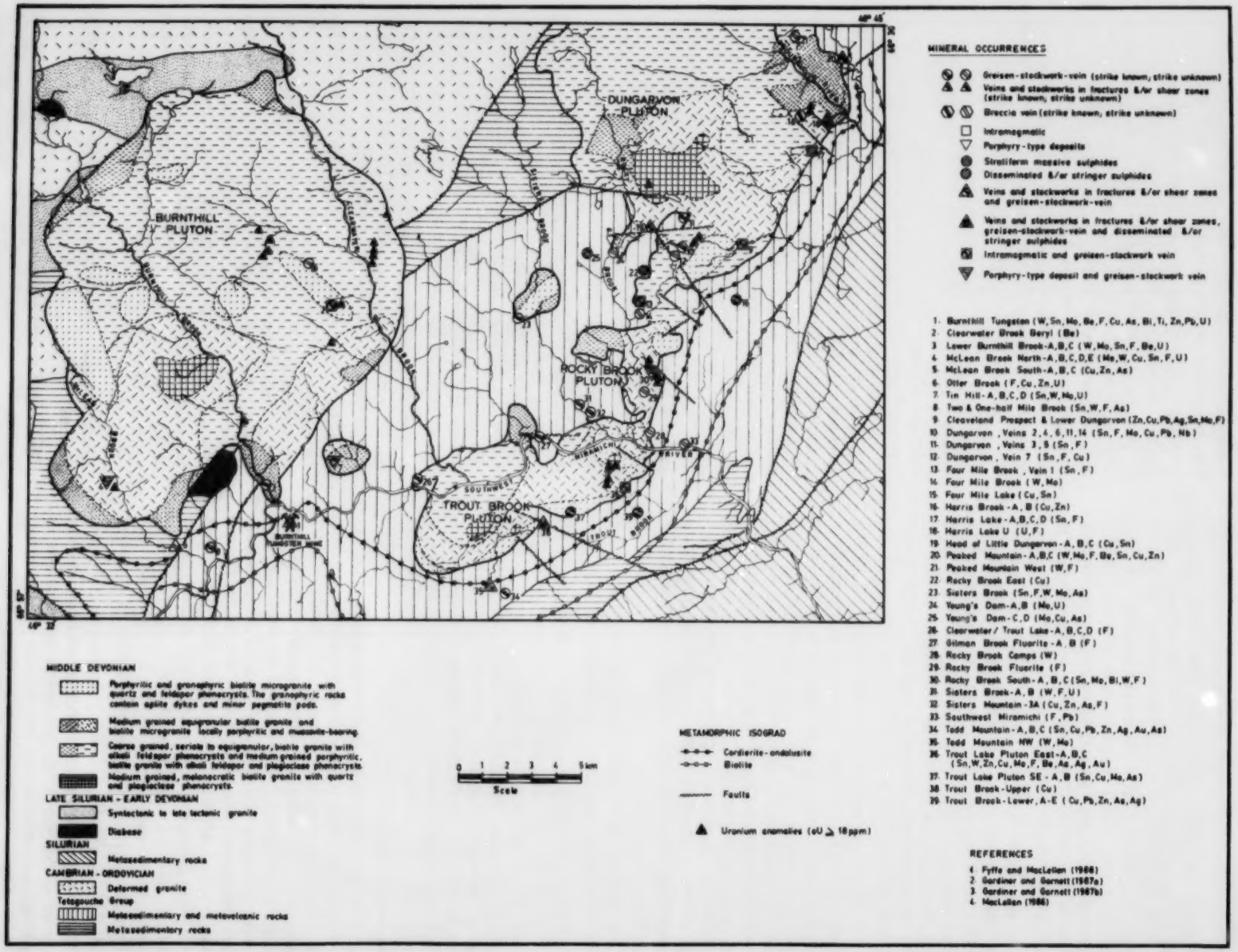
DUNGARVON PLUTON
BURNTHILL PLUTON
ROCKY BROOK PLUTON
TROUT BROOK PLUTON
MINERAL OCCURRENCES
Greisen-stockwork-vein (strike known; strike unknown)
Veins and stockworks in fractures &/or shear zones (strike known, strike unknown)
Breccia vein (strike known; strike unknown)
Intramagmatic
Porphyry-type deposits
Stratiform massive sulphides
Disseminated &/or stringer sulphides
Veins and stockworks in fractures &/or shear zones and greisen-stockwork-vein
Veins and stockworks in fractures &/or shear zones, greisen-stockwork-vein and disseminated &/or stringer sulphides
Intramagmatic and greisen-stockwork vein
Porphyry-type deposit and greisen-stockwork vein
1- Burnthill Tungsten (W,Sn,Mo,Be,F,Cu,As,Bi,Ti,Zn,Pb,U)
2- Clearwater Brook Beryl (Be)
3 Lower Burnthill Brook-A,B,C (W,Mo,Sn,F,Be,U)
4- McLean Brook North-A,B,C,D,E (Mo,W,Cu,Sn,F,U)
5- McLean Brook South-A,B,C (Cu,Zn,As)
6- Otter Brook (F,Cu,Zn,U)
7- Tin Hill-A,B,C,D (Sn,W,Mo,U)
8- Two & One-half Mile Brook (Sn,W,F,As)
9- Cleaveland Prospect & Lower Dungarvon (Zn,Cu,Pb,Ag,Sn,Mo,F)
10- Dungarvon, Veins 2,4,6,11,14 (Sn,F,Mo,Cu,Pb,Nb)
11- Dungarvon, Veins 3,5 (Sn,F)
12- Dungarvon, Vein 7 (Sn,F,Cu)
13- Four Mile Brook, Vein 1 (Sn,F)
14- Four Mile Brook (W,Mo)
15- Four Mile Lake (Cu,Sn)
16- Harris Brook-A,B (Cu,Zn)
17- Harris Lake-A,B,C,D (Sn,F)
18- Harris Lake U (U,F)
19- Head of Little Dungarvon-A,B,C (Cu,Sn)
20- Peaked Mountain-A,B,C (W,Mo,F,Be,Sn,Cu,Zn)
21- Peaked Mountain West (W,F)
22- Rocky Brook East (Cu)
23- Sisters Brook (Sn,F,W,Mo,As)
24- Young's Dam-A,B (Mo,U)
25- Young's Dam-C,D (Mo,Cu,As)
26- Clearwater/Trout Lake-A,B,C,D (F)
27- Gilman Brook Fluorite-A,B (F)
28- Rocky Brook Camps (W)
29- Rocky Brook Fluorite (F)
30- Rocky Brook South-A,B,C (Sn,Mo,Bi,W,F)
31- Sisters Brook-A,B (W,F,U)
32- Sisters Mountain-3A (Cu,Zn,As,F)
33- Southwest Miramichi (F,Pb)
34- Todd Mountain-A,B,C (Sn,Cu,Pb,Zn,Ag,Au,As)
35- Todd Mountain NW (W,Mo)
36- Trout Lake Pluton East-A,B,C (Sn,W,Zn,Cu,Mo,F,Be,As,Ag,Au)
37- Trout Lake Pluton SE-A,B (Sn,Cu,Mo,As)
38 Trout Brook-Upper (Cu)
39- Trout Brook-Lower,A-E (Cu,Pb,Zn,As,Ag)
REFERENCES
1. Fyffe and MacLellan (1988)
2. Gardiner and Garnett (1987a)
3. Gardiner and Garnett (1987b)
4. MacLellan (1986)
MIDDLE DEVONIAN
Porphyritic and granophyric biotite microgranite with quartz and feldspar phenocrysts. The granophyric rocks contain aplite dykes and minor pegmatite pods.
Medium grained equigranular biotite granite and biotite microgranite locally porphyritic and muscovite-bearing
Coarse grained, seriate to equigranular, biotite granite with albali feldspar phenocrysts and medium grained porphyritic, biotite granite with albali feldspar and plagioclase phenocrysts
Medium grained, melanocratic biotite granite with quartz and plagioclase phenocrysts.
LATE SILURIAN - EARLY DEVONIAN
Syntectonic to late tectonic granite
Diabase
SILURIAN
Metasedimentary rocks
CAMBRIAN - ORDOVICIAN
Deformed granite
Tetagouche Group
Metasedimentary and metavolcanic rocks
Metasedimentary rocks
METAMORPHIC ISOGRAD
Cordierite-andalusite
Biotite
Faults
Uranium anomalies (eU ≥ 18 ppm)
0 1 2 3 4 5 km
Scale

Figure 6. Generalized geology and uranium occurrences of the granitic plutons, central Miramichi Anticlinorium.

Porphyritic granite

The porphyritic granite is the main phase of the plutons (Fig. 6) as it covers about 50% of the exposed area. Although the dominant texture exhibited by this unit is porphyritic, seriate and equigranular textures are also common. Poole (1963) described it as pink and coarse grained, with subequal amounts of quartz, plagioclase and alkali feldspar (perthite) and with about 5 to 10% biotite. Rapakivi textures are common.

At the border with the country rocks, fine grained porphyritic granite appears and is believed by MacLellan et al. (1986) to be a chilled equivalent to the main phase. This fine grained porphyritic granite is cut by numerous dykes of aplite and porphyritic microgranite (MacLellan and Taylor, 1989). Xenoliths and schlieren of oriented feldspar phenocrysts occur.

Petrographic examination of rock samples from this phase (Laanela, 1980) reveals that it consists essentially of subhedral, tabular crystals of plagioclase, embedded in an interlocking mosaic of quartz and K-feldspar anhedra. Biotite flakes are scattered throughout the rock but only accessory amounts of muscovite are present. Quartz forms irregularly shaped anhedra, of variable size, that range from unstrained to moderately strained in appearance. The plagioclase is unzoned to faintly zoned, with a composition of about An_{12}. The plagioclase crystals are partly altered to sericite.

The K-feldspar is highly perthitic, occurs as large subhedral crystals, and appears to be fresh.

Biotite crystals are irregularly shaped, deep-brown, and characterized by the presence of dark, pleochroic haloes around zircon inclusions. In addition to zircon, other accessory minerals identified are apatite and magnetite. Evidence for deuteric activity in the rock sample is indicated by sericitization and muscovitization of plagioclase, and chloritization of biotite.

Equigranular granite

The equigranular granite is second in abundance within the plutons (Fig. 6), and it is more or less confined to the south and southeastern parts of each body. It is of two textural varieties, one is medium grained and the other is fine grained (microgranite). The contacts between the equigranular granite and the porphyritic granite are gradational. A few phenocrysts of quartz (up to 8 mm) and of feldspar (up to 1 cm) are developed locally (MacLellan et al., 1986). In the Trout Brook Pluton the equigranular granite contains muscovite (Gardiner and Garnett, 1986) in proximity to known greisen veins. The muscovite is therefore believed to be of secondary origin. Miarolitic cavities, either open or filled with fluorite, are common.

Xenoliths, schlieren, and oriented feldspars that are observed in the porphyritic granites described above are absent in this unit.

Petrographic examination of samples from this phase (Laanela, 1980) indicates that it is composed essentially of an interlocking mosaic of quartz, plagioclase, and K-feldspar anhedra through which are scattered occasional flakes of muscovite and accessory amounts of biotite.

Quartz occurs in irregularly shaped anhedra which have a slight to moderate strained appearance. Plagioclase usually forms equidimensional anhedra and it is typically unzoned with a composition of about An_{12}. K-feldspar crystals in the rock are also more or less equidimensional and many are very finely perthitic. In addition to the primary muscovite noted above, primary muscovite also exists. Accessory zircon is rare and usually forms as tiny inclusions within biotite.

Microgranite and associated aplite dykes and minor pegmatite pods

These rocks are the youngest in the plutons and formed late during magma crystallization (Gardiner and Garnett, 1986; MacLellan et al., 1986). They include porphyritic and granophyric biotite microgranite and several generations of aplitic dykes, veins and pods, and sparse pegmatitic pods. Textures are highly variable. The phenocrysts have various sizes and shapes and the groundmass-to-phenocrysts ratio is inconsistent. The phenocrysts range in size from 1 to 25 mm for feldspars, 1 to 6 mm for quartz and 1 to 5 mm for biotite and their proportion varies from 5 to 40% of the rock. The shape of the phenocrysts varies from euhedral to anhedral (MacLellan et al., 1986). The grain size of the groundmass is less than 1 mm.

Age of the granitic plutons

A wide range of K-Ar mineral ages and Rb-Sr whole rock ages have been obtained for the granitic plutons. Most of the age determinations were carried out on the Burnthill Pluton, but the strong similarities in chemical composition, mineralogy, and texture among Burnthill and the other plutons (i.e., Dungarvon, Trout Brook, and Rocky Brook plutons) suggest that they may have similar ages as well.

Potter (1969) reported K-Ar ages of 400, 382, and 377 Ma for hydrothermal muscovite and 346 Ma for biotite in granite from the Burnthill Tungsten Mine.

Recently, MacLellan et al. (1986) have carried out age determination on muscovite separates of various phases of the Burnthill Pluton. Their determinations indicate an age of 379 ± 4 Ma for late stage magmatic activity and 383 ± 3 Ma and 379 ± 3 Ma for hydrothermal alteration activities at Burnthill Tungsten Mine. These are generally in agreement with the results obtained earlier by Potter. On this basis, MacLellan et al. (1986) and later Taylor et al. (1987) have assigned a tentative age of 380 ± 5 Ma (Middle Devonian) to the Burnthill Pluton and mineral deposits related to it.

Depth of emplacement of the central Miramichi granitic plutons

The mineral assemblages (cordierite and andalusite) in the contact thermal aureoles of the granitic plutons of the central Miramichi Anticlinorium (Fig. 6) are indicative of high level (i.e., epizonal) granitoids according to criteria

proposed by Hutchison (1977). Hutchison has investigated the granitoids of the Malaysian Peninsula and found that epizonal granitoids emplaced into sedimentary or metasedimentary rocks are characterized by wide contact thermal aureoles (up to 3 km) which contain cordierite and andalusite. On the basis of the mineral assemblage in the contact aureole, MacLellan et al. (1986) have also suggested that the Burnthill Pluton is a high level granitoid.

By using the normative quartz-orthoclase-albite (Q-Or-Ab) ternary diagram of Tuttle and Bowen (1958) for the fresh rock samples of the Burnthill Pluton (Fig. 7) it is possible to determine to some extent the depth of emplacement of the Burnthill Pluton. With the exception of the melanocratic biotite granite phase of the pluton, the other three younger phases fall well within the 0.5 kb to 1 kb range cotectic contours which is equivalent to a depth of 2 to 3 km. The melanocratic biotite granite phase falls on the 3 kb cotectic contour which is equivalent to a depth of nearly 9 km. This depth of emplacement for the melanocratic biotite granite may support the opinion of MacLellan et al. (1986) that this phase represents a remnant of an early magmatic phase.

The geological features (miarolitic cavities, rapakivi texture, and granophyre aplites) associated with the three younger phases of the pluton also suggest that they have been emplaced at shallow depths.

Structural control of veins and late stage dykes

The posttectonic Middle Devonian granitic plutons (Burnthill, Dungarvon, Trout Brook, and Rocky Brook) exhibit at least two sets of joints (Butler, 1980). One set strikes northwesterly at about 310° and dips 75° southwest. The other strikes northeasterly at 35° and dips 82° southeast. The northwest-trending set forms the main conduit for hydrothermal fluids in the plutons and contains most of the

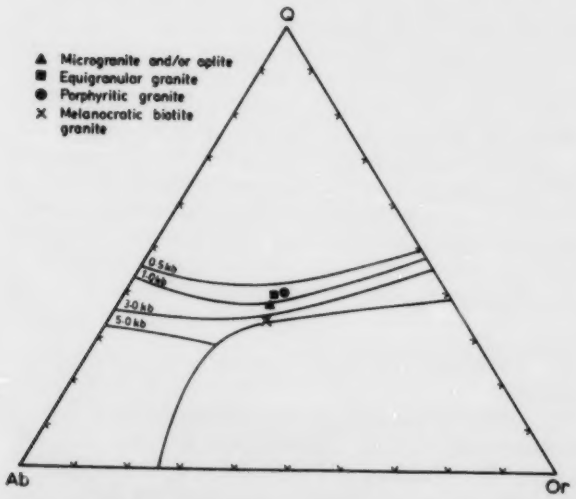

Figure 7. Q-Or-Ab ternary diagram for normative quartz, orthoclase and albite in various phases of the Burnthill Pluton (Diagram after Tuttle and Bowen, 1958).

significant mineral deposits. However, similar mineralization, along the northeast-trending joints, especially in the Trout Lake granite suggests that the two sets of joints may have formed contemporaneously as a conjugate set, with the more productive northwesterly set perpendicular to the extension direction.

A minor set of east-trending fractures is also noticed in the Burnthill Pluton by Butler (1980). This set is suspected to be related to late movement on the Catamaran Fault (Fig. 1).

Mitton (1985) identified different generations of quartz veins, some containing cassiterite, in drill core samples taken from the Dungarvon Pluton. Most were trending 130° which is comparable to those identified in the Burnthill Pluton. Several feldspar veins also were identified in the granitic plutons. They have sharp contact with the host granites and some contain cassiterite (Mitton, 1985).

Aplite dykes and veins (up to 1 m thick) are common especially in hydrothermal alteration zones (Gardiner, 1985), and strike in all directions (MacLellan and Taylor, 1989), but in general they follow three preferred orientations (north, east, and southeast). The aplites formed from the differentiation products of the granite itself. This implies that the joints they occupy were generated when the magma was not entirely crystallized. Mitton (1985) reported as high as 600 ppm Sn in one sample taken from an aplite vein in the Burnthill Pluton.

Wall rock alterations

The posttectonic granitic plutons of the area have undergone extensive hydrothermal alteration of various types as a result of late stage hydrothermal solutions introduced from a final water-rich fluid differentiate (MacLellan et al., 1986). These wall rock alterations are well developed along veined fractures and are characterized by colouring and mineralogical changes marginal to a central quartz vein. Most of the significant mineralization of Sn, W, Mo, and probably U took place at the time of alteration.

The major hydrothermal alteration processes and products as recognized by several investigators are given in Table 1. Of these processes greisenization is the most important. Alteration envelopes containing muscovite ± fluorite ± topaz are well developed within the plutons and most of the Sn, Mo, and W, is typically concentrated during this process. Uranium was probably also redistributed at this stage.

Pagel (1981) has investigated the greisenization processes operative on granitic rocks from Brittany and Cornwall (quoted after Dubessy et al., 1987) and concluded that greisenization is an uranium-conservative process. In contrast, Simpson et al. (1979) concluded that in Cornwall uranium is lost during greisenization. However, despite this contradiction in behaviour during greisenization, the hydrothermal processes are undoubtedly key factors in uranium and certain other metal mineralization.

Mineralization related to the granitic plutons

The Burnthill W-Sn-Mo veins (Fig. 6) occur in the retrograde chlorite aureole 200 m above the contact of the Burnthill Pluton (Fyffe and MacLellan, 1988). The mineralization consists of wolframite, cassiterite, molybdenite, arsenopyrite, pyrite, pyrrhotite, sphalerite, galena, chalcopyrite, native bismuth, scheelite, beryl, anatase, and topaz (Potter, 1969). It occurs within northwesterly (300°) trending greisenized quartz veins (Fyffe and MacLellan, 1988), which range from 1 cm to 2 m in width.

Recent mineral exploration in the area has identified several new occurrences of W-Mo-Sn mineralization that are, like the Burnthill deposit, spatially associated with the granitic plutons (MacLellan et al., 1986; Bourque, 1984). Most occur as greisen veins. They include the McLean Brook South, McLean Brook North, and Tin Hill prospects, all situated along the southwestern part of the Burnthill Pluton, and the Peaked Mountain stockwork zone of quartz veins located close to the eastern margin of the Dungarvon Pluton (Fig. 6). These new discoveries suggest that there exists a widespread potential for the occurrence of W-Sn-Mo mineralization of both endogranite (McLean Brook North and Tin Hill) and exogranitic (McLean Brook South and Tin Hill) types (Taylor et al., 1987).

Mineral occurrences of W, Mo, Sn, and U of different types and styles of deposition were observed in the granitic plutons. Brief descriptions of these occurrences and their geological characteristics are given in Appendix II.

Table 1. Various types and products of hydrothermal alterations identified in the granitic plutons of central Miramichi Anticlinorium.

Original mineral	Alteration process	Mineralogical changes	Chemical changes
Biotite and Feldspars	Greisenization	- K-feldspar - plagioclase - biotite + quartz + mica	- Na_2O + SiO_2 + Al_2O_3
Feldspars and Biotite	Sericitization	- K-feldspar - plagioclase - biotite + sericite	- CaO - K_2O
Biotite	Chloritization	- biotite + chlorite	+ FeO + MgO - K_2O
Feldspars	Albitization	- K-feldspar - Ca-plagioclase + albite	- K_2O + Na_2O
Feldspars	Muscovitization	- K-feldspar - plagioclase - biotite + muscovite	- K_2O
Iron silicates and magnetite	Hematitization	+ hematite	+ FeO

N.B. positive signs indicate substances added whereas negative signs indicate substances subtracted from the system.

REVIEW OF GEOCHEMICAL AND GEOPHYSICAL SURVEYS FOR URANIUM AND OTHER METALS IN THE LONG LAKE AREA AND THE CENTRAL MIRAMICHI ANTICLINORIUM AREA

Overview

Extensive reconnaissance along with detailed geochemical and geophysical surveys were carried out in the Long Lake area and in the central Miramichi Anticlinorium area. These surveys were conducted by several private and governmental exploration organizations in order to trace the source(s) of anomalous quantities of uranium and base metal sulphides previously detected in the area by means of airborne gamma ray spectrometry and routine stream sediment sampling.

Gravity and magnetic geophysical data presented here cannot provide direct evidence for uranium mineralization in the study areas. However, they are able to outline granites known to be enriched with uranium and other metals such as Sn, Mo, and W. For instance, Simpson and Plant (1984) and Plant et al. (1980) have indicated that 'mineralized' granites, such as the Cornubian Batholith of Britain, have a large negative gravity anomaly (>-40 mgals) and a low, poorly defined aeromagnetic anomaly. Similar geophysical anomalies characterize other 'mineralized' granites such as the South Mountain Batholith of Nova Scotia (Chatterjee and Muecke, 1982). Furthermore, granitic-types (i.e., A-, S-, or I-types) that are associated with specific types of minerals (for example U and Sn with S- and A-type granitoids) can be distinguished, to some extent, on the basis of their gravity and magnetic response.

Long Lake area

Geophysical surveys

Gravity

The gravity data over Long Lake area (Fig. 8) indicate a strong negative anomaly (>-48 mgals) over the North Pole Pluton. The centre of this gravity low coincides with the area where brecciation, hydrothermal alteration, and mineralization are intensive (Fig. 3). The centre of the negative gravity anomaly may also coincide with the maximum thickness of the North Pole Pluton.

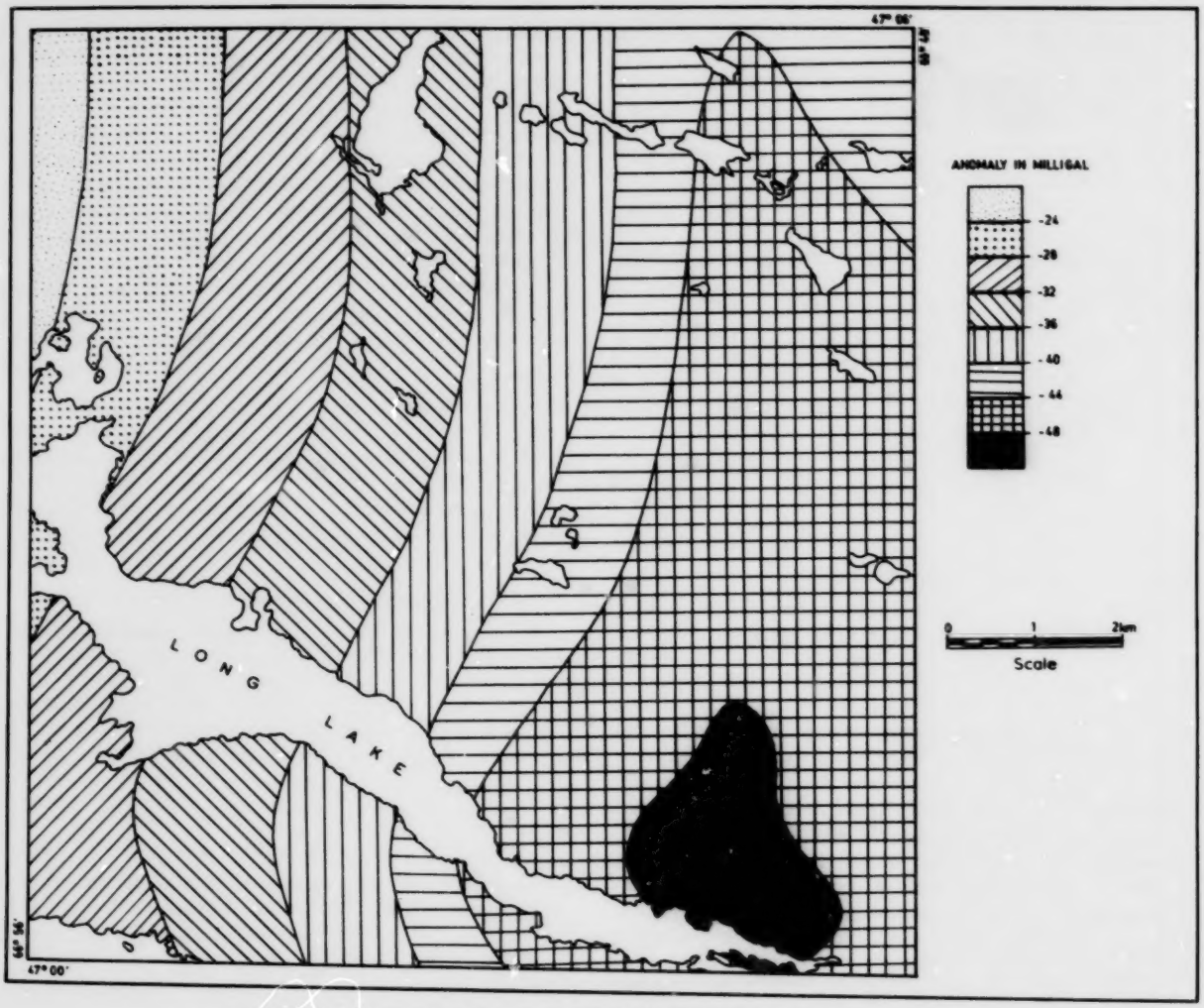

Figure 8. Bouguer gravity data, Long Lake area.

Magnetic

A ground magnetic survey was conducted over Long Lake (Jagodits, 1981) to map the subbottom geology. The survey was unable to detect structural or lithological anomalies. However, a smooth magnetic gradient increasing from south to north of the lake was identified. This gradient may be attributed to decrease in rock magnetism in the south as a result of transformation of magnetite to hematite by hydrothermal alteration.

Airborne total magnetic field data were compiled from a map published by the Geological Survey of Canada (1986), for the Long Lake area (Fig. 9). The survey was made in 1985 by Geophysical Surveys Inc. using a helicopter-borne gradiometer flown at an elevation 150 m above the ground with an average line spacing of 300 m.

By combining the aeromagnetic data (Fig. 9) with the geological data (Fig. 3) it is noted that the North Pole Pluton is associated with a low magnetic response relative to the country rocks. The magnetic contours (Fig. 9) over the pluton are generally smooth with gentle gradients suggesting that the granitic rocks of the North Pole Pluton are homogenous and have not been disturbed extensively by structural deformation.

Very-low frequency electromagnetic technique (VLF)

The VLF survey was mainly performed over Long Lake. It was conducted during the winter of 1981 on the ice (Jagodits, 1981). The objectives of the survey were to map the subbottom geology, particularly the shear zones, with which polymetallic uranium veins are believed to be associated and to check the source of the geochemical anomalies delineated by lake sediment survey.

The survey was able to define several conductors. On the basis of disruptions in the continuity of these conductors three sets of shear zones trending north, north-northeast, and north-northwest were identified.

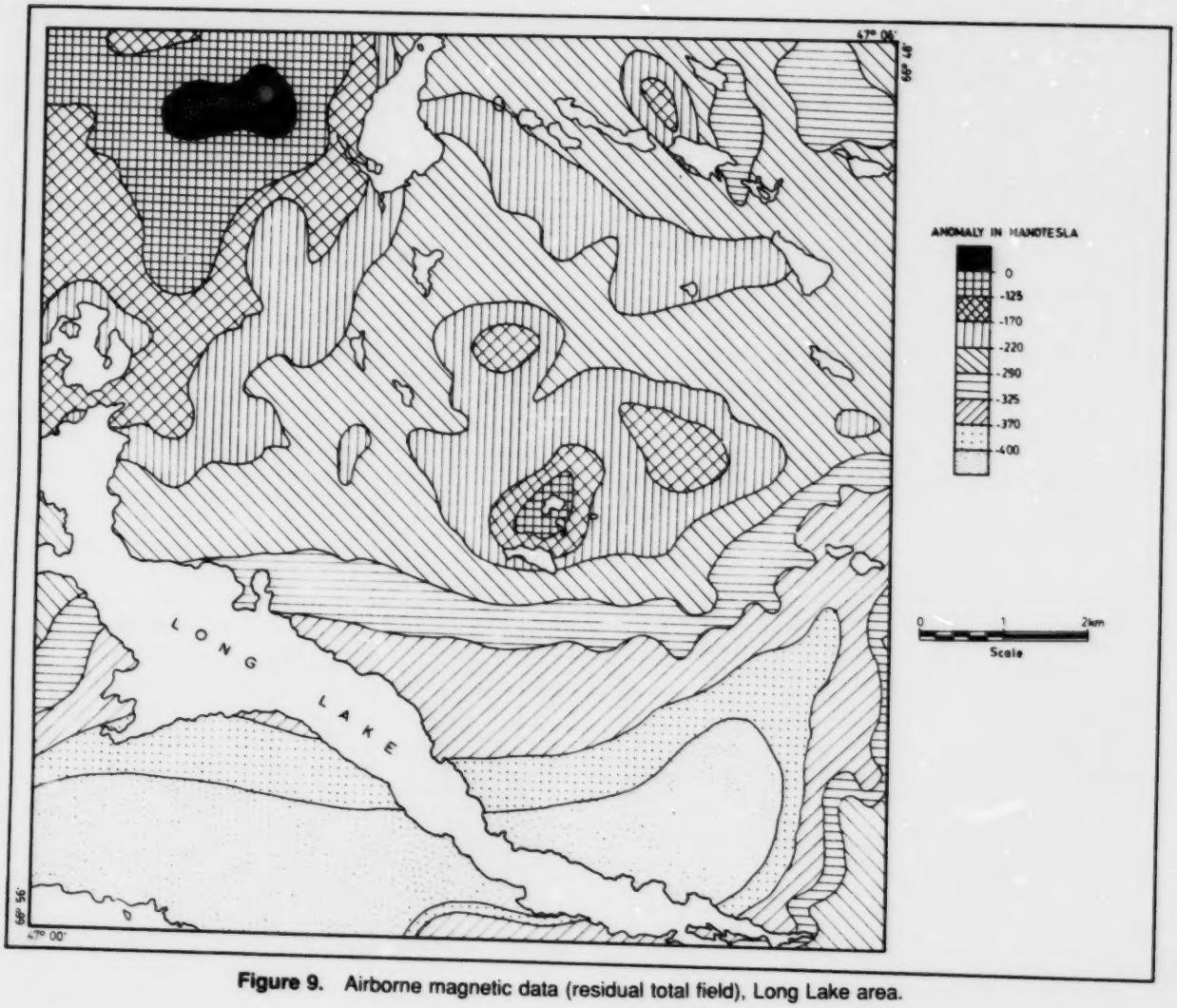

Figure 9. Airborne magnetic data (residual total field), Long Lake area.

Induced polarization (IP)

To verify the results of the VLF survey, an induced polarization survey (apparent resistivity and apparent chargeability) was run over the same lines as the VLF. It was also hoped that faults or breccia zones, particularly mineralized ones, could be defined by areas of low resistivity (high conductivity).

Several low resistivity zones extending through the centre of Long Lake were detected in this survey. The apparent chargeabilities computed over the same profiles produced anomalies coinciding with the low apparent resistivities. These anomalous zones may be related to the presence of polymetallic uranium veins deposited along faults believed to run through the centre of the lake.

Geochemical surveys

Lake sediments geochemistry

Lake sediment sampling was carried out in Long Lake by Canadian Occidental Petroleum to delineate possible areas of uranium and associated metals concentration. The survey was a follow-up to the discovery of mineralized float on the lake shores, in order to identify targets for the drilling program suggested to be carried out on the lake. A total of 439 lake sediment samples were collected and geochemically analyzed for their U, Cu, Pb, Zn, Ag, Mo, and Mn contents (Leonard, 1982). Seventeen multielement anomalies were identified. Uranium along with Zn and Mn are widespread throughout the lake, probably due to their high mobility in the hydromorphic environment.

The multielement anomalies (Leonard, 1982) are generally elongated, suggesting that they may be related to metal concentrations along shear zones. The anomalies have different trends but the majority of them trend either northeast or northwest (see geochemical anomalies over Long Lake in Fig. 45). The northwest-trending anomalies are located in the centre of the lake and appear to be related to a major northwest-trending fault. This, combined with the occurrence of mineralized vein-type float along the lake shore, suggests that vein-type mineralization may indeed be present in the centre of Long Lake. The northeast-trending anomalies, on the other hand, are located mostly near the shores and in the opinion of the authors of this report they may be attributed to a train of mineralized float from the centre of the lake.

Statistical abundances of the metals for which the Long Lake sediments were analyzed, are given in Table 2. The global abundances of these metals in lake sediments are also listed for comparison. With the exception of Cu and Ag, all other elements are exceeding their corresponding global abundances, particularly uranium, which exceeds its global average by an order of six.

Statistical correlation coefficients computed for the 439 samples are given in Table 3. Uranium has a strong positive correlation with Cu and Zn and low to moderate correlations with Ag, Pb, Mo, and Mn. It is of interest to note that only positive correlations were observed among the analyzed elements. This may suggest that they are derived from the same geological source, such as from a fracture-filled vein.

Spring and stream sediments geochemistry

Stream sediments sampling was the first, and probably the most successful survey to locate the mineralization in the Long Lake area. Anomalous U (up to 149 ppm) was identified (1978) in stream sediment samples previously (1971) collected for analysis of Cu, Mo, Zn, and Ag by Canadian Occidental Petroleum (Hauseux, 1980a).

Table 2. Means and ranges of U and other elements analyzed in the Long Lake sediments and their global averages.

Elements	Range	Mean	Global* Average
U (ppm)	0.2 - 215.0	20.0	3.2
Mo (ppm)	0.5 - 126.0	5.0	2.0
Ag (ppm)	0.05 - 2.1	0.4	0.9
Mn (ppm)	73.0 - 12000.0	734.0	670.0
Cu (ppm)	1.0 - 65.0	12.0	57.0
Pb (ppm)	6.0 - 180.0	29.0	20.0
Zn (ppm)	19.0 - 1960.0	302.0	80.0

* Barwise and Whitehead (1983)

Table 3. Correlation coefficients among elements analyzed from 439 lake sediment samples from Long Lake.

	U	Cu	Pb	Zn	Mn	Mo	Ag
Ag	0.27	0.26	0.18	0.18	0.05	0.15	1.00
Mo	0.17	0.14	0.21	0.21	0.39	1.00	
Mn	0.04	0.25	0.27	0.32	1.00		
Zn	0.54	0.61	0.30	1.00			
Pb	0.18	0.36	1.00				
Cu	0.49	1.00					
U	1.00						

Spring and stream sediments sampling also was conducted for the Long Lake area by New Brunswick Department of Natural Resources and Energy (Davies, 1983). The collected samples were analyzed for U, Cu, Pb, Zn, Co, Ni, Mn, Fe, Mo, W, and Ag contents (Appendix III). A compilation map was prepared for the analyzed elements (Fig. 10). The data were treated statistically and the background level chosen at the 50 percentile of the population (median). Different symbols were used to express various levels of anomalies, computed on the basis of 50 percentile, 75 percentile, and 90 percentile levels (Fig. 10). Some of the samples were also analyzed for As, Sb, Ba, and Au contents, however, with the exception of As in a few locations, the metal contents were not anomalous. Unexpectedly, uranium content in the area underlain by the North Pole Pluton is in general moderate, whereas it is high in the area underlain by the Precambrian amphibolite and the Ordovician granite (see Fig. 3). It is possible that uranium migrated either in solution or as particles from the area underlain by the North Pole Pluton (high topography) to areas underlain by Precambrian amphibolites and Ordovician granites (relatively low area). Another possible explanation is that the metal-bearing late phase quartz-feldspar porphyry of North Pole Pluton intruded these rocks (Fig. 3) and provided the uranium and associated metals. No evidence exists to believe that the amphibolites and the deformed granite are the sources of the uranium and the associated metals found in the mineral showings. Statistical abundances of uranium and other metals in the analyzed samples are shown in Table 4.

In order to interpret the results of spring and stream sediment samples in terms of geological controls, a statistical factor analysis was performed on the data by the present authors. Varimax rotated principal component option Statistical Analysis System, (SAS), (1982) was used for this

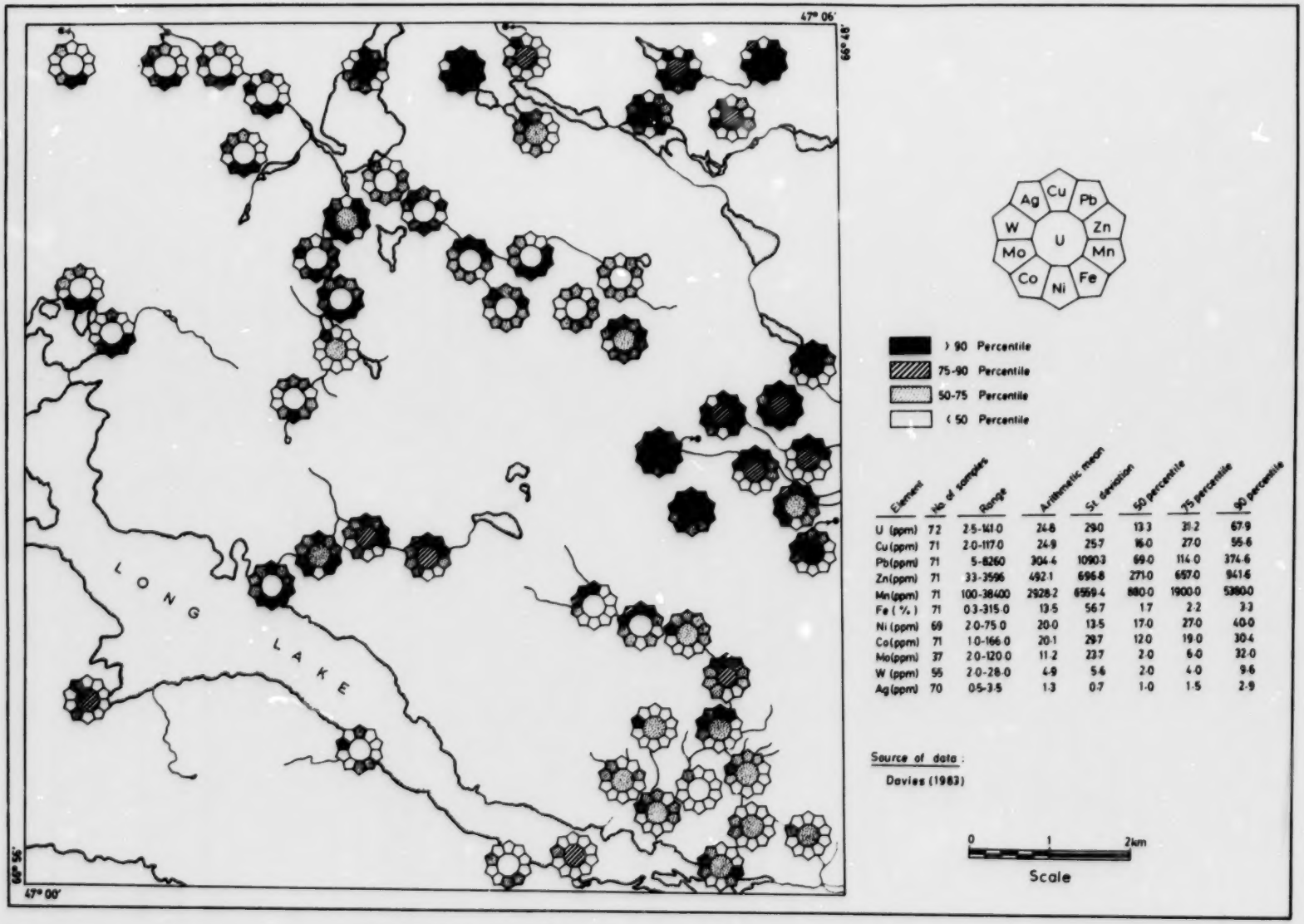

Element	No. of samples	Range	Arithmetic mean	St. deviation	50 percentile	75 percentile	90 percentile
U (ppm)	72	2.5-141.0	24.8	29.0	13.3	31.2	67.9
Cu (ppm)	71	2.0-117.0	24.9	25.7	16.0	27.0	55.6
Pb (ppm)	71	5-8260	304.4	1090.3	69.0	114.0	374.6
Zn (ppm)	71	33-3596	492.1	696.8	271.0	657.0	941.6
Mn (ppm)	71	100-38400	2928.2	6569.4	880.0	1900.0	5380.0
Fe (%)	71	0.3-315.0	13.5	56.7	1.7	2.2	3.3
Ni (ppm)	69	2.0-75.0	20.0	13.5	17.0	27.0	40.0
Co (ppm)	71	1.0-166.0	20.1	29.7	12.0	19.0	30.4
Mo (ppm)	37	2.0-120.0	11.2	23.7	2.0	6.0	32.0
W (ppm)	55	2.0-28.0	4.9	5.6	2.0	4.0	9.6
Ag (ppm)	70	0.5-3.5	1.3	0.7	1.0	1.5	2.9

Figure 10. Contents of spring and stream sediments, Long Lake area.

Table 4. Statistical abundances of elements in spring and stream sediment samples for the Long Lake area.

Element	n*	Range	Mean	St. Dev.	Mode	50 percentile Median	75 percentile	90 percentile	95 percentile	Global@ Averages
U (ppm)	72	2.5 - 141.0	24.8	29.0	4.10	13.25	31.2	67.9	100.2	3.20
Cu(ppm)	71	1 - 117	24.9	25.7	11.00	16.0	27.0	55.6	96.2	55.00
Pb(ppm)	71	5 - 8260	304.4	1090.3	19.00	69.0	114.0	374.6	1424.0	13.00
Zn(ppm)	71	33 - 3596	492.1	696.8	33.00	271.0	657.0	941.6	2028.4	70.00
Mn(ppm)	71	100 - 38400	2928.2	6559.4	1700.00	880.0	1900.0	5380.0	18860.0	950.00
Fe(%)	71	0.3 - 315	13.5	56.7	0.65	1.7	2.2	3.3	99.6	5.00
Ni(ppm)	69	2 - 75	20.0	13.5	27.00	17.0	27.0	40.0	42.0	75.00
Co(ppm)	71	1 - 166	20.1	29.7	5.00	12.0	19.0	30.4	95.8	25.00
Mo(ppm)	37	2 - 120	11.2	23.7	2.00	2.0	6.0	32.0	84.0	1.50
W (ppm)	55	2 - 28	4.9	5.6	2.00	2.0	4.0	9.6	20.8	1.50
Ag(ppm)	70	0.5 - 3.5	1.3	0.7	1.00	1.0	1.5	2.9	3.0	0.07
As(ppm)	19	3 - 85	12.0	19.4	3.00	6.0	10.0	39.0	85.0	1.80
Sb(ppm)	19	0.1 - 0.6	0.2	0.1	0.10	0.1	0.1	0.4	0.6	0.20
Ba(ppm)	19	100 - 360	299.5	50.6	340.00	320.0	340.0	360.0	360.0	425.00

* n = number of samples
@ Barwise and Whitehead (1983)

purpose. Three factors were retained for the analysis. The retained factors show the following metal associations:

Factor I: Zn-Mn-Co-Pb-Ni
Factor II: Ag-U-Cu
Factor III: Fe-Mo

Factor I is composed of Zn, Mn, Co, Pb, and Ni but uranium has no contribution. This factor is probably related to bedrock which is enhanced in these metals. Chemical analyses of samples from the bedrock by Hauseux (1980a) and Fyffe and Pronk (1985) indicate that the uranium content is near normal.

Factor II is composed of U, Ag, and Cu. This factor is probably related to secondary geological processes such as hydrothermal alteration and deposition, and possibly related to vein type mineralization.

Factor III shows that only Fe and Mo are significant. This factor is also related to secondary geological processes which led to Fe and Mo mineralization.

Statistical correlation coefficients among the analyzed metals in spring and stream sediments samples are shown in Table 5. Uranium has a strong positive correlation with Ag and Cu, a pattern also observed in Factor II of factor analysis. Both Ag and Cu can be used as a pathfinder elements for uranium in spring and stream sediments in the area.

Soil geochemistry

The Canadian Occidental Petroleum Company also carried out (1980) a soil sampling search for areas of potential uranium and other metal concentrations. Most of the samples were collected from the area overlying the North Pole Pluton.

Prior to sampling, several test pits were dug in different locations of the study area to determine the relative distribution of metals in various soil horizons. The test indicated that metal concentrations tend to be high in the 'B' horizon. Therefore, whenever it was possible the 'B' horizon was sampled.

Three thousand soil samples were collected in summer of 1980 over the eastern side of Long Lake (Gleeson, 1980) and another 732 samples from the western side of the lake (Lipowicz, 1980). These samples were analyzed for U, Cu, Pb, Zn, Mn, Mo, and Ag contents. Statistical abundances of

Table 5. Correlation coefficients for elements in 72 spring and stream sediment samples of Long Lake area.

	U	Cu	Pb	Zn	Mn	Fe	Ni	Co	Mo	W	Ag
Ag	0.85	0.70	0.52	0.32	0.15	-0.17	0.20	-0.01	-0.05	0.03	1.00
W	-0.03	-0.17	0.06	-0.06	0.02	-0.09	0.04	0.09	-0.17	1.00	
Mo	0.06	-0.32	-0.03	0.07	0.16	0.25	-0.01	0.18	1.00		
Co	-0.08	-0.02	0.32	0.68	0.60	0.37	0.43	1.00			
Ni	0.04	0.12	0.19	0.46	0.38	-0.22	1.00				
Fe	-0.16	-0.01	-0.06	0.00	0.00	1.00					
Mn	-0.12	0.06	0.72	0.92	1.00						
Zn	0.05	0.29	0.67	1.00							
Pb	0.38	0.25	1.00								
Cu	0.58	1.00									
U	1.00										

Table 6. Mean, standard deviations, and ranges of analyzed metals in soils of the Long Lake area.

Metals	n*	Eastern Long Lake		n	Western Long Lake		Global@ Averages
		Ranges	Mean ± St. Dev.		Ranges	Mean ± St. Dev.	
U(ppm)	2990	0.1 - 680	4.5 ± 20.4	732	0.2 - 178.0	2.8 ± 10.1	2.7
Cu(ppm)	2358	0.5 - 3500	25.5 ± 90.5	732	0.5 - 70.0	7.5 ± 5.1	25
Pb(ppm)	2986	0.5 - 7200	73.9 ± 185.4	732	4.0 - 540.0	24.4 ± 22.7	19
Zn(ppm)	2986	2.0 - 21700	190.9 ± 525.3	732	3.0 - 132.0	41.1 ± 21.2	60
Mn(ppm)	2360	6.0 - 99999	927.4 ± 3913.0	732	8.0 - 30200	319.9 ± 1231.3	550
Mo(ppm)	2358	0.5 - 470	4.1 ± 14.9	732	0.5 - 38.0	1.9 ± 2.4	1.0
Ag(ppm)	2360	0.2 - 32	2.1 ± 1.56	732	0.4 - 2.6	1.0 ± 0.3	0.1

* n = number of samples
@ Global average composition from Barwise and Whitehead (1983); Ag from Shacklette and Boerngen (1984).

the analyzed metals are given in Table 6, along with their global averages.

About 54 multielement soil anomalies were located in this survey, the majority of them on the eastern side of Long Lake in an area underlain by the North Pole Pluton. These anomalies have, in general, a linear pattern with west-northwest, east, and northeast trends which could be a reflection of mineralization along linear features such as shear zones.

Other than Mo and U (slightly above global averages) the rest of the metals are generally depleted on the western side of Long Lake.

Two common metal associations were observed in the soil samples. The first is between Cu, Pb, Zn, Mn, and Ag in areas underlain by biotite granite. The second metal association includes U and Mo in northwest-trending anomalies along both the east and west shores of Long Lake.

Till geochemistry

The first direct sign of mineralization in the Long Lake area was in mineralized boulders in glacial tills in the area around Long Lake shores.

Tracing of mineralized boulders has been used for decades as a prospecting method for mineral deposits in glaciated terrains (Dreimanis, 1958). The method is used most successfully for uranium exploration mainly because a scintillometer can easily identify even buried (<50 cm deep) uranium-bearing boulders (Paterson et al., 1979). The Pleutojokk uranium deposit of northern Sweden was discovered in this manner (Gustafsson and Minell, 1977). In Canada, several uranium deposits have been discovered since 1970 by tracing trains of radioactive ore boulders (Seguin et al., 1984).

Uranium is associated with base metal sulphides as well as W, Sn, Mo, and Ag in the Miramichi Anticlinorium (Fig. 1), and it may be possible to locate deposits by tracing radioactive boulders of these metals.

In the Long Lake area, a geochemical study of tills was carried out in the summer of 1983 (Fyffe and Pronk, 1985). Samples collected were analyzed for U, Cu, Pb, Zn, Mn, Fe, Co, Ni, W, Mo, and Au and results are summarized in Table 7.

Anomalous contents of U, Pb, Zn, Cu, and Mn were detected in samples from the area east of Long Lake, which is underlain by granitic rocks of the North Pole Pluton. The anomalies appear to be related to northwest-trending fracture zones in the biotite granite.

Table 7. Statistical abundances of metals in 173 till samples from Long Lake area (after Fyffe and Pronk, 1985).

Element	Range	Mean ± St. Dev.
U (ppm)	1.20 - 9.90	3.60 ± 1.70
Cu (ppm)	1.00 - 76.00	14.20 ± 9.00
Pb (ppm)	9.00 - 183.00	28.70 ± 19.30
Zn (ppm)	12.00 - 515.00	66.10 ± 58.40
Mn (ppm)	40.00 - 710.00	234.70 ± 117.50
Fe (%)	0.71 - 5.30	2.67 ± 0.87
Co (ppm)	3.00 - 22.00	10.60 ± 3.50
Ni (ppm)	3.00 - 59.00	21.00 ± 11.50
Ag (ppm)	0.50 - 3.00	1.20 ± 0.70
Mo (ppm)	2.00 - 8.00	2.10 ± 0.70
W (ppm)	2.00 - 24.00	3.20 ± 2.50
Au (ppm)	0.05	0.05

Uranium anomalies are spatially associated with highly silicified and brecciated granite and with quartz-feldspar porphyry dykes of the North Pole Pluton but not with portions of the pluton composed of biotite-muscovite granite. Fyffe and Pronk (1985) have estimated that the Long Lake anomalies are displaced east-southeastward from their bedrock origin over a distance of 1 to 2 km.

Seep water geochemistry

Limited water sampling was conducted by the Canadian Occidental Petroleum Company (Hauseux, 1980a). Six samples were collected from four seeps in an area underlain by biotite granite at the eastern side of Long Lake, near Cronin Brook. The aim of the survey was to test the level of various elements, particularly uranium, in these water samples in an attempt to define uranium and other metal occurrences in the area. Levels of anion complexes, alkalinity, and conductivity of the water samples were also determined. Results of this survey are summarized in Table 8.

It was expected that the uranium level in the water samples would be low because of their alkaline nature (average pH = 8.54), but it appears that the level of uranium is normal to above normal (Table 8) for natural waters, which is of the order of 0.01 to 0.8 ppb (Boyle, 1982).

Central Miramichi Anticlinorium area

Geophysical surveys

Gravity

Reconnaissance Bouguer gravity mapping was carried out by Earth Physics Branch, Ottawa (Williams, 1978). Gravity stations at 5 km intervals were observed in the survey. The compiled Bouguer gravity map, which is shown in Figure 11, illustrates that the granitic rocks of the Burnthill, Dungarvon, Trout Brook, and Rocky Brook plutons are associated with a single large negative gravity anomaly indicating a strong density contrast between the granitic plutons and the country rocks.

Table 8. Geochemical abundances in six seep water samples from Long Lake area (after Hauseux, 1980a).

Elements	Range	Average
U (ppb)	0.07 - 1.26	0.45
Cu (ppb)	2.00 - 6.00	1.80
Zn (ppb)	4.00 - 6.00	19.20
Mo (ppb)	ND* - 5.00	4.00
Mn (ppb)	ND	ND
Ag (ppb)	ND	ND
Fe (ppb)	ND	ND
Na (ppb)	2560.00 - 5360.00	3918.00
K (ppb)	280.00 - 1860.00	778.00
Ca (ppb)	1800.00 - 7000.00	4040.00
Mg (ppm)	350.00 - 1150.00	728.00
Cl (ppb)	ND - 3770.00	1648.00
F (ppb)	480.00 - 3680.00	1660.00
HCO_3 (ppm)	29.00 - 72.00	41.00
SO_4 (ppm)	10.00 - 22.00	15.40
PO_4 (ppm)	ND - 0.07	0.01
SiO_2 (ppm)	9.30 - 19.70	12.80
pH	6.63 - 9.99	8.54
Conductivity (mho/cm)	55.0 - 174.0	131.0

*ND = Not detected

The centre of the anomaly (<-54 mgal) coincides with the area where hydrothermal activity and resulting mineralization appear to have been most active (i.e., the southeastern margin of the Burnthill Pluton), and may indicate the point above the centre of the magma chamber.

Magnetic

An airborne Fluxgate magnetic survey of the area (GSC, 1965) was made in 1950 by the Geological Survey of Canada (Fig. 12). The survey was flown at a nominal elevation of 150 m above the ground with an average line spacing of 1 km. Figure 12 is derived from the aeromagnetic maps resulting from this survey.

The linear anomalies shown in Figure 12 mostly trend northeasterly, parallel to the prominent structural features exhibited by the Cambro-Ordovician metasedimentary rocks of the Tetagouche Group that host the granitic plutons. The Burnthill Pluton is associated with an insignificant magnetic low, whereas the Dungarvon, Trout Brook, and Rocky Brook plutons lack magnetic anomalies.

Geochemical surveys

Spring and stream sediments geochemistry

Spring and stream sediments sampling was used prior to other exploration methods at least in part because of the abundance of streams and springs in the central Miramichi Anticlinorium area (Fig. 6). A survey conducted by the New Brunswick Department of Natural Resources and Energy

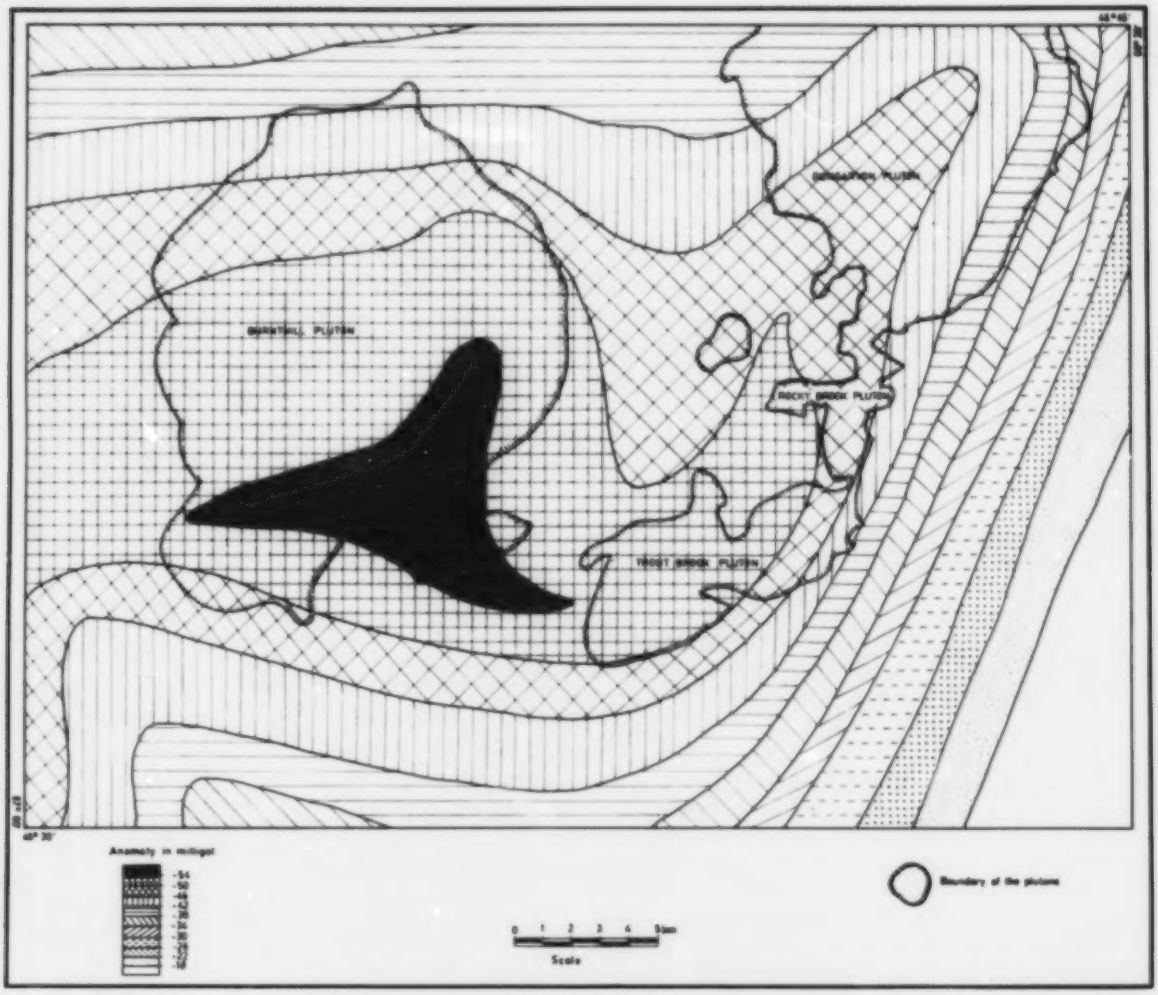

Figure 11. Bouguer gravity map of the granitic plutons, central Miramichi Anticlinorium (after Williams, 1978).

(Austria, 1976, 1977), involved collecting 1065 samples which were analyzed for U, Mo, W, Cu, Pb, Zn, Mn, and Fe contents (Appendix IV). The results of the analysis for the stream sediment samples and the spring sediment samples are shown in Table 9.

Table 9 reveals that only uranium and manganese abundances are significantly different for the two environments. The uranium content is higher in the spring sediment samples than in the stream sediment samples whereas the Mn content is lower in the spring sediment samples relative to the stream sediment samples. Other elements (i.e., Mo, W, Cu, Pb, Zn, and Fe) are more or less similar in abundances in the two environments.

Statistical abundances of U, Mo, W, Cu, Pb, Zn, and Fe in 344 samples of sediments from springs and streams draining the granitic rocks of the Burnthill, Dungarvon, Trout Brook, and Rocky Brook plutons are summarized in Table 10. The results indicate highly anomalous values for U, Mo, W, and to some extent Pb, relative to global averages of these elements in sediments.

If the background level is chosen as the 50 percentile (median) of the population, then, it appears from Table 10 that the average uranium content is higher in the Dungarvon Pluton than in the others. However, variations in uranium distribution, as indicated by great ranges, is high within the Burnthill Pluton relative to other plutons which may suggest that the Burnthill Pluton has a higher potential for uranium mineralization.

Uranium contents in spring and stream sediment samples were contoured for the total area of study (Fig. 13). It is obvious from Figure 13 that the granitic rocks of Burnthill, Dungarvon, Trout Brook, and Rocky Brook plutons are totally anomalous in terms of U content.

In contrast, the country rocks are associated with low uranium values relative to the granitic plutons (Fig. 13). This implies that the main source of uranium in the spring and stream sediments is the granitic plutons.

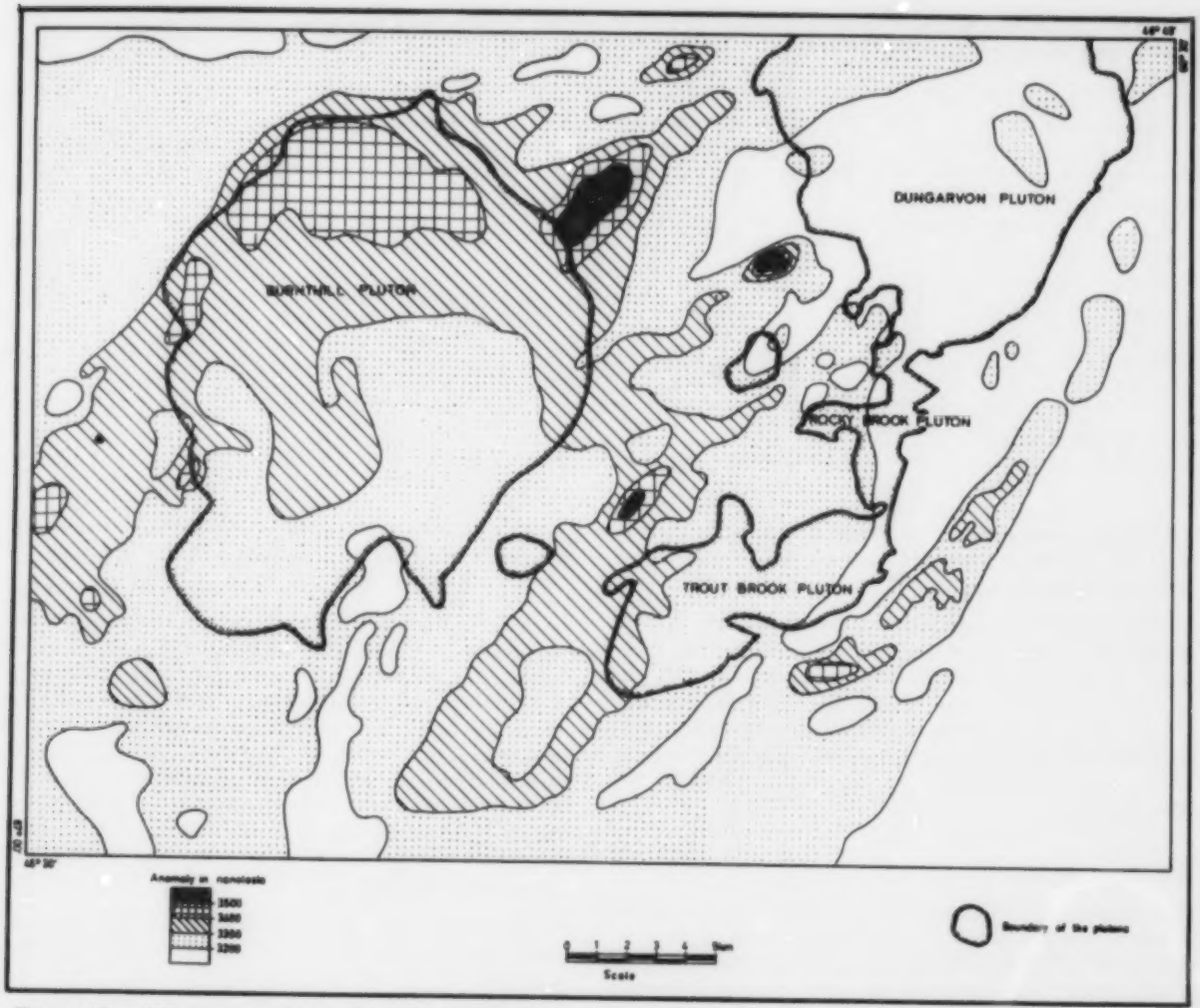

Figure 12. Airborne magnetic data of the granitic plutons, central Miramichi Anticlinorium (after Geological Survey of Canada, 1965).

Nonparametric statistical correlation coefficients were computed between uranium and other elements in the vicinity of the four plutons. The results of the analyses are shown in Table 11. It appears from the result that uranium has a strong positive correlation with molybdenum in the spring and stream sediments overlying the Rocky Brook Pluton. Uranium exhibits a moderate correlation with molybdenum in the Trout Brook Pluton and with base-metal sulphides in the Dungarvon, Trout Brook, and the Rocky Brook plutons. Thus, these correlations possibly suggest that U is associated with Mo and base-metal sulphide deposits in these plutons.

Soil geochemistry

Soil sampling was carried out sporadically in the vicinity of the granitic plutons in the search for mineral deposits. The lack of outcrops and the presence of abundant overburden materials in the area made this technique very useful.

In the present work, the soil profile study carried out by Westmin Resources Limited in the spring of 1981 (Hattie, 1981) was used in order to examine uranium distribution in the soil section. This profile was established over the eastern part of the Burnthill Pluton. Samples from A-, B-, and C-horizons were collected at each of 33 sample sites and chemically analysed for U, Sn, Mo, and W contents (Appendix V).

Statistical means and standard deviations of U, Sn, Mo, and W in different soil horizons are given in Table 12. The results show that U, Sn, Mo, and W contents in the soil samples are in general anomalous as indicated by their comparison with global averages. The results also reveal that uranium content in the soil decreases systematically upward from C-horizon toward A-horizon.

The high uranium content in the C-horizon (contains material derived mostly from the underlying bedrock by weathering) suggests that the uranium was derived from the

Table 9. Comparison between spring and stream sediment samples in terms of trace element contents for the area shown in Figure 13.

Elements	n°	Stream sediment samples mean ± standard deviation	n°	Spring sediment samples mean ± standard deviation
U(ppm)	254	17.2 ± 22.5	43	22.7 ± 20.4
Mo(ppm)	622	6.9 ± 17.0	182	5.9 ± 10.5
W(ppm)	724	9.9 ± 12.7	209	11.2 ± 17.6
Cu(ppm)	823	12.9 ± 12.8	234	12.2 ± 11.6
Pb(ppm)	830	26.2 ± 21.1	235	26.0 ± 20.4
Zn(ppm)	829	89.7 ± 73.1	235	82.0 ± 74.9
Mn(ppm)	830	1931.6 ± 2493.2	234	1646.1 ± 2157.6
Fe(%)	805	2.0 ± 1.2	230	1.8 ± 1.1
n° = number of samples				

underlying granitic rocks. Furthermore, the results suggest that the underlying granitic bedrock has potential for uranium mineralization.

To examine the relationship among U, Sn, Mo, and W in the soil samples, statistical correlation coefficients were established for the samples. Results of this analysis are given in Table 13 which shows that uranium generally correlates moderately with W, Mo, and Sn. This correlation suggests that all these elements may have been derived from similar source rocks such as the granitic rocks of the Burnthill Pluton.

Till geochemistry

Till sampling of the study area was carried out as part of Canada-New Brunswick Mineral Development Agreement during the 1985 and 1986 field season by Lamothe (1989). Each sample was separated into two textural fractions; clay-sized (<2 μm) fraction and clay- plus silt-sized (<63 μm) fraction (Appendix VI). The clay fractions of till samples were analyzed chemically for their U, Sn, Mo, W, F, As, Mn, Fe, Cu, Pb, Zn, Ni, Co, and Cr contents. The clay plus silt fractions were analyzed for their U, Th, Mo, W, Sb, Au, As, Fe, Zn, Ni, Co, and Cr contents. Seventy-seven chemical analyses of till samples covering the granitic plutons of Burnthill, Dungarvon, and Trout Brook were selected for this study in order to detect significant uranium and other elements anomalies and to examine the relationship between uranium and other elements in the till cover.

Statistical abundances of the elements analyzed in the two fractions of till samples are shown in Table 14. With the exception of Cr, all other elements analyzed in the two fractions tend to be enriched in the fine fraction rather than in the coarse fraction (Table 14). This contrast in chemical composition between the two fractions appears to be more obvious for the lithophile elements U, Mo, and W. This may suggest that these elements are associated with the weathering and alteration products of the rocks which are enriched in the fine fraction of till rather than with primary silicate minerals enriched in the coarse fraction. Alternatively, this may reflect the tendency of these elements (i.e., U, Mo, W, and probably Sn) to be absorbed by clays and organic matter that predominate the fine fraction of till samples (Fletcher, 1986).

The 50, 75, and 90 percentile values of uranium content in the clay-sized fraction of till samples (Fig. 14) reveal the presence of several anomalies coincident with areas where the bedrocks are also anomalous, which may indicate that these till samples were derived locally (i.e., from the underlying granitic rocks). Because of the low sampling density of till, it is difficult to define dispersion trains where it is possible to trace these anomalies to their sources, especially if the sources are small, such as veins. However, Figure 14 only outlines areas potentially favorable for uranium exploration.

In order to recognize patterns of elements associated with uranium in the till samples, Spearman rank correlation coefficients were calculated among the elements in the clay fraction and in the clay plus silt fraction (Table 15).

In the clay fraction, significant positive correlations exist only among U, Sn, and W. In the clay plus silt fraction, significant positive correlation exists among U, Th, Mo, and W. It is interesting to note that the correlations among the lithophile elements are stronger in the fine fraction than in the coarse fraction. One explanation is that the portions of the lithophile elements in the coarse fraction are those that are associated with the rock-forming minerals which survived hydrothermal and weathering processes.

GAMMA RAY SPECTROMETRY SURVEYS

Overview

The Miramichi Anticlinorium has been covered by two airborne gamma ray spectrometry surveys. The first was on a reconnaissance basis along flight lines 5 km apart and carried out as part of the Canada-New Brunswick Uranium Reconnaissance Program (URP). The results were released by the Geological Survey of Canada in the spring of 1977 (D.N.R., 1977).

Table 10. Uranium and other trace element contents in spring and stream sediment samples in the Burnthill, Dungarvon, Trout Brook, and Rocky Brook granites.

Elements	Burnthill Granite					Dungarvon Granite					Trout Brook Granite					Rocky Brook Granite					Global[@] Averages
	Range	Mean	St. Dev.	50%	90%	Range	Mean	St. Dev.	50%	90%	Range	Mean	St. Dev.	50%	90%	Range	Mean	St. Dev.	50%	90%	(ppm)
U (ppm)	4.2-171.0	27.2 (70)*	25.1	20.0	50.3	4.3-113.0	36.6 (45)	27.6	26.6	78.1	4.6-96.3	28.2 (11)	28.3	15.8	89.2	6.2-91.5	29.3 (16)	34.1	11.5	91.5	3.2
Mo (ppm)	1.0-300.0	10.0 (160)	27.3	3.0	20.0	1.0-70.0	9.1 (72)	13.1	4.5	44.0	2.0-100.0	13.2 (28)	23.2	4.5	44.0	1.0-20.0	7.1 (10)	7.3	4.0	20.0	1.5
W (ppm)	1.0-80.0	11.6 (175)	13.9	6.0	28.0	1.0-80.0	9.1 (80)	10.6	5.0	20.0	1.0-120.0	20.0 (33)	23.7	12.0	40.0	1.0-40.0	13.7 (10)	11.8	10.0	38.4	1.5
Cu (ppm)	1.0-27.0	4.4 (164)	3.7	4.0	9.0	1.0-22.0	5.4 (100)	4.3	4.0	11.9	1.0-36.0	13.3 (35)	9.0	13.0	25.4	5.0-48.0	16.4 (16)	12.3	13.5	43.7	55
Pb (ppm)	3.0-130.0	23.8 (168)	18.3	19.0	43.0	3.0-110.0	21.5 (101)	19.0	16.0	43.4	3.0-184.0	41.7 (35)	35.1	32.0	89.6	15.0-33.0	20.5 (10)	5.7	18.5	32.2	13
Zn (ppm)	9.8-163.0	42.8 (168)	26.2	38.0	73.5	11.0-370.0	54.8 (101)	47.3	44.0	100.2	13.0-422.0	129.1 (35)	99.0	92.0	258.0	44.0-167.0	85.5 (16)	32.7	83.0	152.4	70
Mn (ppm)	52.0-12240.0	1225.2 (168)	1741.9	630.0	2798.0	70.0-11560.0	1079.7 (101)	1689.4	460.0	2536.0	63.0-15861.0	3448.5 (35)	4472.8	1606.0	12178.0	213.0-2010.0	882.0 (10)	585.9	800.0	1948.0	960
Fe (%)	0.1-4.5	1.1 (166)	0.7	1.0	1.8	0.1-6.0	1.3 (101)	0.9	1.1	2.4	0.1-5.2	1.9 (35)	1.2	1.8	4.0	1.0-3.1	1.9 (10)	0.6	1.8	3.0	5.0

* - number of samples are given in the brackets.
@ - Barwise and Whitehead (1983).

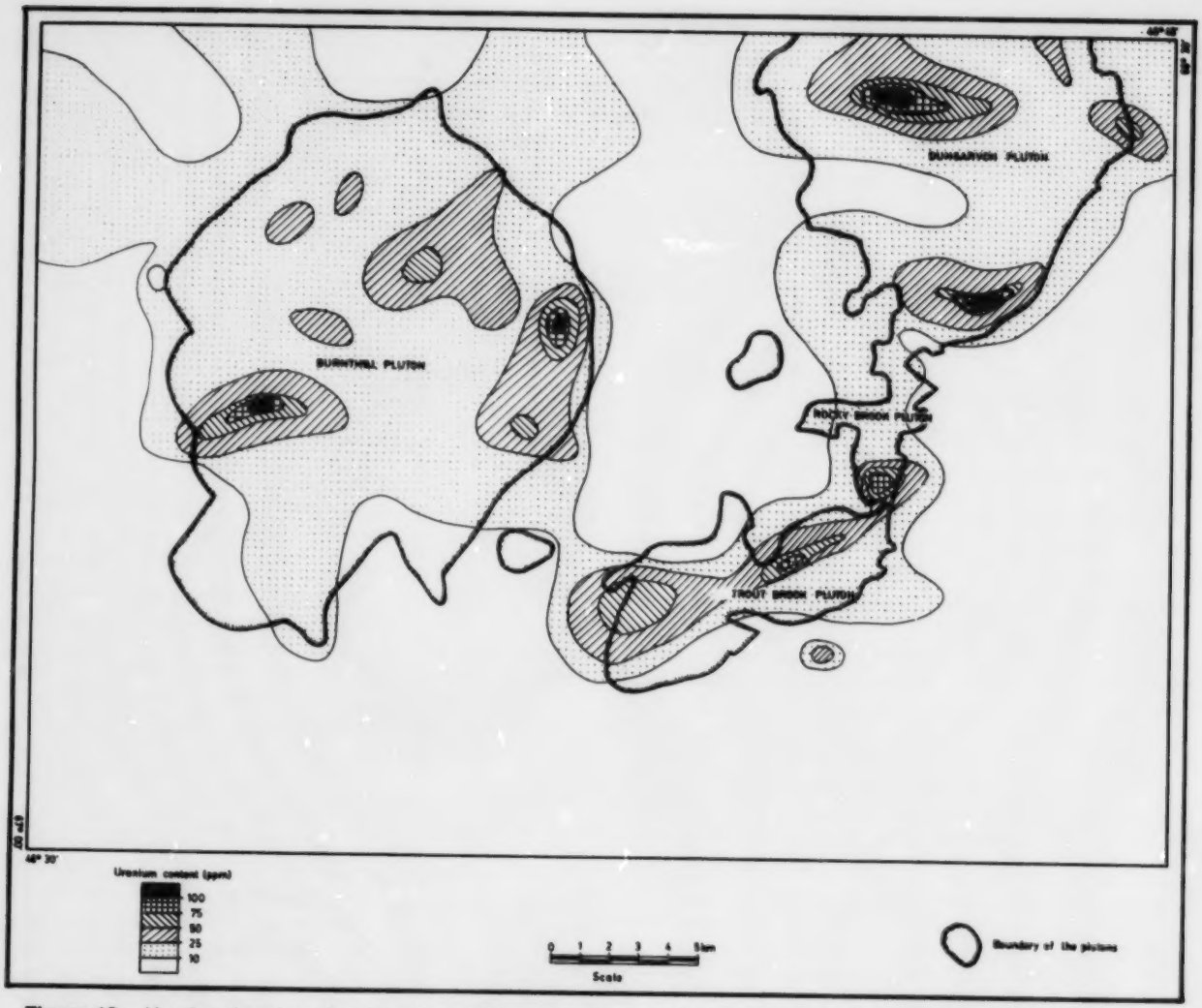

Figure 13. Uranium (ppm) content in spring and stream sediments of the granitic plutons, central Miramichi Anticlinorium.

Table 11. Correlation coefficient between U and other elements in stream and spring sediments of the granitic plutons of the central Miramichi Anticlinorium area.

Element	Burnthill Pluton	Dungarvon Pluton	Trout Brook Pluton	Rocky Brook Pluton
Mo	0.07	0.03	0.32	0.75
W	0.07	0.10	0.21	0.20
Cu	0.04	-0.03	0.36	-0.28
Pb	0.22	0.20	0.44	0.55
Zn	0.09	0.33	0.42	0.47
Mn	0.07	0.29	0.31	0.07
Fe	0.10	-0.06	0.06	-0.36

The second survey was relatively more detailed than the first survey. It was carried out as part of a Canada-New Brunswick Mineral Development Agreement (MDA). The data were released by the Geological Survey of Canada in the spring of 1985 (D.N.R.E., 1986). A 256 channel spectrometer, with twelve 102 x 102 x 406 mm NaI (Tl) detectors, was used in the survey. The lines were flown at a mean terrain clearance of 125 m with flight lines at 1 km line spacing.

The data of the second survey were used in the present work because they are of better quality and resolution than the data of the first survey.

Follow-up in situ gamma ray spectrometry surveys were carried out by the present authors in the area of central Miramichi Anticlinorium in order to examine the response of the aeroradiometric anomalies on the ground and to search for uranium mineralization in the granitic plutons.

Table 12. Soil samples over Burnthill Pluton.

Soil Horizon	n*	MEAN ± STANDARD DEVIATION U(ppm)	Sn(ppm)	Mo(ppm)	W(ppm)
A	33	7.4 ± 22.4	---	1.2 ± 1.2	1.4 ± 0.9
B	25	15.0 ± 4.8	22.3 ± 6.5	3.2 ± 1.1	4.4 ± 1.9
C	25	17.0 ± 3.6	19.9 ± 6.0	3.1 ± 1.2	4.6 ± 1.8
Global Averages @ (ppm)		2.7	10.0	1.0	---

* n = number of samples
@ Global average composition from Barwise and Whitehead (1983).

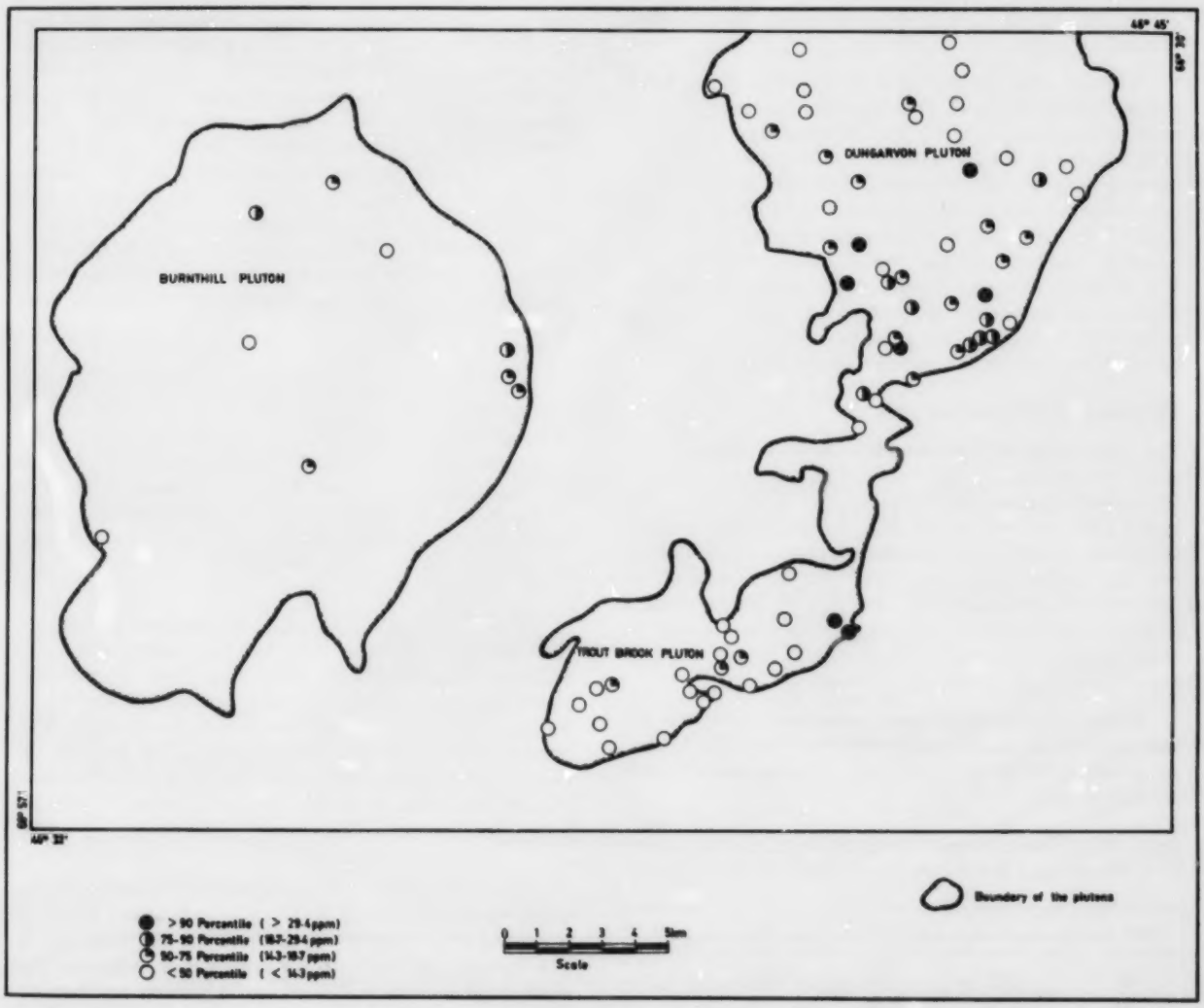

Figure 14. Uranium content in clay-sized (<2 μm) till samples, central Miramichi Anticlinorium, New Brunswick.

The uranium content indicated in spring and stream sediments data was used in conjunction with eU airborne data in order to enhance the search.

Interpretation of airborne gamma ray spectrometry data

General statement

The main objective of an airborne gamma ray spectrometry survey is to delineate potential areas of uranium mineralization. Such surveys have also been useful for mapping various phases of granitic rocks (O'Reilly et al., 1988), and have been used successfully in locating areas enriched with Sn and W (Yeates et al., 1982; Ford and Ballantyne, 1983), because U, Sn, and W are usually concentrated together in the late stage phases of the granites which are crystallized from the residual melts. This appears to be the case with the granitic rocks of the Burnthill, Dungarvon, Trout Brook, and Rocky Brook plutons where U, Sn, and W concentrate more or less in the late stage phases.

O'Reilly et al. (1988) have investigated the airborne gamma ray spectrometry data over the Meguma Zone of Nova Scotia in order to test their applicability in bedrock mapping and mineral exploration, particularly within the granitic rocks of South Mountain Batholith. In addition to being able to delineate various phases of the granites and in locating areas enriched with granophile elements such as U, Sn, W, and Mo, the aeroradiometric survey allows recognition of hydrothermally altered zones within the granitic rocks. Where hydrothermal alteration has lead to substantial redistribution of U, Th, and K within rocks such zones can be easily detected on the aeroradiometric maps.

Miramichi Anticlinorium area

The distribution of known occurrences of uranium and associated elements in the Miramichi Anticlinorium (Fig. 1) illustrates that almost all are located on or adjacent to the granitic plutons. This spatial relationship provides a strong suggestion of genetic relationship including the possibility that the granitic rocks may have been the source of the uranium in these occurrences. Therefore, the present section is largely confined to an investigation of these plutons in order to select the most favourable ones for uranium exploration.

A map showing the airborne radiometric contours of eU was compiled for the Miramichi Anticlinorium (Fig. 15) and areas with different eU values above background (2 ppm) are outlined.

Table 13. Correlation coefficients among U, Sn, Mo, and W in the samples of soil over the Burnthill Pluton.

Element	U	Sn	Mo	W
W	0.35	0.09	0.39	1.00
Mo	0.40	0.18	1.00	
Sn	0.33	1.00		
U	1.00			

The anomalous eU regions (Fig. 15) are at least spatially linked to the granitic plutons (Fig. 1). It also appears that the highest eU radiometric anomalies are closely associated with the W-Sn-Mo-bearing granitic rocks of the Burnthill, Dungarvon, Trout Brook, and Rocky Brook plutons. These granites are also associated with the strongest negative gravity anomalies (Table 16) in comparison to other plutons in the area.

The airborne radiometric data of eU, eTh, and K were digitized at 400 metres square grid for the areas underlain by Burnthill, Dungarvon, and Trout Brook intrusions and at a one square kilometre grid for the others. The grid points that fall on areas covered with water were excluded from the analysis. Average concentrations of eU, eTh, and K calculated from the digitized grids over the plutons are given in Table 16 which illustrates that the Trout Brook, Dungarvon, Mount Elizabeth, and to some extent the Burnthill plutons contain higher eU, eTh, and K relative to other granitic plutons in the anticlinorium. Using these data the Trout Brook Pluton appears to be the most favourable for uranium mineralization (Table 16). The low eU content in the Burnthill and Dungarvon plutons relative to the Trout Brook Pluton may be related to the weathering of the Burnthill and Dungarvon plutons. The Trout Brook Pluton does not exhibit any deep weathering. The Trout Brook, Dungarvon, and Burnthill plutons are all associated with uranium (± W, Sn, Mo) occurrences (Fig. 1). Although the Mount Elizabeth Pluton is not included in the present study it seems to be more favourable for uranium mineralization than originally believed, and should receive further attention in future exploration.

The limited geochemical data compiled for the granitic plutons (Table 16) indicate that most of them are, in general, highly silicic (SiO_2 >73 wt. %). The plots of the mean silica content versus the mean eU and eTh contents respectively (Fig. 16) reveal that both the mean eU and eTh contents increase in general with increasing mean contents of the SiO_2. A somewhat arbitrary grouping of the plutons is shown on the eU versus SiO_2 plot.

On the eTh versus SiO_2 plot, two groups of plutons can be identified as well (Fig. 16). The first group includes the Redstone Mountain, North Pole, Miramichi, Trout Brook, and Dungarvon plutons. In these plutons the mean eTh increases progressively with the increase in the mean SiO_2 content (Fig. 16). In the second group which includes the older granites, Mount Elizabeth Pluton and the Burnthill Pluton, the increase in the mean eTh content with the increase in the mean SiO_2 content is sharper.

All of the granitic plutons appear to be peraluminous where molecular $Al_2O_3/(CaO+Na_2O+K_2O)$ ratios exceed 1.1 (Chappell and White, 1974) and data on this parameter is also included in Table 16 for comparison purposes. The average peraluminous indices are in general comparable, which may suggest that these granitic plutons are derived from anatexial melting of sedimentary protolith, and from a common source magma.

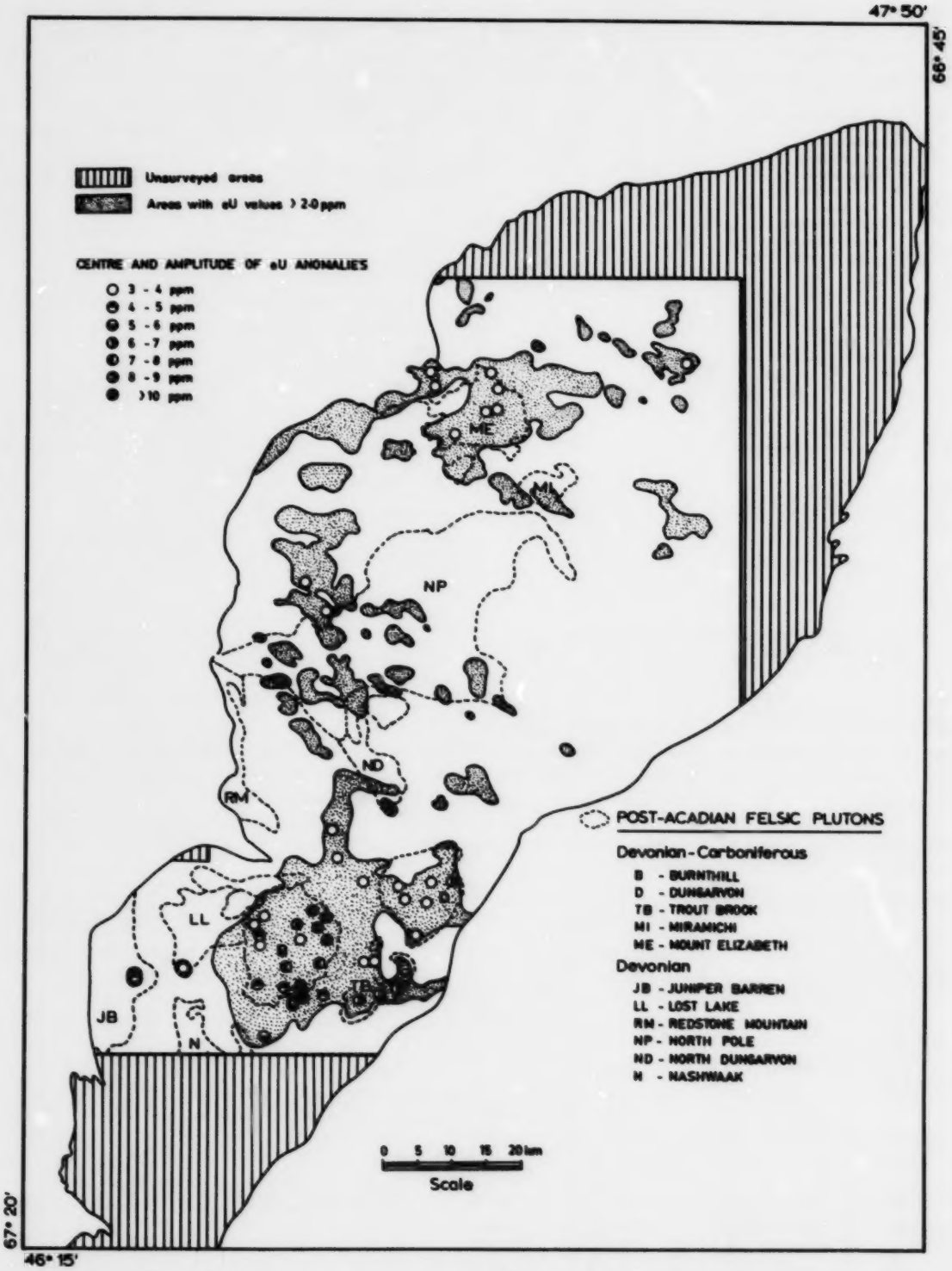

Figure 15. eU airborne gamma ray spectrometry data, Miramichi Anticlinorium, New Brunswick.

The eU, eTh, and K contents in the Miramichi Anticlinorium plutons were plotted on an eU-eTh-K variation diagram (Fig. 17), which illustrates that all of the plutons plot close to each other and that only minor variations exist in terms of radioelement content. Furthermore, Figure 17 indicates that the Trout Brook Pluton is plotted adjacent to uraniferous granites from the Hercynian Cornubian Batholith and the Caledonide Cairngorm granite of Europe (Fig. 17), again suggesting that the Trout Brook pluton is the most favourable for uranium mineralization.

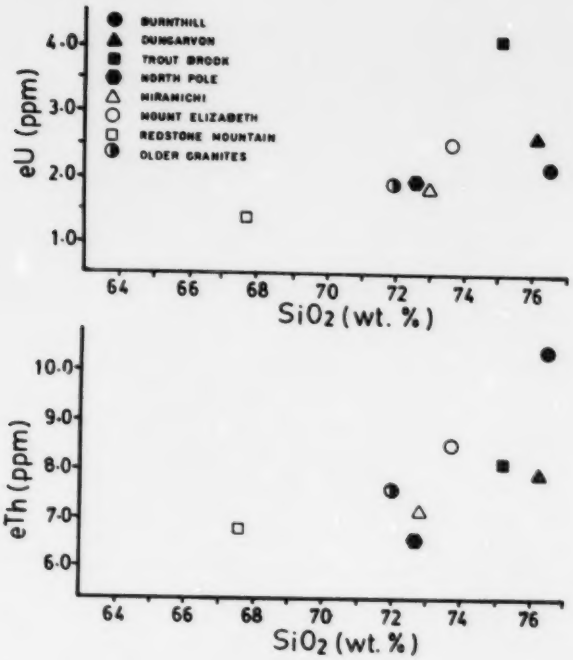

Figure 16. Plots of eU versus SiO_2 and eTh versus SiO_2 for selected granitic plutons in the Miramichi Anticlinorium, showing a general trend of increasing eU and eTh with increase of SiO_2.

Favourability indices of the granitic plutons

In order to rank the granitic plutons of the Miramichi Anticlinorium according to their favourability for uranium mineralization, the quantitative uranium 'favourability indices' developed by Pirkle et al. (1980, 1982) were used. These indices were deduced from the airborne gamma ray spectrometry data, and are based on the assumption that the

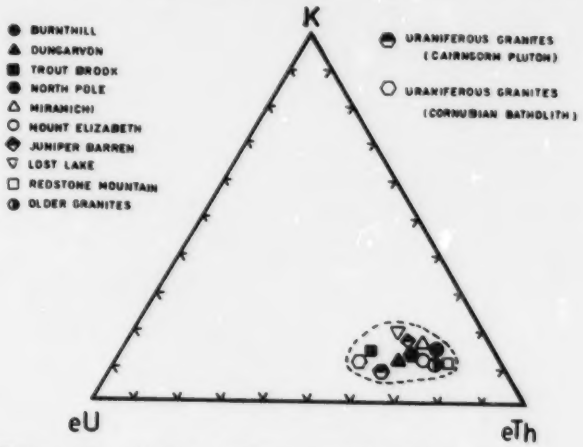

Figure 17. eU-eTh-K ternary variation diagram of the selected granitic plutons in the Miramichi Anticlinorium and for some uraniferous granites.

Table 14. Statistical abundances of metals in till samples overlying the granitic rocks of central Miramichi Anticlinorium plutons.

	<2 µm till fraction (clay)			<63 µm till fraction (clay+ silt)		
ELEMENTS	Mean ± St. Dev.	50 percentile (median)	90 percentile	Mean ± St. Dev.	50 percentile (median)	90 percentile
U (ppm)	15.8 ± 12.4	14.3	29.4	5.4 ± 3.7	3.9	11.4
Th (ppm)	–	–	–	18.8 ± 11.2	15.0	31.4
Sn (ppm)	26.8 ± 33.9	20.0	41.0	–	–	–
Mo (ppm)	4.0 ± 7.2	3.0	7.0	2.6 ± 2.4	2.0	4.0
W (ppm)	14.5 ± 15.1	12.0	24.0	3.2 ± 3.9	2.0	8.8
F (ppm)	872.2 ± 323.6	920.0	1250.0	–	–	–
Sb (ppm)	–	–	–	1.3 ± 1.4	0.9	3.2
Au (ppb)	–	–	–	4.1 ± 6.5	3.0	7.0
As (ppm)	57.5 ± 58.2	40.0	136.4	23.8 ± 26.1	18.5	56.4
Mn (ppm)	800.2 ± 346.9	800.0	1120.0	–	–	–
Fe (%)	4.2 ± 0.7	4.1	5.0	3.8 ± 1.1	3.8	5.1
Cu (ppm)	45.4 ± 26.8	39.0	80.0	–	–	–
Pb (ppm)	45.5 ± 14.6	43.0	67.0	–	–	–
Zn (ppm)	142.3 ± 84.8	122.0	197.0	102.6 ± 57.3	100.0	190.0
Ni (ppm)	50.0 ± 19.3	50.0	77.2	31.2 ± 18.0	30.0	57.4
Co (ppm)	19.5 ± 7.3	19.0	28.0	12.7 ± 6.1	12.0	20.0
Cr (ppm)	64.2 ± 15.2	66.0	80.4	93.9 ± 30.7	94.0	140.0

Table 15. Matrix of Spearman rank correlation coefficients for metals in 77 till samples overlying the granitic rocks of central Miramichi Anticlinorium plutons (upper left corner, <2 μm till fraction; lower right corner, <63 μm till fraction).

	U	Sn	Mo	W	F	As	Mn	Fe	Cu	Pb	Zn	Ni	Co	Cr	
Cr	−0.16	−0.18	0.22	−0.05	−0.01	0.13	0.15	0.36	0.37	−0.13	0.08	0.42	0.39	1.00	
Co	0.06	0.02	0.23	0.19	0.17	0.15	0.42	0.29	0.48	−0.09	0.07	0.50	1.00		
Ni	−0.12	−0.08	0.13	0.09	0.16	0.37	0.29	0.41	0.54	0.03	0.36	1.00			
Zn	0.06	0.15	0.01	0.16	0.25	0.30	0.25	0.26	0.30	0.36	1.00			1.00	U
Pb	0.22	0.23	0.18	0.23	0.12	0.30	0.10	−0.08	0.15	1.00			1.00	0.95	Th
Cu	0.13	0.15	0.36	0.29	0.22	0.45	0.37	0.29	1.00			1.00	0.50	0.57	Mo
Fe	−0.15	−0.07	0.10	−0.01	0.10	0.12	0.19	1.00			1.00	0.40	0.65	0.77	W
Mn	0.29	0.31	0.13	0.22	0.37	0.19	1.00			1.00	0.08	0.14	−0.27	−0.19	Sb
As	0.08	0.12	0.39	0.31	0.14	1.00			1.00	0.04	−0.20	−0.06	−0.08	−0.10	Au
F	0.22	0.16	0.03	0.16	1.00			1.00	−0.10	0.51	0.53	0.11	−0.04	0.13	As
W	0.38	0.45	0.40	1.00			1.00	0.59	−0.18	0.66	0.28	0.08	−0.31	−0.20	Fe
Mo	0.19	0.20	1.00			1.00	0.51	0.56	−0.11	0.57	0.17	0.15	−0.12	−0.05	Zn
Sn	0.54	1.00			1.00	0.55	0.76	0.59	−0.12	0.67	0.15	0.12	−0.31	−0.20	Ni
U	1.00			1.00	0.75	0.42	0.80	0.50	−0.11	0.57	0.32	0.07	−0.15	−0.02	Co
			1.00	0.57	0.75	0.47	0.72	0.42	−0.04	0.50	−0.07	−0.22	−0.60	−0.50	Cr
			Cr	Co	Ni	Zn	Fe	As	Au	Sb	W	Mo	Th	U	

Table 16. Aeroradiometric abundances of eU, eTh, and K; silica, aluminum, and alkali contents and the amplitude of gravity anomalies for the granitic rocks of the Miramichi Anticlinorium.

Plutons	Aeroradiometric data					Geochemical data							Amplitude of Bouguer gravity anomaly (Mgal)
	n*	eU (ppm)	eTh (ppm)	eTh /eU	K (%)	n*	SiO_2 (%)	Al_2O_3 (%)	CaO (%)	Na_2O (%)	K_2O (%)	$\frac{Al_2O_3}{(CaO+Na_2O+K_2O)}$	
Burnthill	701	2.1 ± 4.1	10.4 ± 2.3	5.0	1.8 ± 0.3	17	76.5	12.7	0.6	3.5	4.7	1.4	-54
Dungarvon	361	2.6 ± 0.8	7.9 ± 1.2	3.0	1.4 ± 0.2	8	76.1	12.9	0.7	3.7	4.6	1.4	-48
Trout Brook	107	4.1 ± 1.2	8.1 ± 1.0	2.0	1.7 ± 0.2	7	75.2	12.9	0.7	3.4	4.6	1.5	-53
North Pole	38	1.9 ± 0.4	6.5 ± 1.0	3.4	1.5 ± 0.2	7	72.7	14.4	1.0	3.4	4.4	1.6	-48
Mount Elizabeth	106	2.5 ± 0.6	8.5 ± 1.9	3.4	1.7 ± 0.4	14	73.7	13.6	1.4	4.6	3.6	1.4	-20
Miramichi		1.9 ± 0.4	7.1 ± 1.2	3.7	1.6 ± 0.2	2	72.8	16.2	1.9	4.3	3.3	1.7	-25
Lost Lake	61	1.7 ± 0.2	5.5 ± 1.1	3.2	1.6 ± 0.2								-50
Redstone Mountain	55	1.4 ± 0.3	6.7 ± 2.3	4.8	1.2 ± 0.5	2	67.6	15.5	2.9	2.2	5.0	1.5	-30
Juniper Barren	110	1.3 ± 0.4	4.5 ± 1.2	3.5	1.1 ± 0.3								-50
Old Granites	61	1.9 ± 0.3	7.6 ± 0.8	4.0	1.4 ± 0.1	15	72.0	14.7	1.4	4.3	3.2	1.4	-35

*n = number of samples.

radioelement concentration in the overburden material is proportional to the amount of radioelement in the underlying bedrocks. The indices thus are believed to be useful in areas covered by overburden material and where outcrops are scarce such as in the Miramichi Anticlinorium.

Pirkle's indices are based on principal component analysis (a multivariate statistical technique that models the distribution of data variance). The variabiality of eU, eTh, and K are attributed to geological processes operating in rocks such as supergene and hydrothermal processes that usually lead to uranium depletion in certain parts of the plutons and its concentration in others.

Under secular equilibrium, the amount of U, Th, and K in rocks is proportional to the radioactive daughter isotopes ^{214}Bi, ^{208}Tl, and ^{40}K respectively.

In airborne gamma ray spectrometry data, the three principal component (PC) analyses for the three variables eU, eTh, and K can be represented as follows:

$$PC1 = a_1K + b_1Bi + c_1Tl \quad \ldots\ldots\ldots\ldots\ldots\ldots \quad (1)$$

$$PC2 = a_2K + b_2Bi + c_2Tl \quad \ldots\ldots\ldots\ldots\ldots\ldots \quad (2)$$

$$PC3 = a_3K + b_3Bi + c_3Tl \quad \ldots\ldots\ldots\ldots\ldots\ldots \quad (3)$$

a, b, and c = factor loadings.

At present we are interested primarily in uranium, therefore we only examine the ^{214}Bi (emitted by U) loadings on PC1, PC2, and PC3 which are designated as UPC1, UPC2, and UPC3, respectively. These loadings can be described as follows:

UPC1 = fraction of U originally deposited within a geological unit.

UPC2 = fraction of U that has been mobilized by concentrating or leaching mechanisms.

UPC3 = portion of U that has not been affected by concentrating or leaching mechanisms and, thus, the amount of nonmobilized U present.

The two uranium favourability indices and their meanings as explained by Pirkle et al. (1982) are:

a) |UPC1/UPC3| ratio:

The ratio provides an indicator of the absolute uranium mobilization. Large values indicate that most of the originally deposited uranium is available for transportation while small values indicate little uranium available for transportation.

b) |UPC2/UPC3| ratio:

This ratio indicates the proportion of mobilized relative to nonmobilized uranium. Large values indicate that most of the uranium available for transportation has been mobilized and small values of the ratio indicate little mobilization.

A large |UPC1/UPC3| ratio accompanied by large |UPC2/UPC3| ratio means, according to Pirkel et al. (1982), that the geological unit is favourable for uranium mineralization. Hence, the larger the ratio the higher the favourability.

The principal component analysis technique has been tested successfully in uranium-producing areas in U.S.A. such as Shirley Basin, Wind River Basin, and South Texas Coastal Plain (Pirkle et al., 1982). It has been shown that all of the more favourable areas have |UPC1/UPC3| values greater than 2.

Pirkle's technique was applied on the aeroradiometric data of the Miramichi Anticlinorium in order to determine the favourability of the granitic plutons. The ratios of the uranium loadings (|UPC1/UPC3| and |UPC2/UPC3|) were calculated by using a computer program adopted from Statistical Analysis System (1982). The results of the analysis are given in Table 17.

A plot of |UPC1/UPC2| versus |UPC1/UPC3| ratios for the granitic plutons is shown in Figure 18. The plot illustrates that the favourability of the plutons is in the following order: the Miramichi Pluton (least favourable), Lost Lake Pluton, Burnthill Pluton, Dungarvon Pluton, Juniper Barren Pluton, older granites, North Pole Pluton, Redstone Mountain Pluton, Trout Brook Pluton, and the Mount Elizabeth Pluton (most favourable). However, the results of the analysis is not as encouraging as was expected because some plutons with no uranium associations appear to be most favourable (e.g., Mount Elizabeth and Redstone Mountain) while others with known uranium mineralization appear to be less favourable (e.g., Burnthill and Dungarvon plutons). Possible explanation for this situation is that all of these plutons are geochemically favourable for uranium mineralization but the ones with no known uranium association may have suffered less than other plutons in terms of geological disturbances, such as fracturing, veining, hydrothermal alterations, and weathering, that may have aided in uranium leaching and concentration. Alternatively, these plutons have received less attention than the other plutons by exploration companies. However, it is encouraging that application of this technique also indicates the favourability of the Trout Brook Pluton as was noted previously in this section.

Long Lake area

The digitized data of eU, eTh, and K were processed statistically in order to define radioelement anomalies. The statistical abundances of aeroradiometric eU, eTh, and K contents in various rock units of the Long Lake area are shown in Table 18. The data show that the eU, eTh, and K contents in the biotite-muscovite granite are higher than contents in the biotite granite of the North Pole Pluton. Unexpectedly the mean eU and eTh, contents in the older (foliated) granite are higher than the contents in the North Pole Pluton. This situation is also noticed in the geochemical data previously discussed in this report. The arithmetic means and standard deviations of eU, eTh, and K for the Long Lake map area were calculated to be 1.80 ± 0.41 ppm, 6.30 ± 1.20 ppm, and $1.30 \pm 0.30\%$, respectively. The arithmetic means plus two standard deviations were considered as the threshold levels for eU, eTh, and K in the area. Areas with radioelement contents above the arithmetic means are shown on Figure 19. Areas that exceed the mean plus two standard deviations

Table 17. Uranium favourability indices for the granitic plutons in the Miramichi Anticlinorium.

Pluton Name	n*	Eigenvalues	% of Total Variance Explained	Principal Component P.C.	Eigenvectors U	Th	K	Favourability Indices@ |UPC1|/|UPC3|	|UPC2|/|UPC3|
BURNTHILL	189	2.08 0.63 0.28	0.69 0.21 0.10	1 2 3	0.58 -0.57 0.58	0.63 -0.14 -0.76	0.52 0.81 0.27	0.9	0.8
DUNGARVON	101	2.51 0.33 0.15	0.84 0.11 0.05	1 2 3	0.56 0.76 0.34	0.60 -0.09 -0.80	0.57 -0.65 0.50	1.0	1.1
TROUT BROOK	39	2.56 0.38 0.05	0.85 0.13 0.02	1 2 3	0.54 0.81 0.23	0.58 -0.56 0.59	0.61 -0.19 -0.77	6.6	10.5
NORTH POLE (muscovite-biotite phase)	19	2.60 0.32 0.08	0.87 0.11 0.02	1 2 3	0.55 0.81 0.20	0.58 -0.54 0.61	0.60 -0.22 -0.77	2.8	4.1
MIRAMICHI	37	2.54 0.24 0.22	0.85 0.08 0.07	1 2 3	0.58 -0.32 -0.75	0.58 0.81 0.10	0.58 -0.49 0.65	0.8	0.4
MOUNT ELIZABETH	106	2.69 0.25 0.06	0.90 0.08 0.02	1 2 3	0.56 0.83 0.04	0.59 -0.36 -0.72	0.59 -0.42 0.69	14.0	20.8
JUNIPER BARREN	110	2.62 0.30 0.08	0.87 0.10 0.03	1 2 3	0.57 -0.70 0.43	0.60 -0.01 -0.80	0.56 0.71 0.42	1.3	1.6
LOST LAKE	61	1.50 1.01 0.50	0.50 0.34 0.16	1 2 3	0.70 -0.19 0.69	0.11 0.98 0.17	0.71 0.04 -0.70	1.0	0.3
REDSTONE MOUNTAIN	55	2.64 0.28 0.08	0.88 0.09 0.03	1 2 3	0.55 0.82 0.16	0.60 -0.25 -0.76	0.58 -0.52 0.63	3.4	0.4
OLDER GRANITE	61	1.98 0.72 0.30	0.66 0.24 0.10	1 2 3	0.49 0.84 0.23	0.59 -0.51 0.62	0.64 -0.17 -0.75	2.1	3.7

@ UPC1 represents original U deposited in rock unit
UPC2 represents the mobilized U
UPC3 represents the nonmobilized U
*n = number of samples.

(anomalous values) are also indicated on Figure 19, which shows two prominent anomalous areas, one located on the eastern side of Long Lake over the North Pole Pluton and the other in the northeastern corner over the Ordovician (deformed) granites (Fig. 19). The radiometric anomaly over the North Pole Pluton coincides with anomalous uranium concentrations along highly altered and brecciated quartz-bearing faults (Fig. 3), and with a large negative Bouguer gravity anomaly (Fig. 8).

The radiometric anomaly over the Ordovician granites (Fig. 19) is oriented parallel to a fracture system (northwest-trending) known to intersect the granite, and may be related to a late phase uranium-bearing quartz-feldspar porphyry dyke of the North Pole Pluton (Fig. 3).

Airborne radiometric profiles of eU and eTh concentrations and eU/eTh ratios across the Long Lake area were plotted against their corresponding geological cross-sections for comparison (Fig. 20, 21, and 22). The locations of these profiles are shown on Figure 19.

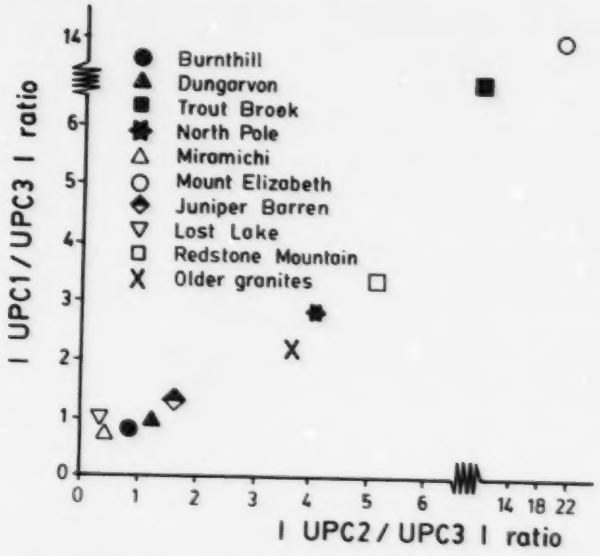

Figure 18. Plot of |UPC1/UPC3| versus |UPC2/UPC3| ratio for selected granitic plutons in the Miramichi Anticlinorium. The higher ratios indicate higher favourability for uranium occurrences.

The mean eU and eTh concentrations and eU/eTh ratios were assumed to represent the background levels of these parameters in the Long Lake area. Charbonneau et al. (1976) found that in the Canadian Shield, an airborne measurement of 1 to 2 ppm eU corresponds to a concentration of 2 or 3 ppm in the overburden, and 4 to 6 ppm eU in the underlying bedrock. Following the same technique described by Charbonneau et al. (1976), Chandra (1981) has established a relationship between measurements made with the hand-held sensor and the airborne gamma ray spectrometer over several areas in New Brunswick. He demonstrated that about 3 to 4 ppm eU on the airborne maps is related to 5 to 7 ppm eU in drift-covered areas and to 13 to 18 ppm eU in the underlying bedrock. From these results it is reasonable to assume that areas with eU above 1.9 ppm (Fig. 20) are anomalous.

Several narrow and isolated peaks of high eU (Fig. 20) values are apparent along the profiles particularly near Long Lake. These anomalies could be related to U concentration along shear zones, veins, and rock boulders scattered in the area especially on the eastern side of the lake. Furthermore, the anomalies of eU appear to be stronger in the southern part of the area relative to the northern part (Fig. 20).

The aeroradiometric eTh concentration profiles (Fig. 21) appear to have smooth patterns of distribution in comparison with the eU profiles. Furthermore, the values of eTh along the profiles are more or less close to the background level (Fig. 21).

Table 18. Statistical abundances of aeroradiometric eU, eTh, and K contents in various rock units of the Long Lake area.

Rock Units		No. Samples	Mean ± St. Dev.			
			eU (ppm)	eTh (ppm)	K %	$\frac{eU}{eTh}$
Lower Devonian	Biotite-muscovite granite	19	1.96 ± 0.36	6.56 ± 1.08	1.58 ± 0.17	0.30 ± 0.06
	Biotite granite	19	1.83 ± 0.42	6.52 ± 0.89	1.46 ± 0.28	0.28 ± 0.04
	Gabbro	5	1.24 ± 0.29	4.82 ± 0.40	0.86 ± 0.05	0.26 ± 0.05
Ord.	Foliated granite	25	2.05 ± 0.35	7.06 ± 1.05	1.31 ± 0.20	0.29 ± 0.02
Cambro-Ord.	Metasedimentary rocks	31	1.57 ± 0.29	5.47 ± 0.83	1.05 ± 0.21	0.29 ± 0.05
Precam.	Amphibolite	3	1.81 ± 0.15	6.83 ± 0.86	1.45 ± 0.82	0.27 ± 0.01

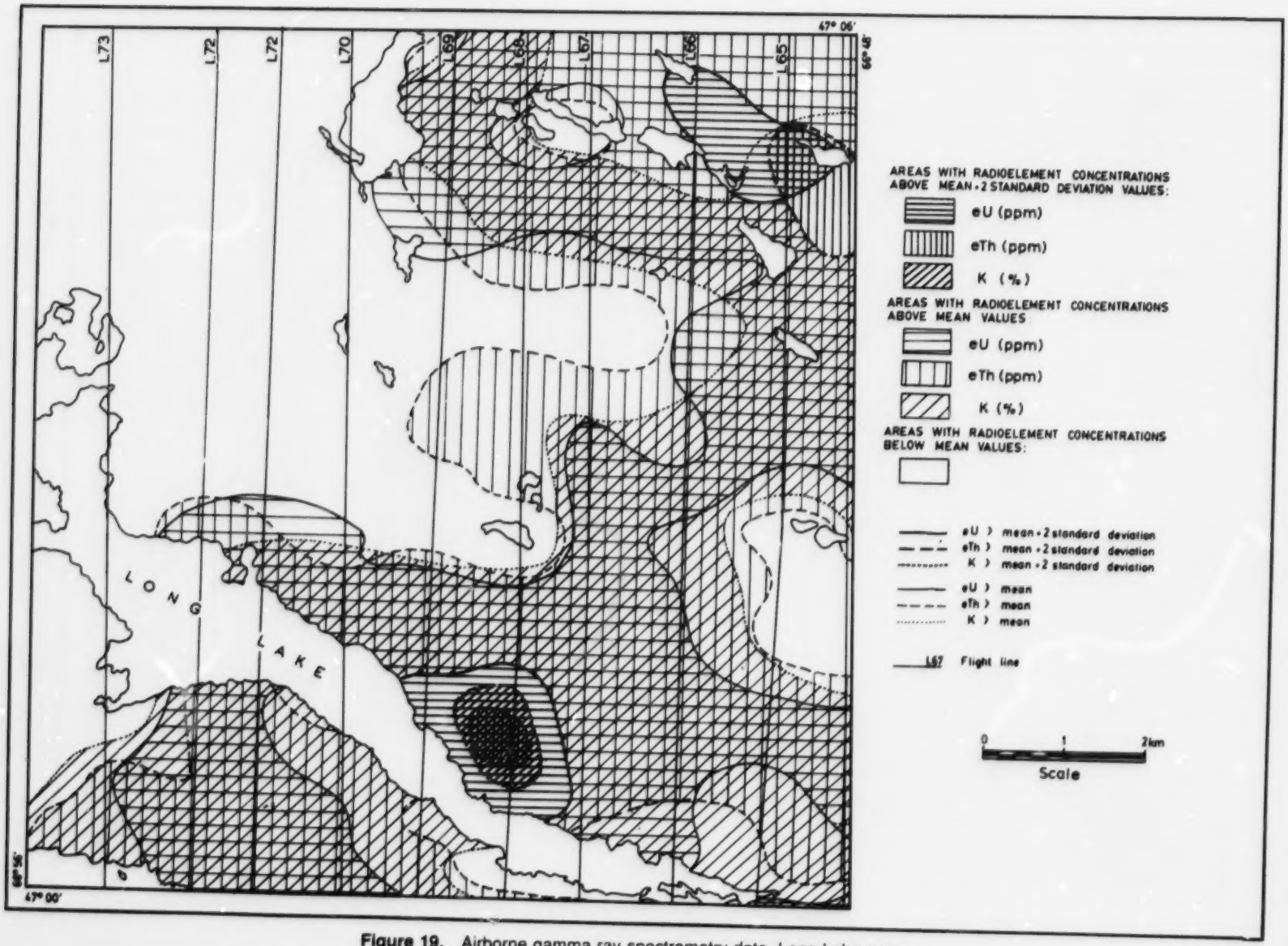

Figure 19. Airborne gamma ray spectrometry data, Long Lake area.

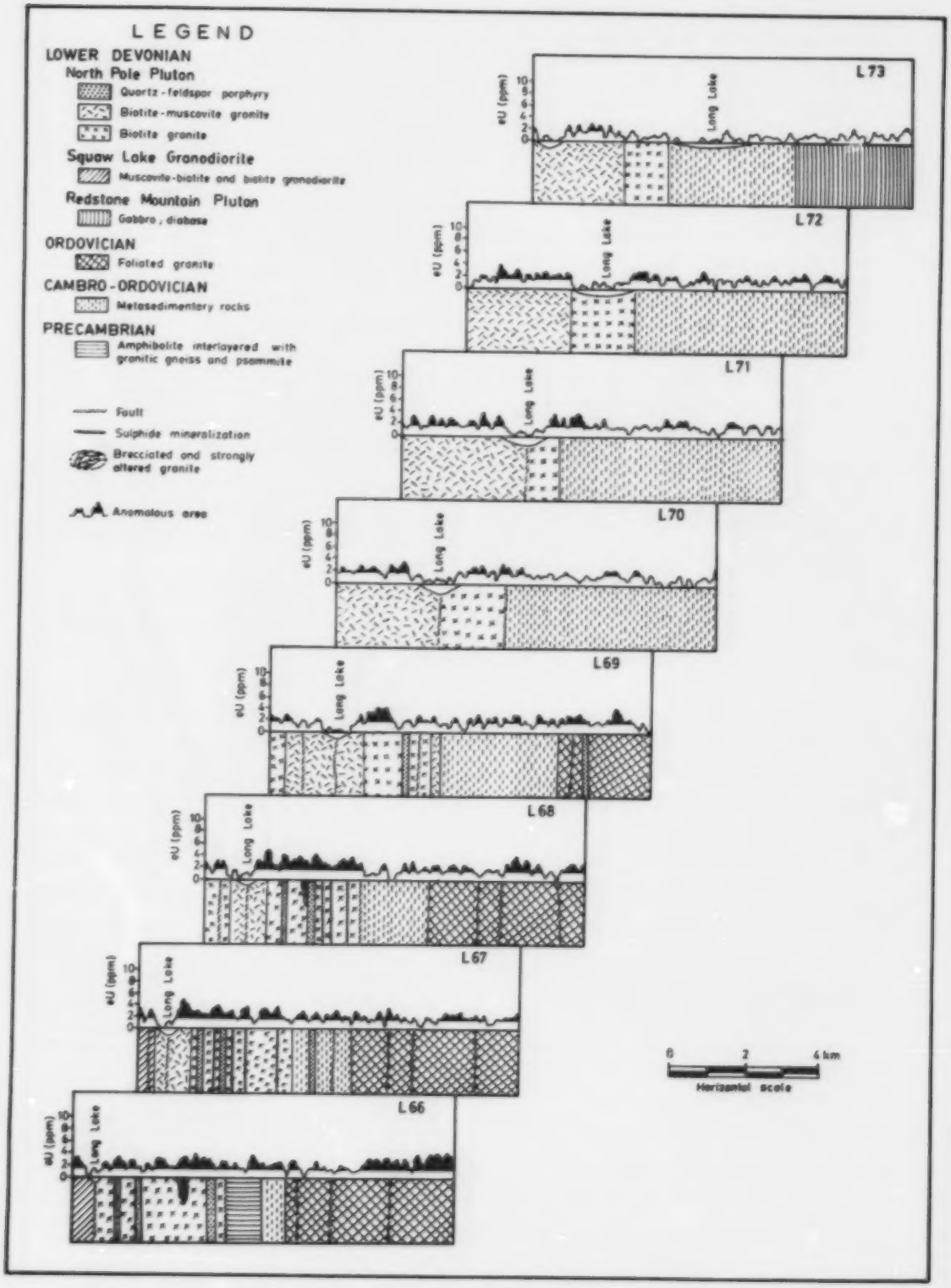

Figure 20. Plots of airborne eU profiles across the Long Lake area.

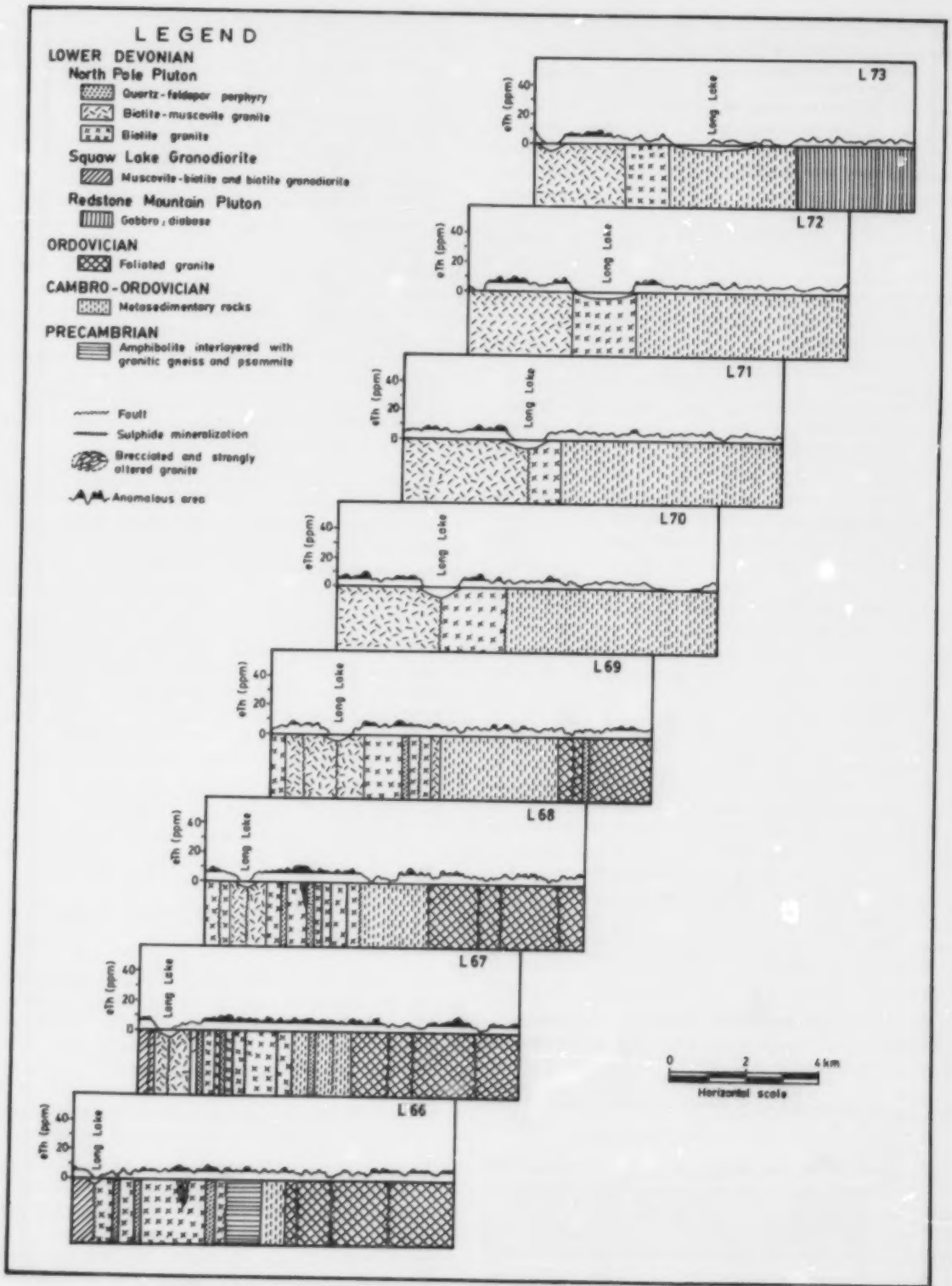

Figure 21. Plots of airborne eTh profiles across the Long Lake area.

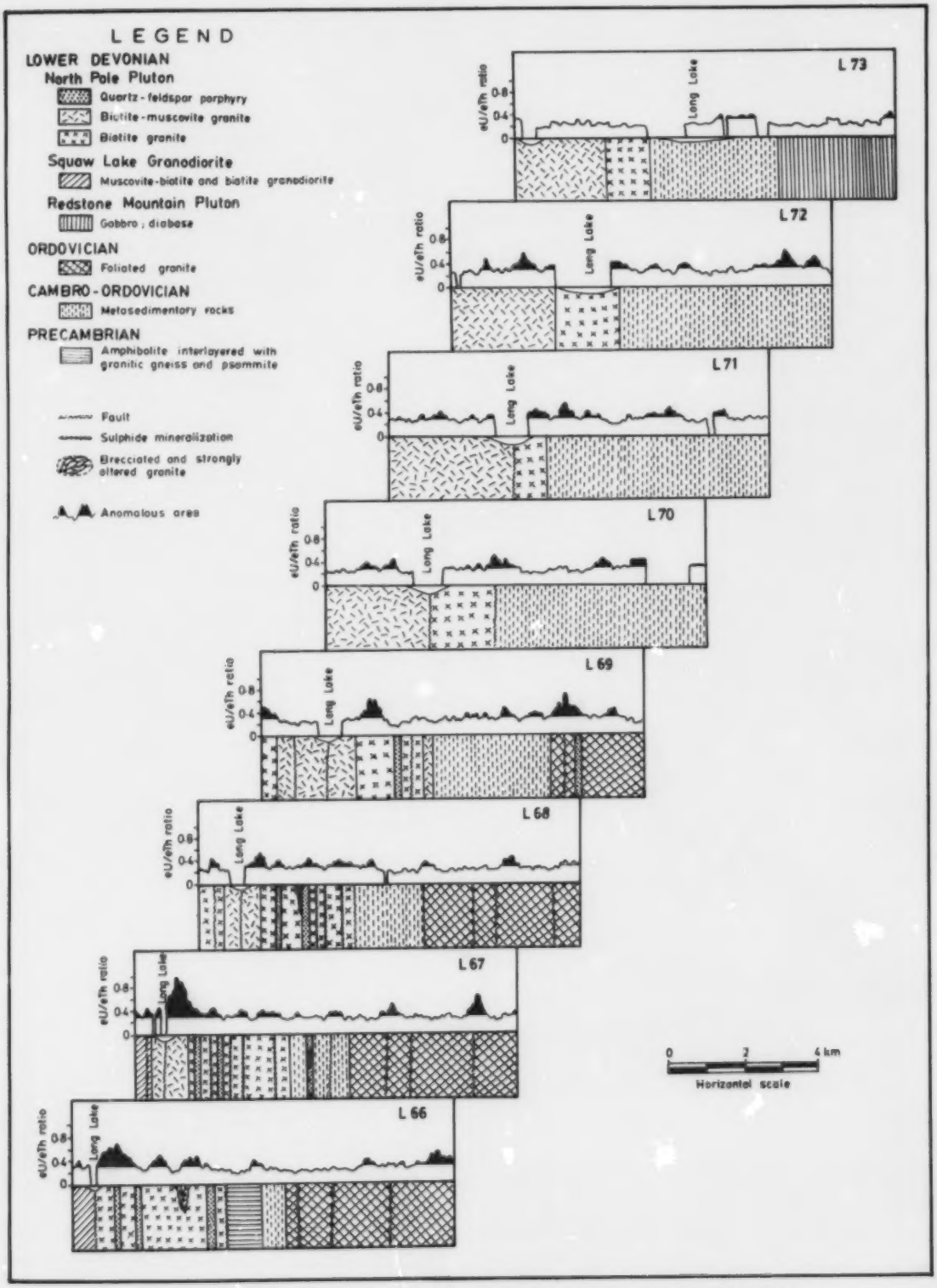

Figure 22. Plots of airborne eU/eTh ratio profiles across the Long Lake area.

The uniform distribution of eTh along the profiles and its near normal concentration relative to eU distribution might be explained by the geochemical behaviour of U and Th in crystalline rocks. During magmatic evolution (reducing environment), both U and Th are tetravalent and have similar ionic radii. They therefore behave similarly and become progressively concentrated in later phases of crystallization. In the late stages of magma crystallization, and during postcrystallization processes (oxidation environment) such as weathering, metamorphism, and hydrothermal alteration, tetravalent uranium is unstable and readily changes to the hexavalent state, whereas Th retains its tetravalent state. Uranium and thorium therefore follow strikingly different paths because of the decrease in the "ionic radius" of uranium consequent to its transformation to the hexavalent state, which makes it readily mobilized from the rocks and available to enter hydrothermal solutions or low temperature meteoric water. Thorium is retained in the rocks and more or less maintains its level of concentration.

On the eU/eTh ratio profiles (Fig. 22), several narrow and isolated peaks of highly anomalous values are shown. These peaks are intensified in the southern part of the area relative to its northern part. A strong eU/eTh anomaly appears on the eastern side of Long Lake where most of the uranium mineralization occurs.

It is of interest also to note that some anomalous peaks of eU/eTh ratio occur above the Ordovician (older) granites (Fig. 22). Visual inspection of these peaks reveals that they are correlated well with faults. This also conforms with the geochemical data in which anomalous uranium in spring and stream sediment samples was found in the area underlain by the Ordovician granites (see Fig. 10).

Narrow eU anomalies accompanied by narrow eU/eTh ratio anomalies such as the one shown in Long Lake area are considered to be the most desirable type of anomaly for uranium exploration (Richardson and Carson, 1976).

Central Miramichi Anticlinorium area

Aeroradiometric data

Visual inspection of the aeroradiometric maps of the area reveals that the granitic plutons are associated with high eU, eTh, and K anomalies. A contour map of the aeroradiometric eU data is shown in Figure 23. The strongest and the broadest eU anomalies are associated with the Burnthill Pluton. Most are confined to the eastern and southeastern margins of the intrusion where much of the Sn, W, and Mo mineralization has been reported to occur.

By combining the aeroradiometric eU map (Fig. 23) with the Bouguer gravity map of the same area (Fig. 11), it is shown that the highest eU anomalies coincide with the centre of the large negative gravity anomaly, a feature noticed by the present authors (Hassan and McAllister, 1988) in the U-bearing granites of the Lower Devonian North Pole Pluton.

The airborne gamma ray spectrometry data of eU, eTh, and K over the granitic rocks of the Burnthill, Dungarvon, Trout Brook, and Rocky Brook plutons are digitized at 400 m square grids. The digitization was performed in order to interpret the data semi-quantitatively.

Means and standard deviations of eU, eTh, and K contents were computed for various phases of the granitic plutons. Results are summarized in Table 19. Within individual plutons, the equigranular and the melanocratic granite phases have slightly higher U and Th contents than other phases. On average, the Trout Brook Pluton has the highest eU and to lesser extent eTh and K contents of the four (Table 19).

The 50 percentile (median) and the 90 percentile values for eU were calculated for the aeroradiometric data in the granitic plutons (Table 19). The median of the data was chosen to represent the threshold level of eU as indicated on the airborne data. Anomalous areas (> 50 percentile) of eU and highly anomalous areas (> 90 percentile) in the airborne data were plotted on a map (Fig. 24). By combining the eU anomalies map (Fig. 24) with the geological map (Fig. 6), it is shown that the granitic plutons are associated with anomalous eU. The Dungarvon Pluton is associated with an eU aeroradiometric anomaly in its northeastern part (Fig. 24), where uranium mineralization has been located along shear zones trending northwesterly (Fyffe and MacLellan, 1988). The granitic rocks of the Trout Brook Pluton are totally anomalous in eU with the highest anomalous eU values restricted to its centre. Visual inspection of the maps reveals that the eU anomalies are generally associated with the equigranular granite phase of the plutons.

In situ gamma ray spectrometry data

The eU anomalies outlined on the airborne gamma ray spectrometry maps (Fig. 23) were examined on the ground by the authors. In situ gamma ray spectrometry was used to determine the amount of eU, eTh, and K in the rocks. Although most of the anomalies were found to be associated with granitic rocks that contain above average eU and eTh relative to normal granites, no economically significant deposits were found. Some anomalies appeared also to be fictitious, resulting either from large areas of rock outcrops surrounded by dense soil-covered areas or to hill or cliff exposures of granitic rocks.

In situ gamma ray spectrometry values of eU, eTh, and K determined for various rock types of the plutons are given in Appendix VII. These data confirm that the late stage equigranular phase of the granite in the plutons is associated with a relatively higher amount of radioelements than the seriate porphyritic granite.

Means and standard deviations of eU, eTh, and K contents for various phases of the granitic plutons are given in Table 19. The mean eU and eTh contents of the rocks of the Burnthill, Dungarvon, Trout Brook and Rocky Brook plutons are 15.0 ppm, 12.9 ppm, 21.3 ppm and 13.7 ppm, respectively for eU and 35.3 ppm, 26.1 ppm, 23.4 ppm, and 30.0 ppm, respectively for eTh (Table 19). These values exceed the global average for uranium and thorium in granitic rocks by substantial amounts (according to Taylor, 1964, granites contain, on average, worldwide, 4.0 ppm U

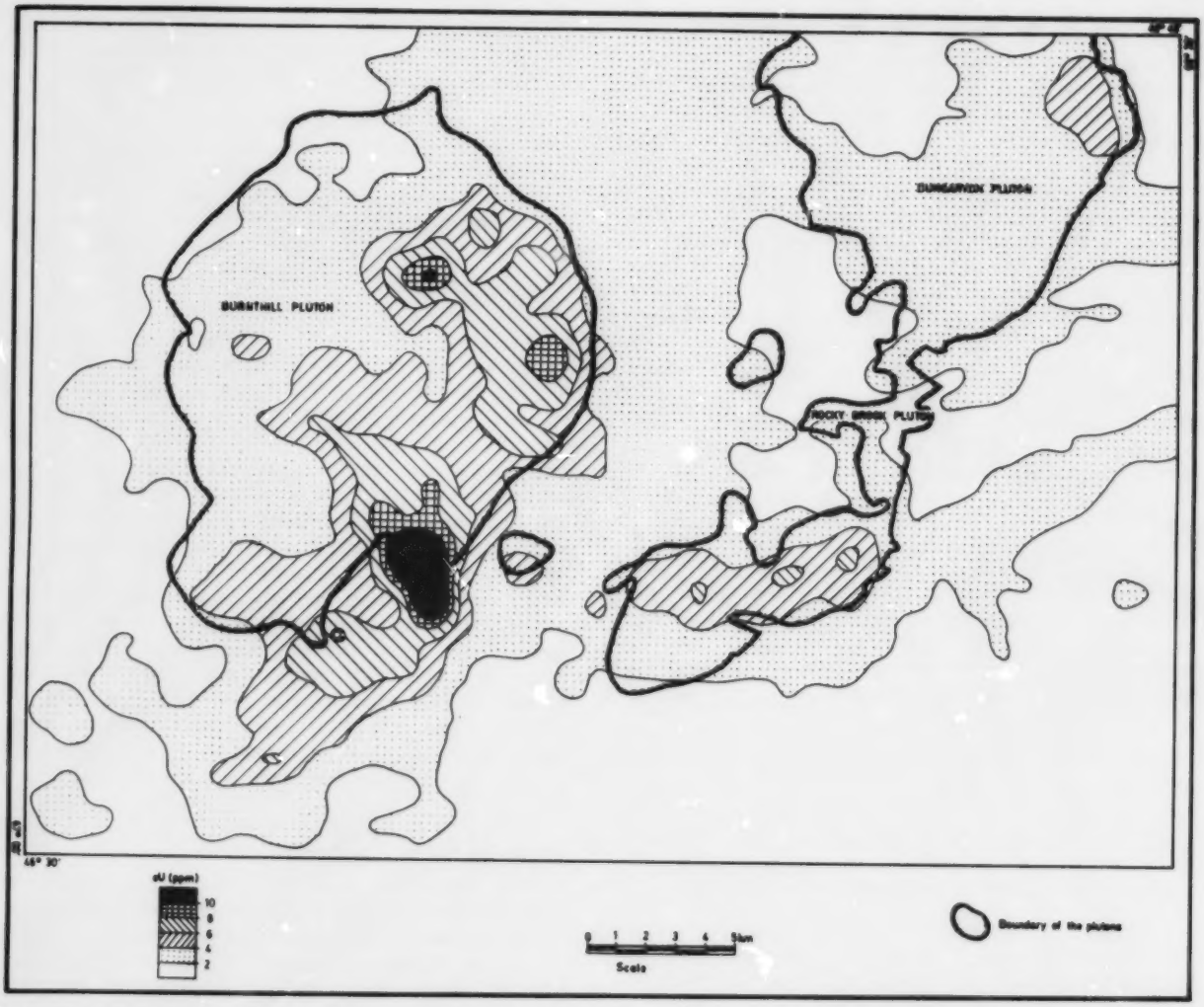

Figure 23. Equivalent uranium aeroradiometric map of the granitic plutons, central Miramichi Anticlinorium.

and 17.0 ppm Th). Furthermore, Table 19 indicates that eU and to some extent eTh contents tend to increase in the younger granitic phases. The in situ data also confirm the airborne data that the Trout Brook pluton contains more uranium than the others.

In situ radiometric determinations of eU, eTh, and K were also made for the dykes and pods that intruded the plutons (Table 20). They are in general enriched with both U and Th. Both eU and eTh appear to be high in the aplitic dykes relative to other types of dykes.

A triangle plot of in situ gamma ray data for eU, eTh, and K contents in the granitic plutons illustrates that the Burnthill, Dungarvon, and Rocky Brook plutons lie close to each other on the diagram (Fig. 25). The Trout Brook Pluton, however, contains a higher amount of eU and lower eTh than the others. It was also previously identified (Fig. 18) as being more favourable for uranium mineralization than the Burnthill and Dungarvon plutons on the basis of their uranium favourability indices.

In order to determine the role of postmagmatic geological processes on the distribution of eU, eTh, and K a set of in situ gamma ray spectrometry readings were taken over rocks effected by weathering, alteration, and joints. The mean values are shown in Table 21. These data are illustrated graphically on a diagram (Fig. 26). For consistency, only readings from one phase of the granite, the coarse grained seriate porphyritic granite is represented.

It is obvious from Figure 26, that eU was slightly depleted in the weathered and altered granites relative to fresh granites. However, eU appears to be concentrated along fractures. With regard to eTh, it more or less retains constant concentration in the weathered and altered rocks but its concentration apparently has increased in the fractured rocks. Potassium appears to follow behaviour similar to thorium.

Table 19. Means and standard deviations of U, Th, and K contents and 50 and 90 percentile contents of U measured by means of in situ and airborne gamma ray spectrometry for different rock types of the granitic plutons (aeroradiometric data are in brackets).

ROCK TYPE	BURNTHILL PLUTON				DUNGARVON PLUTON				TROUT BROOK PLUTON				ROCKY BROOK PLUTON			
	n*	U (ppm)	Th (ppm)	K (%)	n	U (ppm)	Th (ppm)	K (%)	n	U (ppm)	Th (ppm)	K (%)	n	U (ppm)	Th (ppm)	K (%)
Microgranite	31	17.0±10.2	35.3±9.5	5.6±1.5	2	17.1	31.9	5.91	1	25.0	24.2	6.9	–	–	–	–
and aplite	57	(3.9±1.5)	(12.1±2.0)	(1.8±0.2)	–	–	–	–	–	–	–	–	–	–	–	–
Equigranular	27	16.4±3.6	32.7±6.9	5.8±0.9	13	12.2±3.7	24.5±5.8	4.7±0.8	55	21.3±4.5	23.4±4.1	6.3±1.0	49	14.0±3.2	30.6±4.8	5.7±0.6
granite	176	(5.2±2.5)	(11.6±2.0)	(1.8±0.3)	150	(2.9±0.9)	(8.4±1.4)	(1.5±0.2)	46	(4.0±1.4)	(8.0±1.3)	(1.7±0.3)	17	(2.4±0.4)	(7.1±1.1)	(1.3±0.1)
Porphyritic	94	14.5±5.2	36.4±9.5	5.8±0.9	41	13.0±2.1	27.4±3.9	5.1±0.5	–	–	–	–	–	–	–	–
granite	445	(4.3±1.9)	(9.7±2.1)	(1.8±0.2)	189	(2.3±0.6)	(7.5±1.0)	(1.4±0.1)	60	(4.2±1.0)	(8.2±0.8)	(1.7±0.2)	4	(2.1±0.1)	(5.9±0.4)	(1.2±0.1)
Melanocratic	–	–	–	–	17	13.3±3.9	24.8±5.6	5.3±0.9	–	–	–	–	–	–	–	–
granite	23	(5.2±1.1)	(11.6±1.5)	(1.6±0.2)	22	(2.5±0.3)	(8.6±0.6)	(1.6±0.0)	1	(5.4)	(9.0)	(2.0)	–	–	–	–
Average	174	15.0±6.3	35.3±10.3	5.7±1.1	75	12.9±3.1	26.1±5.1	5.1±0.7	57	21.3±4.4	23.4±4.0	6.3±1.0	54	13.7±3.3	30.0±6.1	5.5±0.9
(all phases)	701	(2.1±4.1)	(10.4±2.3)	(1.8±0.3)	361	(2.6±0.8)	(7.9±1.2)	(1.4±0.2)	107	(4.1±1.2)	(8.1±1.0)	(1.7±0.2)	21	(2.3±0.3)	(6.9±1.1)	(1.3±0.1)
50 percentile	174	14.0	–	–	75	12.6	–	–	57	21.2	–	–	54	12.9	–	–
(all phases)	701	(4.1)	–	–	361	(2.5)	–	–	107	(4.2)	–	–	21	(2.3)	–	–
90 percentile	174	22.1	–	–	75	17.2	–	–	57	26.2	–	–	54	19.2	–	–
(all phases)	701	(7.2)	–	–	361	(3.4)	–	–	107	(5.6)	–	–	21	(2.9)	–	–

* n = number of samples

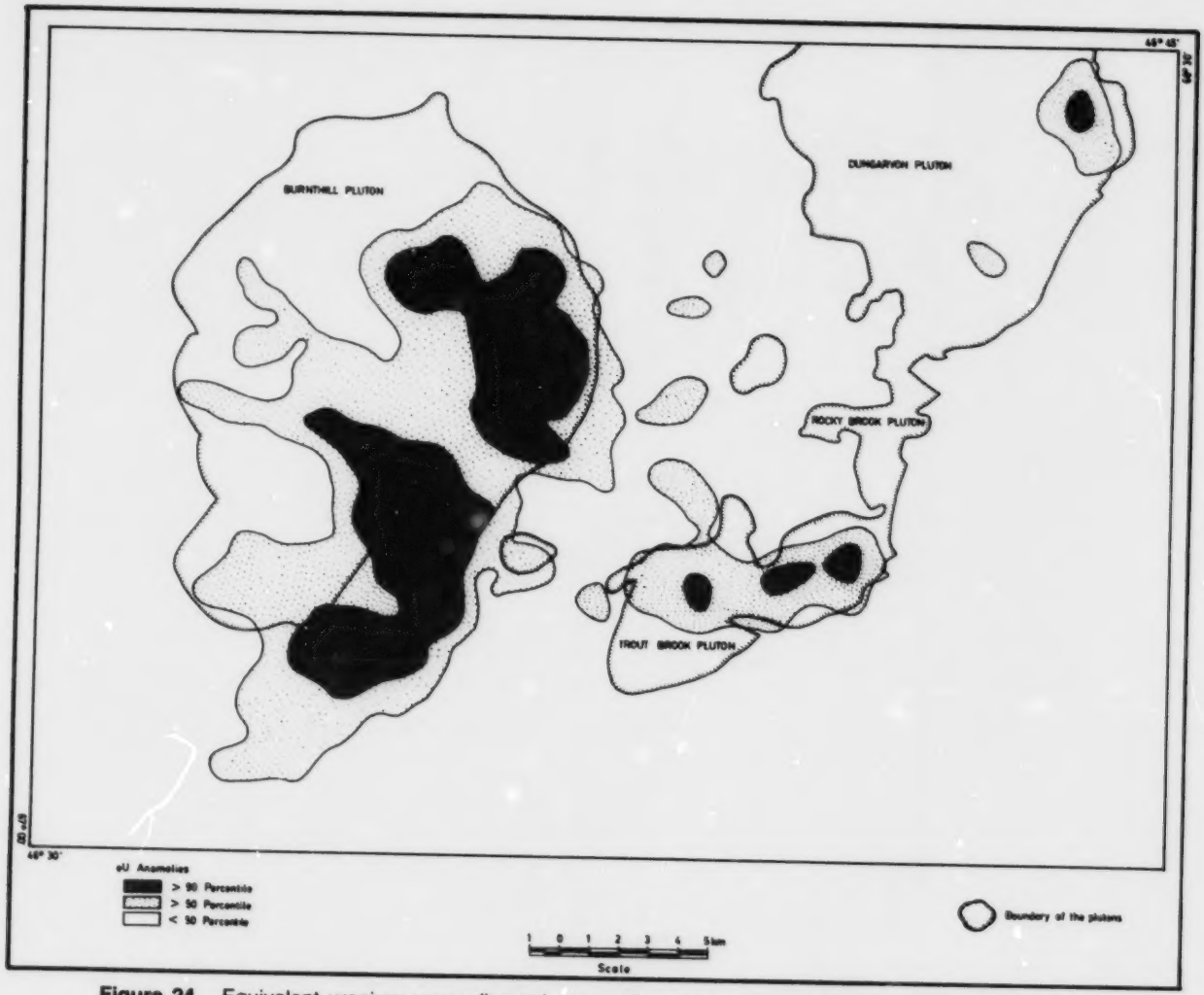

Figure 24. Equivalent uranium aeroradiometric anomalies of the granitic plutons, central Miramichi Anticlinorium.

RELATIONSHIPS OF URANIUM AND OTHER METALLOGENIC ELEMENTS TO THE PETROCHEMICAL CHARACTERISTICS OF THE GRANITIC ROCKS

Overview

Uranium and other metallogenic elements such as those found in Sn, W, and Mo deposits around the world are directly linked to granitic rocks. This link can be observed also in the Miramichi Anticlinorium (Fig. 1) where these elements appear to be associated in time and space with the younger postorogenic, undeformed, granitic plutons. The apparent genetic role of the plutons, as established by the temporal and spatial relationship with the mineral deposits, is further explained below by examining those petrochemical features which may be useful in identifying those granitic bodies most likely to have produced ore bodies.

North Pole Pluton

Whole rock geochemistry

A total of nineteen whole rock analyses, including both fresh and variably altered samples, were obtained from the New Brunswick Department of Natural Resources and Energy (Fyffe and Pronk, 1985) and used in the present work. Sample locations and the analytical results are given in Appendix VIII.

Averages for the major and selected trace elements as well as the normative composition of various phases of the North Pole Pluton are presented in Table 22. Geochemical abundances of these elements in normal granites and uraniferous granites are also given in Table 22 for comparison.

Geochemically the North Pole Pluton is a highly evolved granite (SiO_2 >70 wt. %), and, as are uraniferous granites, is characterized by high SiO_2, K_2O, and Na_2O

Table 20. Means and standard deviations of in situ radiometric eU, eTh, and K contents in various types of dykes and pods intersecting the granitic plutons.

	n*	eU(ppm)	eTh(ppm)	K(%)
BURNTHILL				
Aplite dyke	13	15.2 ± 5.8	37.6 ± 15.3	6.0 ± 0.9
Pegmatite pod	5	12.3 ± 3.4	35.0 ± 15.8	5.8 ± 1.1
Quartz dyke	1	10.5	30.2	4.5
Mafic dyke	3	4.6 ± 2.1	11.6 ± 4.1	3.4 ± 2.0
DUNGARVON				
Aplite dyke	1	9.4	18.5	4.1
Feldspar dyke	1	5.4	13.4	4.1
TROUT BROOK				
Feldspar dyke	1	22.7	23.2	7.4
ROCKY BROOK				
Aplite dyke	1	10.5	25.4	5.0
Quartz dyke	4	10.9 ± 22.9	22.9 ± 4.4	3.3 ± 1.0

* n = number of samples

Table 21. In situ gamma ray spectrometry values of eU, eTh, and K in the coarse grained seriate porphyritic granitic rocks that have undergone various postmagmatic processes.

	n*	eU(ppm)	eTh(ppm)	K(%)
Apparently fresh samples	65	15.1	35.7	5.8
Weathered	9	13.0	36.5	5.4
Altered	7	12.0	34.1	5.4
Fractured	5	18.9	44.5	6.4

* n = number of samples.

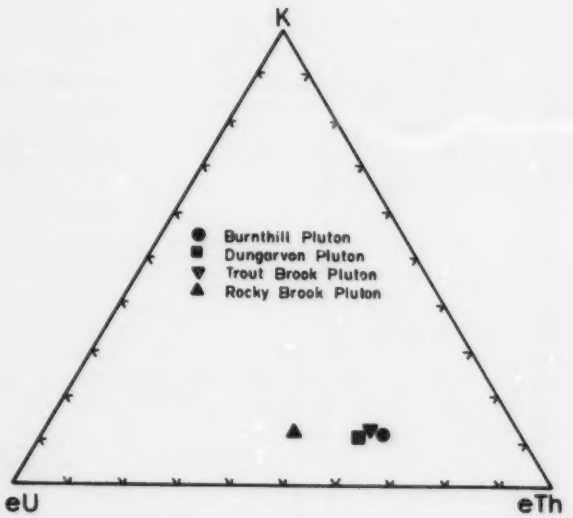

Figure 25. eU-eTh-K ternary variation diagram for in situ gamma ray data of U, Th, and K contents in the granitic plutons, central Miramichi Anticlinorium.

contents relative to normal granites, particularly for the two-mica phases (Table 22). The TiO_2, Fe_2O_3, FeO, MgO, and CaO contents are low in both North Pole Pluton and uraniferous granites relative to normal granites.

The trace element composition varies dramatically within the various phases of the North Pole Pluton (Table 22). The biotite granites and the biotite-muscovite granites contain base metal values higher than in normal granites. Tin abundance is high in the biotite-muscovite granites in comparison to normal granites and uraniferous granites (Table 22). The Ba, F, and Li contents are low in North Pole Pluton relative to normal and uraniferous granites. Rubidium values are high relative to normal granites (a feature of uraniferous granite as well). Strontium and zirconium contents in the North Pole Pluton are lower than in normal granites and in uraniferous granites (Table 22).

Uranium content in the various granitic phases of North Pole Pluton is slightly higher than the average uranium content in normal granites but is lower than in the uraniferous granites of the British Isles and Nova Scotia (Table 22). This may suggest that the North Pole Pluton is derived from rocks originally poor in uranium. Alternatively, uranium may have been depleted from the surface rocks, possibly by meteoric water.

Table 22. Average of major and trace elements in fresh and altered rocks of various phases of the North Pole Pluton and their comparison with normal and uraniferous granites.

Chemical composition	Biotite Granite				Biotite–muscovite granite				Quartz–feldspar porphyry						(a) Average normal granites	Uraniferous Granites	
	Unaltered		Altered with sulphide mineralization		Unaltered		Silicified and brecciated		Unaltered		Mildly altered		Intensely altered			(b) British Caledonides (n = 69)	(c) South Mountain Batholith (n = 136)
	n*	average	n	average	n	average	n	average	n	average	n	average	n	average			
SiO_2(%)	4	71.2	5	72.7	2	73.9	2	83.6	1	76.5	1	76.5	3	76.8	71.3	–	74.48
TiO_2(%)	4	0.44	5	0.39	2	0.15	2	0.14	1	0.15	2	0.12	3	0.14	0.31	0.13	0.06
Al_2O_3(%)	4	14.8	5	14.0	2	14.2	2	8.7	1	13.3	2	13.4	3	12.8	14.32		13.90
Fe_2O_3(%)	4	0.53	5	1.83	2	0.55	2	0.67	1	0.70	2	0.87	3	1.85	1.21	0.88	
FeO(%)	4	2.0	5	3.1	2	1.1	2	0.34	1	0.64	2	0.49	3	1.90	1.64		0.93
MnO(%)	4	0.07	5	0.13	2	0.04	2	0.02	1	0.05	2	0.03	3	0.24	0.05		0.02
MgO(%)	4	0.75	5	0.69	2	0.44	2	0.18	1	0.30	2	0.25	3	0.24	0.71	0.13	0.05
CaO(%)	4	1.29	5	0.12	2	0.74	2	0.11	1	0.28	2	0.09	3	0.10	1.84	0.26	0.75
K_2O(%)	4	4.1	5	4.0	2	4.9	2	3.6	1	4.9	2	5.2	3	3.8	4.07	5.0	4.39
Na_2O(%)	4	3.5	5	0.2	2	3.3	2	0.19	1	3.4	2	0.86	3	0.16	1.68	3.13	3.48
P_2O_5(%)	4	0.10	5	0.09	2	0.09	2	0.06	1	0.0	2	0.03	3	0.06	0.12		0.44
CO_2(%)	4	0.06	5	0.04	2	0.01	2	0.04	1	0.18	2	0.06	3	0.04	0.05		
Be(ppm)	4	6.0	5	4.8	2	6.0	2	7.15	1	6.8	2	8.25	3	5.7	5.0		
Ba(ppm)	4	507.5	5	271.0	2	435.0	2	220.0	1	300.0	2	175.0	3	168.3	600	258	39
Cu(ppm)	4	12.5	5	73.4	2	10.5	2	6.0	1	3.0	2	37.5	3	93.7	10.0	0.0	31
F (ppm)	4	362.5	5	796.0	2	305.0	2	385.0	1	600.0	2	450.0	3	673.3	810.0		4500
Mo(ppm)	4	1.75	5	9.4	2	0.75	2	7.0	1	1.0	2	3.0	3	6.67	1.8		1.4
Pb(ppm)	4	24.0	5	99.6	2	25.0	2	75.0	1	18.0	2	129.5			20.0	26.0	
Rb(ppm)	4	163.8	5	337.0	2	219.0	2	228.5	1	201.0	2	280.0	3	370.7	150.0	455.0	769
B (ppm)	4	4.5	5	27.0	2	3.0	2	52.5	1	–	2	10.0	3	11.3	12		
Sn(ppm)	4	6.73	5	99.8	2	41.0	2	7.05	1	4.6	2	8.0	3	75.3	3.0		39
Sr(ppm)	4	117.0	5	5.67	2	68.5	2	14.5	1	99.0	2	13.5	3	7.0	285.00	67.0	38
Zn(ppm)	4	180.5	5	419.0	2	52.5	2	60.0	1	96.0	2	202.5	3	1313.0	40.0	28.0	86
W (ppm)	4	4.0	5	14.4		–		–		–	2	4.0	3	6.0	1.5		2
Li(ppm)	4	12.75	5	23.8	2	24.0	2	96.0	1	6.0	2	9.5	3	19.0	30.0	75.0	517
Bi(ppm)	4	0.06	5	3.36	2	0.6	2	0.06		–	2	0.08	3	2.2	.15-2		
Zr(ppm)	4	138.8	5	273.0	2	87.5	2	72.5	1	75.0	2	60.0	3	78.3	180.0	65	
S (ppm)	4	62.5	5	1224.0	2	20.0	2	370.0	1	120.0	2	40.0	3	5906.7	330		
U (ppm)	4	5.1	5	5.3	2	4.2	2	7.75	1	4.9	2	17.65	3	11.53	4.0	12.60	8.3
Q(%)	4	30.8	5	54.9	2	33.3	2	69.9	1	37.0	2	52.3	3	60.8	29.06		
C(%)	4	2.5	5	9.6	2	2.3	2	4.5	1	2.1	2	6.4	3	8.5	0.92		
Or(%)	4	24.8	5	24.4	2	29.2	2	22.0	1	29.0	2	31.1	3	23.1	24.50		
Ab(%)	4	29.7	5	1.6	2	28.4	2	1.6	1	28.3	2	7.6	3	1.3	31.13		
An(%)	4	5.8	1	0.7	2	3.1	2	0.1	1	1.1	2	0.3	2	0.2	8.04		
En(%)	4	1.9	5	1.8	2	1.1	2	0.5	1	0.8	2	0.6	3	0.6	–		
Fs(%)	4	2.6	4	4.9	2	1.3	2	0.0	1	0.4	2	0.7	2	3.2	–		
Mt(%)	4	0.8	5	2.4	2	0.8	2	0.5	1	1.0	2	0.8	2	2.0	1.75		
Il(%)	4	0.8	5	0.8	2	0.3	2	0.3	1	0.3	2	0.2	2	0.3	0.58		
Ap(%)	4	0.2	5	0.2	2	0.2	2	0.7	1	0.1	2	0.2	3	0.1	0.28		

(a) Average major oxides and normative composition from Le Maitre (1976); Sr, Rb, Zr, Ni, Zn, Cu, Cr, U, Th, Pb, Co, Li and Be from Taylor (1964); F from Allman and Koriting (1978).

(b) Data from Simpson et. al. (1979) and Plant et. al. (1980).

(c) Data from Clarke and Meucke (1985); U from Chatterjee and Meucke (1982).

* n = number of samples

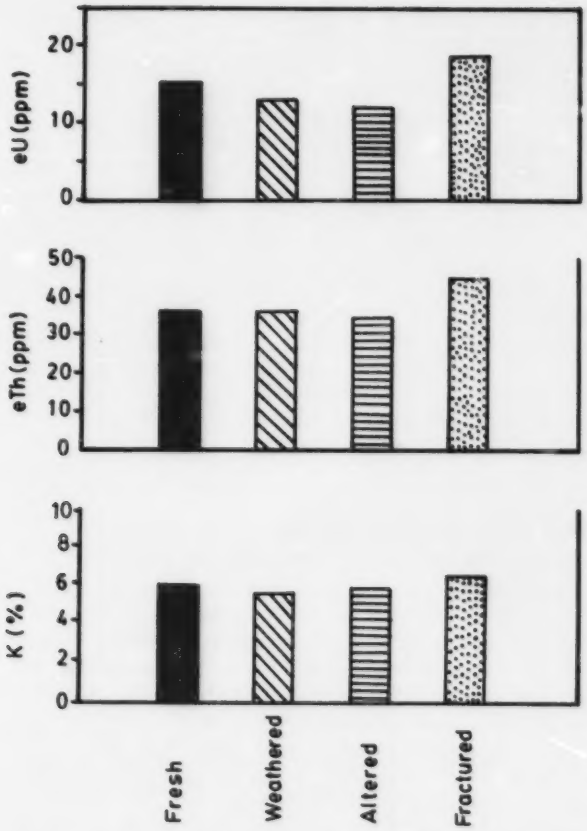

Figure 26. The eU, eTh, and K contents in fresh, weathered, altered, and fractured rock samples of the Burnthill Pluton.

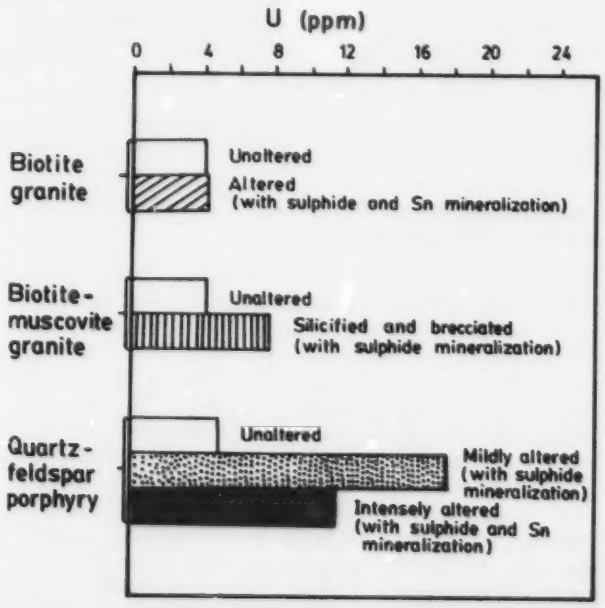

Figure 27. The effect of alteration on uranium content in the North Pole Pluton.

Variation of uranium contents with respect to alteration and mineralization

Variation in uranium content with respect to hydrothermal alteration and mineralization within the various phases of the North Pole Pluton is illustrated in Figure 27. The content appears to be increased considerably in response to hydrothermal alteration, which is apparent in the biotite-muscovite granites where a two-fold increase is noted (Fig. 27), but is most pronounced in the quartz-feldspar porphyry. Furthermore, it appears that uranium in mildly altered rock is more highly concentrated than in intensely altered rocks (Fig. 27).

The effect of mineralization on uranium seems to be varied (Fig. 27). Generally, wherever sulphide mineralization occurs alone in the rocks, uranium content tends to increase considerably, but when sulphide mineralization is accompanied by tin mineralization (Fig. 27), uranium content appears to be lower. This may indicate that uranium and tin have been partitioned from each other during the mineralizing process. Both uranium and tin are incompatible elements and behave similarly at the magmatic stage, but there is evidence that they behave differently during hydrothermal and other mineralization processes (Dubessy et al., 1987; Zagruzina et al., 1987).

Dubessy et al. (1987) have studied the behaviour of uranium and tin during the hydrothermal stage related to the Hercynian granites of France and Great Britain and found that temperature and fugacity of oxygen fO_2 are the main parameters responsible for the contrasting behaviour of the two elements. They found, in general, that at high temperature (>300°C) and low fO_2 (reducing condition), uranium tends to precipitate in the host rocks. Meanwhile, Sn remains in such solutions and is transported to be deposited elsewhere.

Zagruzina et al. (1987) reached similar conclusions during their investigations of about 1000 samples containing uranium and tin from 55 tin deposits in USSR, Czechoslovakia, Mongolia, China, Malaysia, and Australia. They found that much of the uranium in the tin orebodies has been deposited later than the cassiterite (i.e., at lower temperatures). These parameters (T and fO_2) may also be partly responsible for the temporal and sometimes spatial separation of tin and uranium in the granitic rocks of the North Pole Pluton.

Uranium variation with petrochemical indices of North Pole Pluton

Variation diagrams were prepared for U versus SiO_2, U versus felsic index, and U versus degree of oxidation for the granitic rocks of the North Pole Pluton.

The mean U values versus the mean SiO_2 values plot (Fig. 28) for various phases of the North Pole Pluton show that the higher values of U in general are in the more siliceous parts of the granitic rocks. The enrichment of U in the rocks, however, appears to be higher in the altered rocks.

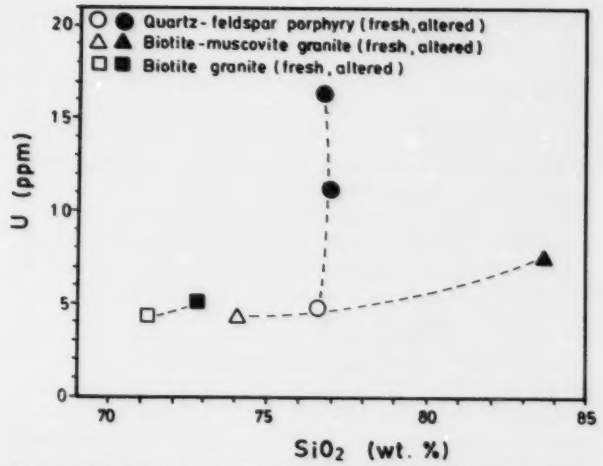

Figure 28. Plot of uranium versus silica, showing for each of the three phases of the North Pole Pluton an increase in uranium content with increase in silica.

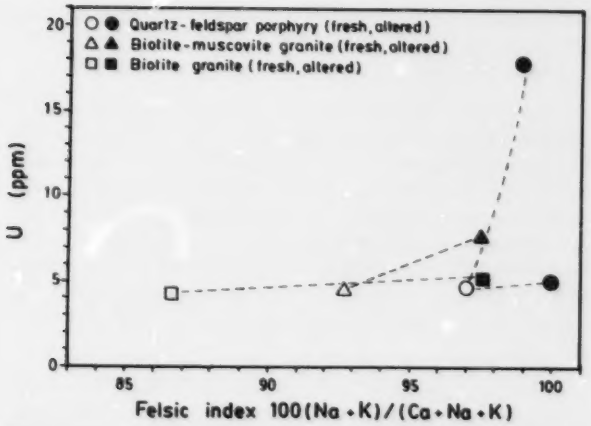

Figure 29. Plot of uranium versus felsic index, showing for each of the three phases of the North Pole Pluton an increase in uranium content with increase in the index.

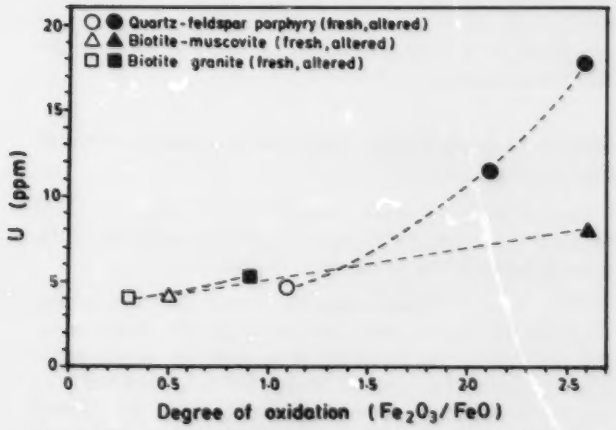

Figure 30. Plot showing increase of uranium with degree of oxidation in the rocks of the North Pole Pluton.

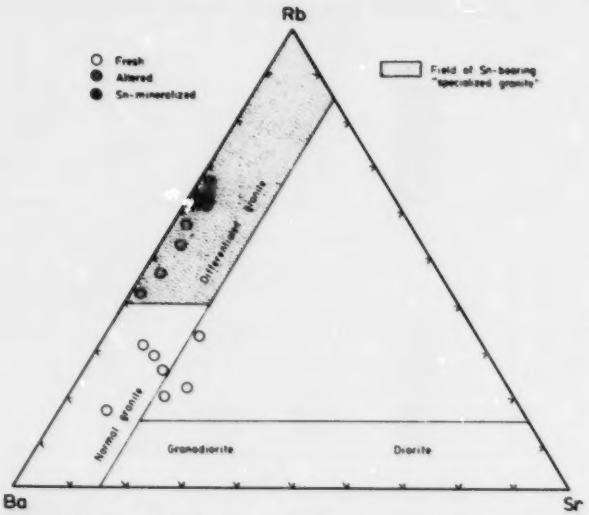

Figure 31. A Rb-Sr-Ba ternary variation diagram for the rocks of the North Pole Pluton (after El Bouseily and El Sokkary, 1975).

The uranium versus felsic index plot (Fig. 29) in granitic rocks of North Pole Pluton reveals that (despite significant degree of magmatic differentiation as represented by the felsic index) the uranium content is almost constant within the fresh rocks of different phases of the pluton. The increase of uranium content with felsic index is most pronounced in the altered rocks of the late-phase quartz-feldspar porphyry (Fig. 29).

The significant effect of fO_2 on behaviour of uranium in the North Pole Pluton is shown in Figure 30, in which the degree of oxidation (Fe_2O_3/FeO) is plotted against uranium content (Fig. 30). The effect is insignificant in fresh rocks but in the altered rocks, uranium increases substantially with degree of oxidation, particularly in the quartz-feldspar porphyry (Fig. 30).

Uranium and tin specialization of the granitic rocks of the North Pole Pluton

The posttectonic, peraluminous, Hercynian granitoids of Europe, and North America are known to contain economic U, Sn, and W deposits (Tischendorf, 1977; Chatterjee et al., 1983; Poty et al., 1986). Attempts have been made by various researchers to distinguish between the specialized granites commonly associated with these deposits and normal granitoids (Tischendorf, 1977; Stemprok, 1979; El Bouseily and El Sokkary, 1975; Chatterjee et al., 1983). Most of these attempts were dependant upon the use of whole rock geochemistry. For example El Bouseily and El Sokkary (1975) used a Rb-Sr-Ba ternary variation diagram (Fig. 31) to classify granites, evaluate differentiation trends, to detect specialization in Sn-bearing granites, and ultimately, to discriminate between Sn-bearing granites (Sn-specialized) and Sn-barren granites.

The Rb, Sr, and Ba contents of the North Pole Pluton have been plotted in such a Rb-Sr-Ba variation diagram (Fig. 31). As shown in Figure 31, the unaltered rocks of the pluton fall within the area of normal granites, and hence they can not be considered as specialized granites. However, the altered and Sn-bearing rocks, which are also enriched with uranium, fall within the area of specialized granites suggesting that both uranium and tin mineralization may favour altered rocks with chemical characteristics of specialized granites.

Among other geochemical criteria used to distinguish between Sn-specialized and normal granitoids are the K-Rb and K-Na ratios. According to Tischendorf (1977) the K-Rb ratio is greater than 100 in normal granites and less than 100 in Sn-bearing (specialized) granites. The K-Rb ratio for the rocks of the North Pole Pluton (Table 23) appears to be lower than 100 in the intensely altered quartz-feldspar porphyry and in the altered biotite granite with sulphide mineralization. These two rocks contain a high tin concentration (Table 23) relative to their corresponding fresh rocks.

The K-Na ratio which, according to Stemprok (1979), is about 1.2 in normal granites and 1.6 in Sn-specialized granites also indicates, with the exception of the unaltered biotite granite, that the granitic rocks of the North Pole Pluton in general are not specialized (Table 23).

Table 23. Selected geochemical parameters distinguishing specialized granites from normal granites for the rocks of the North Pole Pluton.

Rock types	n*	U(ppm)	Sn(ppm)	K/Rb	K/Na
Quartz-feldspar porphyry					
unaltered	1	4.9	4.6	204	1.6
mildly altered	2	17.7	8.0	154	7.2
intensely altered	3	11.5	75.3	86	32.0
Biotite-muscovite granite					
unaltered	2	4.2	41.0	131	30.0
silicified and brecciated	2	7.8	7.1	187	1.7
Biotite granite					
unaltered	4	5.1	6.7	208	1.3
altered and sulphide mineralization	5	5.3	99.8	98	22.0

*n = number of samples

Statistical relationship between uranium and other elements in the North Pole Pluton

Major oxides

To determine the relationship between the contents of uranium and the major mineral-forming oxides of the granitic rocks of the North Pole Pluton, Spearman rank correlation coefficients were calculated (Table 24). In the presumably fresh rocks, uranium correlates weakly to moderately (positive or negative) with the major oxides of the rocks. The only significant and positive correlation is noted between U and Fe_2O_3, SiO_2 and CO_2. The correlation coefficients between uranium and the major oxides in the mineralized samples are more or less the same with the exception of those between U, Na_2O, and Fe_2O_3 which are substantially different, reflecting the redistribution of elements by postmagmatic hydrothermal processes.

Correlation coefficients between uranium and the normative composition of the unaltered granitic rocks of North Pole Pluton were also calculated (Table 25), and show that uranium significantly and positively correlates with corundum, quartz, and orthoclase. On the other hand, uranium has a significant negative correlation with enstatite, anorthite, and albite.

To delineate patterns of elemental association, with respect to uranium within the granitic rocks of North Pole Pluton, varimax rotated factor (principal components) analysis was performed using Statistical Analysis System, (1982) on the major oxides of the fresh, altered, and mineralized rock samples. Plots of loadings on three retained factors for the major oxides of the pluton are given in Figure 32. Loadings with values above ± 0.50 were selected for the interpretation.

Factor I, separates SiO_2 from TiO_2, Al_2O_3, CaO, MgO, FeO, and P_2O_5 (Fig. 32). This factor, as indicated from its constituents, is related to magmatic processes. Although uranium has low contribution in this factor, it follows SiO_2 during magmatic processes. The low contribution of uranium during magmatic processes is also evident in the low uranium content in the unaltered rocks of the North Pole Pluton (Table 22).

Uranium has a larger contribution in Factor II, where it accompanied Fe_2O_3, FeO, and MnO. This factor is related to secondary enrichment of uranium during postmagmatic activities such as hydrothermal and supergene processes. Uranium has no significant contribution in Factor III (Fig. 32).

Trace elements

Spearman rank correlation coefficients were also computed among the trace element contents of North Pole Pluton (Table 26). In the apparently fresh rocks, uranium shows significant positive correlations with the trace elements Be, Mo, Sn, Rb, and Sr as well as with the volatile elements F and S. The positive correlation with F and S may suggest that these volatiles played a significant role in uranium transportation during the magmatic stage.

In the altered and mineralized rock samples, uranium has a significant negative correlation with the volatile elements S and F (Table 26) possibly as a result of their escape (degassing) from the hydrothermal systems. A significant negative relationship of U with Sn, Mo, and W was also noted in the mineralized samples (Table 26). Thus, it is possible to conclude that U, Sn, Mo, and W behaved similarly during the magmatic stage but during the hydrothermal and subsequent mineralization stage, U partitioned from Sn, Mo, and W. The volatile elements F

Table 24. Matrix of Spearman rank correlation coefficients for U and major oxides in fresh (n = 7; upper left corner) and mineralized (n = 12; lower right corner) rock samples of the North Pole Pluton.

Element	U	SiO_2	TiO_2	Al_2O_3	Fe_2O_3	FeO	MnO	MgO	CaO	K_2O	Na_2O	P_2O_5	CO_2
CO_2	0.34	0.44	-0.22	-0.07	0.30	-0.19	-0.28	-0.26	-0.44	0.07	-0.48	0.12	
P_2O_5	-0.14	-0.58	0.51	0.77	-0.41	0.77	0.29	0.67	0.58	-0.69	-0.19		-0.45
Na_2O	0.18	-0.14	0.07	-0.21	0.32	0.11	0.13	0.04	0.11	-0.21		-0.03	0.17
K_2O	0.11	0.86	-0.86	-0.64	0.32	-0.93	-0.83	-0.86	-0.82		0.34	-0.06	0.43
CaO	-0.23	-0.86	0.75	0.79	-0.71	0.89	0.79	0.85		-0.19	0.18	0.24	-0.18
MgO	0.02	-0.89	0.93	0.82	-0.36	0.96	0.77		0.10	-0.12	-0.20	0.30	-0.53
MnO	0.29	-0.88	0.90	0.41	-0.34	0.74		0.40	-0.38	-0.45	-0.59	0.14	-0.46
FeO	0.02	-0.86	0.86	0.86	-0.43		0.71	0.80	-0.16	-0.29	-0.25	0.45	-0.60
Fe_2O_3	0.47	0.39	-0.18	-0.61		0.45	0.36	0.27	0.32	-0.22	-0.10	0.55	-0.19
Al_2O_3	0.16	-0.57	0.57		0.43	0.62	0.35	0.67	-0.27	0.27	-0.32	0.45	-0.09
TiO_2	-0.11	-0.93		0.57	0.37	0.65	0.23	0.87	0.30	-0.04	0.01	0.50	-0.46
SiO_2	0.38		-0.78	-0.77	-0.40	-0.90	-0.50	-0.95	0.06	0.06	0.22	-0.33	0.47
U		0.44	-0.40	-0.02	-0.51	-0.41	0.03	-0.40	-0.50	0.31	-0.29	-0.26	0.44

Table 25. Matrix of Spearman rank correlation coefficients for normative composition in fresh rock samples (n = 7) of the North Pole Pluton.

	U	Q	C	Or	Ab	An	En	Fs	Mt	Il	Ap
Ap	-0.17	-0.42	0.21	-0.35	-0.07	0.42	0.36	0.36	-0.01	0.23	1.00
Il	-0.38	-0.72	0.07	-0.77	0.33	0.72	0.87	0.74	-0.20	1.00	
Mt	0.25	0.33	0.03	0.25	0.28	-0.33	-0.23	-0.69	1.00		
Fs	-0.42	-0.98	-0.07	-0.86	0.33	0.98	0.88	1.00			
En	-0.51	-0.92	-0.22	-0.95	0.53	0.92	1.00				
An	-0.64	-1.00	-0.43	-0.92	0.58	1.00					
Ab	-0.45	-0.58	-0.70	-0.58	1.00						
Or	0.48	0.92	0.30	1.00							
C	0.76	0.43	1.00								
Q	0.64	1.00									
U	1.00										

and S may have acted as a transport mechanism for Sn, Mo, and W during the hydrothermal stage as is shown by the significant positive correlations between F and S with Sn, Mo, and W (Table 26).

Factor analyses performed on the trace elements of fresh, altered, and mineralized rock samples (Fig. 33) illustrate that uranium contribution is significantly high in Factor III where it is most likely attributed to secondary mineralization. Uranium mineralization accompanied Cu and Zn mineralization (Fig. 33). The sulphur contribution is also high in this factor, which may be attributed to the development of a base-metal sulphide mineralization, with which uranium enrichment appears to be associated. Tin, molybdium, and tungsten have higher contribution in Factor II, which is possibly attributed to Sn, Mo, and W mineralization along with Pb, Li, and F enrichments in the rocks. The low contribution of U in Factor I and Factor II may suggest that uranium mineralization in the granitic rocks of North Pole Pluton took place during the late stage hydrothermal processes (i.e., at lower temperature).

Factor II reveals that Sn, Mo, and W mineralization possibly occurred earlier than uranium mineralization during the hydrothermal processes.

Factor I indicates that Rb, Zr, Li, Bi, Sn, Cu, B, F, and Sr have high contribution in the rocks of North Pole Pluton and this factor may be related to magmatic processes.

Central Miramichi Anticlinorium granitic plutons

General statement

Data on 52 whole rock analyses (Appendix IX) from samples collected from the granitic plutons during the period 1985-1987 by the staff of New Brunswick Department of Natural Resources and Energy (Fyffe and MacLellan, 1988; MacLellan and Taylor, 1989) were obtained. Of these samples, 34 were from the Burnthill, Dungarvon, Trout Brook, and Rocky Brook plutons and most were mineralized. In this report the term "mineralized samples" refers to those that containing visible economic minerals. Cassiterite, molybdenite, wolframite, and base-metal sulphides are the main economic minerals of the mineralized samples.

Whole rock geochemistry for the granitic plutons, general review

The average uranium and thorium contents as well as the major, minor, and trace element contents in the apparently fresh rocks and in the mineralized rocks of the central Miramichi plutons are given in Tables 27 and 28 respectively. The global averages of major oxides, minor and trace elements in granitic rocks are also given in these two tables for comparison.

Table 27 illustrates that the apparently fresh rocks of the plutons are highly evolved (SiO_2 >74 wt. %) in that, compared to global averages for granites, they have high SiO_2 and Na_2O contents whereas the contents of TiO_2, Al_2O_3, MgO, CaO, and P_2O_5 are relatively low.

Both uranium and thorium contents appear to be elevated in the apparently fresh rocks of the plutons in comparison to global averages (Table 27), as are other trace elements such as Rb, Y, Sn, and to some extent Zn and F, whereas Sr, Ba, and Nb are apparently depleted. This pattern of trace element enrichment and depletion also has been observed by Chatterjee and Strong (1984) in the uraniferous Sn-W-bearing granitoids of the South Mountain Batholith, Nova Scotia.

Table 26. Matrix of Spearman rank correlation coefficients for U and other trace elements in fresh (n = 7; upper left corner) and mineralized (n = 12; lower right corner) rock samples of the North Pole Pluton.

	U	Be	Ba	Cu	F	Mo	Pb	Rb	B	Sn	Sr	Zn	W	Li	Bi	Zr	S
S	0.38	0.32	-0.44	-0.46	0.48	0.31	-0.21	-0.45	0.68	-0.30	0.77	0.56	–	-0.88	0.34	-0.09	
Zr	-0.69	-0.90	0.07	0.07	-0.45	0.16	0.04	-0.70	0.66	0.23	0.11	0.70	–	0.30	0.26		-0.02
Bi	0.17	-0.17	0.00	0.17	-0.17	0.00	-0.45	-0.17	0.43	0.00	0.34	0.17	–	0.17		0.55	0.35
Li	-0.52	-0.40	0.45	0.50	-0.61	-0.46	0.20	0.32	-0.41	0.16	-0.64	-0.36	–		-0.09	0.24	0.14
W	–	–	–	–	–	–	–	–	–	–	–	–		0.38	0.21	0.59	0.04
Zn	-0.34	-0.41	0.04	-0.02	0.13	0.46	-0.14	-0.96	0.67	-0.16	0.64		0.15	-0.54	-0.11	-0.11	0.11
Sr	0.34	0.02	-0.04	-0.04	0.13	0.50	0.16	-0.68	0.58	0.05		-0.12	-0.65	-0.16	-0.87	-0.58	-0.51
Sn	0.25	-0.61	-0.11	-0.06	-0.61	0.29	0.33	0.00	0.45		-0.34	0.27	-0.07	-0.22	0.44	0.40	0.29
B	-0.15	-0.74	-0.66	-0.65	-0.47	0.16	0.16	-0.67		0.07	0.13	-0.60	0.35	0.63	-0.13	0.41	-0.25
Rb	0.31	0.49	-0.16	-0.09	-0.05	-0.58	0.02		-0.12	0.55	-0.73	-0.02	-0.22	-0.07	0.67	0.45	0.27
Pb	-0.21	-0.22	-0.10	-0.20	-0.71	-0.41		-0.18	-0.04	-0.06	-0.06	0.49	0.86	-0.20	-0.31	0.08	-0.22
Mo	0.39	-0.16	0.31	0.31	0.45		-0.13	0.07	0.13	-0.16	-0.31	-0.20	0.51	0.43	0.13	-0.05	0.71
F	0.37	0.67	0.11	0.09		0.27	-0.10	0.62	0.05	0.32	-0.93	0.06	0.42	0.25	0.80	0.60	0.35
Cu	-0.06	-0.02	0.98		0.28	-0.04	-0.15	0.50	-0.39	0.80	-0.48	0.40	-0.34	-0.38	0.48	0.23	0.59
Ba	-0.13	0.00		-0.04	0.32	-0.03	0.51	-0.13	0.14	-0.05	-0.68	0.15	0.80	0.41	0.12	0.55	0.00
Be	0.54		0.04	0.28	0.40	-0.01	0.27	0.68	0.13	0.39	-0.66	-0.18	0.07	-0.11	0.46	0.39	0.12
U		-0.03	-0.15	-0.39	-0.31	-0.38	0.38	-0.05	-0.32	-0.28	0.26	0.29	-0.37	-0.19	-0.53	-0.55	-0.46

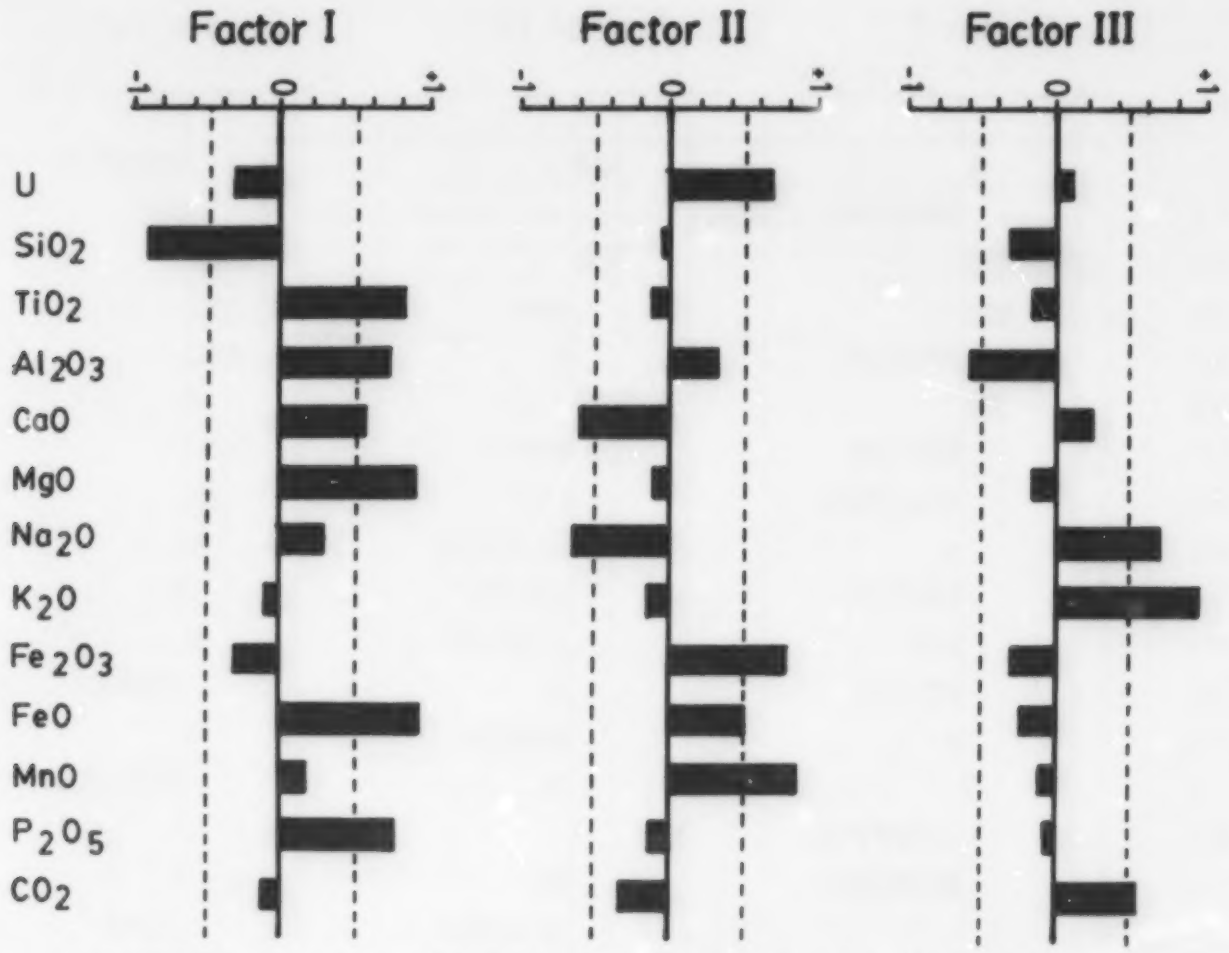

Figure 32. Plots of Factor I, II, and III loadings for major oxide contents in the rocks of the North Pole Pluton.

The major oxide and trace element contents in the mineralized rock samples are highly variable as expressed by their high standard deviations (Table 28). These variations are possibly attributed to the high degree of depletion and concentration by hydrothermal solutions. The CaO content appears to be more susceptible than other oxides to redistribution by hydrothermal solutions as indicated by its extreme compositional variation (Table 28). It is depleted in the Burnthill and Trout Brook plutons but enriched relative to global averages in the Dungarvon and the Rocky Brook plutons. The high variation in CaO content in the plutons may be related to high activity of F in the mineralizing fluids. Silica and to lesser extent Na_2O are also highly variable.

Uranium and to a lesser extent thorium contents in the mineralized rocks (Table 28) are anomalous relative to normal granites. The mean values of U for the plutons range from 7.4 ppm in the Rocky Brook Pluton, to 11.1 ppm in the Burnthill Pluton, values which are more than two to three times the world average of granites (Table 28). The Th-U ratio of the mineralized rock samples varies in the four plutons studied. All except Burnthill show a low Th-U ratio relative to global averages. This suggests that uranium may be preferentially enriched relative to thorium in the granitic rocks.

Among the trace elements in the mineralized samples (Table 28), Rb, Cs, Be, Li, Bi, B, S, As, Sb, Ag, Au, Sn, Mo, W, Cu, Zn, Pb, Ta, Tl, and Cd values are above the average values for normal granites, whereas Co, V, Cr, Mn, Ni, Zr, La, Ce, Nd, Sm, Eu, Gd, Dy, and Er have lower values.

In order to determine the relationship of uranium and thorium contents to the mean contents of the rare-earth elements (REE) in the mineralized rock samples, the chondrite-normalized patterns of REEs of the granitic plutons of the central Miramichi Anticlinorium were plotted (Fig. 34). The patterns for global average granites and of a U-mineralized sample (U = 207 ppm) were also plotted. The curves show a depletion in REEs in the central Miramichi Anticlinorium plutons relative to global average granites. The depletion is most obvious in the U-mineralized

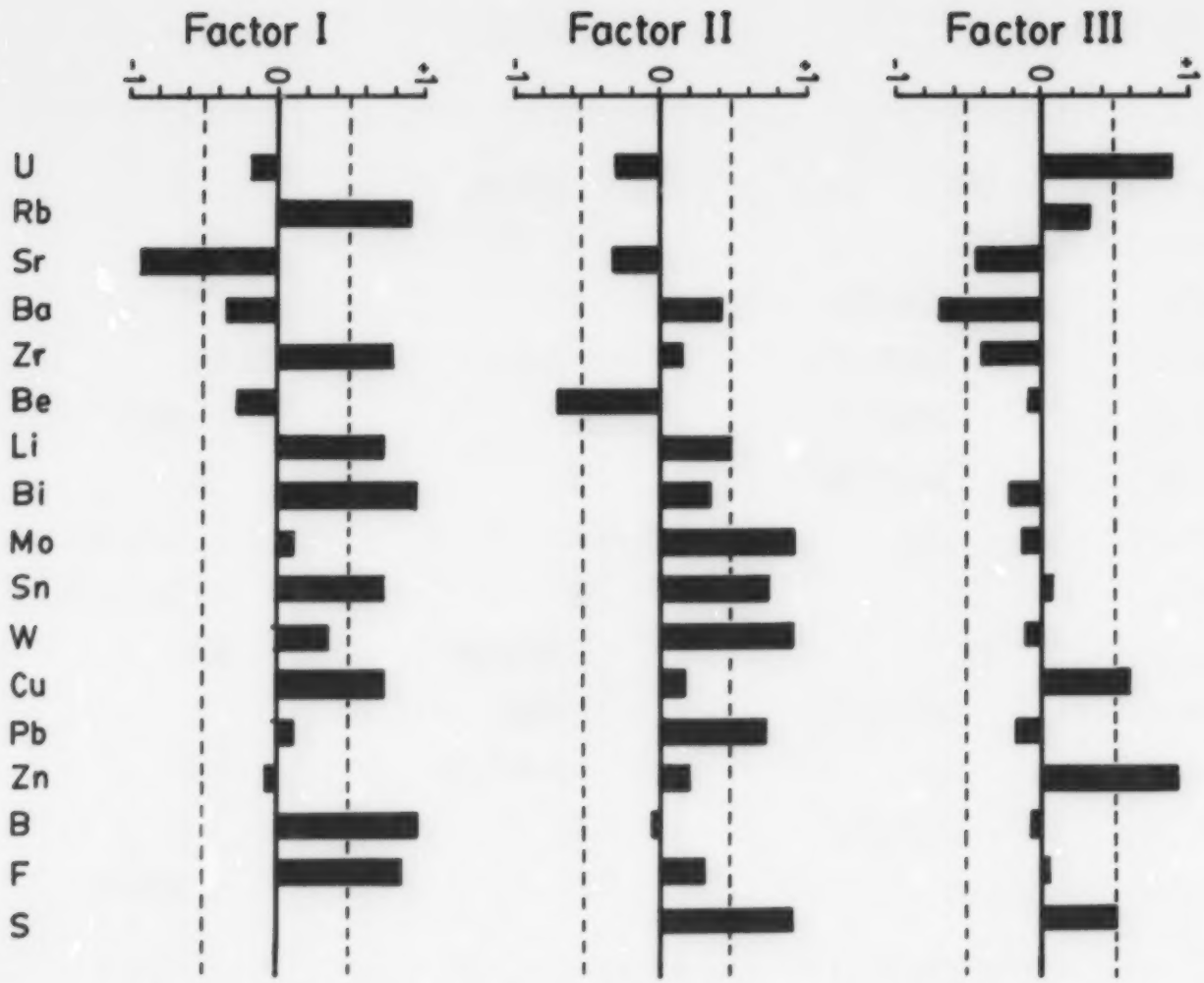

Figure 33. Plots of Factor I, II, and III loadings for trace element contents in the rocks of the North Pole Pluton.

sample of the Dungarvon Pluton. It is also noted that the decrease in light rare-earth elements (LREEs) relative to world average is much greater than the decrease in heavy rare-earth elements (HREE) content.

The depletion in REEs contents with an increase in uranium content may suggest that a large portion of uranium is not contained in accessory minerals. This has an economical implication because accessory minerals are resistant to alteration and weathering. Thus, any uranium incorporated with them will be immobile and not available to later U-forming hydrothermal solutions (see also Barbier, 1974; Duex and Henry, 1985; Frick, 1986).

Burnthill Pluton

Whole rock geochemistry

Table 29 shows the mean and standard deviations of the major oxide and trace element contents and the normative contents of the apparently fresh, altered, and mineralized rock samples of the Burnthill Pluton.

For the major oxides, SiO_2, K_2O, and to some extent CaO and Na_2O contents appear to decrease progressively in abundance in the altered and the mineralized rocks relative to the fresh rocks (Table 29). In contrast, FeO_T (total iron expressed as FeO) MnO, and to some extent TiO_2 and P_2O_5 contents increase progressively from the fresh to the mineralized rocks.

Both uranium and thorium decrease systematically in abundance from the fresh rocks to the mineralized rocks (Table 29). The low uranium and thorium contents in the altered and mineralized rock samples relative to fresh samples may be explained by the fractionation of uranium and thorium from the Sn, Mo, and W concentrated in the mineralized rocks during hydrothermal or other mineralization processes.

The trace elements Rb, Cs, W, Sn, Zn, and to some extent F show systematic increase from the fresh rocks to the mineralized rocks (Table 29). On the other hand Ta and Lu appear to decrease.

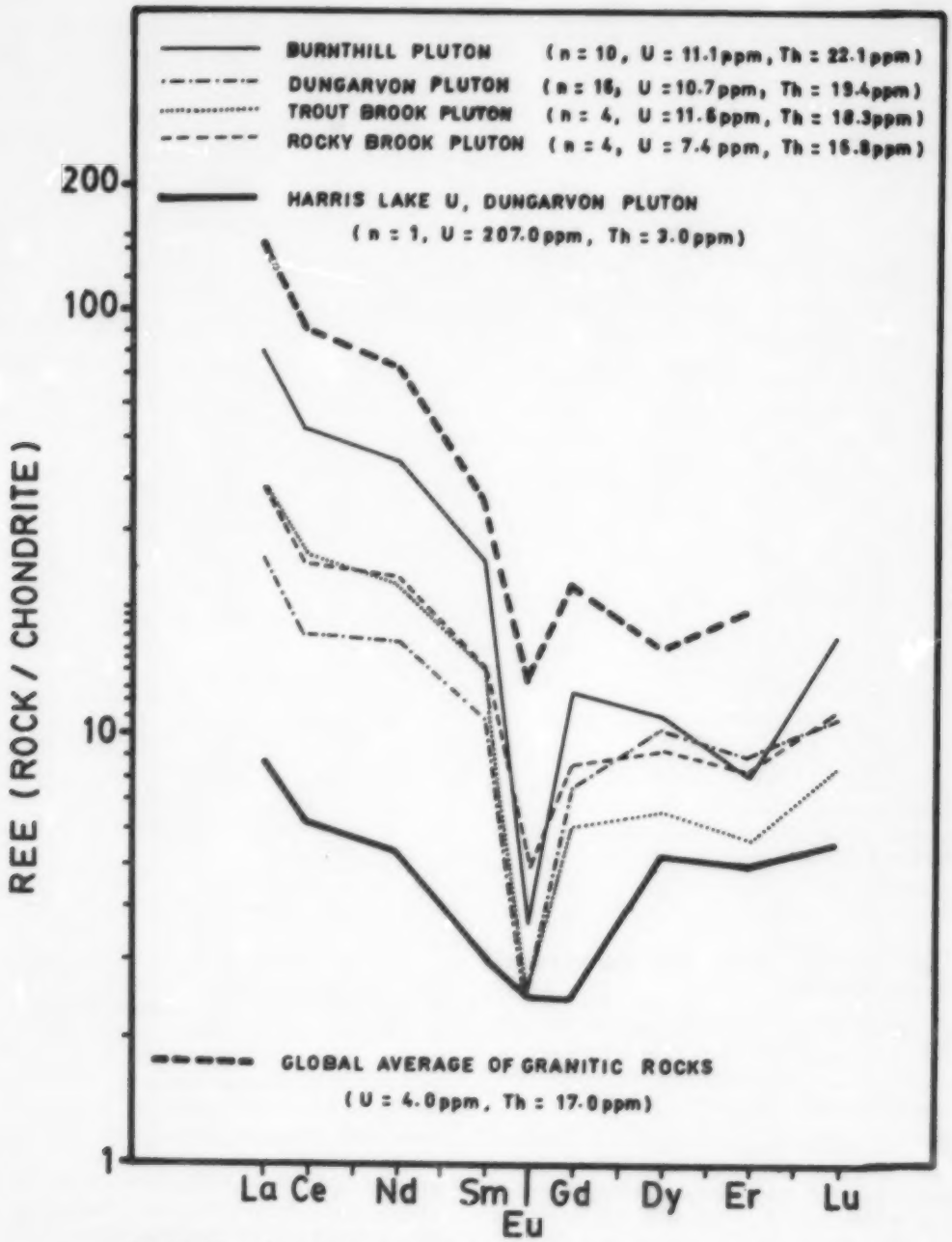
BURNTHILL PLUTON (n = 10, U = 11.1ppm, Th = 22.1ppm)
DUNGARVON PLUTON (n = 16, U = 10.7ppm, Th = 19.4ppm)
TROUT BROOK PLUTON (n = 4, U = 11.6ppm, Th = 18.3ppm)
ROCKY BROOK PLUTON (n = 4, U = 7.4 ppm, Th = 16.8ppm)
HARRIS LAKE U, DUNGARVON PLUTON
(n = 1, U = 207.0ppm, Th = 3.0ppm)
GLOBAL AVERAGE OF GRANITIC ROCKS
(U = 4.0ppm, Th = 17.0ppm)
REE (ROCK / CHONDRITE)
200
100
10
1
La Ce Nd Sm Eu Gd Dy Er Lu

Figure 34. Chondrite-normalized REE plot for mineralized granitic rocks of central Miramichi Anticlinorium plutons.

Table 27. Average U, Th, major oxides, and trace elements in fresh rock samples of the Burnthill, Dungarvon, and Trout Brook plutons and their global averages.

Chemical composition	Dungarvon Pluton (n = 10)*	Burnthill Pluton (n = 15)	Trout Brook Pluton (n = 9)	Global@ averages
SiO_2 (%)	75.68	76.3	74.60	71.3
TiO_2 (%)	0.16	0.2	0.15	0.31
Al_2O_3 (%)	13.13	12.9	13.41	14.32
FeO_T (%)	1.46	1.2	1.91	1.21
MnO (%)	0.05	0.1	0.08	0.05
MgO (%)	0.28	0.3	0.17	0.71
CaO (%)	1.00	0.3	0.90	1.84
K_2O (%)	4.65	6.2	4.20	4.07
Na_2O (%)	3.62	4.5	3.66	1.68
P_2O_5 (%)	0.05	0.05	0.05	0.12
Rb (ppm)	358.0	421.1	379.2	150
Sr (ppm)	58.2	60.3	161.2	285
Ba (ppm)	171.8	151.1	213.9	600
Y (ppm)	50.4	64.7	43.0	42
Zr (ppm)	87.4	106.3	117.9	180
Nb (ppm)	23.0	26.5	14.6	23.5
F (ppm)	604.4	841.7	989.0	810
Sn (ppm)	22.5	15.9	32.7	3.0
Zn (ppm)	54.7	45.1	110.6	40.0
U (ppm)	11.7	16.7	8.6	4.0
Th (ppm)	29.8	35.5	21.0	17.0
Th/U	2.8	2.5	3.2	3-4

@ Average major oxides composition from LeMaitre (1976); Rb, Sr, Ba, Y, Zr, Nb, Sn, Zn, U, and Th from Taylor (1964); F from Allman and Koriting (1978).

*n = number of samples.

Uranium and thorium variations with petrochemical indices of Burnthill Pluton

The contents of U, Th, and the Th-U ratio in the fresh granitic rocks of the Burnthill Pluton were plotted against selected petrochemical indices in an attempt to monitor their behaviour during magmatic evolution.

Plots of U, Th, and the Th-U ratio versus SiO_2 contents of the granitic rocks are shown in Figure 35. Uranium content tends to increase curvilinearly with the amount of SiO_2 increase. Within individual rock units the increase is more obvious (Fig. 35).

The increase in uranium appears to be sharp when the amount of SiO_2 reaches 75% (Fig. 35), a phenomenon probably arising out of enrichment in the silica-rich residual melt during crystallization. Hence granitic rocks with SiO_2 content of greater than 75 wt. % appear to be potential sources for uranium deposits.

Thorium tends to decrease with increase of SiO_2. The decrease is sharp when the SiO_2 content reaches 75%. Thus, it is possible to suggest that a major partitioning of uranium and thorium is most marked when SiO_2 content in the magma reaches 75% by weight, with uranium becoming enriched in the residual melt while thorium is retained in the rocks. This is also evident in the decrease of the Th-U ratio with increasing amounts of SiO_2 (Fig. 35). The decrease in Th-U ratio with increase in SiO_2 content in granitic rocks is rare. However, Chatterjee and Muecke (1982) have observed the same relationship in the uraniferous granites of the South Mountain Batholith of Nova Scotia. Granites showing this trend are more likely to generate uranium ores than the ones showing increasing Th-U ratio with the SiO_2 increase.

The plots of U, Th, and Th-U ratio versus the total alkali ($Na_2O + K_2O$) contents of the rocks (Fig. 36) indicate a strong relationship between uranium content and the total

Table 28. Average U, Th, major oxides, and trace elements in mineralized rock samples of the Burnthill, Dungarvon, Trout Brook, and Rocky Brook, plutons and their global averages.

Elements	Burnthill n* = 10	Dungarvon n = 16	Trout Brook n = 4	Rocky Brook n = 4	Global@ Average
SiO_2(%)	67.05 ± 15.85	71.90 ± 15.26	73.65 ± 9.04	51.18 ± 24.13	71.3
TiO_2(%)	0.27 ± 0.32	0.12 ± 0.11	0.11 ± 0.06	0.29 ± 0.36	0.31
Al_2O_3(%)	13.01 ± 7.69	9.51 ± 5.87	13.69 ± 4.63	11.48 ± 7.31	14.32
CaO(%)	0.24 ± 0.24	3.58 ± 10.58	0.37 ± 0.28	19.00 ± 31.12	1.84
MgO(%)	0.34 ± 0.42	0.19 ± 0.28	0.10 ± 0.06	1.21 ± 2.04	0.71
Na_2O(%)	0.29 ± 0.30	2.04 ± 1.90	1.51 ± 2.07	2.06 ± 1.78	1.68
K_2O(%)	5.16 ± 3.41	3.68 ± 2.92	6.11 ± 2.46	4.54 ± 3.82	4.07
Fe_2O_3(%)	5.74 ± 5.82	1.95 ± 2.34	2.52 ± 0.70	3.88 ± 3.67	1.21
MnO(%)	0.34 ± 0.31	1.13 ± 0.07	0.13 ± 0.08	0.23 ± 0.14	0.05
P_2O_5(%)	0.07 ± 0.08	0.05 ± 0.09	0.07 ± 0.03	0.07 ± 0.04	0.12
Li(ppm)	196.0 ± 301.70	160.0 ± 181.2	167.5 ± 96.7	65.0 ± 26.5	30.0
Be(ppm)	7.5 ± 4.25	19.7 ± 42.4	10.0 ± 10.0	11.3 ± 9.5	5.0
Rb(ppm)	685.6 ± 384.3	261.6 ± 320.3	744.0 ± 202.7	380.5 ± 300.0	150.0
Sr(ppm)	42.4 ± 35.57	86.1 ± 93.3	54.5 ± 44.4	113.0 ± 134.2	285.0
Cs(ppm)	27.1 ± 30.1	11.6 ± 15.5	26.0 ± 16.87	13.8 ± 11.2	3-6.0
Ba(ppm)	234.5 ± 116.7	226.8 ± 163.1	332.5 ± 430.8	269.0 ± 207.2	600.0
B(ppm)	18.0 ± 6.3	18.2 ± 5.3	27.5 ± 9.6	12.5 ± 5.0	12.0
S(ppm)	270.0 ± 252.3	1383.5 ± 2498.5	950.0 ± 1700.0	2527.5 ± 3842.6	330.0
As(ppm)	190.6 ± 565.6	23.9 ± 47.6	6.0 ± 5.9	29.0 ± 24.1	1.5
Sb(ppm)	0.5 ± 0.30	1.4 ± 2.8	0.2 ± 0.0	0.5 ± 0.3	0.2
Y(ppm)	37.1 ± 30.5	32.4 ± 30.0	32.5 ± 17.3	20.5 ± 9.0	42.0
Zr(ppm)	107.0 ± 107.2	55.0 ± 69.1	72.5 ± 59.3	75.0 ± 47.2	180.0
Nb(ppm)	72.7 ± 110.5	25.0 ± 24.7	19.5 ± 10.4	13.3 ± 3.8	23.5
V(ppm)	19.0 ± 19.1	24.1 ± 26.9	10.0 ± 0.0	42.5 ± 58.5	44.0
Cr(ppm)	3.4 ± 1.9	4.1 ± 1.1	3.0 ± 1.2	4.0 ± 0.0	25.0
Mn(ppm)	196.7 ± 41.6	161.1 ± 111.1	110.0 ± 70.0	61.0 ± 69.3	600.0
Co(ppm)	3.3 ± 4.5	3.4 ± 6.5	1.3 ± 0.5	7.0 ± 7.8	5.0
Ni(ppm)	5.6 ± 3.9	2.8 ± 1.7	1.8 ± 0.9	20.5 ± 37.7	8.0
Cu(ppm)	96.8 ± 74.6	81.0 ± 288.6	24.4 ± 43.8	14.0 ± 20.4	10.0
Zn(ppm)	147.4 ± 251.3	30.1 ± 20.0	98.0 ± 128.2	83.8 ± 98.0	40.0
Pb(ppm)	70.0 ± 92.9	32.4 ± 44.2	17.0 ± 17.8	14.0 ± 17.0	20.0
Hf(ppm)	3.6 ± 2.3	2.8 ± 2.1	4.0 ± 0.8	3.0 ± 1.4	4.0
Ta(ppm)	3.8 ± 3.7	3.2 ± 2.7	8.0 ± 4.2	2.5 ± 1.3	1.5
Ga(ppm)	29.1 ± 20.0	15.94 ± 10.3	26.8 ± 12.2	17.5 ± 10.1	20.0
Mo(ppm)	84.6 ± 161.6	40.6 ± 72.9	20.0 ± 9.8	10.5 ± 8.1	0.8
Ag(ppm)	1.8 ± 2.0	0.8 ± 1.1	0.5 ± 0.0	0.6 ± 0.3	0.07
Cd(ppm)	1.6 ± 1.6	1.0 ± 0.0	1.0 ± 0.0	1.0 ± 0.0	0.2
In(ppm)	1.8 ± 1.1	1.1 ± 0.2	1.3 ± 0.5	1.3 ± 0.5	0.02
Sn(ppm)	1591.3 ± 3336.3	1614.2 ± 3685.7	112.5 ± 181.4	24.5 ± 12.4	3.0
W(ppm)	609.7 ± 598.6	33.7 ± 110.0	25.5 ± 31.2	4.8 ± 3.5	1.5
Au(ppb)	0.12 ± 0.03	2.2 ± 2.5	1.0 ± 0.00	1.3 ± 0.5	0.004
Tl(ppm)	5.1 ± 4.0	2.7 ± 1.6	4.8 ± 1.5	3.5 ± 2.1	0.45
Bi(ppm)	54.1 ± 60.2	17.3 ± 31.8	89.1 ± 169.3	49.1 ± 90.7	0.15-2.0
La(ppm)	27.2 ± 21.1	8.9 ± 7.2	13.5 ± 8.3	13.5 ± 10.5	50.0
Ce(ppm)	57.8 ± 44.7	19.3 ± 17.3	29.3 ± 17.4	28.0 ± 23.6	100.0
Nd(ppm)	27.5 ± 20.4	10.1 ± 8.3	14.0 ± 7.8	14.5 ± 10.8	46.0
Sm(ppm)	5.9 ± 4.0	2.6 ± 2.3	3.3 ± 1.4	3.3 ± 2.1	8.3
Eu(ppm)	0.3 ± 0.2	0.2 ± 0.1	0.2 ± 0.2	0.4 ± 0.4	1.1
Gd(ppm)	4.3 ± 3.1	2.6 ± 2.4	2.1 ± 0.9	3.0 ± 1.6	7.6
Dy(ppm)	3.8 ± 2.2	3.5 ± 2.3	2.3 ± 1.3	3.2 ± 0.8	5.5
Er(ppm)	2.0 ± 1.9	2.2 ± 1.5	1.4 ± 1.0	2.0 ± 0.4	4.7
Lu(ppm)	0.6 ± 1.0	0.4 ± 0.2	0.3 ± 0.1	0.4 ± 0.1	--
U(ppm)	11.1 ± 7.8	10.7 ± 10.40	11.6 ± 7.9	7.4 ± 7.0	4.0
Th(ppm)	22.1 ± 12.8	19.38 ± 18.61	18.3 ± 4.8	16.8 ± 13.1	17.0
Th/U	3.4 ± 4.1	1.8 ± 1.2	2.3 ± 1.6	2.5 ± 1.3	3-4

@ Average major oxides composition from Le Maitre (1976); Cr, Mn, Co, and Ni from Vinogradov (1962); other trace elements from Taylor (1964).

* n = number of samples.

Table 29. Average U, Th, major oxides, trace elements, and norms in fresh, altered, and mineralized rock samples of the Burnthill Pluton.

Chemical composition	BURNTHILL PLUTON		
	Fresh Mean ± St. Dev. (n* = 15)	Altered Mean ± St. Dev. (n = 3)	Mineralized Mean ± St. Dev. (n = 10)
SiO_2 (%)	76.3 ± 1.6	70.1 ± 6.1	67.1 ± 15.9
TiO_2 (%)	0.2 ± 0.1	0.2 ± 0.1	0.3 ± 0.3
Al_2O_3 (%)	12.9 ± 0.5	15.9 ± 2.9	13.0 ± 7.7
FeO_T (%)	1.2 ± 0.4	1.8 ± 0.8	5.7 ± 5.8
MnO (%)	0.1 ± 0.0	0.13 ± 0.0	0.3 ± 0.3
MgO (%)	0.3 ± 0.1	0.3 ± 0.1	0.3 ± 0.4
CaO (%)	0.3 ± 0.2	0.3 ± 0.2	0.2 ± 0.2
K_2O (%)	6.2 ± 5.1	6.2 ± 5.1	5.2 ± 3.4
Na_2O (%)	4.5 ± 4.1	4.5 ± 4.1	0.3 ± 0.3
P_2O_5 (%)	0.05 ± 0.04	0.05 ± 0.04	0.1 ± 0.1
Rb (ppm)	421.1 ± 82.0	515.7 ± 417.0	685.6 ± 384.3
Sr (ppm)	60.3 ± 77.3	109.3 ± 114.6	42.4 ± 35.6
Cs (ppm)	9.7 ± 2.85	10.7 ± 10.3	27.1 ± 30.1
Ba (ppm)	151.1 ± 116.9	277.7 ± 302.0	234.5 ± 116.7
Y (ppm)	64.7 ± 21.1	67.7 ± 13.5	37.1 ± 30.5
Zr (ppm)	106.3 ± 36.1	117.7 ± 46.5	107.0 ± 107.2
Nb (ppm)	26.5 ± 12.0	22.0 ± 14.8	72.7 ± 110.5
Hf (ppm)	4.4 ± 0.42	4.7 ± 0.4	3.6 ± 2.3
Ta (ppm)	7.8 ± 4.7	6.3 ± 4.9	3.8 ± 3.7
La (ppm)	24.6 ± 9.2	55.7 ± 48.9	27.2 ± 21.1
Lu (ppm)	0.9 ± 0.4	0.8 ± 0.27	0.6 ± 1.0
Sc (ppm)	5.2 ± 0.8	4.6 ± 0.5	–
Tb (ppm)	1.6 ± 0.5	1.9 ± 0.2	–
Yb (ppm)	6.7 ± 2.6	7.1 ± 2.4	–
F (ppm)	841.7 ± 562.9	1110.0 ± 896.2	–
W (ppm)	4.5 ± 8.7	4.7 ± 2.1	609.7 ± 598.6
Sn (ppm)	15.9 ± 6.6	23.0 ± 16.1	1591.3 ± 3336.3
Zn (ppm)	45.1 ± 29.3	112.7 ± 102.8	147.4 ± 251.3
U (ppm)	16.7 ± 7.4	13.4 ± 11.3	11.1 ± 7.8
Th (ppm)	33.5 ± 10.5	27.3 ± 0.6	22.1 ± 12.8
Th/U (ppm)	2.5 ± 1.4	3.4 ± 2.7	3.4 ± 4.1
Quartz (%)	35.8 ± 2.7	19.2 ± 16.4	
Calcite (%)	0.9 ± 0.4	1.5 ± 0.8	
Orthoclase (%)	26.6 ± 1.3	36.8 ± 30.6	
Albite (%)	30.5 ± 2.4	38.2 ± 34.8	
Anorhite (%)	3.4 ± 2.1	1.0 ± 1.0	
Diopside (%)	0.4 ± 0.6	–	
Hypersthene (%)	1.7 ± 1.3	1.9 ± 1.7	
Magnetite (%)	0.6 ± 0.4	1.0 ± 0.1	
Ilmonite (%)	0.3 ± 0.2	0.3 ± 0.2	
Apatite (%)	0.1 ± 0.1	0.1 ± 0.1	

* n = number of samples.

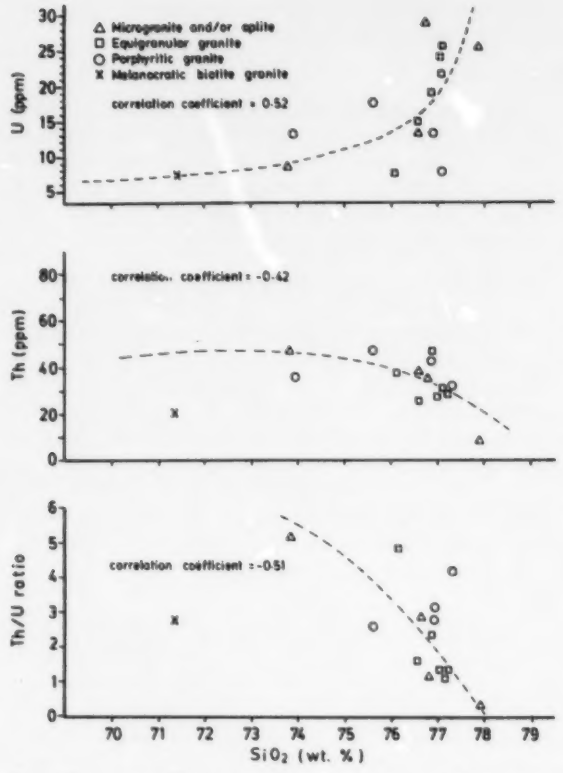

Figure 35. Plot of U, Th, and Th-U ratio versus SiO_2 for the rocks of the Burnthill Pluton, showing an increase of uranium, decrease of thorium, and a decrease of Th-U ratio with silica increase.

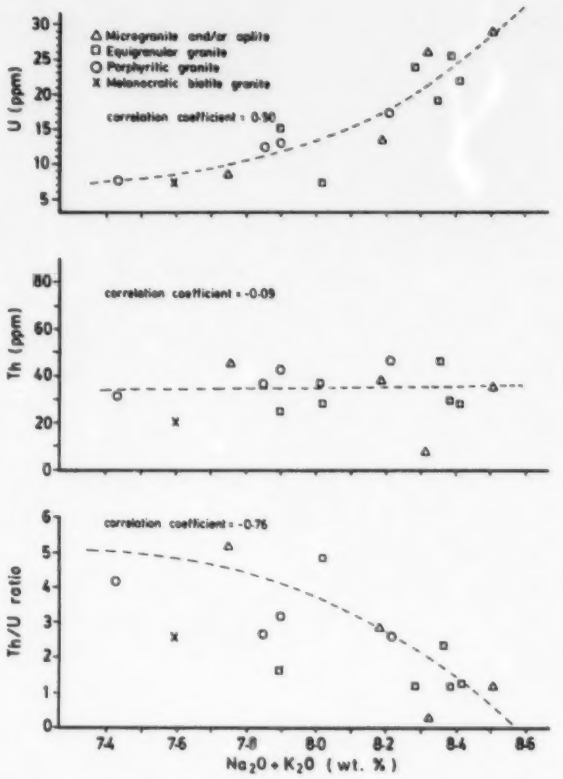

Figure 36. Plot of U, Th, and Th-U ratio versus total alkalies for the rocks of the Burnthill Pluton, showing an increase in uranium, nearly constant Th, and decrease in Th-U ratio with increase in $Na_2O + K_2O$.

alkali content, a relationship also manifested by the strong positive correlation coefficient (r = 0.90) between uranium and the total alkalies. This relationship suggests that uranium may have been partly contained in the alkali minerals and more readily released from the rocks by hydrothermal and weathering processes than if tied up in accessory minerals. The high concentration of uranium in highly alkaline parts of the granite may also be explained by a development of a Na and K metasomatic phase in late stages of magmatic evolution.

Unlike uranium, thorium tends to retain virtually a constant concentration with increase or decrease of total alkali content in the rocks (Fig. 36). There is thus a decrease in the Th-U ratio with the increase of the amount of the total alkalies (Fig. 36).

Uranium, Th, and the Th-U ratio in the granitic rocks were also plotted against the light rare-earth to heavy rare-earth elements ratios as represented by the La-Yb ratio (Fig. 37). The plots reveal an inverse relationship between U and the La-Yb ratio and a positive relationship between Th and the La-Yb ratio. These plots clearly indicate that uranium is associated with the HREEs whereas Th is associated with the LREEs.

Uranium and tin specialization of the granitic rocks of the Burnthill Pluton

The Rb, Sr, and Ba contents in the fresh, altered, and mineralized granitic rocks of Burnthill Pluton were plotted on a Rb-Sr-Ba ternary variation diagram (Fig. 38) of El Bouseily and El Sokkary (1975) in order to detect the specialization of the granites in uranium and tin.

Figure 38 indicates that most of the samples (fresh, altered, and mineralized) fall within the area of differentiated (Sn-bearing, specialized) granites. These samples are also uraniferous which suggest that U-specialized granitoids are associated with Sn-specialized granitoids.

The K-Na and K-Rb ratios of the fresh, altered, and mineralized rocks are 1.4, 5.0, and 38.3 respectively for K-Na ratios and 90.8, 104.9, and 64.3 respectively for K-Rb ratios. These also suggest, to some extent, that the Burnthill Pluton is a Sn-specialized granitoid according to criteria established by Stemprok (1979) and Tischendorf (1977).

It is apparent from the limited trace element data presented here that the Burnthill Pluton is somewhat 'specialized' in terms of tin and uranium contents.

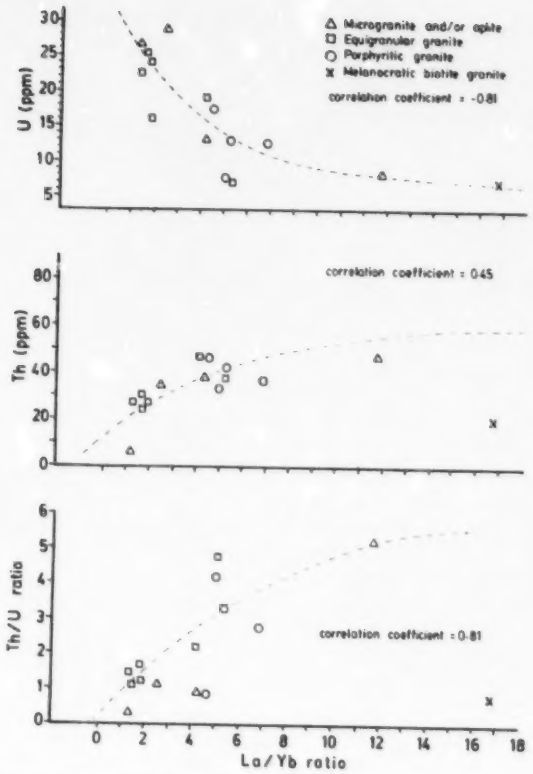

Figure 37. Plot of U, Th, and Th-U ratio versus La-Yb ratio for the rocks of the Burnthill Pluton, showing a decrease in U, increase in Th, and an increase in Th-U ratio with increase in La-Yb ratio.

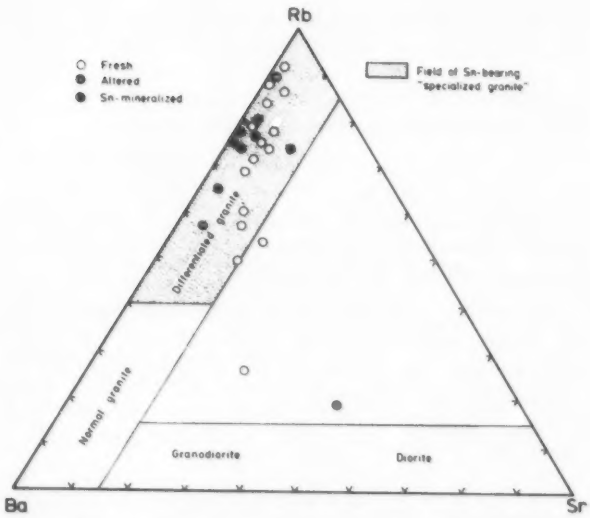

Figure 38. A Rb-Sr-Ba ternary variation diagram for the rocks of the Burnthill Pluton (after El Bouseily and El Sokkary, 1975).

Statistical relationship between uranium and thorium and other elements in the Burnthill Pluton

Major oxides

In order to determine the behaviour of uranium and thorium in the rocks and to establish relationship between uranium, thorium, and the major oxide contents in the fresh and mineralized samples of Burnthill Pluton Spearman rank correlation coefficients were calculated from the data contained in Appendix IX-A (Table 30).

In the fresh samples (Table 30) a significant positive correlation exists between uranium and SiO_2, and uranium and Na_2O. Uranium also shows a strong negative correlation with TiO_2, FeO, MgO, CaO, and P_2O_5. These relationships indicate, as anticipated, that uranium is predominantly associated with the felsic mineral-forming oxides during magmatic evolution of the Burnthill Pluton. Thorium behaves differently, as it correlates negatively with SiO_2 and Na_2O and positively with TiO_2, FeO, MgO, and CaO. This strikingly different behaviour of uranium and thorium in the granite is also evident in the negative correlation coefficient ($r = -0.22$) between uranium and thorium in the fresh rocks (Table 30).

Both uranium and thorium correlate positively with the K_2O content of the rocks. However, the correlation coefficient between Th and K_2O ($r = 0.57$) is far stronger than between U and K_2O ($r = 0.17$). Thus the strong positive correlation between U and Na_2O and low positive correlation between U and K_2O and strong negative correlation between U and CaO may suggest that uranium is associated with albite. In contrast the positive correlation of Th with K_2O and CaO and the negative correlation with Na_2O may suggest that Th favours Ca-plagioclase and orthoclase.

In the mineralized samples (Table 30) uranium lacks or shows low correlations (positive or negative) with most of the major oxides. This can be attributed to fractionation of uranium from the major rock-forming minerals by postmagmatic processes during the mineralization stage. Thorium, on the other hand, shows significant positive correlations with TiO_2, Fe_2O_3, MgO, and P_2O_5 and negative correlations with Na_2O. The persistence of significant correlations between Th and these major oxides in the mineralized rock samples suggest that, unlike U, Th was less mobile during mineralization.

The correlation coefficients among U, Th, and the normative composition of the fresh rocks (Table 31) also indicate uranium associated with albite as was evident in the strong positive correlation coefficient between uranium and albite ($r = 0.74$) in the fresh rocks. Table 31 also suggests that Th may have accompanied Ca-plagioclase and orthoclase during magmatic evolution.

Factor analysis was carried on U, Th, and the major oxide contents in the fresh rock samples. Loadings on three retained factors are shown graphically in Figure 39. Factor I separates SiO_2 from most of the mafic oxides. Uranium follows the SiO_2. This factor, as indicated by its elemental association, is related to magmatic processes. Factor II (Fig. 39), separates Na_2O from TiO, Fe_2O_3, and P_2O_5. Uranium

Table 30. Matrix of Spearman rank correlation coefficients for U, Th, and major oxides in fresh (n* = 15; upper left corner) and mineralized (n = 10; lower right corner) rock samples of the Burnthill Pluton.

	U	Th	SiO_2	TiO_2	Al_2O_3	Fe_2O_3	FeO	MnO	MgO	CaO	K_2O	Na_2O	P_2O_5
P_2O_5	-0.69	0.17	-0.41	0.83	0.54	0.21	0.65	0.36	0.88	0.70	-0.40	-0.35	
Na_2O	0.74	-0.43	0.23	-0.60	0.17	-0.34	-0.51	0.05	-0.55	-0.31	-0.19		-0.18
K_2O	0.17	0.57	-0.13	-0.09	-0.09	-0.01	-0.02	-0.31	-0.22	-0.14		0.16	0.23
CaO	-0.55	0.39	-0.48	0.84	0.41	0.06	0.73	0.08	0.84		-0.20	-0.07	-0.05
MgO	-0.77	0.36	-0.48	0.92	0.42	0.06	0.82	0.27		-0.07	0.33	-0.51	0.60
MnO	-0.22	-0.18	-0.47	0.19	0.17	0.09	0.40		0.24	0.24	-0.14	-0.90	-0.10
FeO	-0.68	0.49	-9.82	0.85	0.48	-0.09		--	--	--	--	--	--
Fe_2O_3	-0.15	0.25	-0.13	0.16	-0.33		--	0.14	0.73	-0.07	0.42	-0.33	0.69
Al_2O_3	-0.28	0.07	-0.40	0.43		0.51	--	-0.14	0.51	-0.20	0.82	-0.02	0.32
TiO_2	-0.83	0.42	-0.65		0.45	0.76	--	0.14	0.76	-0.04	0.27	-0.36	0.77
SiO_2	0.52	-0.42		-0.36	-0.73	-0.51	--	-0.14	-0.42	0.11	-0.56	0.29	-0.23
Th	-0.22		-0.07	0.63	0.16	0.47	--	0.24	0.64	-0.16	-0.02	-0.42	0.51
U		0.11	0.20	0.18	-0.20	-0.07	--	-0.24	-0.07	0.20	-0.20	0.20	0.28

* n = number of samples.

Table 31. Matrix of Spearman rank correlation coefficients for normative composition in fresh rock samples (n* = 15) of the Burnthill Pluton.

	U	Th	Q	C	Or	Ab	An	Hy	Mt	Il	Ap
Ap	-0.71	0.09	-0.32	0.43	-0.31	-0.30	0.60	0.59	0.22	0.83	1.00
Il	-0.78	0.37	-0.35	0.47	-0.03	-0.55	0.79	0.75	-0.02	1.00	
Mt	-0.04	0.25	0.22	0.24	-0.14	-0.06	-0.01	-0.41	1.00		
Hy	-0.65	0.43	-0.48	0.21	0.16	-0.44	0.75	1.00			
An	-0.64	0.46	-0.59	0.09	0.00	-0.42	1.00				
Ab	0.74	-0.41	-0.35	-0.60	-0.35	1.00					
Or	0.04	0.64	0.03	-0.19	1.00						
C	-0.63	0.03	0.47	1.00							
Q	-0.05	-0.23	1.00								
Th	-0.22	1.00									
U	1.00										

* n = number of samples.

follows Na_2O while Th follows the second group. This factor may be attributed to late stage magmatic processes where U is predominantly associated with albite. In Factor III, U has a low contribution whereas Th has a high contribution and follows K_2O. This factor may indicate that Th follows orthoclase during late stage magmatic processes.

Trace elements

Correlation coefficients among U, Th, and other trace elements in the fresh and mineralized rock samples of the Burnthill Pluton are given in Table 32.

In the fresh rocks, a significant positive correlation exists for U with Rb, Y, Nb, Ta, Lu, and W and a significant negative correlation with Sr, Ba, Zr, Hf, La, and to some extent with F. Those elements exhibiting positive correlations with uranium are mostly incompatible elements that are generally concentrated in late stage residual fluids by magmatic processes. There is a lack of correlation of U with Sn and Zn contents of the rocks (Table 32).

Thorium in the fresh rocks correlates positively with Sr, Zr, Hf, and La and negatively with Rb, Y, Nb, Ta, W, Sn, and Zn. This pattern of correlations suggest that Th is associated with accessory minerals.

The low negative correlation of both uranium and thorium with fluorine (Table 32) in the fresh rocks of Burnthill Pluton may be attributed to the escape of fluorine from the magma during the final stages of differentiation. This was also evident from the negative correlation coefficients (r = -0.45) between fluorine and silica calculated for the fresh rock samples.

In the mineralized rock samples (Table 32) uranium has a significant positive correlation with Y, Ta, Lu, and to some extent with W. The degree of negative correlation between U and Sn, and positive correlation with Zn increased in the mineralized samples in comparison to the fresh samples. This may indicate that fractionation between uranium and tin took place during the mineralization processes and that uranium may partly accompany base-metals during its mineralization.

Factor analyses were carried out on the trace element data in the fresh rocks (Fig. 40). Loadings on Factor I reveals that Rb, Y, Nb, Ta, Lu, Tb, and Yb separate from Sr, Ba, Zr, Zn, Cs, and La. Uranium follows the former group. This factor may be attributed to magmatic processes where uranium becomes enriched along with other incompatible trace elements in the late stage residual phase of the magma.

In Factor II (Fig. 40), uranium has no contribution, whereas thorium has a large contribution and it is associated to some extent with hafnium.

Factor III (Fig. 40) is related to uranium enrichment during late stage magmatic processes and shows that uranium makes a large contribution and is associated with niobium.

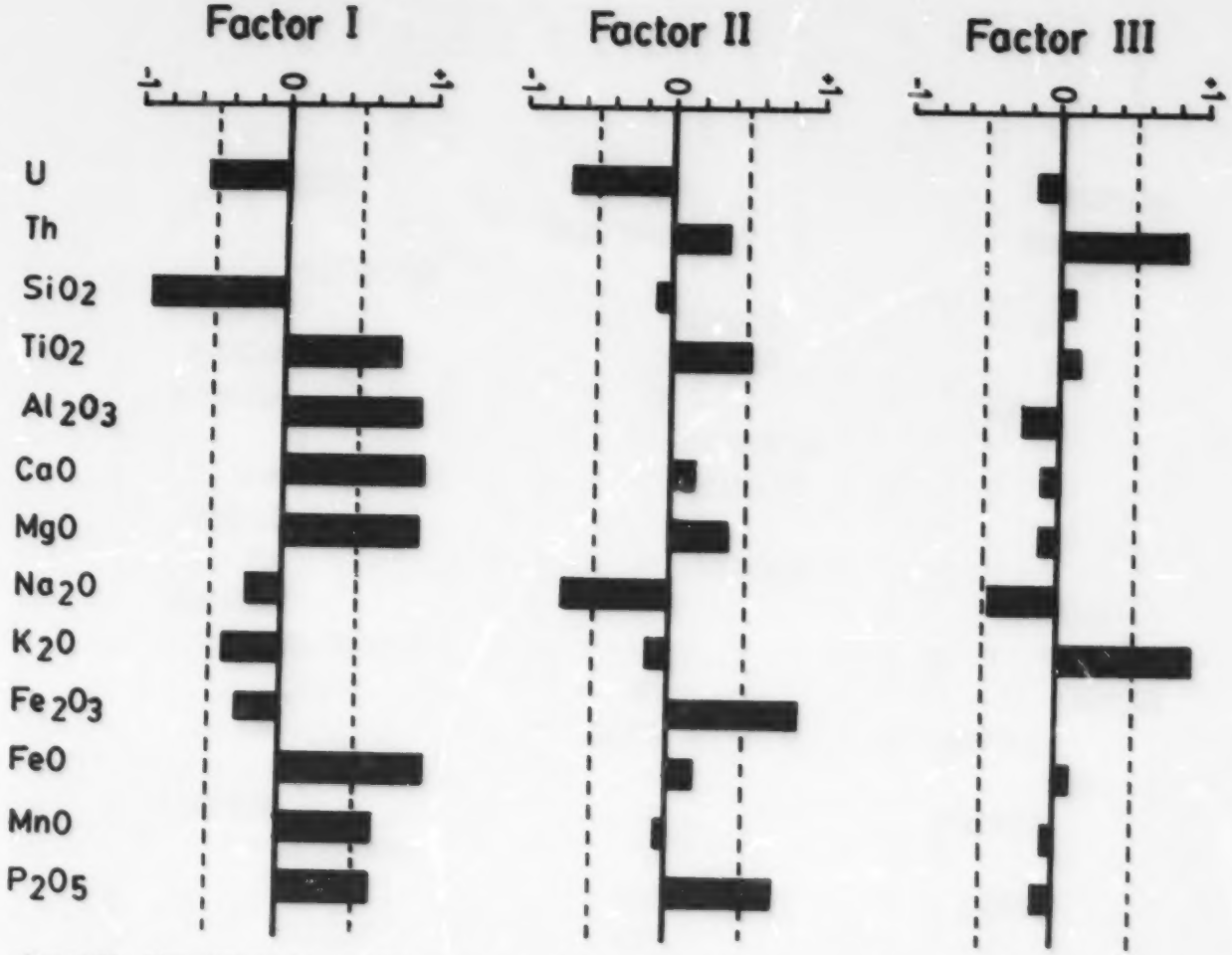

Figure 39. Plots of Factor I, II, and III loadings for major oxide contents in the unmineralized rocks of the Burnthill Pluton.

URANIUM AND ASSOCIATED ELEMENTS CONTENTS WITH RESPECT TO THE GRANITIC TYPES

General statement

Great progress has recently been made in establishing that certain genetic types of granitic plutons are associated with specific types of metal deposits. For instance, Sn, W, F, and U mineralization is generally associated with peraluminous granites that were derived from a sedimentary protolith by anatexis (Chatterjee et al., 1983; Plant et al., 1985; Dubessy et al., 1987). Therefore it is important to establish the genetic types of the granitic plutons in order to assess their potential for uranium and other metals.

At least three groups of granites exist with distinctive mineral associations: I-type, S-type, and A-type granites. Exploration for minerals in granites is usually based on these three types of granitic genesis. For instance many Cu-Mo prophyry deposits are associated with I-type granites (Takahashi et al., 1980) whereas U, Sn, and W are usually associated with S-type and A-type granites (Oshin and Rahman, 1986; Sawka and Chappell, 1986; Barreto et al., 1988).

Chappell and White (1974) have divided the granites of eastern Australia into I- and S-type which correspond to some extent to the calc-alkaline and alkali granites (Moreau, 1976; Pitcher, 1979), respectively. The I-type granites are considered to have been generated from igneous source rocks whereas the S-type granites generated from sedimentary rocks (Chappell and White, 1974; White and Chappell, 1983). The S- and I-type classification is genetic. Ishihara (1977) has added a new classification which is descriptive, in which he classified the granitic rocks of Japan into an ilmenite-series and a magnetite-series. Magnetite-series granites are equivalent to I-type granites whereas the ilmenite-series granites include both I- and S-type granites. The granitoids of magnetite-series are believed to be derived from the mantle whereas the granitoids of ilmenite-series are believed to be derived from reducing, carbon-bearing sedimentary sources. Ilmenite-series granites of Japan are enriched with tin in greisen whereas magnetite-series have associated molybdenum and base-metal deposits.

Table 32. Matrix of Spearman rank correlation coefficients for U, Th, and other trace elements in fresh (n* = 15; upper left corner) and mineralized (n = 10; lower right corner) rock samples of the Burnthill Pluton.

	U	Th	Rb	Sr	Cs	Ba	Y	Zr	Nb	Hf	Ta	La	Lu	F	W	Sn	Zn
Zn	0.02	-0.41	-0.06	-0.06	0.67	-0.01	-0.22	0.08	0.24	0.08	-0.01	-0.09	-0.11	0.24	0.34	0.27	
Sn	-0.04	-0.78	0.40	-0.25	0.05	-0.22	0.36	-0.29	0.13	-0.30	0.31	-0.27	0.38	0.36	0.77		0.74
W	0.31	-0.82	0.53	-0.53	-0.09	-0.46	0.46	-0.58	0.36	-0.42	0.51	-0.58	0.44	0.18		-0.32	-0.16
F	-0.12	-0.18	-0.14	0.16	0.35	0.04	-0.11	0.15	-0.05	-0.27	-0.09	0.32	-0.16		--	--	--
Lu	0.53	-0.37	0.91	-0.82	-0.62	-0.74	0.94	0.75	0.59	-0.38	0.78	-0.64		--	0.02	-0.56	-0.18
La	-0.73	0.59	-0.71	0.84	0.31	0.64	-0.57	0.86	-0.72	0.65	-0.74		-0.12	--	-0.20	0.62	0.51
Ta	0.76	-0.47	0.82	-0.88	-0.24	-0.72	0.78	-0.56	0.81	-0.38		0.34	0.11	--	0.05	0.30	0.39
Hf	-0.39	0.48	-0.40	0.49	0.24	0.35	-0.34	0.56	-0.35		0.82	0.80	0.05	--	-0.17	0.43	0.32
Nb	0.88	-0.37	0.64	-0.91	-0.04	-0.69	0.61	-0.72		0.03	0.22	0.03	0.61	--	0.21	-0.15	0.16
Zr	-0.79	0.51	-0.86	-0.92	-0.48	0.80	-0.71		-0.11	0.93	0.66	0.90	-0.06	--	-0.33	0.55	0.56
Y	0.53	-0.30	0.87	-0.78	-0.57	-0.78		0.13	0.62	0.37	0.43	0.14	0.71	--	0.26	-0.46	-0.01
Ba	-0.72	0.25	-0.89	0.90	0.46		-0.76	0.16	-0.51	-0.12	-0.21	0.09	-0.59	--	-0.09	0.33	0.15
Cs	-0.30	-0.12	-0.56	0.41		0.62	-0.29	0.67	-0.24	0.48	0.28	0.74	-0.58	--	-0.17	0.62	-0.59
Sr	-0.82	0.41	-0.93		0.50	0.22	-0.08	0.34	-0.55	0.35	0.13	0.28	-0.53	--	0.13	0.04	-0.19
Rb	0.65	-0.36		0.40	0.96	0.67	-0.32	0.61	-0.24	0.44	0.28	0.65	-0.59	--	0.05	0.57	0.58
Th	-0.22		0.26	0.48	0.41	-0.28	0.37	0.80	-0.03	0.87	0.70	0.74	0.01	--	-0.48	0.39	0.43
U		0.11	0.02	-0.16	-0.10	-0.08	0.52	0.22	0.07	0.29	0.46	0.01	0.45	--	0.32	-0.35	0.18

* n = number of samples.

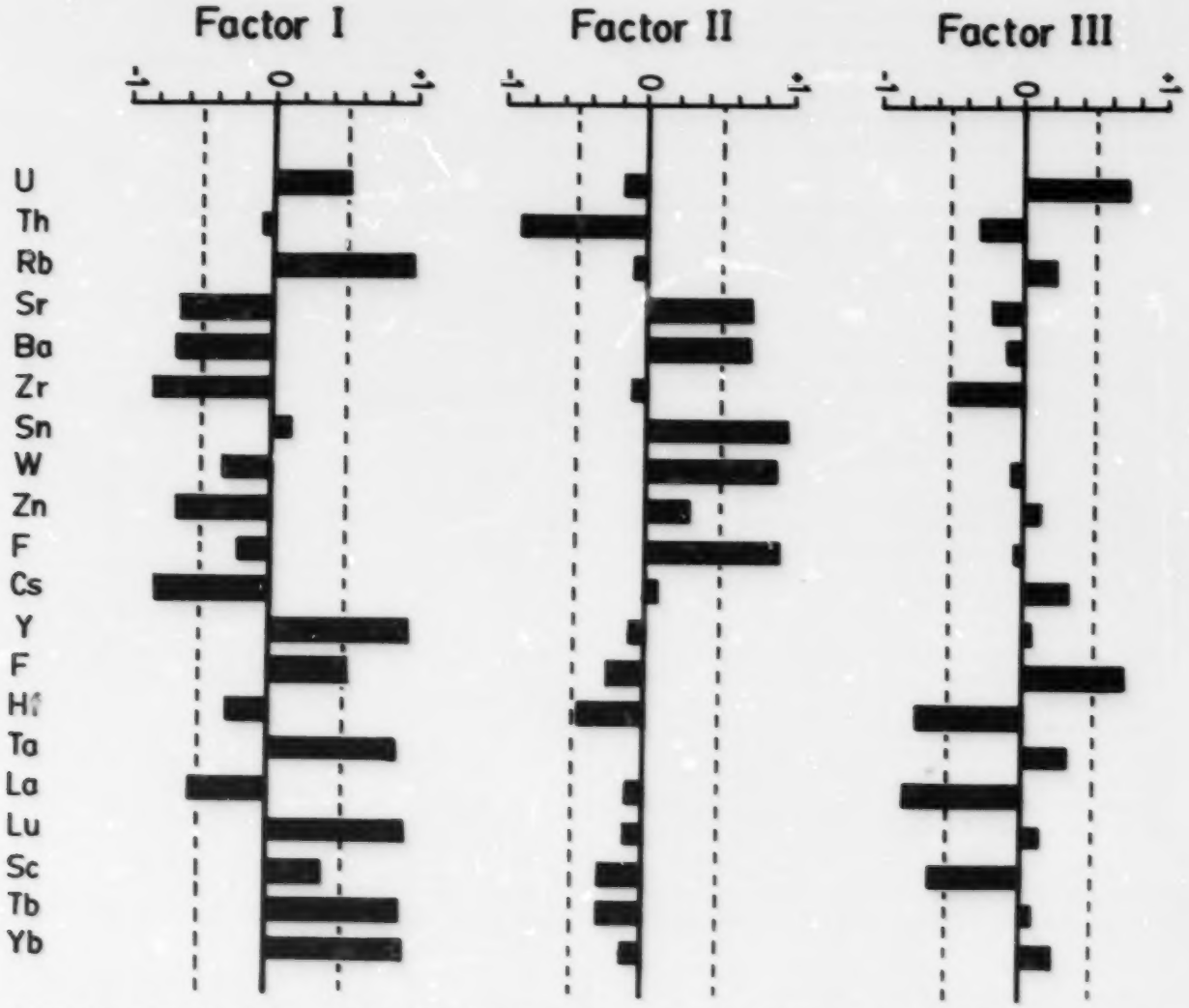

Figure 40. Plots of Factor I, II, and III loadings for trace element contents in the unmineralized rocks of the Burnthill Pluton.

An additional type has been added to the classification, A-type (anorogenic or alkaline) granites, by Loiselle and Wones (1979). Collins et al. (1982) and Loiselle and Wones (1979) believed that the A-type granites formed by crystallization of magma derived from a granulite terrane from which an earlier magma had been produced, i.e., formed late in the magmatic cycle. Recently, Whalen et al. (1987) suggested that A-type granites were probably derived from partial melting of fluorine and/or chlorine enriched, dry, granulitic residue remaining in the lower crust after extraction of an orogenic granite. Anderson (1983) suggested an alternative source for anorogenic granitic magmas, i.e. fusion of the lower crust containing I-type granite.

Granite types of the North Pole and the Burnthill plutons

Ruitenberg and Fyffe (1982) have classified the granitic rocks of Burnthill, Dungarvon, Trout Brook, and Rocky Brook plutons as belonging to S-type granitoids. However, Whalen (1986) and more recently MacLellan and Taylor (1989) have classified these granitic plutons as A-type granites on the basis of their high silica content (SiO_2, >74 wt. %) and elevated abundances of Rb, Ga, Y, Zr, and Nb and their low Sr and Ba values.

The North Pole Pluton and the Burnthill Pluton intruded after the closure of the Iapetus Ocean, as did other Paleozoic granitoid rocks of the Appalachian Orogen (Chatterjee and Strong, 1985) and therefore later than the subduction process. They are not characteristic I-type granitoids of a circum-Pacific type. Furthermore, the granitic rocks of the North Pole and the Burnthill plutons intruded sedimentary rocks and peraluminous Ordovician granites and cogenetic silicic volcanic rocks that presumably derived by partial melting of continental crust (van Staal, 1987). Hence, granitic rocks such as those of North Pole and Burnthill plutons, derived from partial melting of these sedimentary, granitic, and silicic volcanic rocks are expected to be of S- or A-type affinities.

The general geological features of the North Pole and the Burnthill plutons are compared and contrasted with typical I-, S-, and A-type granitoids (Table 33). Both of these plutons are comparable to S-type and A-type granitoids. However, their whole rock geochemical compositions (Table 34) show greater similarity with the A-type than with the S-type.

The plot of molecular Al_2O_3/Na_2O+K_2O values versus molecular Al_2O_3/Na_2O+K_2O+CaO values for the apparently fresh rock samples of the North Pole and the Burnthill plutons (Fig. 41) reveals that these rocks are predominantly peraluminous. This suggests that they are derived from partial melting of crustal rocks (i.e., S-type granitoids). The S-type affinities of the North Pole and the Burnthill plutons are further supported by using the ACF ternary diagram (Fig. 42) of Takahashi et al. (1980). It is obvious from Figure 42 that most of the fresh samples fall well within the field of typical 'S-type' granitoids.

The oxygen-fugacities (fO_2), as expressed by atomic $Fe^{3+}/Fe^{2+}+Fe^{3+}$ ratio, for the fresh granitic rock samples of the North Pole (average 0.35) and the Burnthill (average 0.52) plutons are low to intermediate, respectively. The ratio $Fe^{3+}/Fe^{2+}+Fe^{3+}$ is considered by Ishihara (1977) as a convenient parameter for distinguishing the magnetite-series from the ilmenite-series granitoids. The atomic $Fe^{3+}/Fe^{2+}+Fe^{3+}$ is relatively high in magnetite-series granitoids and low in ilmenite-series granitoids. The classification of the granitic rocks into magnetite- and ilmenite-series has some implications in mineral exploration. According to Ishihara (1977), Sn, W, Nb, and Ta deposits are associated with ilmenite-series granitoids whereas Mo, Cu, Pb, Zn, Ag, and Au deposits are associated with magnetite-series.

The above discussion suggests that the North Pole and the Burnthill plutons belong to the ilmenite-series granitoids of S-type. However, the enrichment of the granites, particularly the Burnthill Pluton, with F, Nb, Ta, and Y and their depletion with V, Ni, Co, and Cr suggests that the Burnthill Pluton and to some extent the North Pole Pluton are of A-type granitoids.

Granite type determination of the North Pole and the Burnthill plutons by using discriminant analyses

The classification of granitoids into I-, S-, and A-types is based mainly on chemical analyses and a comparison of their compositions with those of rocks already classified. However, the large number of chemical criteria are not always in agreement and uncertainties as to classification may arise. Therefore, in this work an attempt is made to classify rocks quantitatively into their genetic types by using a multivariate statistical technique known as discriminant analyses. Discriminant analyses are used to classify specimens into one, two or more alternative groups on the basis of a set of measurements.

Suppose that rock samples from three suites of granitoids of known genetic types (i.e., from I-, S-, and A-type granitoids) are collected and chemically analyzed. From these analyses it is possible to find by discriminant analyses linear functions that produce the maximum differences among the three defined types. Using these linear functions it is possible to assign samples of unknown origin to one of the known granitoid suites.

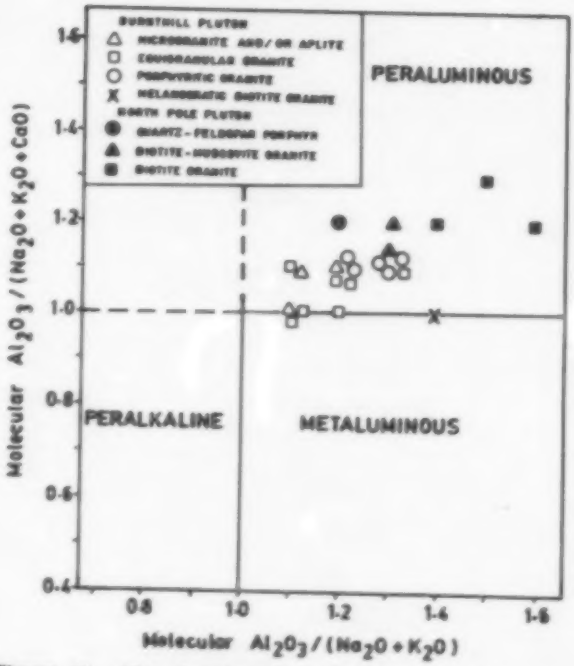

Figure 41. Plot of molecular $Al_2O_3/(Na_2O + K_2O)$ versus molecular $Al_2O_3/(Na_2O + K_2O + CaO)$ for the rocks of the North Pole and Burnthill plutons.

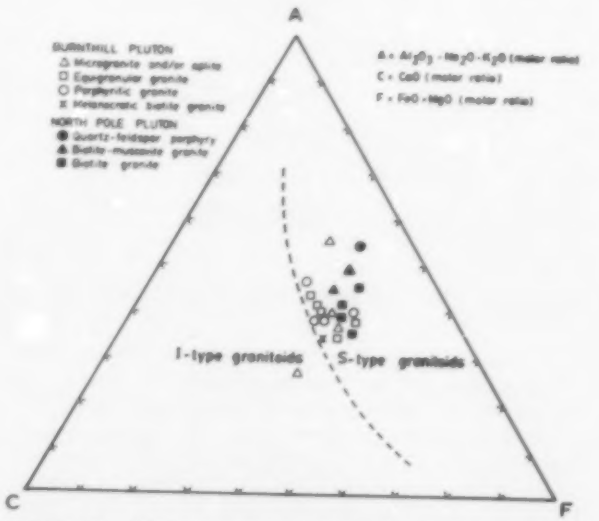

Figure 42. ACF plot of the granitic rocks of the North Pole and Burnthill plutons (after Takahashi et al., 1980).

The discriminant analysis used in the present work was adapted from the 'Statistical Analysis System' (1982). A detailed explanation of the theoretical aspects of the technique is beyond the scope of the present work, but the results and the application of the technique are discussed briefly.

Table 33. Geological features of the North Pole and Burnthill plutons and their comparison to I-, S-, and A-type granitoids.

CRITERIA	I-TYPE GRANITOIDS	S-TYPE GRANITOIDS	A-TYPE GRANITOIDS	NORTH POLE PLUTON	BURNTHILL PLUTON
EXAMPLES	– Sierra Nevada Batholith, U.S.A. – Cairngurm Pluton, British Caledonia	– Hercynian granites of Massif Central, France – Hercynian granites of SW England – South Mountain Batholith, N.S.	– Nigerian Younger granites – Cornwall granite, England – Pike Peak Batholith, U.S.A.		
ORIGIN	– Generated at deeper level in the earth's crust over subduction zones	– Generated by anatexis in areas of thickened silicic crust as a result of collision of an island arc with a stable craton	– Generated along rift zones and within stable continental block (anorogenic)	– Partial melting of sedimentary protolith	– Partial melting of sedimentary protolith
ASSOCIATED MINERAL DEPOSITS	Cu–Mo porphyry	U–Sn–W–F	U–Sn–W–Mo–Zn–Nb–F	U–Sn–W–Mo–Cu–Pb–Zn–Ag–Au	U–Sn–W–Mo–F
MINERALOGY	– Hornblende and sphene are common – Presence of magnetite – Normative diopside or corundum (<1%)	– Absence of hornblende and sphene – Absence of magnetite – Presence of biotite, muscovite, garnet, cordierite, sillimanite, and andalusite. – Normative corundum (>1%)	– Hastingsite and biotite are common – The feldspar is mainly alkali feldspar – Micrographic intergrowth of quartz and alkali feldspar are very common.	– Biotite and muscovite are common – Presence of garnet – Normative corundum (>1%)	– Biotite and muscovite are common – Presence of garnet – Absence of hornblende – Normative corundum (>1%)
CHEMISTRY	– Broad SiO_2 composition (53–76 wt.%) – Mol.$[Al_2O_3/(Na_2O+K_2O+CaO)]$ <1 – High Na_2O content – (Na_2O > 3.2% in felsic members and Na_2O > 2.2% in mafic members) – High CaO content – Relatively high fO_2 – Variation diagrams are linear or near linear – Low Cr and Ni contents – Low K_2O/Na_2O – Low initial $^{87}Sr/^{86}Sr$ ratio (0.704–0.706) – $\delta^{18}O$ low (–6–10% SMOW)	– Restricted SiO_2 composition (>70 wt.%) – Highly peraluminous Mol. $[Al_2O_3/(Na_2O+K_2O+CaO)]$ >1 – Low Na_2O content (Na_2O < 3.2% in felsic members and < 2.2% in mafic members) – Low CaO content – Significantly low fO_2 – Variation diagrams are irregular – Low Sr content – High Cr, Ni, Ti, V, Co, Cu, and Zn contents. – High K_2O/Na_2O – Low Rb/Sr, K/Rb, Zr/Sn and V/Nb – High initial $^{87}Sr/^{86}Sr$ ratio (>0.708) – $\delta^{18}O$ high (>10% SMOW)	– Restricted SiO_2 composition (often near 76 wt.%) – Mostly metaluminous but peraluminous and peralkaline also found – High Na_2O content (>3%) – Low CaO content – Low to moderate fO_2 – High in trace element contents; (REEs except Eu), Zr, Nb, Ta, Ga, Y, Ce – Low in compatible trace element contents; Co, Cr, Ni, Sr, Ba, and Sc – High F and Cl contents – High K_2O/Na_2O – Low f_{H_2O} – High HF/H_2O ratio in the magma – Initial $^{87}Sr/^{86}Sr$ ratios (0.703–0.712)	– Restricted SiO_2 composition (av. 73 wt.%) – Peraluminous Mol. $[Al_2O_3/(Na_2O+K_2O+CaO)]$ >1 – High Na_2O content (3.3%) – Low CaO – Variation diagrams are irregular – Low fO_2 – High K_2O/Na_2O – High Rb/Sr – High initial $^{87}Sr/^{86}Sr$ ratio (>0.706)	– Restricted SiO_2 composition (av. 76 wt.%) – Peraluminous Mol. $[Al_2O_3/(Na_2O+K_2O)]$ >1 – High Na_2O content (av. 4.5%) – Low CaO – High Rb, Y, Nb and Ta contents – Low Sr, Ba, Cr, and Co – Low fO_2 – High K_2O/Na_2O – High Rb/Sr

Table 34. Average major oxides and trace element contents in the North Pole Pluton and the Burnthill Pluton and their comparison to I-, S-, and A-type granitoids.

Elements	I-type* (n = 532)	S-type* (n = 316)	A-type* (n = 31)	North Pole (n = 7)	Burnthill (n = 15)
SiO_2 (%)	68.0	69.1	73.6	72.7	76.3
TiO_2 (%)	0.5	0.6	0.3	0.3	0.2
Al_2O_3 (%)	14.5	14.3	12.7	14.4	12.9
Fe_2O_3 (%)	1.3	0.7	1.0	0.6	0.8
FeO (%)	2.6	3.2	1.7	1.5	1.0
MnO (%)	0.1	0.1	0.1	0.1	0.1
MgO (%)	1.8	1.8	0.3	0.6	0.3
CaO (%)	3.8	2.5	1.1	1.0	0.3
Na_2O (%)	3.0	2.2	3.3	3.4	4.5
K_2O (%)	3.1	3.6	4.5	4.5	6.2
P_2O_5 (%)	0.11	0.13	0.09	0.09	0.05
Rb (ppm)	132	180	199	185	421
Sr (ppm)	253	139	105	101	60
Ba (ppm)	520	480	605	457	151
Y (ppm)	27	32	76	--	65
Zr (ppm)	143	170	342	115	106
Nb (ppm)	9	11	22	--	27
La (ppm)	29	31	55	--	25
Sc (ppm)	15	14	14	--	5
Zn (ppm)	52	64	102	132	45
Cu (ppm)	11	12	6	11	--
Pb (ppm)	16	27	29	23	--
Ni (ppm)	9	17	2	--	5
Cr (ppm)	27	46	3	--	14
V (ppm)	74	72	10	--	4

*Data obtained from White and Chappell (1983).
n = number of samples.

Only major oxide contents were used to discriminate between different granitoid suites. The data for typical I- and S-type granitoids were taken from analyses of the Koaciusko Batholith, Australia (Hine et al., 1978) whereas that of typical A-type granitoids were obtained from the Mumbulla Suite granites, southeastern Australia (Collins et al., 1982). Afterward two types of discriminant techniques, stepwise and canonical, were performed on the compiled data.

Stepwise discriminant analysis is used to select the variables (the major oxides in our case) that contribute most in recognizing the differences among the I-, S-, and A-type granitoids. In this case the procedure was able to select Al_2O_3, TiO_2, MnO, Na_2O, K_2O, and P_2O_5 as the best discriminators among the three granitoid suites. This selection appears to be reasonable since Al_2O_3, K_2O, and Na_2O contents are critical to differentiate among I-, S-, and A-types.

Following this, canonical discriminant analysis was carried out by using only the selected variables, and was used to obtain the discriminant functions which are simply linear combinations of the variables involved, in this case Al_2O_3, TiO_2, MnO, Na_2O, K_2O, and P_2O_5. The canonical function has the following form:

$$D=\mu_0 + \mu_1X_1 + \mu_2X_2 \ldots + \mu_pX_p \quad \ldots\ldots\ldots\ldots\ldots\ldots \quad (4)$$

where:

D=the value on the canonical discriminant function in the group,

μ=coefficient which produces the desired characteristics in the function, and

X=the values on discriminating variables.

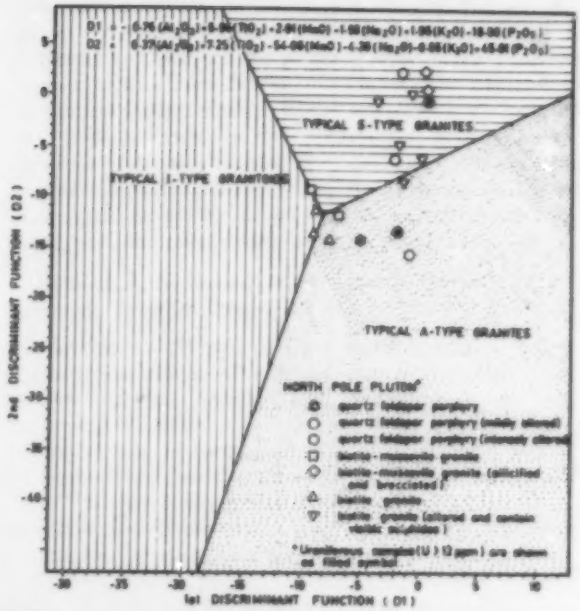
TYPICAL S-TYPE GRANITES
TYPICAL I-TYPE GRANITOIDS
TYPICAL A-TYPE GRANITES
NORTH POLE PLUTON*
quartz feldspar porphyry
quartz feldspar porphyry (mildly altered)
quartz feldspar porphyry (intensely altered)
biotite-muscovite granite
biotite-muscovite granite (silicified and brecciated)
biotite granite
biotite granite (altered and contain visible sulphides)
* Uraniferous samples (U > 12 ppm) are shown as filled symbol
2nd DISCRIMINANT FUNCTION (D2)
1st DISCRIMINANT FUNCTION (D1)

Figure 43. Plot of the granitic rock samples of the North Pole Pluton on the proposed discriminant diagram used to distinguish I-, S-, and A-type granitoids.

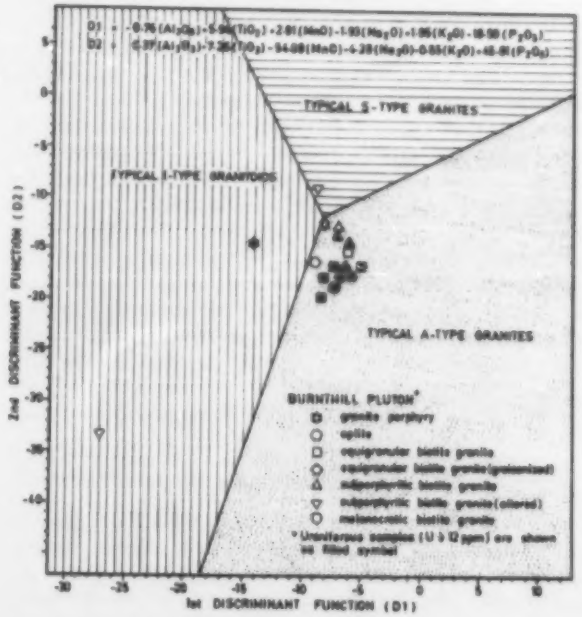

Figure 44. Plot of the granitic rock samples of the Burnthill Pluton on the proposed discriminant diagram used to distinguish I-, S-, and A-type granitoids.

Since only three groups (I-, S-, and A-type) of granitoids are involved, two canonical discriminant functions were obtained and are as follows:

$$D_1 = -0.76(Al_2O_3) + 5.96(TiO_2) + 2.91(MnO) - 1.93(Na_2O) + 1.95(K_2O) - 18.50(P_2O_5) \quad \ldots\ldots\ldots\ldots\ldots\ldots \quad (5)$$

$$D_2 = 0.37(Al_2O_3) + 7.25(TiO_2) - 54.08(MnO) - 4.28(Na_2O) - 0.55(K_2O) + 45.81(P_2O_5) \quad \ldots\ldots\ldots\ldots\ldots\ldots \quad (6)$$

A diagram showing the zones defined by I-, S-, and A-type granitoids was plotted (Fig. 43, 44).

The Al_2O_3, TiO_2, MnO, Na_2O, K_2O, and P_2O_5 contents in the rocks of the North Pole and the Burnthill plutons were substituted in equations (5) and (6) and the values of D_1 and D_2 for the two plutons were projected on figures 43 and 44, respectively.

The samples of the North Pole Pluton are mainly scattered between the zones defined by typical S- and A-type granitoids (Fig. 43). Interestingly most of the fresh rocks fall within the zone of typical A-type granitoids whereas the altered and mineralized samples fall within the zone of S-type granitoids. Thus, it is possible to assume that hydrothermal alteration may have modified part of the pluton from A- to S-type composition. Similar changes have been documented elsewhere, (for example, Simpson et al., 1982; Pitcher, 1987) and attributed to metasomatic alterations. Unlike the North Pole Pluton, the Burnthill Pluton retained its original type even after interaction with hydrothermal solutions.

According to this analysis, rocks of the Burnthill Pluton are predominantly of A-type as shown in Figure 44, which supports the suggestion previously put forward by Whalen (1986) and MacLellan and Taylor (1989).

METALLOGENIC MAPS AND CONCEPTUAL MODELS FOR URANIUM AND ASSOCIATED ELEMENTS DISTRIBUTION IN NORTH POLE AND CENTRAL MIRAMICHI ANTICLINORIUM PLUTONS

Metallogenic maps

General statement

One aim of this study has been to assess the North Pole and central Miramichi Anticlinorium plutons and surrounding rocks (Fig. 1) in terms of their favorability for uranium mineralization. To this end a generalized metallogenic map has been compiled to assist in exploration for uranium and associated metals.

Using the limited data available the maps have been divided into uranium-barren areas, here defined as those which contain below the background level values of uranium (50 percentile or median), where uranium mineralization is unlikely to take place, and uranium-bearing areas, defined as those which contain anomalous values of uranium (greater than 50 percentile), where U mineralization is more likely to occur.

Long Lake area

The staff of Canadian Occidental Petroleum collected a considerable number of samples (float, outcrop, and trench) during their exploration program. These samples were

Table 35. Statistical abundances of elements in bedrock and float samples in the Long Lake area.

Element	BEDROCK SAMPLES						FLOAT SAMPLES					
	n	Mean ± St.Dev.	50 Percentile (Median)	75 Percentile	90 Percentile	95 Percentile	n	Mean ± St. Dev.	50 Percentile (Median)	75 Percentile	90 Percentile	95 Percentile
U (ppm)	54	93.6 ± 427.8	6.4	14.8	70.0	503.7	31	274.2 ± 672.6	26.4	130.0	1202.0	2256.0
Th(ppm)	52	68.3 ± 119.9	24.0	41.8	208.7	394.8	25	11.9 ± 8.4	11.0	16.5	22.8	31.0
Cu(ppm)	55	2172.7 ± 6745.0	92.0	196.0	5828.0	21840.0	31	83.5 ± 203.8		83.0	160.0	660.0
Pb(ppm)	54	929.2 ± 2482.0	168.0	800.0	2760.0	3130.0	31	241.0 ± 409.6	100.0	240.0	816.0	1460.0
Zn(ppm)	55	2990.3 ± 7020.6	480.0	2270.0	9420.0	19560.0	31	800.9 ± 3284.1	48.0	219.0	1044.0	8115.9
Mo(ppm)	51	76.6 ± 288.3	11.0	24.0	117.6	408.0	26	4693.0 ± 23519.0	15.5	101.5	451.0	78370.3
Sn(ppm)	15	150.1 ± 253.2	58.0	134.0	653.8	976.0	-	-	-	-	-	-
Ag(ppm)	47	17.9 ± 48.1	2.0	8.0	57.2	106.8	15	2.7 ± 4.3	1.0	3.0	11.0	17.0
Au(ppb)	5	1168.2 ± 1498.2	200.0	2800.0	3000.0	3000.0	6	18.3 ± 12.0	17.5	31.0	31.0	31.0

n = number of samples

chemically analyzed for U, Th, Cu, Pb, Zn, Mo, Sn, Ag, and Au contents. Results of the analyses are listed in Appendix X. Most of the samples were taken from the granitic rocks of the North Pole Pluton. The contents of uranium and other element in the samples were processed statistically to determine their abundances. Because almost all the float samples are mineralized and their sources were not fully identified, they were dealt with separately. On the other hand, the trench samples of the bedrock were combined with the outcrop samples in the statistical analyses.

Statistical abundances of elements in the bedrock and float samples in the Long Lake area are given in Table 35.

The median (50 percentile) of the data was chosen to represent the threshold level of elements. Locations of bedrock and float samples with anomalous levels (>50 percentile) of uranium and thorium were plotted on the geological map of Long Lake area (Fig. 3). Furthermore, the uranium and thorium anomalies were classified according to their statistical element abundances (75 percentile, 90 percentile, and 95 percentile; Table 35) into three different classes; low, medium, and high (Fig. 3). Anomalous levels of Cu, Pb, Zn, Mo, Sn, Ag, and Au in the samples are also given beside U and Th on the map (Fig. 3). As shown in Figure 3, most of the highly anomalous occurrences are located on the eastern side of Long Lake, in close association with the quartz-feldspar porphyry dykes, particularly with the highly altered and brecciated zones of the dykes.

On the basis of geochemical anomalies (soils, lake sediments, spring and stream sediments, bedrock and drill cores) and radiometric anomalies, the Long Lake area is divided into favourable and unfavourable areas for uranium and associated elements exploration (Fig. 45). The favourable areas are further subdivided into six zones with different orders of favourability. These zones of favourability were delineated according to the quantity and quality of the data used in their identifications. For example, in the first-order favourability zones, positive signs of mineralization were obtained from drill cores, overburden materials, bedrock and radiometric data. In the sixth-order favourability anomalous uranium was found only in spring and stream sediment samples. The best target, as the available data indicates, for uranium exploration in the area would be the centre of Long Lake and its eastern side.

Central Miramichi Anticlinorium area

A total of 40 mineral occurrences (Appendix II) of endo- and exo-granitic types were plotted on a recent geological map of the area (Fig. 6). These occurrences are closely related to the granitic rocks of the Burnthill, Dungarvon, Trout Brook, and Rocky Brook plutons.

The main types of mineralization shown on the metallogenic map (Fig. 6) are as follows:

a. Veins and stockworks
b. Intramagmatic
c. Porphyry type
d. Disseminated and/or stringer sulphides
e. Combination of two or more of the above (a-d) types

On the basis of the type of mineralization, each occurrence is represented by a specific symbol (Fig. 6). For structurally controlled deposits, the preferred direction of mineralization is shown.

In addition to the 40 mineral occurrences, the highly anomalous eU values (>90 percentile) of rock samples determined by in situ gamma ray spectrometry (Appendix VII) were plotted on the same geological map (Fig. 6). Anomalous levels of uranium appear to be associated with the eastern and southeastern portion of the Burnthill Pluton, eastern and southern portion of the Dungarvon Pluton and eastern portion of the Rocky Brook and Trout Brook plutons. Furthermore, the uranium anomalies are more or less spatially associated with the equigranular granitic phases of the plutons.

Conceptual models

General statement

The geological data and geological concepts established throughout this study have led to consideration of a number of models describing the geological processes that led to uranium mineralization in the North Pole and central Miramichi Anticlinorium plutons.

The magmatic-hydrothermal model described by Simpson et al. (1982) and Chatterjee et al. (1982) as well as the 'per descensum' model of Barbier (1974) are applicable to some extent. In the former model, a melt (usually granitic in composition) produces uranium and other metal enriched hydrothermal fluids that move upward from deeper zones in the Earth's crust to deposit these metals at higher levels.

In the 'per descensum' model, highly oxidized meteoric waters produced during continental weathering deplete uranium from surface rocks and deposit it wherever a suitable reduction zone is intersected.

Uranium deposits similar to those described in the present work are found in many places in the world. Most are associated with peraluminous two-mica granites, and many are also connected with hydrothermally altered and brecciated zones. The best examples are those associated with granitic rocks of Massif Central of France (Moreau, 1976), the Hercynian granites of Great Britain (Simpson and Plant, 1984), the two-mica granites in Schwarzach area of Germany (Dill, 1985) and the granitic rocks of South Mountain Batholith of Nova Scotia (Chatterjee and Strong, 1985). Both hypogene (hydrothermal fluids) and supergene (meteoric waters) processes have been proposed as being active in the formation of uranium deposits.

As in any other model of similar nature, the source of the uranium and associated metals, mechanism of their mobilization, and precipitation in suitable areas are the main factors considered.

North Pole Pluton

The brecciation of the host granites along fractures, alteration of wall rocks, and the formation of quartz veins in the

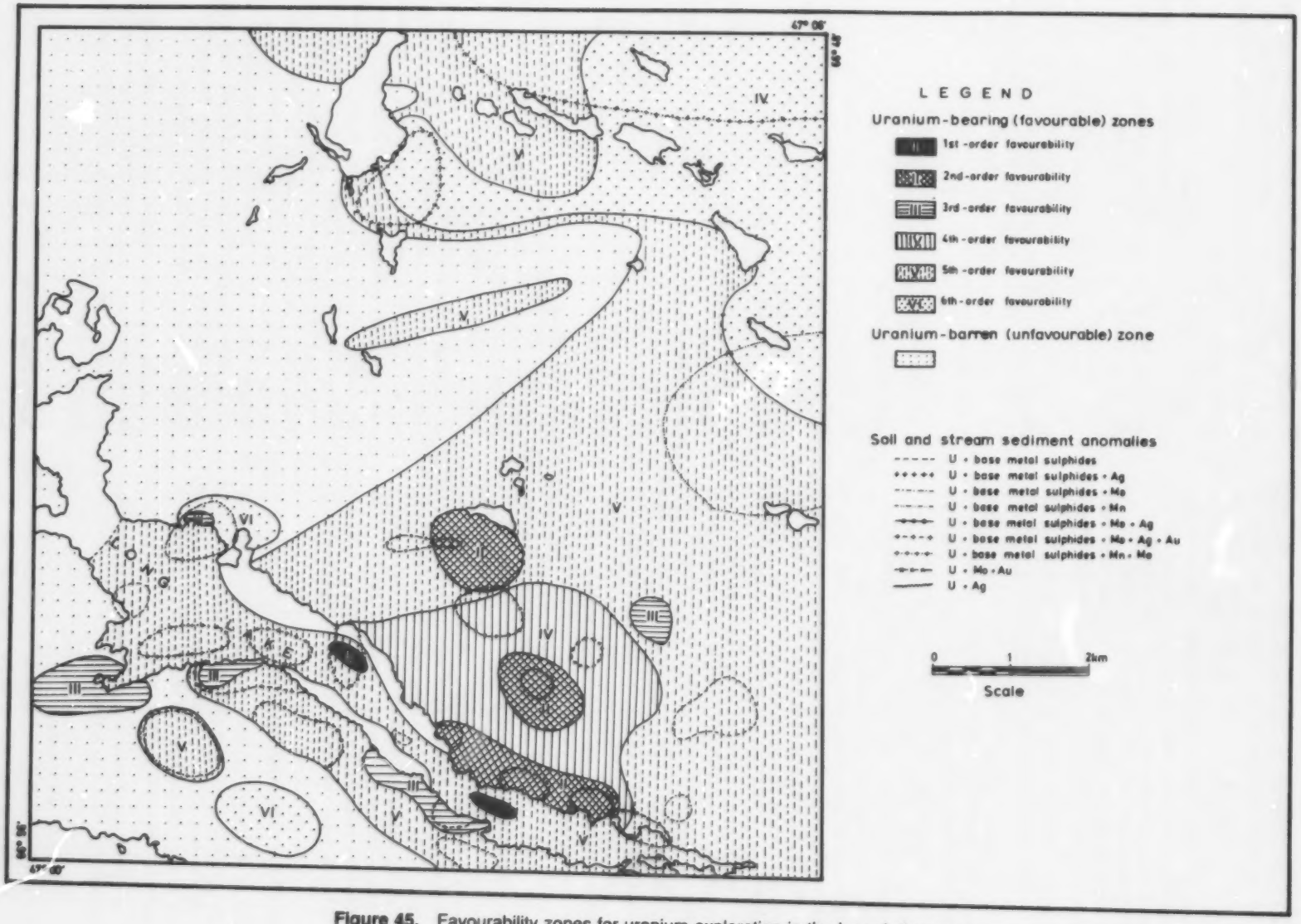

Figure 45. Favourability zones for uranium exploration in the Long Lake area.

North Pole Pluton are some of the features that support the hydrothermal model. The supergene model is supported by secondary uranium mineralization (autunite-torbernite) found in float. These two minerals are usually formed in supergene deposits (Dill, 1983). It may be that they were deposited in bedrock near the surface prior to their separation and transportation by weathering and/or glacial processes.

Metals, including uranium, could have been introduced into the Long Lake area during the generation of the highly evolved granite of North Pole Pluton (Fig. 46) as the chemical data suggest. The pluton was probably derived from metal-enriched sedimentary rocks as indicated by its peraluminous nature. Furthermore, the magma was apparently enriched with water (Fyffe and Pronk, 1985), and therefore capable of producing a hydrothermal system as a separate magmatic aqueous phase (hydrothermal fluid) upon cooling and crystallization (Burnham and Ohmoto, 1980). Such fluids could have acted independently as a mineralizing fluid, or may have contributed to convective cells generated in meteoric waters by magmatic or radiogenic heat. Such cells may act over long periods of time (Fehn et al., 1978).

As the magma moved upward in the Earth's crust to crystallize in the epizone, its content of uranium and other metals might have been enhanced as a result of its contamination with country rocks (Cambro-Ordovician metapelites).

The structural features produced (faults, joints, fractures, and brecciation) within the granitic rocks of North Pole Pluton as a result of the Acadian Orogeny played an important role in uranium mineralization. These structural features increased the permeability of the wall rocks and acted as conduits for hydrothermal fluid flow in the rocks and thus, enhanced the capacity of hydrothermal solutions for mineralization (Plant et al., 1985).

The continuity of flow and circulation in the hydrothermal fluids of a convective cell were probably maintained by periodic opening of fractures as a result of consecutive seismic activities (Mawer and Williams, 1985), similar to the recent series of earthquakes (M_b = 5.7) in the study area with the epicentre located within the North Pole Pluton (Berry et al., 1982). Studies by several investigators elsewhere also have indicated that vein-type hydrothermal deposits are frequently formed in seismically active areas (Golovin, 1979; Sibson et al., 1975; Plant et al., 1985; Durrance, 1985). The seismic activity in the area may also generate heat needed to maintain the convective cell.

Chemical reactions between the metal-bearing hydrothermal fluids and the wall rocks along the fractures may have resulted in the precipitation of quartz (chalcedony) along with uranium and associated metals. The wall rocks in turn were altered to chlorite, sericite, calcite, and kaolinite. A chemical environment favourable for reduction and precipitation of uranium could have been provided by sulphide minerals precipitated along the fractures prior to uranium mineralization (Fig. 5). The loss of CO_2 from the hydrothermal fluids to the wall rocks during carbonization may also have led to uranium mineralization (Rich et al., 1977).

The loss of alkalies (K and Na) as a result of more rock sericitization may have led to precipitation of silica (quartz or chalcedony) along veins. The data showed that uranium deposition accompanied chalcedony precipitation more than quartz precipitation. Quartz is a stable form of silica at P-T conditions found in hydrothermal systems and its presence usually indicates a slow change in chemical conditions accompanied by precipitation (Fournier, 1986). In contrast, chalcedony precipitates under rapid changes in the physical or chemical conditions of the fluids at temperature below 180°C. These conditions are: (1) rapid cooling, (2) mixing of different waters, (3) pH changes, and (4) reaction of the fluids with the silica in the host rocks (Fournier, 1986). Therefore, it is possible to assume that precipitation of uranium in the North Pole Pluton was favoured by some combination of these physicochemical changes.

Meteoric water (Fig. 46) containing dissolved oxygen could have dissolved phosphates from the Cambro-Ordovician metasedimentary rocks and become slightly acidic during its percolation in the rocks. When such water passed through the fractures of the North Pole Pluton it could have dissolved uranium along with copper. The sulphide minerals that were precipitated along fractures during hydrothermal processes may have provided the reduction zone favourable for secondary deposition of autunite and torbernite.

Central Miramichi Anticlinorium plutons

Uranium along with other metals, particularly Sn and W may have been initially enriched in the source materials of the granites (sedimentary rocks on the basis of being peraluminous 'S-type' granites) and concentrated in the granitic rocks of the plutons by partial melting of the source rocks (Fig. 47). The uranium content (and other metals) was further enhanced by magmatic differentiation which led to concentration of uranium and other incompatible elements (i.e., Sn, W, Mo, F, Bi, Li, Rb) in late stage differentiates of the granites. Thus, the late stage pods and dykes of granite porphyry, aplite, and granophyric granite phases of the pluton (Fig. 47) contain higher levels of uranium (and other metals) than the porphyritic granite phase.

A separate magmatic acqueous phase may have been developed within the magma during its late stage crystallization. This is indicated by the presence of aplitic and pegmatitic pods and miarolitic cavities. The aqueous phase was probably enriched in uranium and other incompatible elements, and transported uranium and other elements along fractures to suitable sites of deposition. The data presented here indicate that tin, tungsten, and molybdenum were probably deposited earlier at higher temperatures (associated with greisenization) whereas uranium was deposited later during the cooling of the hydrothermal fluids (i.e., at lower temperature). This is also evidenced by the association of uranium with low temperature alteration such as albitization.

Meteoric water containing dissolved oxygen may have been periodically added to the hydrothermal fluids. This meteoric water could have dissolved more uranium during

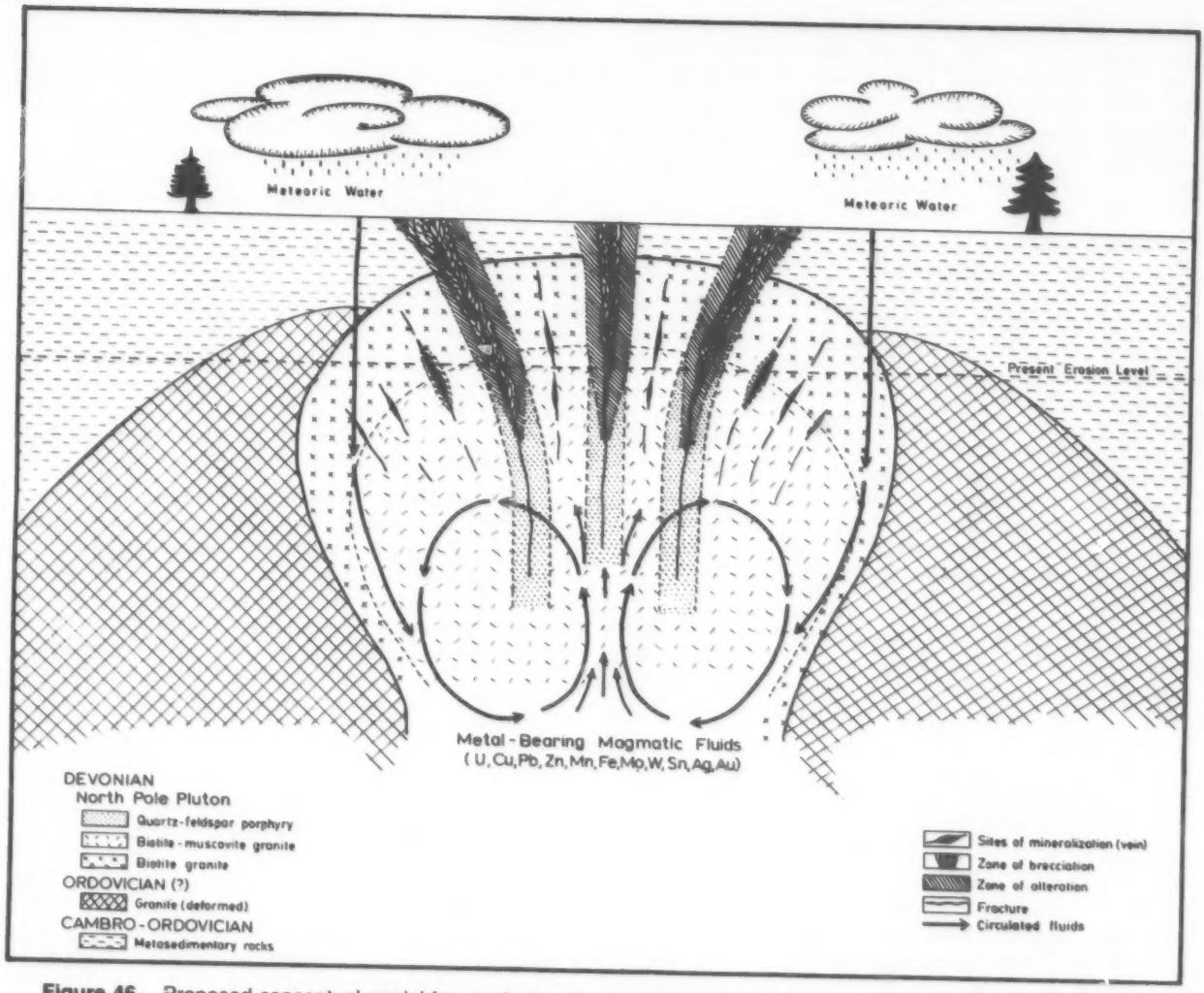

Figure 46. Proposed conceptual model for uranium and associated metals concentration in the North Pole Pluton.

its percolation in the metasedimentary rocks. The base-metal sulphides within the granitic rocks and in their vicinity may also have been derived from the metasedimentary rocks by meteoric waters.

Chemical reaction between the metal-bearing hydrothermal fluids and the wall rocks along fractures may have resulted in the precipitation of uranium (and other elements). The presence of fluorite in the uranium occurrence discovered in the northeastern part of the Dungarvon Pluton by R. Shives of the Geological Survey of Canada (Appendix II) may suggest that uranium existed in the hydrothermal solution as uranous fluoride complexes. The precipitation of fluorine ions as fluorite reduces uranous ion mobility in solutions and leads to the precipitation of uranium (Langmuir, 1978).

CONCLUSIONS AND GUIDELINES FOR FUTURE EXPLORATION

Conclusions

The Miramichi Anticlinorium metallogenic domain is part of a uranium-bearing belt that extends from Europe (Jachymov and P'ríbram areas, Czechoslovakia; Schwarzach area, Germany; Massif Central, France; Hercynian and Caladonian granites, Great Britain) to North America (South Mountain Batholith, Nova Scotia). The polymetallic vein-type uranium deposits in this belt have a common characteristic in that they all occur in late tectonic plutons and fractures. The mineralization is associated with re-activated faults intersecting highly evolved peraluminous two-mica granites. It appears also that uranium and other lithophile elements such as Sn, W, and Mo in this belt were at least temporally associated with the main orogenic events; Hercynian Orogeny in Europe and Acadian Orogeny in North America. Hence, it is assumed that the Acadian Orogeny (400 Ma) may represent a major metallogenic epoch for U, Sn, W, and Mo mineralization in the Miramichi Anticlinorium domain.

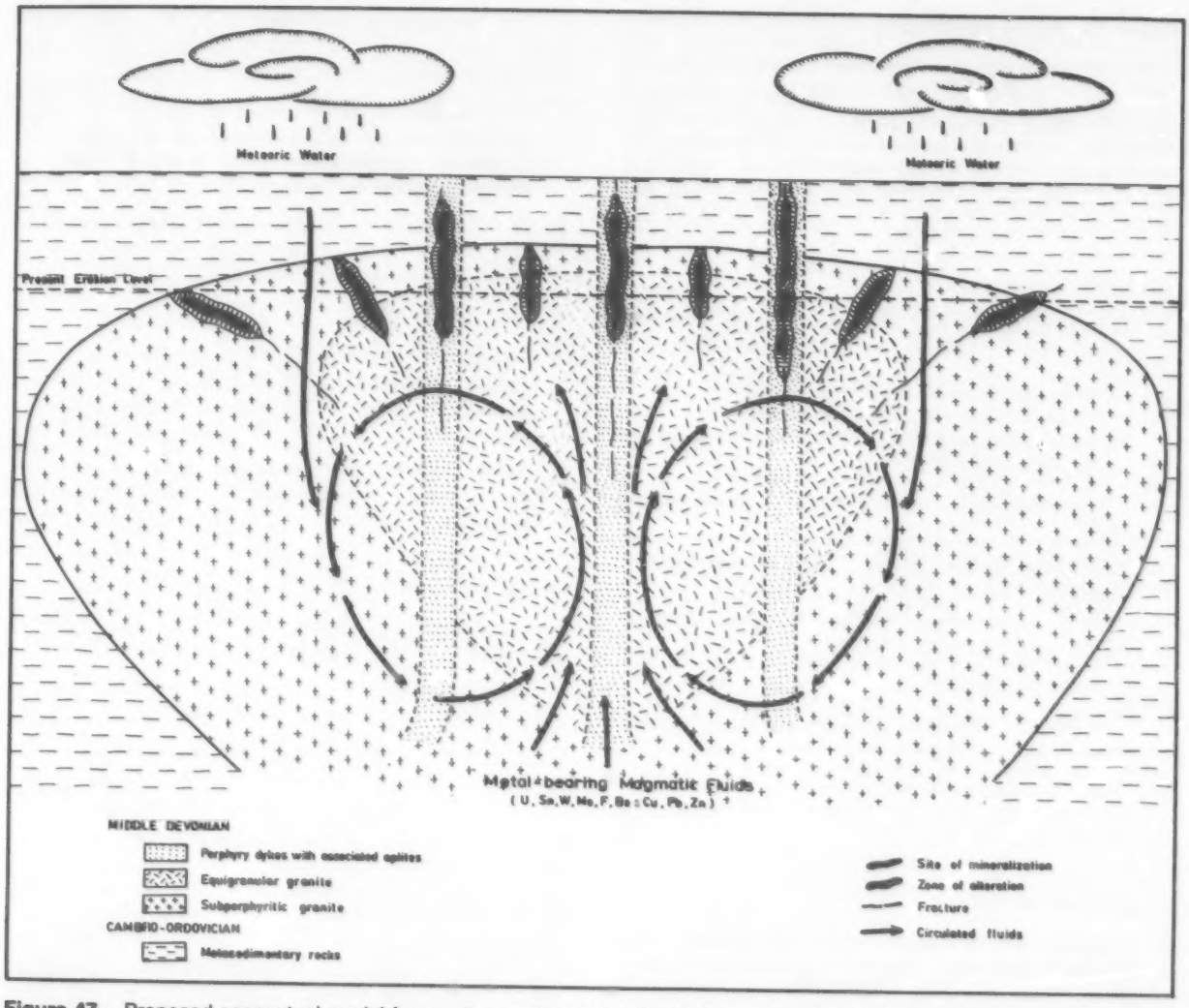

Figure 47. Proposed conceptual model for uranium and associated metals concentration in the granitic rocks of the central Miramichi Anticlinorium plutons.

The Acadian granitic plutons of the North Pole Pluton (Long Lake area) and the Burnthill, Dungarvon, Trout Brook, and Rocky Brook plutons (central Miramichi Anticlinorium) have been examined with respect to their potential for uranium mineralization by using integrated geological, geochemical, and geophysical data.

Low grade uranium concentrations occur within and around the granitic plutons of central Miramichi Anticlinorium. These uranium occurrences are commonly associated with economically important elements, especially with Sn, W, Mo, and base-metal sulphides.

The uranium deposits near Long Lake occur as polymetallic vein-type and are concentrated along at least four northwest-trending chalcedony-filled fractures that crosscut the Lower Devonian granitic rocks of North Pole Pluton. The uranium deposits are mostly associated with Cu, Pb, Zn, Sn, W, Mo, Bi, Ag, and Au. Pyrite, chalcopyrite, sphalerite, galena, covellite, and molybdenite are the major sulphide minerals identified in the veins. Small amounts of arsenopyrite, matildite, and native bismuth were also identified. No mineral identification was carried out for uranium in these veins. However, autunite and torbernite have been recognized in float samples.

Uranium occurrences in the central Miramichi Anticlinorium are associated with late phase differentiates of the granitic plutons. In addition to uranium, these granites host Sn, W, Mo, and F minerals.

The available data support a combination of magmatic and hydrothermal processes for uranium and associated elements concentrations in the plutons in the two areas.

Guide for future exploration

Within the granitic plutons examined here, there appear to be specific geological, geochemical, and geophysical signatures that may be useful guides for uranium and other lithophile elements exploration and should be taken into consideration in future exploration. These distinctive signatures that characterize the host granites are outlined below:

Geological signatures

1. Emplaced at shallow depth (<3 km) in the crust (i.e., epizonal) in a relatively seismically active zone.
2. The plutons are in general relatively small in outcrop area, particularly the Burnthill, Dungarvon, Trout Brook, and Rocky Brook plutons, which host the W, Sn, W, Mo, and F deposits.
3. The plutons are discordantly emplaced in the country rocks.
4. The host granites formed late in the tectonomagmatic sequence. They postdate the earlier (Taconian) and more recent (Acadian) tectonic activities.
5. The host granites are usually associated with low- to medium-grade thermal aureole metamorphism.
6. The host granites usually exhibit a high variation in textures and appear to be intruded in multiple stages.
7. The mineralization appears to favour late-formed fractures and, more specifically those which have undergone brecciation.

Geochemical signatures

1. The host granite and the overburden materials (i.e., soils, till, sediments, and waters) show high contents of uranium (at least three times the average background value). There is also a strong variation in uranium values within these materials as reflected in their high standard deviation.
2. The host granites are peraluminous (molecular $Al_2O_3/Na_2O+K_2O+CaO > 1$) and highly evolved ($SiO_2$ >70 wt.%) and generally contain two types of mica (biotite and muscovite).
3. The host granites have affinities toward S-type and A-type granitoids.
4. They appear to form under a reducing condition (atomic $Fe^{+3}/Fe^{+2}+Fe^{+3}$ ratios are low to intermediate) and they have affinities toward ilmenite-series granitoids.
5. The uranium mineralizations are either associated with specialized granites or with altered granites that have chemical characteristics of specialized granites.
6. The uranium content in the host granites displays a curvilinear increase with the increase in SiO_2 content. The increase in SiO_2 is accompanied by a decrease in the Th-U ratio.
7. The host granites have high SiO_2, K_2O, and Na_2O contents and low TiO_2, CaO, MgO, and P_2O_5 contents in comparison to global averages.
8. The host granites are enriched with incompatible trace elements such as Rb, Y, and Ta and depleted of compatible trace elements such as Sr, Zr, and Ba relative to global averages.
9. The host granites are impoverished in some transition elements such as Ni, Cr, Co, and V and enriched with other transition elements such as Cu and Zn.
10. The host granites are depleted in REE content.
11. The uranium mineralization appears to favour low to medium temperature hydrothermal alteration such as hematitization and albitization rather than greisenization.
12. The host granites contain a high content of normative quartz and orthoclase and a lower content of plagioclase feldspar relative to global averages.

Geophysical signatures

1. The host granites are associated with high eU, eTh, and K airborne gamma ray spectrometry anomalies.
2. The host granites are associated with strong negative (>-40 mgals)Bouguer gravity anomalies.
3. The host granites are associated with low (not well defined) magnetic anomalies.

REFERENCES

Allman, R. and Koriting, S.
1978: Fluorine; in Handbook of Geochemistry, K.H. Wedepohl, (ed.); v. 2, no. 1, Springer-Verlag, Berlin, p. 9-A-1-9-0-4.

Allman-Ward, P., Halls, C., Rankin, A., and Bristow, C.M.
1982: An intrusive hydrothermal breccia body at Wheal Remfry in the western part of the St. Austell Granite Pluton, Cornwall, England; in Metallization Associated with Acid Magmatism, A.M. Evans (ed.); John Wiley and Sons Ltd., New York, p. 1-28.

Anderson, F.D.
1972: The Catamaran Fault, north-central New Brunswick; Canadian Journal of Earth Sciences, v. 9, p. 1278-1286.

Anderson, J.L.
1983: Proterozoic anorogenic granite plutonism of North America; Geological Society of America, Memoir 161, p. 133-154.

Austria, V.
1976: Stream and spring sediment geochemistry maps of Cu, Pb, Zn, Mn, Fe, Mo and W, Hayesville (21J/10); New Brunswick Department of Natural Resources, Map Plate 76-77(a-g) scale 1:50 000 and Map Plate 76-78(a-g) scale 1:50 000.
1977: Uranium content of stream and spring sediments, Hayesville (21J/10); New Brunswick Department of Natural Resources, Map Plate 77-26, scale 1:50 000.

Barbier, M.J.
1974: Continental weathering as a possible origin of vein-type uranium deposits; Mineralium Deposita, v. 9, p. 271-286.

Barreto, P.M.C., Tassinari, C.C.G., Cordani, L.K., and Costa, C.C.
1988: Uranium in granites - an approach for identification of uranium provinces in Brazil: Part I - The Sao Francisco Craton and its marginal belts (abstract); Chemical Geology, v. 70, p. 191.

Barwise, A.J.G. and Whitehead, E.V.
1983: Fossil Fuel Metals; in The significance of trace elements in solving petrogenetic problems and contraversies, S.S. Augustithis (ed.), Theophrastus Publications, S.A. Athens, Greece, p. 599-643.
Berry, M.J., Wetmiller, R.J., Stevens, A.E., Hasegawa, H.S., and Adams, J.
1982: The Miramichi, New Brunswick earthquake sequence of January, 1982 (abstract); Canadian Geophysical Society, 9th Annual Meeting, p. 10.
Bloemraad, J. and Reid, G.L.
1980: Geological, geophysical and geochemical report on the Cleaveland claim group; New Brunswick Department of Natural Resources, Assessment Report 472514, Beth-Canada Mining Co.
Bourque, W.
1984: A petrographic study of samples from cassiterite bearing localities in central New Brunswick, Fontao, Spain and Echassieres, France; B.Sc. thesis, University of New Brunswick, Fredericton, 164 p.
Boyle, R.W.
1982: Geochemical prospecting for thorium and uranium deposits; in Developments in Economic Geology 16, Elsevier Scientific Publishing Company, 498 p.
Brulé, D.
1982: Geochemistry, geology and trenching, Trout Lake; New Brunswick Department of Natural Resources, Assessment Report 472809, Eldorado Nuclear Ltd.
Burke, K.B.S. and Chandra, J.J.
1983: Gravity survey of the epicentral area of the main sequence of 1982 Miramichi earthquakes; New Brunswick Department of Natural Resources, Open File 83-3, 27 p.
Burnham, C.W. and Ohmoto, H.
1980: Late-stage processes of felsic magmatism; Mining Geology Special Issue, Published by The Society of Mining Geologist of Japan, no. 8, p. 1-11.
Butler, R.B.
1980: Geological, geophysical and geochemical surveys and trenching, Otter Brook; New Brunswick Department of Natural Resources, Assessment Report 472523, Western Mines Ltd.
Canadian Mines Handbook
1986-87: The Northern Miner Press Ltd., Toronto, Canada, p. 72.
Carmichael, I.S.E., Turner, F.J., and Verhoogen, J.
1974: Igneous petrology; McGraw Hill Inc., New York, 739 p.
Chandra, J.J.
1981: Ground investigation of airborne gamma-ray radiometric anomalies in New Brunswick by truck-mounted and hand-held gamma-ray sensor; M.Sc. thesis, University of New Brunswick, Fredericton, 99 p.
Chappell, B.W. and White, A.J.R.
1974: Two contrasting granite types; Pacific Geology, v. 8, p. 173-174.
Charbonneau, B.W., Killeen, P.G., Carson, J.M., Cameron, G.W., and Richardson, K.A.
1976: Significance of radio element concentration measurements made by airborne gamma-ray spectrometry over Canadian Shield; in Exploration for uranium ore deposits, International Atomic Energy Agency, p. 35-53.
Chatterjee, A.K. and Muecke, G.K.
1982: Geochemistry and the distribution of uranium and thorium in the granitoid rocks of the South Mountain Batholith, Nova Scotia: some genetic and exploration implications; in Uranium in Granites, Y.T. Maurice (ed.); Geological Survey of Canada, Paper 81-23, p. 11-17.
Chatterjee, A.K. and Strong, D.F.
1984: Discriminant and factor analysis of geochemical data from granitoid rocks hosting the Millet Brook uranium mineralization South Mountain Batholith, Nova Scotia; Uranium, no. 1, p. 289-305.
1985: Review of some chemical and mineralogical characteristics of granitoid rocks hosting Sn, W, U, Mo deposits in Newfoundland and Nova Scotia; in High heat production (HHP) granites, hydrothermal circulation and ore genesis, Bulletin of the Institution of Mining and Metallurgy, London, p. 489-516.
Chatterjee, A.K., Robertson, J., and Pollock, D.
1982: A summary on the petrometallogenesis of the uranium mineralization of Millet Brook, South Mountain Batholith, Nova Scotia; in Mineral Resources Division, Nova Scotia Department of Mines, Report of Activities, p. 57-66.
Chatterjee, A.K., Strong, D.F., and Muecke, G.K.
1983: A multivariate approach to geochemical distinction between tin-specialized and uranium-specialized granites of southern Nova Scotia; Canadian Journal of Earth Sciences, v. 20, p. 420-430.
Clarke, D.B. and Muecke, G.K.
1985: Review of the petrochemistry and origin of the South Mountain Batholith and associated plutons, Nova Scotia, Canada; in High heat production (HHP) granites, hydrothermal circulation and ore genesis, The Institution of Mining and Metallurgy, p. 41-54.
Collins, W.J., Beams, S.D., White, A.J.R., and Chappell, B.W.
1982: Nature and origin of A-type granites with particular reference to southeastern Australia; Contributions to Mineralogy and Petrology, v. 80, p. 189-200.
Crocco, P.E.
1975: A summary report on the granitic rocks of New Brunswick; New Brunswick Department of Natural Resources, Topical Report 75-6, 150 p.
Crouse, G.W.
1977: Geological notes, Long and Trousers Lakes (map area K-11), New Brunswick; New Brunswick Department of Natural Resources, Geological Notes Series 77-191, 18 p. (map revised 1982).
1981: Geology of parts of Burnt Hill, Clearwater and McKiel Brooks; New Brunswick Department of Natural Resources, Map Report 81-5, 46 p.
Davies, J.L.
1983: Stream and spring sediment geochemistry maps, Serpentine Lake (210/2), Cu, Pb, Zn, U, Ag, Co, Mn, Fe, Ni, Mo, and W; New Brunswick Department of Department of Natural Resources, Map Plates 83-33 (A-K), scale 1:50 000.
Department of Natural Resources
1977: Airborne gamma-ray spectrometric contour maps, 1976 Canada - New Brunswick Uranium Reconnaissance Program, Campbellton (210); New Brunswick Department of Natural Resources, Map Plate, 77-48 (a-g), scale 1:50 000.
Department of Natural Resources and Energy
1986: Geological series maps of airborne gamma ray spectrometric survey, Miramichi Highlands; New Brunswick Department of Natural Resources & Energy, Map Plates 86-55 (a-g), scale 1:50 000.
Dill, H.
1983: On the formation of vein-type uranium "yellow ores" from the Schwarzach Area (NE-Bavaria, Germany) and on the behaviour of P, As, V and Se during supergene processes; Geologische Rundschau, v. 72, p. 955-980.
1985: Granite-related and granite-induced ore mineralization on the western edge of the Bohemian Massif; in high heat production (HHP) granites, hydrothermal circulation and ore genesis, Bulletin of the Institution of Mining and Metallurgy, p. 55-70.
Dreimanis, A.
1958: Tracing ore boulders as a prospecting method in Canada; Canadian Institute of Mining and Metallurgy, v. 61, p. 49-56.
Dubessy, J., Ramboz, C., Nguyen-Trung, Ch., Cathelineau, M., Charoy, B., Cuney, M., Leroy, J., Poty, B., and Weisbrod, A.
1987: Physical and chemical controls (fO_2, T, pH) of the opposite behaviour of U and Sn-W as examplified by hydrothermal deposits in France and Great Britain, and solubility data; Bulletin de Minéralogie, v. 110, p. 261-281.
Duex, T.W. and Henry, C.D.
1985: Uranium mobility in late magmatic and hydrothermal processes; in Uranium deposits in volcanic rocks, International Atomic Energy Agency, p. 365-377.
Durrance, E.M.
1985: Hydrothermal circulation and isostasy, with particular reference to the granites of southwest England; in High heat production (HHP) granites, hydrothermal circulation and ore genesis, The Institution of Mining and Metallurgy, p. 71-85.
El Bouseily, A.M. and El Sokkary, A.A.
1975: The relation between Rb, Ba and Sr in granitic rocks; Chemical Geology, v. 16, p. 207-219.
Fehn, U., Cathles, L.M., and Holland, D.H.
1978: Hydrothermal convection and uranium deposits in abnormally radioactive plutons; Economic Geology, v. 73, p. 1556-1566.

Fisher, J.C.
1976: Remote sensing applied to exploration for vein-type uranium deposits, Front Range, Colorado; Ph.D. thesis, Colorado School of Mines, Boulder, Colorado, 141 p.

Fletcher, C.J.N.
1977: The geology, mineralization and alteration of Ilkwang Mines, Republic of Korea. A Cu-W-bearing tourmaline breccia pipe; Economic Geology, v. 72, p. 753-768.

Fletcher, W.K.
1986: Analysis of soil samples; in Exploration geochemistry: design and interpretation of soil surveys, J.M. Robertson (ed.); Society of Economic Geologists, p. 79-96.

Ford, K.L.
1982: Investigation of regional airborne gamma ray spectrometric patterns in New Brunswick and Nova Scotia; Geological Survey Canada, Paper 82-1B, p. 177-194.

Ford, K.L. and Ballantyne, S.B.
1983: Uranium and thorium distribution patterns and lithogeochemistry of Devonian granites in the Chedabucto Bay area, Nova Scotia; in Current Research, Part A; Geological Survey Canada, Paper 83-1A, p. 109-119.

Fournier, R.O.
1986: The behaviour of silica in hydrothermal solutions; in Geology and Geochemistry of Epithermal Systems, B.R. Berger and P.M. Bethke (ed.); Reviews in Economic Geology, v. 2, p. 45-61.

Frick, C.
1986: The behaviour of uranium, thorium and tin during leaching from coarse-grained porphyritic granite in an arid environment; Journal of Geochemical Exploration, v. 25, p. 261-282.

Fyffe, L.R.
1976: Correlation of geology in the southeastern and northern parts of the Miramichi Zone; in 139th Annual Report, New Brunswick Department of Natural Resources, p. 137-141.
1982a: Taconian and Acadian structural trends in central and northern New Brunswick; Geololgical Association of Canada, Special Paper 24, p. 117-130.
1982b: Geology in the vicinity of the 1982 Miramichi earthquake; in Earth Physics Branch, Energy Mines and Resources, Ottawa, Open File 82-24, p. 44-46.

Fyffe, L.R. and MacLellan, H.E.
1988: Lithogeochemistry (including gold) of altered and mineralized samples from the Burnthill Brook area (NTS 21J/10) of central New Brunswick; New Brunswick Department of Natural Resources and Energy, Geoscience Report 88-1, 92 p.

Fyffe, L.R. and Pronk, A.G.
1985: Bedrock and surficial geology-rock and till geochemistry in the Trousers Lake area, Victoria County, New Brunswick; New Brunswick Department of Natural Resources, Report of Investigation, no. 20, 74 p.

Fyffe, L.R., Pajari, G.E., Jr., and Cherry, M.E.
1981: The Acadian plutonic rocks of New Brunswick; Maritime Sediments and Atlantic Geology, v. 17, p. 23-36.

Gardiner, W.B.
1985: Dungarvon claims (21J/10E), New Brunswick; New Brunswick Department of Natural Resources, Assessment Report 473103, Kidd Creek Mines Ltd.

Gardiner, W.W. and Garnett, K.
1986: A field investigation of granites in the Dungarvon area of New Brunswick; New Brunswick Department of Natural Resources, Information Circular 86-2, p. 57-60.
1987a: Geology of the Dungarvon and Sister Brook granites; New Brunswick Department of Natural Resources, Map Plate 87-55, scale 1:20 000.
1987b: Geology of the Trout Lake and Rocky Brook granites; New Brunswick Department of Natural Resources, Map Plate 87-57, scale 1:20 000.

Gasparrini, C.
1981: Identification and description of the uranium minerals in a rock sample, project Campy (Long); New Brunswick Department of Natural Resources, Assessment Report 472695, no. 239, Canadian Occidental Petroleum.

Geological Survey of Canada
1965: Aeromagnetic maps of Campbellton (210) and Woodstock (21J) areas; Geological Survey of Canada, Maps GSAM 7046G and GSAM 7041G, scale 1:253 440.
1986: Magnetic anomaly map (residual total field): Serpentine Lake area; Map C21310G, scale 1:50 000.

Gleeson, C.F.
1980: Soil geochemistry of the Long claims; New Brunswick Department of Natural Resources, Assessment Report 472695, Interim Report, Canadian Occidental Petroleum.

Golovin, Ye.A.
1979: Possible mechanism for formation of stratiform uranium deposits in non-magmatic seismoactive regions; International Geology Review, v. 21, no. 11, p. 1297-1300.

Gustafsson, B. and Minell, H.
1977: Case history of discovery and exploration of Pleutojokk uranium deposit, northern Sweden; in Prospecting in Areas of Glaciated Terrain, The Institution of Mining and Metallurgy, p. 72-79.

Hassan, H.H. and McAllister, A.L.
1988: Geological, geochemical and geophysical favourabilities for polymetallic vein-type uranium mineralization in the Long Lake area and in the Miramichi Anticlinorium, New Brunswick; Geological Survey of Canada, Open File 1821, 86 p.

Hassan, H.H., Hale, W.E., and Chrzanowski, M.
1987: Geology of uranium and associated elements in New Brunswick; Geological Survey of Canada, Open File 1769, 65 p.

Hattie, D.W.
1981: Report on drilling and geophysical and geochemical tests in March 1981, Otter Brook; New Brunswick Department of Natural Resources, Assessment Report 472712, Westmin Resources Ltd.

Hauseux, M.
1980a: Diamond drilling summer 1980, Long claim group; New Brunswick Department of Natural Resources, Assessment Report 473155, Canadian Occidental Petroleum.
1980b: Geology and geochemistry of Long claim group; New Brunswick Department of Natural Resources, Assessment Report 472695, Canadian Occidental Petroleum Ltd.
1981: Trenching, diamond drilling and rock geochemistry, Long South Claim Group; New Brunswick Department of Natural Resources, Assessment Report 473156, Canadian Occidental Petroleum.
1982: Diamond drilling, winter 1982, Long Lake, Long South, Shawn, Shawn North and Swamp claims; New Brunswick Department of Natural Resources, Assessment Report 473157, Canadian Occidental Petroleum.

Hine, R., Williams, I.S., Chappell, B.W., and White, A.J.R.
1978: Contrasts between I- and S-type granitoids of the Kosciusko Batholith; Journal of the Geological Society of Australia, v. 25, p. 219-234.

Holdaway, M.J.
1971: Stability of andalusite and the aluminum silicate phase diagram; American Journal of Science, v. 271, p. 97-131.

Hosking, K.F.G.
1977: Known relationships between the "hard rock" tin deposits and the granites of Southeast Asia; Geological Society of Malaysia Bulletin, v. 9, p. 141-157.

Hutchison, C.S.
1977: Granite emplacement and tectonic subdivision of Peninsular Malaysia; Geological Society of Malaysia Bulletin, v. 9, p. 187-207.

Irrinki, R.R.
1979: Geology of north and south Little Sevogle River - north branch, Little southwest Miramichi River - McKendrick and Catamaran Lakes region Map-Areas 0-12, N-12, and N-13; New Brunswick Department of Natural Resources, Map Report 79-1, 35 p.

Ishihara, S.
1977: The magnetite-series and ilmenite-series granitic rocks; Mining Geology, Published by The Society of Mining Geologist of Japan, v. 27, p. 293-305.

Jagodits, F.L.
1981: Geophysical survey on Shawn claim group; New Brunswick Department of Natural Resources, Assessment Report 472796, Barclay Exploration Services Ltd. to Canadian Occidental Petroleum.

Kents, P.
1964: Special breccias associated with hydrothermal developments in the Andes; Economic Geology, v. 58, p. 1551-1563.

Keppie, J.D.
1977: Plate tectonic interpretation of Paleozoic World Maps; Nova Scotia Department of Mines, Paper 77-3, 45 p.

Laanela, H.
1980: Trout Brook claim group, New Brunswick; New Brunswick Department of Natural Resources, Assessment Report 472652, Eldorado Nuclear Ltd.

Lafontaine, M.A.G.
1980: Geology, soil geochemistry and radiometry, Trout Lake; New Brunswick Department of Natural Resources, Assessment Report 472517, Eldorado Nuclear Ltd.

Lamothe, M.
1989: Till geochemistry over the central part of the Miramichi Zone and vicinity, New Brunswick; Geological Survey of Canada, Open File 1967, 70 p.

Langmuir, D.
1978: Uranium solution-mineral equilibria at low temperatures with applications to sedimentary ore deposits; Geochimica et Cosmochimica Acta, v. 42, p. 547-569.

LeMaitre, R.W.
1976: The chemical variability of some common igneous rocks; Journal of Petrology, v. 17, p. 589-637.

Leonard, K.W.
1982: Geology and geochemistry of Long Lake claim group; New Brunswick Department of Natural Resources, Assessment Report 472797, Canadian Occidental Petroleum.

Lindsey, D.A. and Fisher, F.S.
1985: Mineralized breccias in intrusive complexes of Late Cretaceous and Paleocene age, North-central Montana; U.S. Geological Survey, Professional Paper 1301A, p. 3-34.

Lipowicz, T.
1980: Geology and geochemistry of the northern part of the Shawn claim group; New Brunswick Department of Natural Resources, Assessment Report 472697, Canadian Occidental Petroleum.

Loiselle, M.C. and Wones, D.R.
1979: Characteristics and origin of anorogenic granites; Geological Society of America Abstract, v. 11, p. 468.

MacLellan, H.E.
1986: Geology of the Burnthill granite (21J/10); New Brunswick Department of Natural Resources and Energy, Map Plate 86-241, scale 1:20 000.

MacLellan, H.E. and Taylor, R.P.
1989: Geology and geochemistry of the Burnthill Granite and related W-Sn-Mo-F mineral deposits, central New Brunswick; Canadian Journal of Earth Sciences, v. 26, p. 499-514.

MacLellan, H.E., Taylor, R.P., and Lux, D.R.
1986: Geologic and geochronologic investigations of the Burnthill Granite; New Brunswick Department of Natural Resources, Information Circular 86-2, p. 48-56.

Mawer, C.K. and Williams, P.F.
1985: Crystalline rocks as possible paleoseismicity indicators; Geology, v. 13, p. 100-102.

McKerrow, W.S., and Ziegler, A.M.
1971: The Lower Silurian paleogeography of New Brunswick and adjacent area; Journal of Geology, v. 71, p. 635-646.

Mitton, B.
1985: Hydrothermal alteration of granitoids associated with Little Dungarvon Tin Deposit, N.B.; B.Sc. thesis, University of New Brunswick, Fredericton, New Brunswick, 75 p.

Moreau, M.
1976: L'uranium et les granitoides: essai d'interpretation; in Geology, Mining and Extractive Processing of Uranium, M.J. Jones (ed.); The Institution of Mining and Metallurgy, p. 83-102.

Nowlan, G.S.
1981: Some Ordovician conodont faunules from the Miramichi Anticlinorium, New Brunswick; Geological Survey of Canada, Bulletin 345, 35 p.

O'Reilly, G.A., Corey, M.C., and Ford, K.L.
1988: The role of airborne gamma-ray spectrometry in bedrock mapping and mineral exploration: case studies from granitic rocks within the Meguma Zone, Nova Scotia; Maritime Sediments and Atlantic Geology, v. 24, p. 47-60.

Oshin, I.O. and Rahman, M.A.
1986: Uranium favourability study in Nigeria; Journal of African Earth Sciences, v. 5, no. 2, p. 167-175.

Pagel, M.
1981: Facteurs de distribution et de concentration de l'uranium et du thorium dans quelques granites de la chaine hercynienne d'Europe; thesis, Nancy University, 566 p.

Paterson, N.R., Bonnchart, R., Misener, D.J., and Watson, R.K.
1979: Geophysical prospecting for uranium in the Athabasca Basin; Canadian Mining Journal, p. 32.

Pirkle, F.L., Beckman, R.J., and Fleischhauer, H.L., Jr.
1982: A multivariate uranium favourability index using aerial radiometric data; Journal of Geology, v. 90, p. 109-124.

Pirkle, F.L., Campbell, K., and Wecksung, G.W.
1980: Principal components analysis as a tool for interpreting NURE aerial radiometric survey data; Journal of Geology, v. 88, p. 57-67.

Pitcher, W.S.
1979: The nature, ascent and emplacement of granitic magmas; Geological Society of London Journal, v. 136, p. 627-662.
1987: Granites and yet more granites forty years on; Geologische Rundschau, v. 76, no. 1, p. 51-79.

Plant, J., Brouen, G.C., Simpson, P.R., and Smith, R.T.
1980: Signatures of metalliferous granites in the Scottish Caledonides; Transactions of The Institution of Mining and Metallurgy, section B, v. 89, p. B198-B210.

Plant, J.A., O'Brien, C., Tarney, J., and Hurdley, J.
1985: Geochemical criteria for the recognition of high heat production granites; in High heat production (HHP) granites, hydrothermal circulation and ore genesis, The Institution of Mining and Metallurgy, p. 263-285.

Poole, W.H.
1963: Geology of Hayesville map-area, New Brunswick; Geological Survey of Canada, Map 6-1963, scale 1:63 360.

Potter, R.R.
1969: The geology of the Burnt Hill area and ore controls of the Burnt Hill tungsten deposit; Ph.D. thesis, Carleton University, Ottawa, 136 p.

Poty, B., Leroy, J., Cathelineau, M., Cuney, M., Friedrich, M., Lespinasse, M., and Turpin, L.
1986: Uranium deposits spatially related to granites in the trench part of the Hercynian Orogen; in Vein type uranium deposits, International Atomic Energy Agency, p. 215-246.

Rast, N.
1983: The northern Appalachian traverses in the Maritimes of Canada; in Profiles of Orogenic Belts, N. Rast and F.M. Delany, (ed.); Geodynamics Series Volume 10, American Geophysical Union, Washington, D.C., 310 p.

Rast, N., Kennedy, M.J., and Blackwood, R.R.
1976: Comparison of some tectonostratigraphic zones in the Appalachians of Newfoundland and New Brunswick; Canadian Journal of Earth Sciences, v. 13, p. 868-875.

Rich, R.A., Holland, H.D., and Peterson, U.
1977: Hydrothermal uranium deposits: Developments in Economic Geology, no. 6, Elsevier Scientific Publishing Company, N.Y., 264 p.

Richardson, K.A. and Carson, J.M.
1976: Regional uranium distribution in northern Saskatchewan; in Uranium in Saskatchewan, C.E. Dunn, (ed.); Saskatchewan Geological Society, Special Publication, no. 3, p. 27-50.

Ruitenberg, A.A. and Fyffe, L.R.
1982: Mineral deposits associated with granitoid intrusions and related subvolcanic stocks in New Brunswick and their relationship to Appalachian tectonic evolution; Canadian Institute of Mining and Metallurgy, v. 75, no. 842, p. 83-97.

Ruitenberg, A.A., Fyffe, L.R., McCutcheon, S.R., St. Peter, C.J., Irrinki, R.R., and Venugopal, D.V.
1977: Evolution of Pre-Carboniferous Tectonostratigraphic Zones in the New Brunswick Appalachians; Geoscience Canada, v. 4, p. 171-181.

Sawka, W.N. and Chappell, B.W.
1986: The distribution of radioactive heat production in I- and S-type granites and residual source regions: implications to high heat flow areas in the Lachlan Fold Belt, Australia; Australian Journal of Earth Sciences, v. 33, p. 107-118.

Sawkins, F.J.
1969: Chemical brecciation, an unrecognized mechanism for breccia formation?; Economic Geology, v. 64, p. 613-617.

Scherkenbach, D.A.
1982: Geologic, mineralogic, fluid inclusion and geochemical studies of the mineralized breccias at Cumobabi, Sonora, Mexico; Ph.D. thesis, University of Minnesota, Minneapolis, Minnesota, 190 p.

Seguin, M.K., Gaucher, E., and Desbiens, R.
1984: Beep Mat 1 - an automated miniaturized EM mineral detector; in Prospecting in areas of glaciated terrain 1984; The Institution of Mining and Metallurgy, p. 193-200.

Shacklette, H.T. and Boerngen, J.G.
1984: Element concentrations: in soils and other surficial materials of the conterminous United States; Geological Survey Professional Paper 1270, 105 p.

Sibson, R.H., Moore, J.McM., and Rankin, A.H.
1975: Seismic pumping - A hydrothermal fluid transport mechanism; Geological Society of London Journal, v. 131, p. 653-659.

Simmons, S.F. and Sawkins, F.J.
1983: Mineralogic and fluid inclusion studies of the Washington Cu-Mo-W-bearing breccia pipe, Sonora, Mexico; Economic Geology, v. 78, p. 521-526.

Simpson, P.R. and Plant, J.A.
1984: Role of high heat production granites in uranium province formation; in Uranium geochemistry, mineralogy, geology, exploration and resources, B. DeVivo, F. Ippolito, G. Capaldi, and P.R. Simpson (ed.); The Institution of Mining and Metallurgy, p. 167-178.

Simpson, P.R., Brown, G.C., Plant, J., and Ostle, D.
1979: Uranium mineralization and granite magmatism in the British Isles; Philosophical Transactions of the Royal Society of London, series A, v. 291, p. 385-412.

Simpson, P.R., Plant, J.A., Watson, J.V., Green, P.M., and Fowler, M.B.
1982: The role of metalliferous and mineralised uranium granites in the formation of U provinces; in Proceedings of the Symposium on Uranium Exploration Methods, Review of the Nuclear Energy Agency, International Atomic Energy Agency, Research and Development Program, Paris, p. 157-170.

Skinner, P.
1974: Geology of the Tetagouche Lakes, Bathurst and Nepisiquit Falls map areas, New Brunswick; Geological Survey of Canada, Memoir 371, 133 p.

Sotnikov, V.I., Berzina, A.P., Nikitina, E.I., Skuridin, V.A., and Proskuryakov, A.A.
1974: Relationship between copper-molybdenum mineralization and subvolcanic granitoids; in Metallization Associated with Acid Magmatism, M. Stemprok (ed.); v. 1, p. 123-126.

Statistical Analysis System
1982: Statistical Analysis System user's guide: Statistics; SAS Instit. Inc., Cary, North Carolina, p. 584.

Stemprok, M.
1979: Mineralized granites and their origin; Episodes, v. 1979, no. 3, p. 20-24.

St. Julien, P. and Béland, J.
1982: Orogenies; in Major structural zones and faults of the Northern Appalachians, Geological Association of Canada, Special Paper 24, p. 6-9.

Takahashi, M., Aramaki, S., and Ishihara, S.
1980: Magnetite-series/Ilmenite-series vs. I-type/S-type granitoids; Mining Geology, Published by the Society of Mining Geologist of Japan, Special Issue, no. 8, p. 13-28.

Taylor, R.P., Lux, D.R., and Hubacher, A.F.
1987: Age and genesis of granite-related W-Sn-Mo mineral deposits, Burnthill, New Brunswick, Canada; Economic Geology, v. 82, p. 2197- 2208.

Taylor, S.R.
1964: Abundance of chemical elements in the continental crust: A new table; Geochimica et Cosmochimica Acta, v. 28, p. 1273.

Tischendorf, G.
1977: Geochemical and petrographic characteristics of silicic magmatic rocks associated with rare-element mineralization; in Metallization Associated with Acid Magmatism, M. Stemprok, L. Burnol and G. Tischendorf (ed.); v. 2, Prague, p. 41-96.

Tuttle, O.F. and Bowen, N.L.
1958: Origin of granite in the light of experimental studies in the system $NaAlSi_3O_8$-$KAlSi_3O_8$-SiO_2-H_2O; Geological Society of America, Memoir, no. 74, 153 p.

van Staal, C.R.
1987: Tectonic setting of the Tetagouche Group in northern New Brunswick: implications for plate tectonic models of the northern Appalachians; Canadian Journal of Earth Sciences, v. 24, p. 1329-1351.

Venugopal, D.V.
1979: Geology of Debec Junction-Gibson Millstream-Temperance Vale-Meductic area; New Brunswick Department of Natural Resources, Map Report 79-5, 36 p.

Vinogradov, A.P.
1962: Average contents of chemical elements in the principal types of igneous rocks of earth crust; Geochemistry, no. 7, p. 641-664.

Whalen, J.B.
1986: A-type granites in New Brunswick; in Current Research, Part A; Geological Survey of Canada, Paper 86-1A, p. 297-300.

Whalen, J.B., Currie, K.L., and Chappell, B.W.
1987: A-type granites: geochemical characteristics, discrimination and paragenesis; Contributions to Mineralogy and Petrology, v. 95, p. 407-419.

White, A-J.R. and Chappell, B.W.
1983: Granitoid types and their distribution in the Lachlan Fold Belt, southeastern Australia; Geological Society of America, Memoir 159, p. 21-34.

Williams, D.A.
1978: Compilation Bouguer gravity map of Woodstock (21J); New Brunswick Department of Natural Resources, Map Plate, 78-42E, scale 1:250 000.

Williams, H.
1979: Appalachian orogen in Canada; Canadian Journal of Earth Sciences, v. 16, no. 3, p. 792-807.

Yeats, A.N., Wyall, B.W., and Tucker, D.H.
1982: Application of gamma-ray spectrometry to prospecting for tin and tungsten granites, particularly within the Lachlan Fold Belt, New South Wales; Economic Geololgy, v. 77, p. 1725-1738.

Zagruzina, I.A., Pinskii, E.M., and Savinova, I.B.
1987: Uranium in cassiterite of tin deposits; International Geology Review, v. 29, p. 94-109.

Appendix I

Best overall analytical results for elements in different types of samples* for the Long Lake area (after Hauseux, 1982).

Elements	Concentrations/Thickness	Sample Types
U	8800 ppm	Float
Mo	120 000 ppm	Float
Sn	2868 ppm	Float
Au	30 000 ppb	Vein
As	8095 ppm	Vein
Bi	1980 ppm	Vein
Cu	40 000 ppm/0.30 m	Drill hole
Pb	25 000 ppm/0.09 m	Drill hole
Zn	153 000 ppm/0.30 m	Drill hole
Ag	86 ppm/0.30 m	Drill hole
Cd	44 ppm/0.53 m	Drill hole
Hg	280 ppm/0.08 m	Drill hole
In	134 ppm/0.30 m	Drill hole
Sb	96 ppm/1.30 m	Drill hole

*All these samples were collected from the eastern side of Long Lake.

Appendix II

Brief description of the mineral occurrences associated with the Burnthill (BH); Dungarvon (D), Trout Brook (TB), and Rocky Brook (RB) plutons (compiled after Fyffe and MacLellan, 1988).

NO.	NAME OF DEPOSIT	LATITUDE ° ′ ″	LONGITUDE ° ′ ″	ELEMENTS PRESENT	METALLIC MINERALS	NONMETALLIC MINERALS	ALTERATION PRODUCTS	DEPOSIT TYPE	STYLE OF MINERALIZATION	REMARKS
BH-1	BURNTHILL TUNGSTEN	46 34 10	66 48 50	W, Sn, Mo, Be, F, Cu, As, Bi, Ti, Zn, Pb	wolframite, cassiterite, molybdenite, arsenopyrite, pyrite, pyrrhotite, sphalerite, galena, chalcopyrite, native bismuth	scheelite, beryl, anatase, quartz, topaz	muscovite, silica, sericite, fluorite	Quartz-carbonate veins. Greisen vein.	NW-trending greisenized veins cutting Cambro-Ordov. metasedimentary rocks.	Veins range from 1 cm to 2 m width, and are mineralized in a zone 300 x 150 m to a depth of 200 m.
BH-2	CLEARWATER BROOK (North and South)	46 38 50	66 47 30	Be		beryl		Intramagmatic. Greisen vein.	Mineralization associated with pegmatite and greisen veins in Burnthill Pluton	
BH-3	LOWER BURNTHILL BROOK	46 34 58	66 49 36	W, Mo, Sn, F, Be	wolframite, molybdenite, cassiterite	beryl, quartz	muscovite, fluorite	Greisen-stockwork vein	Mineralization occurs in quartz veins with greisen borders cutting Burnthill Pluton.	The veins trend 110° and 120°.
BH-4	McLEAN BROOK NORTH	46 35 04	66 54 30	Mo, W, Cu, Sn, F	molybdenite, W minerals, chalcopyrite, pyrite, cassiterite	quartz	epidote, silica, fluorite	Porphyry-type. Greisen-stockwork vein.	Mineralization occurs as disseminations and smears on fractures and in quartz veinlets cutting the Burnthill Pluton.	
BH-5	McLEAN BROOK SOUTH	46 33 37	66 52 23	Cu, Zn, As	chalcopyrite, sphalerite, arsenopyrite, pyrite, pyrrhotite			Quartz carbonate veins and stockworks in fractures		The mineralization occurs within biotite isograd of contact metamorphic aureole.
BH-6	OTTER BROOK	46 39 48	66 48 15	F, Cu, Zn	chalcopyrite, sphalerite, pyrite, pyrrhotite, hematite	quartz	muscovite, epidote, illite, fluorite	Greisen-stockwork vein.	Fluorite occurs in veins and as vug fillings in quartz veins. Sulphides occur as disseminations in veins and along fractures.	Greisen alteration of the granite borders the veins. The veins crosscut the Burnthill Pluton.
BH-7	TIN HILL	46 35 30	66 47 27	Sn, W, Mo	cassiterite, wolframite, molybdenite, magnetite, pyrite	quartz	sericite, chlorite	Greisen-stockwork vein. Porphyry-type.	Mineralization occurs in greisen-bordered quartz vein swarm in feldspar-porphyritic granite.	The veins trend 120°.

NO.	NAME OF DEPOSIT	LATITUDE ° ′ ″	LONGITUDE ° ′ ″	ELEMENTS PRESENT	METALLIC MINERALS	NONMETALLIC MINERALS	ALTERATION PRODUCTS	DEPOSIT TYPE	STYLE OF MINERALIZATION	REMARKS
BH-8	TWO and ONE-HALF MILE BROOK	46 33 36	66 51 15	Sn, W, F, As	cassiterite, wolframite, arsenopyrite	quartz	fluorite	Greisen-stockwork vein	Mineralization occurs in quartz veins and veinlets cutting Cambro-Ordovician metasedimentary rocks.	The veins are closely spaced (1-5 cm) and parallel to each other. They strike 110°-120°. The veins are located within biotite isograd of contact metamorphic aureole.
D-1	CLEAVELAND PROSPECT and LOWER DUNGARVON	46 40 11	66 34 30	Zn, Cu, Pb, Ag, Sn, Mo	chalcopyrite, galena, sphalerite, silver, cassiterite, molybdenite, pyrite	quartz K-feldspar	sericite, chlorite, illite, hematite, fluorite	Greisen-stockwork vein. Intra-magmatic.	Sulphides occur within a musco-vite-quartz greisen vein. Cassiterite and fluorite occur in quartz/ feldspar veins.	The greisen vein strikes 105° with a width of 1.2 m. The quartz-felds-par veins strike 130°. The veins crosscutting the Dungarvon Pluton.
D-2	DUNGARVON (VEINS 2, 4, 6, 11, 14)	46 40 08	66 36 29	Sn, F, Mo, Cu, Pb, Nb	cassiterite, molybdenite, chalcopyrite, pyrite, magnetite,	quartz, anhydrite, calcite, epidote, chalcedony, K-feldspar	fluorite, kaolin, chlorite, illite, hematite	Greisen-stockwork vein.	Mineralization occurs in feldspar and quartz veins as well as in tabular quartz stockwork zone and in quartz breccias.	Veins are 1 cm to 2 m wide. Stock-works are up to 15 m wide. All veins cut medium-to coarse-grained Dungarvon Pluton. All veins and stockwork zones trend 130° and are associated with two major 85° and 130° trending faults.
D-3	DUNGARVON (VEINS 3 and 5)	46 40 48	66 36 20	Sn, F	cassiterite, pyrite,	quartz, K-feldspar, chalcedony	fluorite, chlorite, illite, hematite	Greisen-stockwork vein.	Mineralization occurs in veins of many gener-ations.	The veins are up to 50 cm wide. They strike 130° and dip vertically.
D-4	DUNGARVON (VEIN 7)	46 39 58	66 36 38	Sn, F, Cu	cassiterite, pyrite, chalcopyrite	quartz	fluorite, illite, hematite	Greisen-stockwork vein.	Mineralization occurs in 2 m wide fault zone filled with massive quartz-fluorite. Quartz veinlets in surrounding granite carry cassiterite. Fifty metres west of fault are numerous veins of fluorite, pyrite and chalco-pyrite.	

Appendix II (cont.)

NO.	NAME OF DEPOSIT	LATITUDE ° ′ ″	LONGITUDE ° ′ ″	ELEMENTS PRESENT	METALLIC MINERALS	NONMETALLIC MINERALS	ALTERATION PRODUCTS	DEPOSIT TYPE	STYLE OF MINERALIZATION	REMARKS
D-5	FALL BROOK (JOHNSTON)	46 46 38	66 32 33	Sn, W, Mo, F	cassiterite, wolframite, molybdenite, pyrite	K-feldspar, quartz	fluorite, sericite, hematite, illite	Greisen-stockwork vein. Intra-magmatic.	Molybdenite and wolframite are in quartz veins. Cassiterite occurs in quartz-greisen veins. Fluorite occurs as veinlets and as vug fillings in quartz and/or feldspar veins.	
D-6	FALL BROOK SOUTH	46 45 18	66 32 27	Mo	molybdenite			Porphyry-type.	Molybdenite stringers cutting medium grained granite of Dungarvon Pluton.	
D-7	FOUR MILE BROOK (VEIN 1)	46 38 56	66 37 45	Sn, F	cassiterite, pyrite	quartz, chalcedony, K-feldspar	illite, fluorite	Greisen-stockwork vein. Intra-magmatic.	Tin occurs in quartz veins, aplites and in feldspar veins.	Veins trend 130° and are steeply dipping. Veins may be locally brecciated.
D-8	FOUR MILE BROOK (W-Mo)	46 38 41	66 37 47	W, Mo	wolframite, molybdenite, pyrite, pyrrhotite	quartz		Greisen-stockwork vein.	Sulphides and wolframite occur in quartz veins cutting hornfelsed Ordovician siltstone ≈ 200 m from the Dungarvon Pluton.	Veins are generally randomly oriented. Veins within cordierite-andalusite isograd of contact metamorphic aureole.
D-9	FOUR MILE LAKE	46 39 00	66 34 40	Cu, Sn	chalcopyrite, cassiterite, pyrite, pyrrhotite	quartz		Greisen-stockwork vein. Contact metasomatic	Sulphides occur as disseminations and stringers in hornfelsed Ordovician metasediments. Tin occurs in a calc-silicate horizon.	Showings within biotite isograd of contact metamorphic aureole.
D-10	HARRIS BROOK	46 42 53	66 31 46	Cu, Zn	chalcopyrite, sphalerite, pyrite			Quartz-carbonate veins and stockworks in shear zones.	Stringer sulphides cutting granite and hornfelsed greywackes.	Mineralizations are within contact metamorphic aureole.
D-11	HARRIS LAKE (Sn and F)	46 42 17	66 32 18	Sn, F	cassiterite	K-feldspar	illite, hematite, fluorite	Greisen-stockwork vein. Intra-magmatic.	Cassiterite and fluorite in K-feldspar veins. Fluorite also occurs as veinlets.	All cutting medium grained granite.
D-12	HARRIS LAKE (U)	46 43 00	66 32 36	U, F		U minerals, fluorite, quartz		Quartz-carbonate veins and stockworks	A 130° trending quartz-fluorite breccia in the granite hosts the U.	The breccia zone is in a fault/shear zone. At least 1 m wide and traceable for 400 m

NO.	NAME OF DEPOSIT	LATITUDE ° ′ ″	LONGITUDE ° ′ ″	ELEMENTS PRESENT	METALLIC MINERALS	NONMETALLIC MINERALS	ALTERATION PRODUCTS	DEPOSIT TYPE	STYLE OF MINERALIZATION	REMARKS
D-13	HEAD OF LITTLE DUNGARVON	46 40 32	66 37 26	Cu, Sn	chalcopyrite, pyrite			Quartz-carbonate veins and stockworks. Greisen-stockwork vein.	Sulphides occur as stringers along fractures in granite and as disseminations in bleached granite. Tin occurs in fault gouge.	All the mineralizations are closely associated with 2 sets of faults trending 085° and 130°.
D-14	PEAKED MOUNTAIN	46 44 15	66 31 15	W, Mo, F, Be, Sn, Cu, Zn	wolframite, molybdenite, cassiterite, chalcopyrite, sphalerite, pyrite	scheelite, molybdo-scheelite, beryl, quartz	biotite, sericite, fluorite	Greisen-stockwork vein. Quartz-carbonate veins and stockworks	W and Mo occur as disseminations around quartz veins and as dustings in the veins. W, Mo, Be, F in greisen veins.	Quartz veins are up to 5 cm wide and rimmed by biotite. They trend roughly 110°-120°.
D-15	PEAKED MOUNTAIN WEST	46 44 45	66 32 47	W, F	pyrite,	scheelite, quartz	illite, hematite, fluorite	Greisen-stockwork vein.	W occurs in quartz and/or fluorite veinlets.	
D-16	ROCKY BROOK EAST	46 39 13	66 37 43	Cu	chalcopyrite, pyrite			Strati-form massive sulphides	Disseminated sulphides along laminations and bands within cherts and slates	Mineralization occurs within cordierite-andalusite isograd of contact metamorphic aureole.
D-17	YOUNG'S DAM (A and B)	46 40 00	66 38 31	Mo	molybdenite, pyrite		sericite	Greisen-stockwork vein.	Greisenized granite cut by molybdenite stringers. Pyrite as disseminations.	
D-18	YOUNG'S DAM (C and D)	46 40 02	66 39 27	Mo, Cu, As	molybdenite, chalcopyrite, arsenopyrite, pyrite	quartz		Greisen-stockwork vein.	Sulphides occur as stringers, disseminations and in quartz veinlets. Mo in quartz veinlets.	Mineralization within contact metamorphic aureole.
TB-1	CLEARWATER/ TROUT LAKE	46 35 02	66 44 47	F		quartz, K-feldspar	fluorite	Greisen-stockwork vein.	Mineralization occurs in fluorite veinlets or in feldspar vein with disseminated and stringer fluorite.	All the veins trend roughly 130°. They are cutting the Trout Brook Pluton.
TB-2	GILMAN BROOK FLUORITE	46 36 00	66 40 55	F	pyrite		fluorite	Greisen-stockwork vein.	Mineralization occurs as fluorite vein and as fluorite and pyrite in a wide shear zone at the intersection of two faults in granite.	The mineralization is associated with two sets of faults. The E-W fault is 1-2 m wide marked by a zone of breccia. The NW-SE fault is a 50-100 m wide fracture zone and is probably the younger of the two.

Appendix II (cont.)

NO.	NAME OF DEPOSIT	LATITUDE ° ′ ″	LONGITUDE ° ′ ″	ELEMENTS PRESENT	METALLIC MINERALS	NONMETALLIC MINERALS	ALTERATION PRODUCTS	DEPOSIT TYPE	STYLE OF MINERALIZATION	REMARKS
TB-3	ROCKY BROOK CAMPS	46 36 08	66 37 26	W	wolframite	quartz		Greisen-stockwork vein.	Wolframite crystals (up to 2 cm) occur in quartz veins (up to 5 cm in width).	The veins cut Cambro-Ordovician metasedimentary rocks, approximately 150 m from Trout Brook Pluton
TB-4	SISTER BROOK	46 36 44	66 39 42	W, F	wolframite	quartz	fluorite, sericite	Greisen-stockwork vein.	Wolframite and fluorite occur in quartz veins. Wolframite also occurs in greisen-bordered quartz veins.	Veins trend 120°-140°. All cut the Cambro-Ordovician metasedimentary rocks.
TB-5	SISTER MOUNTAIN	46 36 32	66 39 17	Cu, Zn, As, F	chalcopyrite, sphalerite, arsenopyrite, pyrite	quartz	fluorite	Greisen-stockwork vein.	Mineralization occurs in quartz veins.	The veins cutting the Cambro-Ordovician metasedimentary rocks. The veins are mariolitic and strike 110°-130°. Dipping steeply.
TB-6	SOUTHWEST MIRAMICHI	46 35 52	66 36 19	F, Pb	galena, pyrite		fluorite	Greisen-stockwork vein.	Fluorite and galena occur in hornfelsed greywacke. Fluorite also occurs in a fracture zone in granite. Pyrite is disseminated.	Mineralization occurs within biotite isograd of contact metamorphic aureole.
TB-7	TODD MOUNTAIN	46 32 35	66 42 00	Sn, Cu, Pb, Zn, Ag, Au, As	cassiterite, chalcopyrite, galena, sphalerite, pyrite, pyrrhotite, arsenopyrite, silver, gold, magnetite	quartz, graphite	chlorite, muscovite	Greisen-stockwork vein.	Sulphides occur as nodules, disseminations and stringers associated with quartz-chlorite-arsenopyrite-muscovite in joints.	Host rocks are (partly bleached) pyritic and graphitic siltstone and fine calc-silicate hornfels ('chert') overlying argillite and quartzite.
TB-8	TODD MOUNTAIN NW	46 32 44	66 42 22	W, Mo	wolframite, molybdenite	tourmaline,		Quartz-carbonate veins and stockwork. Greisen-stockwork vein.	Wolframite with minor molybdenite and tourmaline, in a quartz vein, cutting metasedimentary rocks.	The deposit lies 800 m south of the Trout Brook Pluton

NO.	NAME OF DEPOSIT	LATITUDE ° ′ ″	LONGITUDE ° ′ ″	ELEMENTS PRESENT	METALLIC MINERALS	NONMETALLIC MINERALS	ALTERATION PRODUCTS	DEPOSIT TYPE	STYLE OF MINERALIZATION	REMARKS
TB-9	TROUT LAKE PLUTON EAST	46 34 55	66 38 10	Sn, W, Zn, Cu, Mo, F, Be, Bi, As, Ag, Au	cassiterite, wolframite, sphalerite, chalcopyrite, molybdenite, bismuthinite, arsenopyrite, silver, gold, pyrite, hematite, magnetite.	beryl, quartz, K-feldspar	fluorite, sericite, chlorite, illite	Greisen-stockwork vein. Intra-magmatic.	Mineralization occurs in greisen-bordered quartz veins in granitic rocks of the Trout Brook Pluton.	Veins are most abundant in the fine- to medium-grained phase of the granite.
TB-10	TROUT LAKE PLUTON SE	46 34 24	66 39 57	Sn, Cu, Mo, As	cassiterite, chalcopyrite, bornite, molybdenite, arsenopyrite, pyrite	quartz	muscovite, hematite	Greisen-stockwork vein.	Disseminated arse-nopyrite and pyrite in hematically-altered granite. Sn, Cu and Mo disseminations occur in quartz (± muscovite) greisen vein in granite.	
TB-11	TROUT BROOK/ UPPER	46 34 05	66 40 48	Cu	chalcopyrite, pyrite, pyrrhotite			Greisen-stockwork vein. Quartz-carbonate veins and stockworks.	Sulphides in quartz string-ers cutting hornfelsed Ordovician conglomerate.	Veins within cordierite-andalu-site isograd of contact meta-morphic aureole.
TB-12	TROUT BROOK/ LOWER	46 34 23	66 37 49	Cu, Pb, Zn, As, Ag	chalcopyrite, galena, sphalerite, pyrite, pyrrhotite, arsenopyrite, silver	quartz		Greisen-stockwork vein.	Quartz stringers with sulphides cutting siltstones; disseminated sulphides occur along laminations and bands in cherts and slates.	Mineralization is within the biotite isograd of a con-tact metamorphic aureole.
RB-1	ROCKY BROOK SOUTH	46 37 26	66 37 28	Sn, Mo, Bi, W, F	cassiterite, molybdenite, bismuthinite, wolframite, pyrite	quartz, K-feldspar	sericite, anhydrite, fluorite, hematite, illite, kaolinite	Porphyry-type. Greisen-stockwork vein.	Sn segregation in quartz vein. Mo and Bi in quartz stock-work. W and Mo in greisenized granite.	Veins cut granitic rocks of Rocky Brook Pluton. Feldspar content of veins suggests late magmatic to early hydrothermal origin of veins. Veins trending 120°-140°.
RB-2	ROCKY BROOK FLUORITE	46 37 00	66 37 33	F	pyrite	quartz	fluorite	Greisen-stockwork vein.	Fluorite occurs in fracture and/or breccia zones as matrix.	Fracture/breccia zones trend 120°-140° and are up to 100 m wide, of which 1.5 m can be 100% fluorite. Most veins are endo-granitic. The exo-granitic veins are smaller.

Appendix II (concl.)

Appendix III

Element contents in spring and stream sediment samples in the Long Lake area (data compiled from Davies, 1983).

No.	U ppm	Cu ppm	Pb ppm	Zn ppm	Mn ppm	Fe %	Ni ppm	Co ppm	Mo ppm	W ppm	Ag ppm	As ppm	Sb ppm	Ba ppm
1	10.6	4	19	40	140	0.63	7	5	–	–	0.5			
2	9.2	4	19	38	260	0.65	7	5	–	–	0.5			
3	13.7	7	31	44	100	0.7	10	8	2	2	1.5			
4	28.9	6	5	87	2300	1.75	9	11	2	4	1.0			
5	15.6	–	–	0	–	–	–	–	–	2	–			
6	18.7	4	32	45	400	0.76	6	6	2	2	0.5			
7	3.6	13	63	214	820	0.71	16	11	–	–	1.0	9	0.1	220
8	5.4	5	74	33	900	0.37	5	9	2	2	1.0			
9	9.7	11	71	99	830	0.51	5	4	–	–	1.0			
10	19.1	17	62	315	1200	0.83	7	7	–	4	1.0			
11	13.2	9	59	271	980	0.65	5	5	–	4	1.0			
12	15.2	7	50	310	520	0.32	4	3	–	2	1.0			
13	3.5	14	27	54	250	1.74	20	9	–	2	0.5	6	0.1	340
14	31.9	2	9	33	180	0.31	4	1	–	2	0.5	3	0.1	360
15	27.4	20	69	338	740	0.85	8	9	2	8	1.0			
16	19.4	7	36	124	500	0.30	4	4	–	20	0.5	6	0.1	320
17	28.6	108	129	207	790	0.59	8	9	2	4	1.0	7	0.1	260
18	7.4	23	42	94	480	1.94	20	11	–	4	0.5	10	0.2	340
19	29.8	11	120	231	4000	2.28	16	12	8	24	2.0			
20	40.1	33	114	507	1400	0.83	10	13	4	2	1.5			
21	15.3	24	72	428	880	0.65	8	9	–	4	1.0			
22	5.5	27	269	305	860	2.10	14	12	2	4	1.5	39	0.4	220
23	3.7	49	48	146	730	0.47	10	4	2	–	3.0			
24	5.8	57	60	184	190	0.79	10	5	2	8	3.0	12	0.1	220
25	21.6	34	89	801	2600	1.16	16	12	–	2	1.0			
26	13.5	50	109	694	3200	2.90	2	50	28	2	1.0			
27	12.8	36	107	565	2300	2.51	40	23	2	2	1.0	10	0.2	320
28	141.0	18	77	224	410	0.46	–	8	2	5	1.5			
29	19.7	32	123	767	970	1.92	14	26	4	12	1.5			
30	63.3	25	263	818	740	2.09	–	19	6	28	1.5			
31	67.4	41	687	528	900	0.67	15	8	–	4	2			
32	99.3	117	399	952	1900	1.86	23	20	4	4	3.5			
33	102.0	50	2336	959	5700	3.29	18	25	6	8	3.0			
34	48.8	111	8260	1156	2400	2.18	15	10	3.5	18	–			
35	31.7	82	3722	3596	29500	2.97	27	31	15	2	3.0			
36	32.4	80	816	900	240	0.33	13	5	2	–	3.0			
37	89.4	89	608	516	100	0.49	15	5	2	4	3.0			
38	16.3	27	102	804	1600	1.73	19	12	–	2	1.5			
39	9.3	18	68	519	1700	1.86	24	16	–	–	1.0			
40	12.9	20	71	657	1100	1.72	26	15	–	2	1.5	3	0.1	300
41	12.3	15	76	554	800	1.74	22	12	–	2	1.0			
42	5.4	10	34	772	3000	2.19	25	22	2	2	1.0			
43	4.1	9	31	622	1500	2.13	27	17	–	2	1.0	7	0.1	230
44	5.3	9	34	772	4100	2.41	27	27	2	2	1.0	10	0.1	320
45	4.1	47	192	674	1700	1.36	17	14	2	2	2.0			
46	6.3	13	40	737	2800	2.43	28	20	2	2	1.0			
47	3.1	19	104	163	1300	2.06	29	17	–	–	1.0			
48	7.2	17	107	142	850	1.47	22	13	–	2	1.5			
49	13.2	15	53	188	270	0.69	14	7	–	–	1.5			
50	2.8	8	33	86	490	1.33	21	11	–	–	0.5			
51	8.1	16	98	356	6600	2.69	29	39	4	8	1.0			
52	7.1	14	69	300	920	2.01	28	16	–	8	1.0			
53	6.9	14	80	260	1100	1.73	75	14	2	8	1.0			
54	13.3	15	129	3483	19100	1.00	41	77	15	8	1.0	6	0.1	240
55	6.5	11	28	567	890	1.87	24	13	–	2	1.0			
56	11.4	17	62	502	720	1.87	27	13	–	2	1.0			
57	21.7	16	42	180	510	0.80	17	8	2	2	2.0			
58	70.8	11	72	274	1700	3.21	16	13	40	2	2.0			
59	54.5	8	78	201	960	0.99	11	8	6	–	1.5			
60	34.5	6	202	220	18700	8.64	21	124	80	–	1.5	85	0.6	320
61	103.0	11	277	1038	38400	8.18	27	156	120	–	1.5			
62	68.1	23	160	3337	18600	10.70	57	166	30	–	2.0			
63	55.6	12	30	60	680	0.62	13	5	2	–	1.5			
64	4.1	18	20	66	560	2.16	38	19	–	2	1.0	5	0.1	320
65	3.2	21	23	119	340	2.18	37	16	–	4	0.5	3	0.1	340
66	3.5	19	23	120	390	2.42	40	17	–	2	0.5	3	0.1	340
67	4.0	18	29	177	390	2.33	40	17	–	4	1.0	3	0.1	360
68	2.7	15	28	64	490	2.54	43	18	–	–	1.0	6	0.1	300
69	2.6	17	28	55	550	3.15	41	23	–	2	1.0	5	0.1	340
70	2.5	16	54	140	3800	2.29	21	28	2	2	1.5			
71	58.3	11	38	61	660	0.89	13	12	–	–	1.5			
72	16.4	5	19	46	170	0.84	9	7	–	2	1.0			

Appendix IV

Element contents in spring and stream sediment samples (after Austria, 1976, 1977).

SN	ST	RU	U ppm	Mo ppm	W ppm	Cu ppm	Pb ppm	Zn ppm	Mn ppm	Fe %	LATITUDE ° ' "	LONGITUDE ° ' "
0001	*	OG			4	14	19	68	1388	2.9	46 44 55	66 56 50
0002	*	OG			2	8	22	50	790	2.2	46 44 45	66 55 15
0003	+	OG		2	4	11	28	118	2670	3.3	46 44 43	66 55 08
0004	+	OG			2	5	22	78	390	2.1	46 44 30	66 55 25
0005	+	OG	20.1		2	8	22	103	1180	3.1	46 44 15	66 55 08
0006	*	LG	13.2			14	34	138	1870	5.1	46 43 50	66 54 52
0007	+	OG	5.2		4	9	22	108	510	3.2	46 44 00	66 57 00
0008	*	OG				12	50	68	2236	3.6	46 44 03	66 56 40
0009	*	LG			4	4	9	20	170	0.3	46 43 45	66 57 19
0010	+	LG			2	8	30	138	570	2.8	46 44 00	66 58 33
1011	+	S			4	46	33	100	1827	3.0	46 31 15	66 33 20
0012	+	LG		2		11	51	183	6570	4.3	46 43 48	66 58 28
0013	+	LG		1		15	36	109	2540	3.4	46 43 30	66 58 25
0014	+	LG	24.9	8		8	54	195	3840	5.0	46 43 46	66 55 27
0015	+	LG		10	4	10	45	236	6260	4.3	46 43 37	66 59 42
0016	+	LG		10	4	6	69	145	2250	3.9	46 43 36	66 59 15
0017	+	LG		2	2	4	57	74	4800	3.2	46 43 30	66 59 28
0018	+	LG		6		7	57	240	5750	5.1	46 43 30	66 58 53
0019	+	LG	25.6	2	2	11	36	112	2610	3.4	46 43 17	66 58 30
0020	+	LG	14.9		2	11	36	140	2000	3.2	46 43 17	66 58 27
0021	+	LG		1	4	13	24	92	1390	2.0	46 43 00	66 58 05
0022	+	OG		1	2	16	30	121	1820	2.0	46 42 47	66 57 45
0023	+	LG		1	2	4	22	54	520	1.2	46 42 57	66 58 43
0024	+	LG		4	2	4	28	96	1920	2.0	46 42 45	66 58 18
0025	+	OG	16.3		2	2	13	22	340	0.4	46 42 37	66 57 50
0026	+	OG			2	2	3	20	40	0.2	46 42 38	66 57 52
0027	+	LG		1	2	6	22	52	630	1.5	46 42 45	66 59 30
0028	+	LG		1		5	22	87	950	1.5	46 42 45	66 59 25
0029	+	LG		1	2	3	16	57	230	0.7	46 42 33	66 58 58
0030	+	LG		1	2	4	13	49	180	0.8	46 42 28	66 58 30
0031	+	OG			3	2	13	32	70	0.4	46 42 18	66 57 58
0032	+	OG	13.2		2	3	3	40	470	0.7	46 42 30	66 57 42
0033	+	OG		1	2	6	22	43	450	1.8	46 42 20	66 56 09
0034	+	OG		1	4	14	15	43	730	1.4	46 42 26	66 55 05
0035	+	OG			2	13	15	19	380	0.7	46 42 17	66 55 08
0036	+	OG		1	2	34	30	52	1000	1.5	46 42 11	66 55 14
0037	+	OG	17.1			4	19	54	910	1.4	46 42 02	66 55 31
0038	+	OG		2	4	5	13	51	840	1.3	46 41 55	66 57 56
0039	+	OG		2	2	7	30	66	2600	2.3	46 41 38	66 57 34
0040	+	OG		1	2	5	20	59	1690	1.4	46 41 30	66 57 42
0041	+	OG	14.2	1	2	4	13	37	250	1.0	46 41 20	66 57 25
0042	*	LG	15.6		4	6	19	83	1060	0.8	46 42 05	66 59 57
0043	+	LG	22.9			4	12	35	712	0.7	46 41 57	66 59 50
0044	*	LG	13.3		4	2	12	25	330	0.5	46 41 52	66 59 55
0045	*	LG	17.1			4	19	40	630	0.8	46 41 46	66 59 40
0046	*	LG		4	2	6	37	78	6370	2.9	46 41 42	66 59 30
0047	*	LG			2	2	16	33	470	0.6	46 41 35	66 59 46
0048	+	LG	12.4			3	22	18	490	0.2	46 41 31	66 59 50
0049	+	LG				4	19	35	700	0.5	46 41 32	66 59 32
0050	+	LG	26.0		2	4	22	58	1410	1.1	46 41 37	66 59 30
0051	+	LG				4	25	68	1680	1.6	46 41 27	66 59 28
0052	*	LG		2	2	3	16	33	1220	0.6	46 41 25	66 59 30
0053	*	LG			2	9	22	75	1690	1.8	46 41 08	66 59 11
0054	*	LG		1		4	16	42	790	0.8	46 40 45	66 59 00
0055	*	LG	17.1		2	2	22	25	2520	0.9	46 40 57	66 58 45
0056	+	LG	9.3			4	22	81	2300	1.6	46 41 01	66 57 10

LEGEND

SN = Sample number
ST = Sample type
+ stream sediment samples
* spring sediment samples

RU = Rock unit underneath sample
OG = Ordovician granites
LG = Lower Devonian granites
BG = Burnthill Pluton
DG = Dungarvon Pluton
TG = Trout Brook Pluton
RG = Rocky Brook Pluton

S = Silurian metasedimentary rocks

CO = Cambro-Ordovician metasedimentary rocks

Appendix IV (cont.)

SN	ST	RU	U ppm	Mo ppm	W ppm	Cu ppm	Pb ppm	Zn ppm	Mn ppm	Fe %	LATITUDE ° ' "	LONGITUDE ° ' "
0057	+	LG		2	4	4	22	81	2700	1.7	46 40 40	66 57 20
0058	+	LG	14.0	8	4	5	28	71	5250	2.5	46 40 25	66 57 18
0059	+	LG	34.6	6	4		30	73	2810	1.8	46 40 27	66 57 11
0060	+	LG		2	2	6	15	51	4360	1.5	46 40 10	66 57 30
0061	+	LG		4	4	6	15	56	2980	1.0	46 40 12	66 57 11
0062	+	BG	19.8	1	4	4	19	40	470	0.8	46 41 08	66 55 50
0063	+	LG		2	2	4	19	74	1090	1.6	46 40 57	66 56 25
0064	+	LG		2	2	3	28	54	1430	1.9	46 40 38	66 56 30
0065	*	BG		4	4	4	16	37	980	1.0	46 40 25	66 56 04
0066	+	BG		50	1	10	130	53	9530	4.5	46 40 07	66 55 53
0067	+	BG		2	6	9	47	103	4500	1.4	46 40 04	66 55 33
0068	+	BG		20	2	6	19	50	530	0.8	46 40 03	66 55 08
0069	*	BG		20	16	5	35	45	243	2.1	46 40 01	66 54 30
0070	+	OG			2	10	29	105	630	2.4	46 44 15	66 53 42
0071	+	LG		4	2	11	28	138	1390	2.9	46 44 01	66 53 30
0072	+	LG			2	11	31	98	1480	2.7	46 43 59	66 53 17
0073	+	LG					93	395	12960	5.9	46 43 13	66 53 25
0074	+	LG	23.5		2	5	28	93	890	1.6	46 42 50	66 53 28
0075	*	BG			4	4	37	80	1250	2.2	46 42 30	66 53 30
0076	+	BG		2	4	2	22	38	280	1.1	46 42 15	66 53 43
0077	+	BG		20		4	31	70	1830	1.9	46 42 10	66 53 27
0078	+	BG		6	10	2	31	45	490	1.4	46 41 59	66 53 45
0079	+	BG	12.9	6	4	4	28	48	1470	1.8	46 41 58	66 53 30
0080	+	LG		1	2	12	26	99	830	2.7	46 44 00	66 51 56
0081	+	LG		1	2	7	16	58	620	2.4	46 43 50	66 51 55
0082	+	LG	9.4		2		16	76	960	2.1	46 43 45	66 51 57
0083	+	LG		1	2	11	13	71	830	1.8	46 43 47	66 51 20
0084	+	LG	15.0	2	2	10	13	71	850	1.9	46 43 34	66 51 30
0085	*	LG			2	15	10	55	513	2.0	46 43 30	66 51 35
0086	+	LG	15.8		2	7	13	58	480	1.5	46 43 28	66 51 45
0087	+	BG		2	2	4	6	39	550	1.0	46 43 20	66 51 55
0088	*	BG		2	2	5	10	58	1150	1.2	46 43 16	66 50 51
0089	+	BG	13.3			3	32	32	1100	1.1	46 42 40	66 51 51
0090	*	BG			2	4	22	32	930	1.0	46 42 35	66 51 45
0091	+	BG	36.6			4	41	30	470		46 42 12	66 51 50
0092	+	BG	39.7	1	2	2	19	20	250		46 41 50	66 52 07
0093	+	BG	13.0	1	4		9	17	80		46 41 30	66 52 18
0094	+	BG	12.8	1	2		16	15	80		46 41 30	66 52 18
0095	+	BG	23.6	1	4	3	25	32	820		46 41 32	66 52 55
0096	+	BG	47.3	1	4	5	25	52	1230		46 41 35	66 53 16
0097	+	BG		1	2	2	3	13	120		46 40 52	66 52 36
0098	*	BG		2		5	17	43	390		46 41 00	66 52 55
0099	+	BG		2	4	5	7	49	550		46 40 56	66 53 15
0100	+	BG		4	2	4	29	34	3970		46 40 20	66 53 18
0101	+	BG	12.2		2	4	16	29	440		46 40 00	66 53 28
0102	+	BG		5		5	32	31	6790		46 40 02	66 54 10
0103	+	BG		2	2	1	16	18	520		46 42 18	66 49 50
0104	*	BG		2	2	1	12	23	520		46 42 12	66 49 47
0105	*	BG			2	1	9	30	4506		46 42 06	66 50 00
0106	+	BG		1	2	1	6	18	480		46 41 50	66 50 06
0107	+	BG	21.2		2	2	12	28	390		46 41 35	66 50 06
0108	+	BG		10	20	7	37	43	4910		46 41 28	66 51 04
0109	+	BG			8	6	12	18	350		46 41 26	66 50 42
0110	*	BG		1		1	9	10	320		46 41 22	66 50 27
0111	+	BG			2	4	19	18	90		46 41 15	66 50 30
0112	+	BG	23.4		2	1	6	25	390		46 41 20	66 50 06
0113	+	BG	30.4	1	2	1	12	15	140		46 41 13	66 50 07
0114	+	BG	13.6	1	2	1	9	13	280		46 41 20	66 49 25
0115	+	BG	47.1	2		2	16	28	68		46 41 05	66 49 32
0116	+	BG	82.2		4	1	12	20	250		46 41 00	66 49 35
0117	+	BG	31.9		4	1	16	28	520		46 40 45	66 49 15
0118	+	BG		1	4	1	12	16	1230		46 40 15	66 48 57
0119	*	BG		1	4	3	22	18	2500		46 40 55	66 50 42
0120	+	BG		4	4	4	34	28	218		46 40 45	66 50 41
0121	+	BG		6	16	3	22	30	2080	1.1	46 40 30	66 50 41
0122	+	BG		4	23	4	27	53	1570	1.8	46 40 38	66 50 25
0123	+	BG	76.6	4	4	2	37	40	800	0.7	46 40 40	66 50 00
0124	+	BG		2	16	3	28	50	1570	1.4	46 40 35	66 50 00
0125	+	BG	47.6	1	38	2	22	28	350	1.0	46 40 40	66 49 35
0126	+	BG	45.9	2	20	1	15	21	369	0.6	46 40 33	66 49 15
0127	+	BG		2	8	2	27	37	441	1.4	46 40 28	66 49 18
0128	+	BG			8	3	25	42	307	1.7	46 40 25	66 49 35
0129	+	BG		3	4	2	39	49	97	1.3	46 40 20	66 49 35
0130	+	BG		1	2	2	15	21	492	0.5	46 40 05	66 49 58
0131	+	BG		1	4	1	21	28	215	0.6	46 40 26	66 48 45
0132	*	BG			4	1	21	19	266	0.4	46 40 30	66 48 48
0133	+	BG		1	4	1	18	26	133	0.5	46 40 23	66 48 10
0134	*	BG		1	4	1	18	23	441	0.7	46 40 25	66 48 00
0135	+	BG		1	4	1	21	23	164	0.7	46 40 12	66 47 42
0136	*	BG	41.1	1	16	4	24	30	410	1.2	46 40 08	66 47 50
0137	+	BG	21.0		4	1	9	21	72	0.4	46 40 08	66 47 20

Appendix IV (cont.)

SN	ST	RU	U ppm	Mo ppm	W ppm	Cu ppm	Pb ppm	Zn ppm	Mn ppm	Fe %	LATITUDE ° ' "			LONGITUDE ° ' "		
0138	•	OG				2	49	113	1140	2.5	46	44	57	66	49	56
0139	•	OG		1	4	10	20	103	510	2.7	46	44	41	66	50	20
0140	+	LG				13	43	100	1320	2.6	46	44	22	66	49	35
0141	•	OG			2	22	17	97	620	2.7	46	44	40	66	49	12
0142	•	OG	6.5	1	4	12	13	65	320	2.2	46	44	28	66	49	02
0143	•	LG		8	2	9	17	87	1020	2.0	46	44	09	66	49	01
0144	•	OG		2	8	5	10	58	260	1.3	46	43	40	66	49	38
0145	•	OG		0	10	6	16	68	1630	2.0	46	43	17	66	49	40
0146	•	OG		8	4	6	26	56	2240	2.5	46	43	23	66	49	20
0147	•	OG		2	8	4	6	48	480	1.0	46	43	12	66	49	14
0148	•	OG		1	4	2	3	29	150	0.5	46	43	07	66	49	10
0149	+	OG		1	8	3	6	34	180	0.7	46	43	04	66	48	58
0150	•	OG		4	8	7	19	87	1210	2.4	46	43	48	66	49	06
0151	•	OG		10	8	5	42	97	3920	2.4	46	43	39	66	49	02
0152	+	OG		1	8	4	6	52	470	1.3	46	43	17	66	48	30
0153	+	OG		2	12	1	10	90	900	2.1	46	43	22	66	48	07
0154	+	OG		2	8	6	13	75	1080	1.6	46	43	18	66	48	05
0155	+	OG		4	8	17	13	97	3030	2.5	46	43	20	66	47	54
0156	+	OG		8	32	6	13	167	1560	2.8	46	43	15	66	47	50
0157	+	OG		10	12	15	17	107	3210	3.2	46	43	29	66	47	32
0158	+	OG		15	2	6	17	105	5630	2.7	46	43	58	66	47	40
0159	•	OG	24.1		2	7	10	37	790	1.3	46	43	50	66	47	07
0160	+	OG		2	8	6	17	85	1620	1.7	46	43	48	66	46	53
0161	•	BG	20.2		4	2	18	29	472	1.1	46	42	05	66	47	40
0162	+	BG		1	4	1	9	10	125	0.3	46	41	20	66	47	20
0163	+	BG	16.7	2	4	2	15	30	333	0.9	46	41	15	66	47	20
0164	+	BG	16.3	4	4	3	15	30	575	0.8	46	40	18	66	46	58
0165	+	BG		2	4	2	15	36	542	0.9	46	41	15	66	46	30
0166	•	BG	9.4	4	12	2	28	25	694	0.9	46	41	08	66	46	15
0167	+	BG		8	4	4	21	38	495	1.7	46	40	28	66	46	31
0168	+	BG		4	4	3	28	43	949	1.0	46	40	38	66	46	10
0169	+	BG		2		8	15	72	1306	1.8	46	39	55	66	46	06
0170	•	BG				2	15	20	1083	0.8	46	40	50	66	45	50
0171	•	BG	4.4	4	4	2	21	18	749	0.7	46	40	45	66	45	50
0172	+	OG	11.3	1	4	6	8	35	170	0.9	46	42	52	66	44	36
0173	+	OG		5	2	4	43	40	8320	1.8	46	42	57	66	44	17
0174	+	OG			2	1	5	21	110	0.4	46	42	47	66	44	05
0175	•	OG		2	8	2	19	38	630	1.1	46	41	53	66	44	36
0176	+	CO	5.0	2	8	4	13	40	830	1.7	46	42	11	66	43	20
0177	+	CO		1	2	4	13	55	220	1.1	46	41	38	66	43	20
0178	+	CO		2		18	29	91	2760	1.8	46	41	16	66	43	30
0179	+	CO		2	2	13	29	86	2410	1.8	46	41	26	66	43	05
0180	•	CO		1	2	17	19	94	690	2.6	46	41	22	66	43	00
0181	+	CO				6	13	38	470	1.7	46	41	30	66	43	02
0182	+	CO	7.8		2	6	11	46	400	1.2	46	41	30	66	42	50
0183	+	CO		2	2	8	16	60	800	1.7	46	41	04	66	43	00
0184	•	CO		3	4	10	19	35	480	2.1	46	41	26	66	42	13
0185	+	CO	5.1	2	8	45	216	329	7150	4.1	46	41	12	66	42	13
0186	•	CO		2	2	6	15	30	330	0.7	46	40	59	66	42	20
0187	+	CO	7.3			5	52	92	1710	1.9	46	40	00	66	43	00
0188	+	CO		8	16	20	34	99	2190	2.4	46	39	50	66	42	44
0189	+	OG			2	2	6	23	330	0.7	46	43	50	66	42	50
0190	+	OG	4.2	2	2	5	15	40	49	1.7	46	43	30	66	42	36
0191	+	CO	3.0	2	2	4	12	38	300	1.2	46	43	10	66	42	30
0192	+	CO	3.7	2		3	12	25	290	0.9	46	43	06	66	41	40
0193	+	CO		2	8	3	12	43	830	1.3	46	42	59	66	41	55
0194	+	CO	3.6		2	9	13	54	770	1.8	46	42	17	66	41	26
0195	+	CO			2	4	18	27	3260	1.7	46	42	22	66	41	13
0196	+	CO		6	4	10	44	72	2790	2.7	46	42	02	66	41	34
0197	+	CO			4	8	28	65	790	1.9	46	41	59	66	41	29
0198	+	CO	4.6	4	4	7	9	61	790	1.4	46	41	43	66	41	18
0199	+	CO		4	12	7	19	53	820	2.2	46	41	19	66	41	08
0200	+	CO	3.9	4	12	17	25	53	760	2.3	46	41	01	66	41	11
0201	•	CO			4	5	9	58	140	1.1	46	40	35	66	41	10
0202	+	DG	20.8		4	4	19	57	530	1.3	46	44	57	66	39	40
0203	+	DG		2	4	5	21	11	870	1.6	46	44	50	66	39	38
0204	•	DG		1		2	19	11	510	1.3	46	44	31	66	39	21
0205	+	CO		30	4	8	41	33	4200	1.4	46	44	21	66	41	05
0206	+	CO		40		19	41	101	4690	2.1	46	44	08	66	40	51
0207	+	CO	5.9	4	4	1	6	30	100	0.6	46	44	20	66	40	44
0208	+	DG		8	4	9	9	37	730	1.3	46	44	14	66	40	35
0209	•	DG		10	20	8	72	90	6850	1.7	46	43	55	66	39	07
0210	+	DG		4	2	9	15	55	1210	1.6	46	43	42	66	40	40
0211	+	DG		1	2	10	6	43	400	1.6	46	43	44	66	40	16
0212	+	DG	25.0	10	2	13	24	63	1680	1.9	46	43	38	66	39	58
0213	+	DG	13.4	2	1	3	3	20	180	0.7	46	43	30	66	39	52
0214	•	DG	17.5	1	4	11	21	52	1400	1.8	46	43	25	66	38	55
0215	+	DG			2	1	3	13	150	0.2	46	42	04	66	39	16
0216	+	DG		6	4	5	15	70	920	1.3	46	41	53	66	39	03
0217	+	DG					3	15	100	0.1	46	42	02	66	38	56
0218	+	CO		8		32	154	113	6160	4.1	46	41	33	66	39	25

Appendix IV (cont.)

SN	ST	RU	U ppm	Mo ppm	W ppm	Cu ppm	Pb ppm	Zn ppm	Mn ppm	Fe %	LATITUDE ° ' "	LONGITUDE ° ' "
0219	+	DG		6		13	67	78	2810	2.3	46 41 43	66 39 04
0220	•	CO		10	12	16	24	113	1410	4.0	46 41 20	66 39 38
0221	+	DG	31.5	2	12	9	44	35	810	1.3	46 44 53	66 33 11
0222	+	DG	35.2	6	12	3	31	134	2330	1.3	46 44 43	66 33 10
0223	+	DG	16.1		1	1	9	27	320	0.6	46 44 52	66 34 52
0224	•	DG			2	1	9	23	250	0.8	46 44 41	66 34 34
0225	+	DG		1	2	1	15	32	420	1.0	46 44 23	66 33 58
0226	+	DG		2		1	12	30	400	0.9	46 44 22	66 33 57
0227	+	DG	9.4			2	9	25	260	0.9	46 44 30	66 33 27
0228	+	DG		10	16	3	13	53	1220	1.4	46 44 07	66 37 37
0229	•	DG		1	4	2	8	26	160	0.3	46 44 00	66 37 37
0230	+	DG			2	2	11	22	90	0.4	46 44 06	66 37 27
0231	•	DG	12.6		2	3	13	38	210	1.1	46 44 09	66 37 10
0232	•	DG	38.1		2	2	8	41	200	0.6	46 44 04	66 37 03
0233	+	DG	26.9		12	2	16	50	270	0.9	46 44 00	66 37 00
0234	•	DG	40.9	30		6	80	58	450	3.6	46 43 51	66 36 54
0235	+	DG	98.7		8	4	16	36	540	0.3	46 43 45	66 36 57
0236	+	DG	80.0	1	2	2	13	36	520	0.6	46 43 34	66 37 07
0237	+	DG	55.6	4		2	24	111	2550	1.1	46 43 30	66 37 01
0238	•	DG	70.6	2		3	27	106	2040	1.3	46 44 03	66 36 33
0239	•	DG		1	2	1	8	19	370	0.5	46 44 02	66 36 15
0240	•	DG	12.9	1		3	34	101	1220	1.7	46 44 59	66 36 03
0241	•	DG		3	2	8	19	50	400	1.4	46 43 48	66 35 55
0242	+	DG	52.3	2	4	3	13	46	350	0.7	46 43 52	66 35 36
0243	•	DG	18.0		12	2	6	35	170	0.6	46 43 02	66 34 37
0244	•	DG		6	8	1	16	19	460	0.6	46 43 05	66 35 06
0245	•	DG	33.7	5	4	3	19	48	390	1.4	46 43 23	66 35 18
0246	+	DG	76.9	1		3	15	59	330	1.0	46 43 43	66 35 09
0247	+	DG	27.0			2	6	50	440	1.0	46 43 50	66 35 10
0248	+	DG				1	6	32	380	0.6	46 43 54	66 34 42
0249	+	DG				2	15	37	800	0.8	46 43 59	66 34 19
0250	+	DG				1	6	35	270	0.8	46 44 03	66 33 59
0251	•	DG			4	2	6	23	250	0.5	46 43 58	66 33 58
0252	+	DG			8	4	9	47	360	1.0	46 44 08	66 33 31
0253	+	DG	23.4		12	3	12	30	310	1.1	46 44 16	66 33 10
0254	•	DG	26.3	6	4	4	25	59	560	0.9	46 44 22	66 32 50
0255	•	DG		4	12	2	31	37	2140	2.4	46 44 10	66 32 54
0256	•	DG	12.6	10	2	11	64	28	680	1.7	46 44 00	66 32 17
0257	+	DG		50	16	9	110	370	11560	6.8	46 43 50	66 32 22
0258	•	DG	22.2	2	2	3	13	44	320	1.1	46 43 24	66 31 45
0259	+	DG		20	4	3	12	40	420	0.8	46 43 07	66 31 35
0260	+	DG	10.9		8	4	27	152	3090	2.0	46 43 09	66 31 24
0261	+	DG	69.1	40	8	22	40	153	1780	2.1	46 43 23	66 31 16
0262	+	CO				8	48	94	3860	3.1	46 43 00	66 31 07
0263	+	DG			8	2	8	16	120	0.6	46 42 46	66 37 11
0264	+	DG		4		2	27	97	1140	1.5	46 42 30	66 37 52
0265	+	DG		4	6	2	35	92	870	1.8	46 42 23	66 38 20
0266	+	DG			1	2	3	20	70	0.3	46 42 00	66 38 33
0267	+	DG		2	2	2	9	25	350	0.5	46 41 48	66 38 42
0268	+	DG		10	8	16	24	83	3240	2.9	46 41 45	66 38 45
0269	+	DG		4		7	27	53	1070	1.2	46 41 41	66 38 26
0270	+	DG		6	4	13	18	109	1010	1.7	46 41 32	66 38 32
0271	•	DG		8	8	15	24	75	1220	2.1	46 41 38	66 38 37
0272	+	DG		6	16	3	29	45	530	1.0	46 41 24	66 38 07
0273	•	DG		2		10	53	28	830	0.9	46 41 18	66 36 25
0274	•	DG		10	8	8	27	14	120	0.2	46 41 11	66 36 26
0275	+	DG		6		10	15	68	450	2.0	46 40 13	66 38 40
0276	+	CO		2	2	5	6	50	380	1.4	46 40 00	66 38 50
0277	+	DG		20	28	5	41	77	1730	2.4	46 42 30	66 36 00
0278	+	DG		3	4	5	15	37	300	1.3	46 42 24	66 35 40
0279	+	DG		4	8	5	12	35	230	1.0	46 42 18	66 35 15
0280	+	DG		15	24	5	29	60	560	1.3	46 42 10	66 34 55
0281	+	DG			4	5	9	32	290	0.9	46 42 03	66 34 32
0282	+	DG			2	9	9	46	250	1.3	46 41 52	66 34 14
0283	+	DG	16.7	2	8	2	18	44	410	1.5	46 41 40	66 34 06
0284	+	DG		70	80	18	96	91	7610	3.0	46 41 51	66 35 06
0285	+	DG		20	24	6	21	26	1070	1.5	46 41 46	66 35 07
0286	+	DG		6	16	5	16	58	340	1.3	46 41 40	66 34 35
0287	•	DG		1	4	4	11	22	130	0.5	46 41 33	66 34 27
0288	+	DG	13.7		12	10	15	46	340	1.4	46 41 33	66 34 10
0289	+	DG	65.4	20	24	11	50	109	1940	2.4	46 40 23	66 36 05
0290	•	DG	34.2	2	28	6	19	58	790	1.5	46 40 30	66 36 00
0291	+	DG	113.0	25	12	5	25	71	2620	1.7	46 40 20	66 35 28
0292	+	DG	102.0	50	4	6	61	245	2490	2.8	46 40 11	66 35 06
0293	•	DG			4	1	17	33	460	1.0	46 40 18	66 34 56
0294	+	DG	51.2	2	4	3	19	49	730	0.8	46 40 20	66 34 40
0295	+	DG	66.4			5	16	82	771	0.7	46 40 02	66 35 12
0296	+	DG	55.4	1		4	11	73	552	0.6	46 40 03	66 34 49
0297	+	DG	26.6	4	16	8	11	22	260	0.3	46 40 46	66 34 55
0298	+	DG	4.3	10	16	12	21	50	490	1.9	46 40 40	66 34 40
0299	+	DG	49.5	4	4	2	15	39	1180	0.7	46 40 29	66 33 55

Appendix IV (cont.)

SN	ST	RU	U ppm	Mo ppm	W ppm	Cu ppm	Pb ppm	Zn ppm	Mn ppm	Fe %	LATITUDE ° ′ ″			LONGITUDE ° ′ ″		
0300	+	DG		4	8	12	24	34	240	1.2	46	39	45	66	36	48
0301	+	DG		7	20	4	16	26	660	0.5	46	39	45	66	36	40
0302	+	DG	8.5	2	4	5	3	21	220	0.8	46	41	10	66	32	34
0303	+	DG	24.1	8	12	6	21	46	430	1.1	46	40	58	66	33	19
0304	+	CO	19.8			4	12	44	600	1.3	46	40	42	66	33	18
0305	+	CO	5.8	5	8	5	46	126	4690	2.4	46	41	07	66	31	15
0306	+	CO		2	8	4	46	110	3140	2.3	46	40	54	66	31	24
0307	+	CO		4	6	7	52	206	1630	3.1	46	40	53	66	31	30
0308	+	CO	6.2	2	4	6	43	124	1870	2.6	46	40	30	66	31	16
0309	+	S	4.1		6	9	49	117	1130	2.9	46	40	10	66	31	10
0310	+	S		2	24	8	62	121	2100	3.4	46	39	55	66	31	14
0311	*	S		2	20	8	49	153	1920	3.2	46	39	48	66	31	09
0312	+	S			8	5	49	84	540	2.5	46	39	40	66	31	18
0313	+	CO		1	4	4	15	20	310	0.9	46	42	50	66	30	48
0314	*	CO	3.7	2	2	14	2	99	1650	3.0	46	42	26	66	30	10
0315	+	LG			2	3	7	39	297	0.6	46	39	40	66	59	55
0316	*	LG		1	6	3	3	18	77	0.3	46	39	38	66	59	35
0317	+	LG			2	2	6	27	230	0.3	46	39	30	66	59	32
0318	+	LG			2	3	6	30	350	0.4	46	39	33	66	59	07
0319	+	LG			2	5	3	41	450	1.1	46	39	35	66	58	42
0320	+	LG				2	3	16	30	0.2	46	39	40	66	57	58
0321	*	LG		1	2	2	16	270	30	0.3	46	39	40	66	58	02
0322	+	LG	4.1		2	2	6	24	60	0.1	46	39	28	66	58	01
0323	+	LG			2	4	19	76	500	1.6	46	39	19	66	57	29
0324	+	LG		6	4	4	22	68	1340	1.7	46	39	02	66	57	46
0325	+	OG		4	2	2	16	41	1060	1.2	46	38	56	66	57	20
0326	*	LG			2	5	9	27	230	0.9	46	40	05	66	58	20
0327	+	LG		2	2	4	30	54	5910	2.5	46	40	03	66	57	59
0328	+	LG		1	2	6	27	54	2480	1.2	46	39	59	66	59	33
0329	*	CO		1	2	10	15	42	800	2.1	46	40	00	66	56	58
0330	+	CO		4	4	5	8	58	1160	1.2	46	39	52	66	57	06
0331	+	CO		6	2	6	15	37	1130	1.4	46	39	46	66	56	50
0332	*	OG		2	2	3	10	40	540	0.6	46	39	06	66	56	45
0333	+	LG			2	2	10	22	210	0.5	46	38	56	66	59	56
0334	*	LG			2	2	7	16	66	0.3	46	38	40	66	59	48
0335	+	LG			2	3	6	10	384	0.6	46	38	45	66	59	45
0336	+	BG		6	4	6	22	48	860	1.1	46	40	00	66	55	37
0337	+	BG		2	2	6	125	58	2260	1.3	46	39	58	66	54	38
0338	+	BG		10	8	4	23	86	3380	1.8	46	39	12	66	58	00
0339	*	BG		6	4	13	70	42	480	1.2	46	39	23	66	55	47
0340	*	BG		2	4	5	6	21	280	0.5	46	39	27	66	55	27
0341	+	BG		6	8	4	26	73	1370	1.5	46	39	17	66	55	34
0342	+	BG		2	28	5	16	73	660	1.2	46	39	13	66	55	06
0343	+	BG				5	39	113	2320	1.7	46	39	07	66	55	07
0344	+	BG		2	8	3	6	46	300	0.5	46	38	59	66	55	11
0345	+	BG		4	40	4	13	62	1030	0.9	46	39	10	66	54	40
0346	+	CO			4	2	6	30	120	2.6	46	37	31	66	59	37
0347	+	CO			4	12	31	115	800	2.9	46	37	28	66	59	30
0348	+	OG			4	2	6	25	290	0.3	46	37	11	66	59	36
0349	+	OG			4	4	16	43	360	0.8	46	37	08	66	59	40
0350	+	OG			6	3	19	40	540	0.7	46	37	06	66	59	44
0351	+	OG	8.7		4	1	9	20	90	0.2	46	36	45	66	59	41
0352	+	OG	3.8	1	4	3	16	72	650	0.9	46	38	21	66	58	03
0353	*	OG		4	8	5	54	72	1500	2.5	46	38	18	66	57	57
0354	+	OG		1	2	2	13	57	490	0.6	46	37	58	66	58	00
0355	+	OG			2	3	19	52	1430	0.8	46	37	45	66	57	56
0356	+	OG		1	4	9	16	42	310	0.7	46	37	59	66	58	25
0357	+	OG			2	5	35	54	490	1.7	46	37	40	66	58	00
0358	*	OG		1	2	3	15	33	100	0.9	46	37	30	66	58	03
0359	+	OG	2.6			2	12	19	130	0.2	46	37	21	66	58	03
0360	*	CO			2	2	12	17	400	0.4	46	37	20	66	58	08
0361	+	CO			2	2	15	18	120	0.4	46	34	50	66	57	50
0362	+	CO	1.8		2	2	6	10	30	0.1	46	35	11	66	57	33
0363	+	OG		1	4	9	188	117	2140	1.3	46	38	07	66	56	20
0364	*	BG	32.2	10		3	30	68	560	0.8	46	37	48	66	55	50
0365	+	BG	50.6	1		4	27	60	690	0.5	46	37	37	66	55	46
0366	+	BG	6.2	1		4	17	42	630	0.6	46	37	00	66	55	38
0367	*	BG		4	4	2	3	21	100	0.4	46	36	48	66	55	11
0368	+	BG		2	6	2	17	33	670	1.2	46	36	41	66	55	10
0369	+	BG			4	3	7	31	510	0.6	46	36	20	66	54	41
0370	+	BG		40		20	42	61	4360	1.8	46	35	48	66	55	05
0371	+	BG		30	4	18	39	56	2760	1.5	46	35	35	66	55	05
0372	+	BG		8	20	13	12	40	460	0.6	46	35	30	66	55	10
0373	+	BG	4.2		12	12	27	56	1520	1.3	46	35	27	66	55	54
0374	+	BG		1	20	11	21	53	810	1.0	46	35	24	66	55	30
0375	+	BG	8.4		4	6	21	53	1570	1.1	46	35	18	66	55	30
0376	+	BG		7	4	5	18	43	340	0.7	46	35	00	66	55	42
0377	+	BG	22.7	2	6	3	12	26	600	0.5	46	39	52	66	53	37
0378	*	BG			2	4	3	32	390	0.5	46	39	41	66	53	40
0379	+	BG			4	5	22	43	940	1.7	46	39	58	66	52	50
0380	+	BG		2	8	5	19	25	630	0.5	46	39	54	66	52	49

Appendix IV (cont.)

SN	ST	RU	U ppm	Mo ppm	W ppm	Cu ppm	Pb ppm	Zn ppm	Mn ppm	Fe %	LATITUDE ° ' "	LONGITUDE ° ' "
0381	+	BG	14.5		8	7	19	64	1220	1.3	46 39 28	66 53 36
0382	+	BG		6	20	4	16	59	1070	1.1	46 39 18	66 54 00
0383	*	BG		30	8	7	26	50	2220	2.2	46 39 22	66 54 00
0384	+	BG		6	40	8	13	56	1450	1.1	46 39 11	66 54 12
0385	+	BG		2	2	6	56	58	4580	2.1	46 39 43	66 52 17
0386	+	BG	39.1	4	8	8	28	38	1750	0.7	46 39 43	66 52 20
0387	+	BG		1	6	3	12	18	210	0.5	46 39 30	66 52 00
0388	+	BG		4	6	3	25	38	1120	0.4	46 39 16	66 51 23
0389	+	BG		4	4	3	19	33	620	0.5	46 39 07	66 51 25
0390	+	BG	24.9		4	2	18	25	361	0.3	46 38 57	66 51 06
0391	*	BG		1	2	1	9	18	136	0.4	46 39 01	66 51 01
0392	+	BG		2	2	1	15	13	403	0.2	46 38 42	66 50 50
0393	+	BG		8	4		21	20	861	0.5	46 38 23	66 50 39
0394	+	BG	13.1	4	4	1	21	23	556	0.5	46 38 10	66 50 11
0395	+	BG		2		1	15	25	706	0.3	46 38 03	66 49 42
0396	+	BG			2	1	12	18	153	0.3	46 37 57	66 49 05
0397	*	BG			2	1	12	18	222	0.2	46 37 21	66 49 09
0398	+	BG	13.6	1	2	3	18	21	318	0.5	46 39 53	66 49 53
0399	+	BG	19.5		2	2	18	23	430	0.5	46 39 21	66 50 11
0400	+	BG		1	2	1	6	9	72	0.2	46 39 18	66 49 45
0401	+	BG		9	56	5	25	30	852	0.6	46 39 10	66 48 08
0402	+	BG	27.6			6	62	51	969	1.1	46 39 01	66 47 40
0403	+	BG		2	12	1	22	44	310	1.1	46 39 02	66 47 10
0404	+	BG		4	16	7	12	41	431	0.8	46 39 03	66 46 45
0405	+	BG	30.8	10	80	3	46	30	1156	0.6	46 38 17	66 47 41
0406	+	BG	33.2	6	40	2	31	25	781	0.5	46 37 59	66 47 10
0407	+	BG	34.1		4	5	53	37	1108	1.0	46 38 00	66 48 18
0408	+	BG	25.3	2	16	4	44	44	1763	0.7	46 37 56	66 47 40
0409	+	BG	68.9	4	12	5	25	44	748	0.7	46 37 53	66 47 10
0410	*	BG	65.0	8	24	16	56	78	1652	1.0	46 37 48	66 47 00
0411	+	BG	171.0	3		9	53	153	12240	2.4	46 38 11	66 54 15
0412	*	BG	39.3		20	8	37	95	3970	1.3	46 38 17	66 54 15
0413	+	BG	13.1		8	2	9	30	240	0.1	46 38 24	66 53 45
0414	+	BG	68.9	40	20	10	56	103	3970	1.8	46 38 18	66 53 41
0415	+	BG		20	20	8	37	80	3710	1.2	46 38 06	66 52 45
0416	+	BG			2	5	4	68	780	2.4	46 38 50	66 52 30
0417	+	BG			4	7	18	73	680	2.3	46 38 45	66 52 25
0418	+	BG		8	4	7	18	111	450	3.0	46 38 40	66 52 18
0419	+	BG		20		9	47	100	3150	1.4	46 38 10	66 52 00
0420	+	BG	19.3	4	24	7	54	92	9463	1.8	46 37 32	66 52 30
0421	*	BG		8	28		48	78	190	2.2	46 37 18	66 52 25
0422	+	BG		300	40	7	67	163	10465	3.9	46 37 23	66 51 59
0423	+	BG		20	56	5	33	115	5021	2.8	46 37 32	66 51 40
0424	+	BG	22.9	10	40	4	15	62	1374	1.9	46 37 43	66 51 26
0425	*	BG		1	2	1	12	16	62	0.1	46 37 52	66 51 03
0426	*	BG		2	8	1	42	103	1167	1.5	46 37 48	66 50 48
0427	*	BG		1	2	2	3	23	83	0.5	46 37 11	66 50 48
0428	+	BG	10.9	2	4	2	18	35	374	0.7	46 37 10	66 50 30
0429	+	BG		2	24	5	21	43	348	0.8	46 37 03	66 49 53
0430	+	BG	18.1	2	16	5	15	53	374	0.7	46 37 02	66 50 20
0431	+	BG				2	25	39	1480	1.1	46 36 50	66 52 04
0432	+	BG	12.1	4	16	7	25	44	1350	1.2	46 36 41	66 51 37
0433	+	BG		6	12	10	25	50	1450	1.6	46 36 37	66 51 17
0434	*	BG		1	8	27	28	45	1136	1.0	46 36 43	66 50 00
0435	*	BG		40	28	2	16	33	1825	0.8	46 36 43	66 49 52
0436	*	BG		6	12	6	41	33	3544	1.0	46 37 10	66 49 20
0437	+	BG		1	20	3	15	37	1330	1.2	46 36 23	66 50 39
0438	*	BG		3	16	3	25	39	860	1.2	46 36 22	66 50 45
0439	+	BG	7.9	1	28	2	6	23	212	0.5	46 36 12	66 50 27
0340	+	BG	7.8	40	10	4	24	36	2120	0.8	46 36 22	66 54 35
0441	+	BG		10	6	2	10	26	320	0.5	46 36 35	66 54 30
0442	+	BG		40	8	4	21	36	1820	0.8	46 36 38	66 54 27
0443	+	BG		100	10	12	24	79	2340	1.5	46 36 11	66 54 20
0444	+	BG		20	6	4	3	26	560	0.6	46 35 58	66 54 21
0445	+	BG		100	24	5	24	43	2500	1.7	46 35 53	66 54 22
0446	+	BG		50	24	5	24	43	1440	1.4	46 35 49	66 53 59
0447	+	BG	9.2			9	14	41	680	1.2	46 35 30	66 54 29
0448	+	BG	11.1			9	7	56	1030	1.2	46 35 27	66 54 32
0449	*	BG		30	8	7	17	56	1350	1.8	46 35 10	66 54 12
0450	+	BG	11.1	20	16	8	10	46	1230	1.1	46 34 55	66 54 12
0451	+	BG		10	16	16	24	71	2120	2.3	46 34 50	66 53 51
0452	+	BG		15	20	11	17	54	1430	1.7	46 34 36	66 54 02
0453	+	BG		3	12	1	12	21	62	0.3	46 36 10	66 52 40
0454	+	BG		2	28	1	15	23	393	0.8	46 36 00	66 52 20
0455	*	BG		1	8	1	9	12	52	0.1	46 35 53	66 52 29
0456	+	BG	10.9	2	16	1	15	16	155	0.3	46 35 42	66 51 50
0457	+	CO		2	12	2	12	30	403	0.6	46 35 17	66 51 43
0458	+	BG	6.3	1	24	2	18	25	372	0.5	46 34 56	66 52 00
0459	*	BG	6.0	2	28	2	18	39	124	0.7	46 34 56	66 52 05
0460	+	CO	3.0		4	3	15	38	278	0.6	46 34 49	66 50 40
0461	*	CO		3	12	15	43	182	611	2.0	46 34 49	66 50 30

SN	ST	RU	U ppm	Mo ppm	W ppm	Cu ppm	Pb ppm	Zn ppm	Mn ppm	Fe %	LATITUDE ° ′ ″	LONGITUDE ° ′ ″
0462	+	CO		2	8	3	15	43	708	0.6	46 34 32	66 50 25
0463	•	BG	8.0	2	8	3	21	23	615	0.6	46 35 58	66 50 08
0464	+	BG		2	4	6	71	38	250	0.7	46 35 34	66 49 13
0465	+	BG	5.8	2	4	2	12	43	388	0.5	46 35 11	66 49 40
0466	+	BG	19.3	4	28	5	43	44	1434	1.5	46 37 10	66 48 13
0467	+	BG		2	4	4	43	30	2131	0.6	46 36 40	66 48 00
0468	•	BG		1	8	4	3	18	69	0.2	46 36 34	66 48 05
0469	+	BG		30		5	43	99	518	1.9	46 36 27	66 48 00
0470	+	CO		25	20	9	40	87	3297	1.3	46 36 07	66 47 38
0471	•	CO		70	16	22	43	255	5029	1.9	46 36 02	66 47 40
0472	•	BG		2	24	5	15	30	551	0.3	46 36 40	66 47 19
0473	+	CO			8	2	6	35	138	0.2	46 36 18	66 47 17
0474	+	CO		2	8	1	9	20	792	0.4	46 36 02	66 47 11
0475	+	BG		4	2	1	12	20	647	0.4	46 35 50	66 47 03
0476	+	BG	8.2			3	21	47	759	0.6	46 35 40	66 47 00
0477	+	CO		20		20	31	85	331	1.5	46 35 00	66 48 13
0478	+	CO		8	24	18	26	92	769	1.9	46 35 00	66 48 09
0479	+	CO		40	80	20	45	133	4028	2.9	46 34 52	66 48 06
0480	+	CO				20	54	197	2329	2.0	46 34 57	66 48 00
0481	+	CO	6.8	8	28	13	51	117	2265	1.9	46 34 48	66 48 00
0482	+	CO		15	80	9	43	51	2125	1.7	46 34 50	66 47 50
0483	+	CO	100.0	2	2	3	12	27	201	0.6	46 37 48	66 46 20
0484	+	BG	37.9	8	16	5	18	41	476	0.8	46 37 03	66 46 44
0485	•	BG	31.6	2	8	2	9	25	190	0.6	46 38 37	66 46 01
0486	•	BG		1	8	6	21	62	403	1.3	46 38 40	66 45 40
0487	•	BG		10	6	3	30	48	1515	1.2	46 38 15	66 46 05
0488	•	BG		2	4	2	3	18	122	0.5	46 38 10	66 45 55
0489	+	CO		1	8	3	29	22	2030	0.5	46 38 42	66 44 42
0490	+	CO		1		4	21	34	1330	1.0	46 38 30	66 45 00
0491	+	CO		4	12	2	12	18	597	0.5	46 38 23	66 45 08
0492	•	CO		30	40	19	70	61	8263	2.1	46 38 11	66 45 18
0493	+	CO	8.0	2	16	4	13	24	958	0.7	46 38 09	66 45 20
0494	+	CO	8.5	6	40	5	21	50	752	2.0	46 38 00	66 45 30
0495	+	CO		30	16	16	61	84	4960	3.4	46 37 56	66 44 30
0496	+	CO		9	24	21	27	79	1993	1.3	46 37 35	66 45 08
0497	•	CO		3	16	21	21	34	286	0.9	46 37 18	66 44 54
0498	+	BG	36.4	6	80	3	28	41	970	0.8	46 37 44	66 46 40
0499	+	CO	39.3	2	48	3	37	41	703	0.7	46 37 33	66 46 17
0500	+	CO	34.8	40	20	12	100	158	3661	2.2	46 37 27	66 46 17
0501	+	BG		40	20	9	119	156	3772	1.6	46 37 20	66 46 40
0502	+	CO		2	24	4	19	48	971	0.7	46 37 23	66 46 00
0503	•	CO			12	5	9	21	123	0.6	46 37 20	66 46 02
0504	+	CO		2	80	8	31	50	658	1.3	46 37 15	66 45 27
0505	+	CO		4	24	10	25	48	692	1.4	46 37 09	66 45 08
0506	+	CO				8	21	55	114	1.3	46 36 23	66 44 50
0507	+	CO		10	4	15	15	139	5040	3.9	46 36 27	66 44 00
0508	+	CO		30	8	42	87	160	5470	6.0	46 36 30	66 44 17
0509	+	CO	6.5	20	8	60	56	115	2430	4.5	46 36 20	66 44 37
0510	•	CO		4	8	45	16	48	240	1.4	46 35 58	66 44 20
0511	+	CO	4.7	2		29	31	65	1390	3.0	46 35 40	66 44 22
0512	+	CO		15	16	46	27	95	2870	3.6	46 35 50	66 43 27
0513	+	TG		8	12	22	25	91	1930	2.0	46 35 31	66 43 30
0514	+	TG	15.8	2	4	13	27	93	1420	1.8	46 35 23	66 43 40
0515	•	TG		2	4	12	28	55	1898	2.0	46 35 20	66 44 07
0516	+	BG		1	4	3	12	37	536	0.4	46 35 45	66 46 45
0517	+	BG		6	16	3	18	50	804	0.7	46 35 20	66 46 37
0518	+	CO		2	4	10	24	67	837	1.2	46 35 12	66 46 30
0519	+	CO	8.9			12	35	79	1127	1.3	46 35 00	66 46 20
0520	•	TG	61.0	4	80	18	52	128	1033	1.6	46 34 38	66 44 20
0521	•	TG		20		25	113	160	2011	2.1	46 34 53	66 43 23
0522	•	TG		10	20	14	64	47	722	1.5	46 34 52	66 43 10
0523	•	TG		5	28	14	32	83	911	1.9	46 34 57	66 42 25
0524	•	TG	9.1		40	11	29	92	655	1.3	46 35 00	66 42 08
0525	•	TG		6	28	13	88	164	689	1.7	46 35 04	66 41 50
0526	+	TG		8		5	46	214	3611	2.0	46 35 08	66 41 30
0527	+	TG		4	16	12	52	203	3622	3.4	46 35 54	66 41 10
0528	+	TG	30.8	2	16	17	55	246	2100	1.7	46 35 35	66 40 05
0529	+	TG	96.3	10	28	36	184	422	6302	2.3	46 35 20	66 40 08
0530	+	TG	40.4	4	12	11	44	210	1071	1.2	46 35 39	66 39 40
0531	+	TG	14.5		24	3	14	47	200	0.6	46 35 20	66 39 31
0532	+	CO		6	2	15	18	55	590	1.7	46 38 33	66 43 37
0533	+	CO	5.8	3	4	12	24	64	780	1.9	46 38 20	66 42 57
0534	+	CO		4	12	13	15	34	488	1.3	46 38 43	66 42 47
0535	•	CO		2	4	12	21	44	820	1.5	46 38 15	66 42 49
0536	+	CO				14	21	55	1020	1.5	46 38 60	66 42 43
0537	+	CO		4	8	13	15	60	820	1.6	46 38 02	66 42 46
0538	+	CO	4.6	4	4	12	18	60	740	1.5	46 37 53	66 42 39
0539	+	CO		140	2	9	18	39	360	1.1	46 37 45	66 43 20
0540	+	CO		2	28	16	31	71	390	1.8	46 37 40	66 43 08
0541	+	CO	7.2			16	32	85	1100	2.2	46 37 32	66 42 36
0542	•	CO		4	12	23	18	57	840	1.6	46 37 40	66 42 27

Appendix IV (cont.)

SN	ST	RU	U ppm	Mo ppm	W ppm	Cu ppm	Pb ppm	Zn ppm	Mn ppm	Fe %	LATITUDE ° ' "	LONGITUDE ° ' "
0543	•	CO		8	10	18	27	58	1840	2.1	46 37 28	66 42 20
0544	•	CO		7	20	25	27	81	1000	1.9	46 37 25	66 42 31
0545	+	CO		2		14	27	63	518	1.4	46 37 17	66 44 01
0546	+	CO		5	20	15	21	54	467	1.5	46 37 08	66 43 40
0547	•	CO		6	12	26	30	84	874	2.0	46 37 09	66 43 12
0548	+	CO		4	12	17	21	49	335	1.6	46 37 06	66 43 02
0549	•	CO		4	4	18	15	56	671	1.5	46 37 02	66 43 01
0550	+	CO	5.9	4	12	18	21	63	600	1.4	46 37 03	66 42 40
0551	+	CO	5.0	2	2	16	27	70	630	2.3	46 37 08	66 43 30
0552	+	CO			16	14	16	74	650	1.4	46 36 36	66 42 10
0553	+	CO		2	4	13	22	72	2070	1.7	46 36 25	66 42 30
0554	+	CO			4	14	22	72	1430	1.8	46 36 32	66 42 27
0555	•	CO		2	1	17	22	83	1060	2.2	46 36 33	66 41 37
0556	+	TG	6.6	4	8	16	27	91	880	1.8	46 36 21	66 41 37
0557	+	TG			4	3	11	23	150	0.2	46 36 16	66 41 20
0558	+	CO		20		16	55	89	10640	4.4	46 36 04	66 42 44
0559	+	CO			4	33	33	129	1240	2.2	46 36 00	66 42 27
0560	+	TG		2	8	18	25	106	990	2.1	46 36 00	66 41 57
0561	+	TG		4	8	26	41	201	2060	1.7	46 35 57	66 41 56
0562	+	TG	4.6	4	16	16	30	129	1060	2.0	46 35 70	66 41 41
0563	•	CO	18.5	8	16	11	18	182	1430	1.3	46 36 11	66 40 41
0564	+	CO		2	20	36	29	161	760	3.6	46 39 34	66 44 11
0565	+	CO			12	2	11	24	260	0.5	46 39 24	66 44 40
0566	•	CO		1		6	11	17		0.7	46 39 22	66 44 33
0567	•	CO			8	8	58	106	10250	2.3	46 39 18	66 44 20
0568	+	CO		2	8	6	37	72	2830	2.5	46 39 20	66 44 20
0569	+	CO		10	8	27	58	82	7250	4.4	46 39 39	66 43 42
0570	+	CO		6	4	22	42	84	4405	3.3	46 39 29	66 43 50
0571	+	CO	5.7	2	8	24	29	96	2020	3.7	46 39 25	66 43 53
0572	•	CO		20		17	62	100	3430	2.0	46 38 58	66 43 06
0573	+	CO		8		15	46	89	1250	1.9	46 38 50	66 42 53
0574	+	CO				22	86	161	4600	2.8	46 38 47	66 42 11
0575	+	CO		10	4	17	46	98	1710	2.1	46 38 48	66 41 52
0576	+	CO		10		18	28	89	1150	2.1	46 39 50	66 42 41
0577	•	CO				13	15	62	930	1.7	46 39 41	66 42 12
0578	+	CO	6.0			15	18	87	960	1.9	46 39 27	66 42 06
0579	+	CO		10	28	19	24	99	1380	2.2	46 39 10	66 42 00
0580	•	CO				18	178	316	9480	4.0	46 39 07	66 41 51
0581	•	CO	7.9	4	8	4	20	138	1210	2.5	46 38 03	66 41 00
0582	•	CO		5		20	12	57	470	1.5	46 37 59	66 40 57
0583	+	CO	4.5	4	28	3	20	103	1140	3.3	46 37 27	66 40 30
0584	+	CO		6	8	18	16	74	800	1.8	46 37 03	66 40 17
0585	•	CO		2	16	7	11	43	260	1.2	46 37 00	66 40 13
0586	•	CO		4	16	20	14	84	870	2.4	46 36 57	66 40 02
0587	•	CO		6	28	16	12	46	710	2.0	46 36 50	66 40 20
0588	•	CO	6.3	2	32	12	8	41	410	1.4	46 36 41	66 39 32
0589	+	CO		4	4	10	36	67	490	1.7	46 39 35	66 39 00
0590	+	CO	10.5	1	12	7	21	64	530	1.6	46 39 32	66 39 02
0591	•	CO		6	4	61	24	201	4120	2.7	46 38 31	66 39 41
0592	+	CO		2	8	39	12	88	450	1.4	46 38 19	66 39 28
0593	+	RG		4	8	46	21	88	1290	3.1	46 38 08	66 39 07
0594	+	RG	12.3	2	8	23	18	111	2010	2.5	46 37 57	66 38 47
0595	+	CO		4	8	21	12	93	1420	2.3	46 37 38	66 38 42
0596	+	CO		5	4	26	15	97	2000	2.3	46 37 36	66 38 49
0597	+	CO		8	24	40	29	202	3110	2.1	46 39 10	66 38 38
0598	+	CO	11.3	2	8	2	9	69	480	1.6	46 39 06	66 38 40
0599	•	CO		2	8	4	18	109	1340	1.9	46 38 57	66 38 42
0600	•	CO		2	2	8	11	40	400	1.7	46 38 54	66 35 45
0601	+	CO		70	16	22	30	93	6880	2.5	46 39 20	66 36 10
0602	+	DG	7.7		6	3	3	22	90	0.2	46 39 31	66 36 40
0603	•	DG		4	4	8	11	63	560	0.8	46 39 30	66 37 00
0604	+	DG			24	4	16	41	420	1.0	46 39 08	66 37 17
0605	+	DG	20.1	4	8	5	8	31	446	0.8	46 38 57	66 37 14
0606	+	DG		15	16	11	24	50	5011	2.8	46 38 52	66 36 47
0607	+	DG	11.2	20		13	22	61	5980	3.0	46 38 53	66 37 11
0608	+	CO		6	12	6	13	48	650	1.2	46 38 47	66 37 41
0609	+	CO	13.5	4	12	6	11	50	600	1.1	46 38 37	66 38 05
0610	•	CO		20	8	26	32	159	3040	2.9	46 38 20	66 38 10
0611	+	RG	8.1	1	1	15	16	68	570	1.7	46 38 03	66 38 03
0612	•	RG		6	20	9	15	44	213	1.0	46 37 57	66 38 07
0613	•	RG		10	4	21	25	95	1130	2.2	46 37 49	66 37 51
0614	•	RG		20	12	8	19	95	1390	1.9	46 37 38	66 37 59
0615	+	RG	6.2	2	40	20	18	71	541	2.5	46 37 27	66 38 20
0616	•	CO		6	40	18	12	71	531	2.2	46 37 23	66 38 36
0617	•	RG	46.9	4	24	5	25	78	1030	1.6	46 37 05	66 38 11
0618	+	RG	10.6	2	4	5	15	48	216	1.2	46 36 56	66 38 15
0619	•	RG	91.5	20	16	12	33	157	430	1.6	46 36 49	66 37 52
0620	•	CO		2	2	15	18	78	672	1.9	46 36 32	66 38 10
0621	+	TG	23.3	4	8	11	19	49	270	0.8	46 36 08	66 38 03
0622	•	CO		20	16	16	41	587	3550	3.0	46 35 30	66 37 55
0623	+	CO		70	24	12	60	547	9013	3.3	46 35 19	66 37 37

SN	ST	RU	U ppm	Mo ppm	W ppm	Cu ppm	Pb ppm	Zn ppm	Mn ppm	Fe %	LATITUDE ° ′ ″	LONGITUDE ° ′ ″
0624	•	CO	12.4	5	20	21	30	335	1702	2.1	46 35 33	66 37 30
0625	+	CO		4	12	33	36	343	393	1.1	46 35 38	66 37 38
0626	•	CO		3	26	38	35	209	1591	2.4	46 35 53	66 36 45
0627	•	CO		5	120	22	41	236	898	1.7	46 35 53	66 36 16
0628	+	CO		1	28	33	177	270	1295	1.9	46 35 57	66 36 10
0629	•	CO		4	40	16	90	79	648	1.6	46 35 55	66 36 07
0630	•	CO			30	3	11	25	179	0.4	46 35 45	66 36 18
0631	+	CO		10		30	44	176	5168	5.6	46 35 27	66 36 10
0632	+	CO		2	40	6	22	47	1439	0.9	46 35 33	66 36 11
0633	+	CO		1	35	12	14	47	567	0.7	46 35 37	66 35 50
0634	+	CO	7.3	8	30	31	46	208	6145	5.5	46 35 38	66 35 55
0635	+	CO		4	28	10	20	63	689	1.8	46 34 48	66 37 42
0636	+	CO		2	20	13	20	63	1200	1.7	46 34 38	66 37 20
0637	+	CO		10	56	36	29	119	2678	4.3	46 34 27	66 37 02
0638	+	CO	11.1	20		62	32	145	4544	5.3	46 34 44	66 36 33
0639	+	CO		6	12	10	14	53	978	2.7	46 35 03	66 36 20
0640	+	CO		2	4	47	70	127	7329	2.6	46 35 06	66 36 00
0641	+	CO		8		25	15	56	2690	3.2	46 35 04	66 35 45
0642	+	CO		4	24	34	55	195	6375	3.1	46 35 10	66 35 30
0643	+	CO		1	16	1	6	14	144	0.2	46 35 22	66 35 18
0644	+	CO		1	4	36	35	95	1644	3.2	46 35 46	66 34 50
0645	+	CO		1	4	21	26	122	739	1.8	46 35 33	66 35 09
0646	+	CO	5.3	2	16	40	7	263	1250	2.1	46 35 30	66 35 08
0647	+	CO		3	20		38		7898	4.7	46 35 33	66 34 54
0648	•	CO		6	2	41	33	190	6796	2.8	46 35 49	66 34 37
0649	+	CO		8	28	33	44	186	4155	2.6	46 35 08	66 35 00
0650	+	CO		2	16	32	38	132	1886	2.6	46 34 43	66 34 51
0651	•	CO		2	16	26	32	120	989	2.4	46 34 35	66 34 59
0652	+	CO	6.7			26	20				46 34 35	66 34 45
0653	+	CO		2	20	24	32	114	1445	2.4	46 34 26	66 34 57
0654	+	CO		10	8	38	41	186	5967	4.9	46 34 57	66 34 00
0655	+	CO			8	24	32	154	4933	4.5	46 34 42	66 34 05
0656	•	CO		6	4	34	32	151	4933	3.8	46 34 33	66 34 13
0657	•	CO		4	8	26	23	71	867	2.6	46 34 36	66 34 07
0658	•	CO		4	2	22	23	115	3222	2.9	46 34 40	66 34 02
0659	•	CO		4	4	18	19	149	3026	3.8	46 34 52	66 33 47
0660	+	CO		1	2	25	36	71	3673	2.4	46 34 12	66 34 02
0661	+	CO		1	16	2	11	24	370	0.6	46 38 23	66 35 47
0662	•	CO		2	8	23	19	69	1710	2.7	46 38 10	66 36 00
0663	+	CO		2	12	5	8	48	590	1.1	46 38 09	66 35 51
0664	•	CO		4	8	9	16	64	2020	1.6	46 37 57	66 36 07
0665	+	CO		6	8	13	29	121	5670	1.9	46 37 11	66 36 42
0666	•	CO	2.2	4	12	16	40	143	4050	2.6	46 37 13	66 36 11
0667	+	CO		3	20	5	15	44	450	1.2	46 37 18	66 35 57
0668	•	CO		4	4	12	24	72	980	2.3	46 37 17	66 35 40
0669	+	CO		2	12	9	9	97	2780	2.3	46 37 07	66 35 12
0670	+	CO		2	12	3	12	37	440	1.0	46 36 36	66 35 18
0671	+	CO		2		13	12	97	2140	2.8	46 36 23	66 35 08
0672	+	CO		2	16	36	21	104	2100	2.8	46 36 09	66 35 12
0673	+	CO		6	8	23	20	88	1114	2.8	46 35 50	66 35 37
0674	+	CO		2	12	12	26	124	3295	1.9	46 35 43	66 35 17
0675	•	CO			8	16	16	67	2940	2.1	46 39 07	66 34 20
0676	•	CO	4.2	2	8	5	15	56	520	1.3	46 39 19	66 34 05
0677	+	CO			2	8	8	45	240	1.2	46 38 40	66 34 30
0678	+	CO	3.7		1	8	8	52	270	1.3	46 38 33	66 34 02
0679	+	CO		6	8	12	12	25	1230	3.2	46 38 21	66 34 40
0680	+	CO		4	4	13	13	213	1770	3.7	46 38 18	66 34 01
0681	+	CO		2	2	9	15	119	1860	3.0	46 35 20	66 32 32
0682	+	S		2	16	12	9	101	500	2.7	46 38 05	66 32 22
0683	+	S	3.5		8	8	9	92	870	2.6	46 38 08	66 32 00
0684	+	S			12	10	6	72	540	1.9	46 37 57	66 31 50
0685	+	S	3.0			9	9	82	1083	2.2	46 37 40	66 31 50
0686	•	S		2	4	9	6	7	1420	2.2	46 36 55	66 31 55
0687	+	S		1	8	2	3	47	1060	1.0	46 36 50	66 33 00
0688	+	S	4.2	3	4	15	15	111	3398	4.3	46 36 30	66 32 32
0689	+	S	3.8	2	4	9	9	92	1682	2.6	46 36 30	66 32 26
0690	•	S		4	4	10	15	106	2966	3.6	46 36 27	66 32 20
0691	+	S			4	8	9	74	1625	2.6	46 36 13	66 32 35
0692	+	CO		2	2	4	6	67	1340	1.7	46 36 20	66 33 31
0693	+	CO			2	14	9	77	950	2.7	46 36 10	66 33 30
0694	+	S	2.8		2	2	3	32	511	1.0	46 36 10	66 32 40
0695	+	S		2	2	8	9	82	1398	2.5	46 35 57	66 32 42
0696	+	S		2	28	7	3	74	841	2.2	46 35 37	66 32 55
0697	•	S			2	12	9	144	591	3.1	46 35 32	66 33 04
0698	+	S	2.9	2	24	19	13	104	1478	2.5	46 35 23	66 32 50
0699	•	S		2	16	17	14	71	3326	2.4	46 35 16	66 32 55
0700	+	S	4.2	2	12	13	11	71	1120	2.2	46 35 11	66 32 33
0701	•	S		4	4	19	27	104	3120	3.4	46 35 07	66 32 30
0702	•	S		4	6	15	19	99	3120	3.0	46 35 08	66 32 17
0703	+	S		2	40	16	16	73	1315	2.5	46 35 04	66 32 01
0704	+	S		2	2	28	31	110	1250	3.7	46 35 23	66 31 12

Appendix IV (cont.)

SN	ST	RU	U ppm	Mo ppm	W ppm	Cu ppm	Pb ppm	Zn ppm	Mn ppm	Fe %	LATITUDE ° ′ ″	LONGITUDE ° ′ ″
0705	+	S		2	2	30	34	115	1875	3.9	46 35 18	66 31 30
0706	+	S	4.3		4	26	24	90	1185	3.0	46 35 08	66 31 54
0707	+	S		4	2	26	24	82	984	3.1	46 34 57	66 31 17
0708	+	S		2	8	18	32	144	5096	3.0	46 34 54	66 31 42
0709	+	S		2	2	23	28	73	580	2.8	46 34 52	66 31 28
0710	+	S		2	2	43	30	64	1051	2.7	46 34 50	66 31 23
0711	+	S		4	24	17	19	90	1424	2.4	46 34 45	66 31 43
0712	+	S	6.7	4	12	43	45	82	890	3.1	46 34 42	66 31 39
0713	+	S		2	24	15	13	97	1116	2.4	46 34 24	66 32 04
0714	+	S		2	16	25	27	71	1148	2.3	46 34 22	66 32 00
0715	+	S		2	16	3	6	51	425	1.0	46 34 30	66 32 20
0716	+	S			1	11	6	29	202	0.8	46 34 23	66 32 27
0717	+	S		1	16	5	6	47	287	1.0	46 34 13	66 32 40
0718	+	S		2		18	19	75	1298	2.4	46 34 10	66 32 19
0719	+	S		1	12	9	11	111	950	2.3	46 38 31	66 30 21
0720	+	S	3.9		12	5	8	84	370	1.6	46 38 24	66 30 45
0721	*	S		20	16	9	30	233	10180	4.1	46 38 20	66 30 49
0722	+	S			2	4	16	48	301	1.3	46 36 35	66 30 30
0723	+	S		1	4	12	22	103	770	3.0	46 36 20	66 30 20
0724	+	S		1	24	11	25	96	1205	2.7	46 36 07	66 30 45
0725	+	S	3.0	2	1	14	25	99	1261	3.2	46 35 43	66 31 01
0726	+	S	2.3	2	16	5	3	39	254	1.6	46 35 10	66 30 09
0727	+	OG			4	2	3	28	110	0.4	46 33 55	66 59 46
0728	+	OG	4.5		2	2	3	18	110	0.3	46 33 48	66 59 17
0729	+	CO			2	4	3	33	160	0.6	46 33 53	66 58 52
0730	+	CO			2	4	12	40	1080	1.3	46 34 03	66 58 39
0731	+	CO			2	4	3	18	340	0.5	46 34 20	66 58 30
0732	+	CO	2.7		2	2	9	18	80	0.3	46 34 31	66 58 20
0733	+	CO	2.7		2	2	9	38	390	1.2	46 34 29	66 58 13
0734	+	CO				2	6	28	200	0.6	46 34 40	66 58 11
0735	+	OG		1	2	2	14	27	989	0.8	46 31 57	66 59 12
0736	+	OG		2	2	4	20	94	1795	1.6	46 31 55	66 59 05
0737	+	OG	5.0			3	17	41	1511	1.3	46 31 40	66 49 11
0738	+	OG	7.9	4	4	8	46	94	9784	4.0	46 31 31	66 58 05
0739	+	OG		4	4	5	49	92	6532	3.5	46 31 44	66 58 31
0740	*	OG		2	2	1	6	9	45	0.2	46 31 08	66 58 31
0741	*	OG		2	2	2	9	18	216	0.5	46 31 04	66 58 20
0742	*	OG		2	4	2	17	48	2625	1.8	46 31 19	66 57 44
0743	*	OG		4	2	5	49	45	7700	3.1	46 31 15	66 57 25
0744	+	OG		1	2	2	17	23	1860	1.0	46 30 41	66 57 40
0745	+	OG		2	2	2	29	18	2590	1.2	46 30 35	66 57 12
0746	+	CO		1	2	8	13	76	411	3.1	46 32 10	66 58 08
0747	+	CO		4	2	11	32	92	3155	3.3	46 31 59	66 57 48
0748	+	LG	5.6	2	2	12	23	94	1967	3.1	46 31 58	66 57 22
0749	+	OG		2	4	1	29	76	3344	2.6	46 32 20	66 57 50
0750	+	LG		1	2	6	14	68	644	1.8	46 32 12	66 57 27
0751	+	LG		2	4	3	20	71	211	1.1	46 32 11	66 57 03
0752	+	LG		1	4	5	17	73	755	1.5	46 32 08	66 56 50
0753	+	LG	3.9	4	2	2	46	190	1378	3.1	46 32 04	66 56 31
0754	+	CO		4	4	27	38	300	2767	3.1	46 32 58	66 56 52
0755	*	CO		6	2	48	41	241	3011	4.5	46 32 43	66 56 55
0756	+	CO		2	2	32	55	284	2044	3.5	46 32 48	66 56 43
0757	+	CO		2	2	34	35	328	2633	3.7	46 32 37	66 56 35
0758	+	LG		6	4	39	29	287	1789	3.6	46 32 25	66 56 30
0759	+	LG	3.7	2	3	34	41	287	1544	3.4	46 32 12	66 56 33
0760	+	LG		2	4	15	38	124	833	2.4	46 31 55	66 56 08
0761	+	LG			12	11	11	103	500	2.0	46 31 43	66 55 45
0762	*	LG			2	14	17	76	689	2.3	46 31 53	66 55 45
0763	*	LG		2	2	21	35	140	755	3.3	46 32 14	66 56 00
0764	*	LG		4	4	7	52	64	4033	4.2	46 31 19	66 55 40
0765	+	LG	4.1	2	4	14	14	94	800	2.3	46 31 27	66 55 29
0766	+	LG			10	2	3	41	609	1.2	46 30 50	66 55 55
0767	+	LG		20	8	4	24	64	1079	1.5	46 30 36	66 55 55
0768	+	LG	4.2		4	7	13	54	1244	1.8	46 30 11	66 55 10
0769	+	CO			8	17	35	122	3667	2.2	46 33 57	66 55 20
0770	*	CO		10	8	8	14	61	322	1.6	46 33 53	66 55 00
0771	+	CO			2	34	26	167	1467	2.7	46 33 28	66 55 25
0772	+	CO		2	2	27	29	198	2300	2.0	46 33 23	66 55 09
0773	+	CO		2	12	9	38	243	5567	3.2	46 33 13	66 54 50
0774	+	CO		1	2	17	26	95	1911	2.5	46 33 07	66 56 00
0775	+	CO			2	8	26	88	978	1.7	46 33 00	66 55 32
0776	+	CO			2	8	29	87	1489	1.8	46 32 57	66 55 12
0777	+	CO			2	16	17	124	500	2.6	46 32 53	66 54 49
0778	+	CO	3.4	1	2	29	41	167	967	2.9	46 31 57	66 54 33
0779	+	CO	3.1	2	2	13	38	80	1400	3.3	46 31 33	66 54 22
0780	+	CO		1	4	17	46	221	4055	3.2	46 33 02	66 54 33
0781	+	CO	2.8	2	8	14	35	464	11889	3.3	46 32 55	66 54 20
0782	+	CO	3.2	1		78	67	182	1344	3.2	46 32 50	66 54 22
0783	+	CO	3.0	3	4	12	26	83	611	1.9	46 33 40	66 54 40
0784	+	CO		2	12	9	17	86	422	2.1	46 33 15	66 54 10
0785	+	CO		2	8	12	35	88	444	2.5	46 32 57	66 53 49

SN	ST	RU	U ppm	Mo ppm	W ppm	Cu ppm	Pb ppm	Zn ppm	Mn ppm	Fe %	LATITUDE ° ′ ″	LONGITUDE ° ′ ″
0786	+	CO	3.2	3		10	46	88	889	2.3	46 32 37	66 53 23
0787	•	CO		1	2	4	17	34	89	1.4	46 32 42	66 53 19
0788	•	CO		2	8	16	44	173	2633	3.4	46 32 26	66 53 22
0789	+	CO	3.1	2	4	16	23	97	978	2.5	46 32 17	66 52 50
0790	+	CO	3.6	1	2	12	49	117	2764	3.0	46 31 35	66 53 39
0791	+	CO		2	16	15	26	133	3186	3.3	46 31 22	66 53 33
0792	+	CO			8	9	29	90	1660	2.4	46 31 23	66 53 30
0793	+	CO			2	8	20	153	8333	2.6	46 31 11	66 53 42
0794	+	CO			2	4	12	58	2420	1.4	46 31 04	66 54 00
0795	+	CO			2	10	35	95	1287	2.4	46 31 07	66 53 12
0796	+	CO			4	8	20	97	2250	2.9	46 30 59	66 53 01
0797	+	CO	6.7		6	10	20	121	990	2.5	46 31 01	66 53 00
0798	+	CO		2	2	13	26	231	9740	1.0	46 30 42	66 53 10
0799	+	CO			4	12	14	87	652	2.3	46 30 53	66 52 38
0800	+	CO		1	2	16	26	73	7234	2.5	46 30 37	66 52 25
0801	+	CO		1	2	13	15	170	759	4.8	46 30 42	66 52 18
0802	+	CO			2	10	15	80	665	2.0	46 30 49	66 52 18
0803	+	CO			4	19	60	218	1620	2.9	46 32 13	66 51 45
0804	+	CO			2	19	45	141	1218	2.3	46 32 04	66 51 43
0805	-	BG		20	80	11	23	68	967	1.5	46 34 15	66 53 49
0806	+	CO	13.1	30	40	24	23	97	895	2.0	46 34 02	66 53 39
0807	+	CO			28	10	37	61	895	0.3	46 33 49	66 53 20
0808	+	CO	11.1	6	12	11	17	63	139	1.1	46 33 39	66 52 20
0809	+	CO		8	56	4	9	32	689	0.7	46 34 26	66 51 38
0810	+	CO	7.7	20	28	5	15	57	1250	1.2	46 34 08	66 51 33
0811	+	CO		4	24	5	9	44	731	0.9	46 33 49	66 51 12
0812	+	CO		2	40	12	31	83	593	1.3	46 33 40	66 50 55
0813	+	CO	5.4	4	20	10	18	71	604	1.1	46 33 50	66 50 49
0814	+	CO		4	4	13	70	301	2732	2.7	46 33 11	66 50 48
0815	+	CO		2	4	11	44	197	1477	2.4	46 33 00	66 50 50
0816	+	CO	2.1	1	2	12	38	148	1392	2.4	46 33 13	66 50 18
0817	+	CO		1	8	10	32	126	1012	2.1	46 33 03	66 50 08
0818	+	CO			4	14	35	150	1181	2.5	46 32 51	66 49 58
0819	+	CO		2	4	6	30	80	919	2.3	46 32 52	66 49 42
0820	+	CO	3.1	1	4	6	27	58	694	2.4	46 32 39	66 49 45
0821	+	CO			2	6	15	63	513	2.1	46 32 20	66 49 58
0822	•	CO			2	3	9	25	118	0.9	46 32 28	66 50 00
0823	•	CO			2	14	21	51	897	2.4	46 32 16	66 49 40
0824	+	CO			2	25	33	112	4306	3.1	46 30 56	66 50 50
0825	+	CO			2	10	26	80	1060	2.3	46 31 00	66 50 12
0826	+	CO		1	2	10	23	126	6118	2.7	46 30 56	66 50 15
0827	+	CO		4	2	18	20	133	2190	4.4	46 30 50	66 49 59
0828	+	CO	5.9	4	4	22	23	211	4293	4.6	46 30 41	66 49 39
0829	+	CO		4	4	22	27	228	5620	4.7	46 30 35	66 49 20
0830	+	CO		6	4	69	26	498	18386	5.8	46 30 30	66 49 30
0831	+	CO		4	2	17	39	141	8970	2.7	46 31 18	66 49 39
0832	+	CO	8.0	3	2	39	27	286	15860	3.7	46 31 06	66 49 29
0833	+	CO		6	4	56	24	316	16800	5.3	46 31 00	66 49 15
0834	+	CO		2	8	5	25	68	1111	1.1	46 34 16	66 50 06
0835	+	CO	4.9	2	8	21	34	63	1083	1.8	46 34 05	66 49 49
0836	+	CO	6.1		100	15	42	147	3134	2.7	46 33 50	66 49 36
0837	•	CO		6		22	95	371	9658	4.0	46 33 46	66 49 20
0838	+	CO		8	12	14	60	262	11303	4.0	46 33 32	66 49 17
0839	+	CO		4	4	14	63	143	3184	3.4	46 33 17	66 49 10
0840	+	CO		10	4	16	71	291	13462	4.7	46 33 17	66 48 45
0841	+	CO		4	4	14	45	136	5791	2.7	46 33 10	66 48 29
0842	+	CO		8	8	10	30	194	9626	3.3	46 32 59	66 48 13
0843	+	CO		2	4	16	21	129	4872	3.2	46 32 43	66 48 20
0844	+	CO		4	2	16	39	116	9071	3.2	46 32 23	66 48 30
0845	+	CO		2	2	13	24	87	4476	2.6	46 32 09	66 48 42
0846	+	CO	4.3	2	4	22	54	80	1571	2.8	46 34 17	66 47 02
0847	+	CO	3.3		4	10	29	206	490	2.6	46 30 56	66 47 27
0848	•	CO		2	120	32	42	116	1100	2.6	46 34 17	66 46 58
0849	•	CO		1	20	31	57	114	2244	3.3	46 34 06	66 46 55
0850	+	CO	2.9		4	1	29	78	439	2.3	46 33 09	66 45 41
0851	•	CO		1	10	8	29	86	1624	2.5	46 32 20	66 45 52
0852	+	CO	7.1	20		36	80	488	10854	6.8	46 31 41	66 45 53
0853	+	CO			2	6	16	91	2280	2.5	46 31 08	66 46 00
0854	+	TG			20	25	16	140	2744	2.6	46 34 21	66 44 30
0855	•	TG			40	15	32	74	589	1.7	46 34 21	66 44 20
0856	+	TG		3	12	3	17	66	1606	1.5	46 33 11	66 43 21
0857	+	TG		15	8	10	33	85	3372	2.4	46 33 41	66 43 12
0858	+	TG			1	1	3	13	63	0.1	46 34 02	66 42 18
0859	+	TG		2	2	3	11	48	651	1.2	46 33 58	66 42 42
0860	+	TG	8.2		16	2	6	33	231	0.6	46 33 56	66 42 18
0861	+	TG		6	4	5	28	46	4244	1.6	46 33 50	66 42 18
0862	•	TG		100	24	15	13	267	15599	5.0	46 33 45	66 42 15
0863	+	TG		2	8	4	42	46	8602	1.4	46 33 33	66 42 22
0864	+	TG		8	8	4	66	90	10809	1.9	46 34 03	66 41 17
0866	+	TG		80	32	21	61	401	15861	4.8	46 33 59	66 41 10
0867	+	TG		40	8	35	92	252	14233	5.2	46 33 51	66 41 20

Appendix IV (cont.)

SN	ST	RU	U ppm	Mo ppm	W ppm	Cu ppm	Pb ppm	Zn ppm	Mn ppm	Fe %	LATITUDE ° ' "	LONGITUDE ° ' "
0868	+	CO		10	20	9	19	77	3298	1.9	46 34 05	66 40 30
0869	+	CO	9.0	4	24	6	11	85	746	1.4	46 33 59	66 40 06
0870	+	CO	4.6	6	24	25	19	186	2826	2.0	46 33 54	66 40 03
0871	+	CO		4	6	9	19	85	7763	3.0	46 33 40	66 40 20
0872	+	CO		10	56	25	36	153	2784	2.8	46 33 40	66 40 35
0873	+	CO		2	12	15	25	90	1996	2.3	46 33 46	66 40 37
0874	+	CO		3	8	12	28	79	4202	2.1	46 33 20	66 40 52
0875	+	CO		2	6	11	17	110	1408	1.9	46 34 00	66 39 41
0876	+	CO			12	2	3	28	462	0.5	46 34 10	66 39 26
0877	+	CO		4	12	21	20	86	544	1.4	46 33 35	66 39 11
0878	+	CO		4	8	36	24	131	1844	3.0	46 33 27	66 39 28
0879	+	CO		3	16	24	14	121	2468	1.5	46 32 49	66 40 41
0880	+	CO		1	40	6	8	83	1362	1.2	46 32 33	66 40 20
0881	+	CO		2	40	13	8	230	4532	1.5	46 32 21	66 40 00
0882	+	CO	2.8	4	20	12	14	121	1415	1.7	46 32 08	66 39 46
0883	+	CO	2.8	2	8	10	8	99	383	1.6	46 32 03	66 39 50
0884	+	CO		2		18	14	156	2681	1.6	46 32 03	66 40 12
0885	+	CO		4	4	8	17	116	2149	2.0	46 32 07	66 40 39
0886	+	CO		2		19	28	254	4000	1.9	46 32 19	66 41 10
0887	+	CO		1		19	28	235	2777	1.7	46 32 14	66 41 15
0888	+	CO		6	20	59	45	156	3755	2.4	46 32 13	66 41 48
0889	+	CO		20	8	38	41	209	4989	2.9	46 31 47	66 40 42
0890	+	CO			16	5	11	121	437	1.8	46 31 23	66 40 41
0891	+	CO		1	8	6	16	102	886	1.8	46 31 13	66 40 18
0892	+	S			16	4	14	97	986	2.6	46 31 10	66 40 00
0893	+	S		1	12	6	16	112	1166	2.2	46 31 08	66 39 40
0894	+	S	4.1	1	4	11	14	116	549	2.4	46 30 57	66 39 27
0895	+	S		1	16	9	14	177	1031	2.4	46 30 51	66 39 28
0896	+	CO		6	40	37	35	578	14002	2.7	46 31 48	66 42 38
0897	+	CO		2	16	30	36	239	12500	3.3	46 31 48	66 42 15
0898	+	CO		2	4	15	33	303	1723	3.0	46 31 50	66 42 09
0899	+	CO		1	1	2	16	27	546	0.6	46 31 48	66 42 00
0900	+	CO	2.6	1	8	16	19	136	2321	1.8	46 31 20	66 42 20
0901	+	CO		4		82	27	241	4506	2.9	46 31 17	66 42 27
0902	+	CO		2		33	35	165	3277	2.4	46 31 18	66 42 48
0903	+	CO				52	33	466	5094	2.4	46 31 07	66 42 12
0904	+	CO		6		30	46	265	5819	3.0	46 31 01	66 42 41
0905	+	CO		2	65	20	16	186	2205	1.7	46 30 54	66 42 22
0906	+	CO		2		37	33	388	4170	2.5	46 30 57	66 42 19
0907	+	CO	2.7		16	16	16	218	704	1.8	46 30 43	66 42 16
0908	+	CO			8	21	60	288	1817	2.1	46 30 40	66 42 20
0909	+	CO		2	20	28	101	385	5975	3.3	46 30 40	66 42 42
0910	+	CO	2.5	1	2	11	29	132	10854	3.6	46 31 32	66 45 30
0911	+	CO		2	2	5	52	77	680	2.6	46 32 18	66 44 36
0912	+	CO				4	43	51	640	1.7	46 32 13	66 44 40
0913	+	CO		2	4	6	28	49	950	1.5	46 32 01	66 44 40
0914	+	CO		2	4	8	21	42	400	1.6	46 31 45	66 44 29
0915	+	CO	3.2	4	8	9	26	12	1222	1.8	46 31 33	66 44 17
0916	+	CO		3	1	9	64	56	10778	3.9	46 32 11	66 43 39
0917	+	CO		30	80	22	88	182	701	3.0	46 31 50	66 43 53
0918	+	CO		6	12	34	38	196	5633	3.5	46 31 49	66 43 48
0919	+	CO		2		12	29	122	3511	2.6	46 31 45	66 43 53
0920	+	CO	4.1			30	41	279	11011	3.2	46 31 34	66 44 07
0921	+	CO		8	8	17	26	88	2578	2.7	46 31 17	66 44 07
0922	+	CO		20	2	23	125	133	3500	4.2	46 31 13	66 44 10
0923	+	CO		2	2	5	21	47	870	1.7	46 31 03	66 44 00
0924	+	CO		2	4	8	15	40	730	1.7	46 30 47	66 44 00
0925	+	CO		4	2	9	15	42	190	1.8	46 30 28	66 44 00
0926	+	CO	2.9	10	4	9	24	44	600	1.8	46 30 10	66 44 01
0927	+	CO		2	4	10	23	10	2844	1.9	46 34 04	66 38 55
0928	+	CO	4.2	2	12	9	23	88	2344	1.8	46 33 58	66 38 58
0929	+	CO		3	4	51	35	164	4855	3.1	46 33 40	66 39 05
0930	+	CO		30	24	37	44	189	2078	5.2	46 33 51	66 38 20
0931	+	CO		6	15	27	29	115	2778	3.4	46 33 43	66 38 17
0932	+	CO		30	12	76	41	203	4111	3.8	46 33 33	66 38 38
0933	+	CO		20	12	39	35	173	6167	3.3	46 33 48	66 38 00
0934	+	CO		10	8	22	26	104	2100	3.2	46 34 03	66 34 44
0935	+	CO		2	16	22	19	76	1786	2.2	46 33 36	66 37 00
0936	+	CO		4		79	35	110	6786	2.2	46 33 40	66 36 50
0937	+	CO		4	12	23	28	65	1021	2.5	46 33 12	66 38 07
0938	+	CO		3	12	22	28	96	1936	2.3	46 33 08	66 38 06
0939	+	CO		2	8	12	17	47	345	1.9	46 33 13	66 37 39
0940	+	CO		4	8	26	19	85	1046	2.1	46 33 11	66 37 27
0941	+	CO			16	8	17	112	506	2.7	46 33 15	66 37 06
0942	+	CO			4	3	14	33	226	1.2	46 33 10	66 37 07
0943	+	CO			8	16	22	98	1574	2.4	46 33 17	66 36 30
0944	+	S	4.2	6	4	13	11	96	596	2.4	46 33 06	66 36 27
0945	+	S		2	4	3	22	107	1585	3.2	46 33 11	66 36 10
0946	+	S		2	4	7	22	105	1181	3.2	46 33 10	66 35 33
0947	+	S		6	1	29	8	51	330	1.9	46 33 04	66 35 30
0948	+	CO		1	4	24	39	120	2383	3.2	46 33 13	66 35 41

Appendix IV (cont.)

SN	ST	RU	U ppm	Mo ppm	W ppm	Cu ppm	Pb ppm	Zn ppm	Mn ppm	Fe %	LATITUDE ° ' "	LONGITUDE ° ' "
0949	+	S		8	4	39	22	96	1500	3.3	46 33 39	66 35 11
0950	+	S	5.2	4	2	29	22	100	1117	3.5	46 33 30	66 34 53
0951	+	S		2	2	38	29	118	1477	3.6	46 33 36	66 34 32
0952	+	S	5.0	4	1	48	32	104	1443	3.8	46 33 47	66 34 22
0953	+	S	3.6	2		13	14	89	766	3.0	46 33 24	66 34 53
0954	+	S	3.8	1	4	21	20	85	789	2.5	46 33 30	66 33 40
0955	+	S		1	4	23	20	110	811	2.9	46 33 21	66 33 50
0956	+	S		1	8	28	26	121	1378	2.8	46 33 18	66 34 11
0957	+	S	4.1	1	16	25	20	101	733	2.5	46 32 52	66 35 09
0958	+	S			2	22	17	92	811	2.4	46 32 42	66 35 25
0959	+	S		2	8	26	23	121	121	2.9	46 32 41	66 35 45
0960	+	S		2	4	31	23	147	1522	3.3	46 32 40	66 36 12
0961	+	S	3.5	2	4	24	17	135	911	3.1	46 32 37	66 35 47
0962	+	S	3.5	2	4	29	23	149	1267	3.1	46 32 33	66 35 51
0963	+	S		2	4	23	30	173	1239	2.8	46 32 18	66 36 19
0964	+	S		3	1	30	28	175	1071	3.4	46 32 15	66 36 36
0965	+	S		3	1	29	28	136	1565	3.6	46 32 09	66 37 11
0966	+	S		4	4	40	47	149	4622	3.9	46 32 05	66 37 07
0967	+	S		2	4	26	25	184	1166	3.3	46 32 06	66 37 17
0968	+	CO		4	12	28	23	92	1655	2.8	46 32 49	66 38 33
0969	+	S		35		55	49	397	13689	4.2	46 32 31	66 38 16
0970	+	S	4.8	6		38	29	292	3299	5.2	46 32 12	66 38 05
0971	+	S		10	12	16	44	153	2789	3.3	46 32 20	66 38 36
0972	+	S		10	8	28	35	241	7422	4.8	46 32 10	66 38 13
0973	+	S		8	4	29	38	200	6533	3.9	46 32 00	66 39 00
0974	+	S		8	4	28	41	208	4733	2.8	46 31 59	66 38 35
0975	+	S	2.2			40	52	296	7144	4.2	46 32 02	66 38 00
0976	+	S		1	12	3	6	40	296	0.8	46 34 04	66 33 00
0977	+	S		2	2	9	14	134	3925	2.7	46 33 57	66 33 18
0978	+	S	4.2	2	8	7	11	100	2085	1.9	46 33 44	66 33 29
0979	*	S			4	8	17	67	1250	1.7	46 33 40	66 33 00
0980	*	S		5	20	5	5	21	300	0.8	46 34 03	66 32 20
0981	+	S		1	20	15	16	49	998	1.5	46 33 57	66 32 08
0982	+	S	5.7	1	20	24	19	61	998	2.0	46 33 51	66 31 21
0983	+	S		2	40	16	13	66	901	2.3	46 33 54	66 32 30
0984	+	S		4	12	19	24	75	1281	2.3	46 33 40	66 32 39
0985	*	S			8	36	40	75	1127	2.7	46 33 36	66 32 33
0986	+	S	4.3	7	4	18	48	75	1365	2.4	46 33 22	66 32 47
0987	*	S		3	4	55	61	141	3394	3.7	46 33 07	66 32 30
0988	*	S		1	4	19	28	94	1218	3.0	46 32 57	66 31 59
0989	+	S		2	4	41	71	81	978	3.2	46 32 59	66 32 51
0990	*	S			2	29	17	88	889	2.9	46 32 51	66 32 46
0991	+	S			1	32	20	77	778	3.0	46 32 42	66 32 41
0992	+	S		2	80	11	17	54	411	1.7	46 32 29	66 32 29
0993	+	S			2	47	27	85	1255	3.0	46 32 39	66 32 21
0994	+	S				55	46	95	522	2.3	46 32 26	66 32 13
0996	+	S	3.7		2	38	32	90	1169	2.7	46 32 16	66 32 05
0997	*	S		2	80	16	17	74	933	2.2	46 32 07	66 32 11
0998	+	S		2	2	54	35	92	1189	3.1	46 32 08	66 32 00
0999	+	S		1	1	30	35	94	3498	3.6	46 32 07	66 31 27
1000	+	S				29	53	120	6652	3.8	46 31 55	66 31 37
1001	+	S			1	29	24	113	2811	3.5	46 31 55	66 31 32
1002	+	S	3.0	1	4	20	16	90	1031	2.8	46 31 33	66 31 50
1003	+	S		1	4	17	19	93	1355	2.4	46 31 21	66 31 50
1004	+	S		1		21	19	109	1300	3.3	46 31 27	66 32 11
1005	+	S		2	4	16	22	80	1723	2.6	46 31 13	66 32 11
1006	+	S		1	4	23	19	109	1547	3.4	46 31 30	66 32 30
1007	*	S		2		30	33	165	2758	2.7	46 31 30	66 32 45
1008	+	S		2	8	33	27	93	1973	2.6	46 31 31	66 32 59
1009	+	S	2.8	2	4	21	19	96	1289	3.2	46 31 27	66 33 00
1010	+	S		1	4	27	27	108	1909	2.9	46 31 25	66 33 08
1012	+	S		1	4	23	19	114	1344	3.5	46 31 21	66 33 30
1013	+	S		1	4	23	19	87	1481	2.8	46 31 18	66 33 34
1014	*	S		1	4	24	27	102	1880	3.5	46 31 32	66 34 09
1015	+	S	3.1	2	4	23	22	114	1418	3.6	46 31 32	66 34 10
1016	+	S				20	19	114	1544	3.5	46 31 40	66 34 33
1017	+	S		3	2	19	35	123	2468	3.2	46 31 50	66 34 50
1018	+	S		2	6	22	22	112	1386	3.6	46 31 45	66 34 51
1019	*	S	3.9	1	4	19	36	116	3414	3.0	46 31 45	66 35 10
1020	+	S	2.5	1	4	47	30	87	1355	3.0	46 31 40	66 35 10
1021	+	S		6		18	41	182	4979	3.9	46 31 41	66 35 39
1022	+	S				7	19	81	840	2.4	46 31 43	66 35 55
1023	+	S			4	4	19	83	1670	1.5	46 31 45	66 36 30
1024	+	S			2	5	22	101	1166	1.9	46 31 42	66 36 58
1025	+	S		1	1	19	16	131	1795	2.8	46 31 25	66 35 49
1026	+	S		2	4	13	14	73	936	2.4	46 31 17	66 36 08
1027	+	S	3.2	1	1	15	14	86	837	2.4	46 31 18	66 36 40
1028	*	S		2	1	25	33	107	2962	3.1	46 31 13	66 36 38
1029	+	S		1	2	12	14	118	1266	3.0	46 31 14	66 37 03
1030	+	S			2	13	16	113	1498	2.8	46 31 03	66 37 23
1031	+	S	3.9	2	4	11	14	111	1112	3.2	46 30 56	66 38 07

Appendix IV (concl.)

SN	ST	RU	U ppm	Mo ppm	W ppm	Cu ppm	Pb ppm	Zn ppm	Mn ppm	Fe %	LATITUDE ° ' "	LONGITUDE ° ' "
1032	+	S		1	2	2	14	29	462	0.9	46 30 53	66 38 03
1033	+	S		1	6	8	14	116	2265	2.4	46 30 50	66 38 20
1034	+	S		1	4	6	14	114	1267	2.3	46 30 53	66 38 43
1035	+	S			4	9		24	975	2.2	46 30 55	66 39 00
1036	*	S		1	4	8	14	102	1110	2.3	46 31 00	66 39 00
1037	*	S			2	13	16	68	704	2.1	46 31 16	66 31 27
1038	+	S		1	4	40	33	114	1481	3.6	46 30 38	66 31 30
1039	+	S			2	56	36	112	1702	3.9	46 30 42	66 31 34
1040	+	S		1	4	41	30	116	1397	3.7	46 30 41	66 32 00
1041	+	S		1	4	58	36	110	1649	3.9	46 30 37	66 32 00
1042	+	S	3.0	1	4	33	33	116	1534	2.8	46 30 43	66 32 23
1043	+	S		2	2	34	30	104	1050	3.2	46 30 40	66 32 57
1044	+	S		1	4	33	38	121	1996	3.3	46 30 37	66 33 23
1045	*	S		1	4	52	38	89	1386	3.6	46 30 38	66 33 17
1046	*	S		2	4	42	60	184	6008	3.2	46 30 33	66 33 35
1047	*	S		1	4	19	41	144	3760	3.3	46 30 30	66 33 50
1048	+	S		1	4	22	38	131	2626	3.5	46 30 33	66 33 52
1049	+	S		1	4	15	22	129	1828	3.3	46 30 31	66 34 25
1050	*	S			1	18	25	116	1229	2.8	46 30 29	66 34 25
1051	*	S		1	4	22	46	144	3487	3.8	46 30 30	66 34 50
1052	+	S		2	4	21	35	150	2437	3.2	46 30 36	66 34 56
1053	+	S		1	1	29	24	106	1888	3.6	46 32 03	66 31 18
1054	+	S			1	22	19	85	1202	3.1	46 32 11	66 31 00
1055	+	S	2.0		4	38	24	111	1727	4.0	46 32 15	66 30 36
1056	+	S			1	37	27	101	1438	3.7	46 32 24	66 30 18
1057	+	S			2	37	41	113	2900	3.5	46 31 41	66 30 41
1058	+	S		1	2	43	33	109	1681	4.4	46 31 30	66 30 59
1059	+	S	2.7	1	1	43	28	103	1521	4.2	46 31 23	66 31 09
1060	+	S		2	4	38	47	112	4319	3.8	46 31 33	66 30 20
1061	+	S				39	30	105	2202	3.4	46 31 27	66 30 47
1062	+	S	4.1	2	4	47	31	129	1691	3.2	46 31 17	66 31 04
1063	+	S	2.7			57	36	97	2111	3.6	46 30 44	66 31 10
1064	*	S				37	30	95	1271	3.4	46 30 40	66 31 08
1065	*	S		1		48	50	116	3239	4.2	46 30 51	66 30 38
1066	*	S	4.1	1	12	43	27	95	1649	3.6	46 30 13	66 30 43

Appendix V

Contents of U, Sn, W, and Mo in soil samples, Otter Brook area, Burnthill Pluton*

Sample No.	Latitude °	'	"	Longitude °	'	"	U(ppm) Soil Horizon A	B	C	Sn(ppm) Soil Horizon A	B	C	W(ppm) Soil Horizon A	B	C	Mo(ppm) Soil Horizon A	B	C
OB-1	46	37	54	66	48	28	0.2	20.2	–	–	22	–	<1	4	–	0.7	4	–
OB-2	46	37	54	66	48	28	0.7	–	10.8	–	–	14	1	–	6	0.9	–	3
OB-3	46	37	55	66	48	28	0.5	–	16.0	–	–	19	<1	–	4	0.9	–	4
OB-4	46	37	56	66	48	28	2.2	–	21.3	–	–	23	3	–	4	0.5	–	5
OB-5	46	37	57	66	48	28	1.1	15.6	18.6	–	39	31	2	3	4	0.5	3	4
OB-6	46	37	57	66	48	28	1.3	–	12.7	–	–	14	1	–	6	1.3	–	–
OB-7	46	37	58	66	48	28	0.3	18.2	–	–	22	–	1	4	–	0.8	5	–
OB-8	46	37	59	66	48	28	0.9	–	21.8	–	–	23	1	–	6	1.0	–	5
OB-9	46	37	59	66	48	28	0.3	12.8	–	–	30	–	1	6	–	1.0	4	–
OB-10	46	38	00	66	48	28	0.7	9.9	–	–	13	–	1	6	–	6.5	5	–
OB-11	46	38	01	66	48	28	102.7	–	19.5	–	–	16	3	–	8	3.9	–	3
OB-12	46	38	01	66	48	28	26.9	–	17.6	–	–	17	5	–	6	2.6	–	3
OB-13	46	38	01	66	48	28	5.3	–	15.7	–	–	21	2	–	8	1.0	–	3
OB-14	46	38	02	66	48	28	4.6	13.9	–	–	15	–	3	6	–	<0.5	2	–
OB-15	46	38	03	66	48	28	0.6	18.3	18.7	–	28	20	<1	6	4	1.1	4	4
OB-16	46	38	03	66	48	28	0.6	–	20.9	–	–	31	<1	–	8	0.6	–	5
OB-17	46	38	04	66	48	28	1.4	21.8	–	–	24	–	1	6	–	0.8	5	–
OB-18	46	38	04	66	48	28	5.3	28.8	–	–	27	–	1	10	–	1.7	4	–
OB-19	46	38	05	66	48	28	0.4	20.4	–	–	19	–	1	4	–	0.8	4	–
OB-20	46	38	05	66	48	28	0.2	13.1	13.6	–	17	14	<1	4	4	<0.5	3	3
OB-21	46	38	06	66	48	28	80.9	–	16.9	–	–	20	3	–	4	1.9	–	3
OB-22	46	38	06	66	48	28	0.4	19.0	23.5	–	22	23	1	6	4	1.1	4	4
OB-23	46	38	06	66	48	28	0.2	16.8	–	–	32	–	1	4	–	0.7	3	–
OB-24	46	38	07	66	48	28	0.7	12.1	–	–	29	–	1	4	–	1.0	3	–
OB-25	46	38	07	66	48	28	0.2	13.0	12.6	–	12	15	<1	ND@	4	1.0	4	3
OB-26	46	38	08	66	48	28	0.4	11.9	16.3	–	19	23	1	2	2	0.7	3	2
OB-27	46	38	09	66	48	28	0.4	12.9	15.4	–	14	15	1	2	2	0.8	2	2
OB-28	46	38	10	66	48	28	0.3	16.3	18.9	–	27	34	1	4	4	0.6	3	2
OB-29	46	38	10	66	48	28	0.5	13.1	10.5	–	16	12	1	4	4	0.8	1	3
OB-30	46	38	11	66	48	28	0.5	10.6	22.1	–	22	18	1	6	4	0.6	2	2
OB-31	46	38	12	66	48	28	0.6	9.9	14.0	–	28	17	<1	4	4	0.5	1	1
OB-32	46	38	13	66	48	28	0.6	7.8	16.4	–	19	19	1	3	4	<0.5	3	1
OB-33	46	38	13	66	48	28	1.4	14.5	11.8	–	21	19	1	2	2	0.5	3	2

*Data obtained from Westmin Resources Ltd. (Hattie, 1981).
@ND = not detected.

Appendix VI

Chemical analyses and locations of till samples overlying the granitic plutons of central Miramichi Anticlinorium area (Lamothe, 1989).

A. Clay fraction (<2 μm)

Sample* No.	As (ppm)	Co (ppm)	Cr (ppm)	Cu (ppm)	F (ppm)	Fe (%)	Mn (ppm)	Mo (ppm)	Ni (ppm)	Pb (ppm)	Sn (ppm)	U (ppm)	W (ppm)	Zn (ppm)
BH-86LFA 24701	21	19	74	39	968	5.0	840	2	87	36	7	2.3	3	148
BH-86LFA 30001	11	17	46	17	1175	3.6	490	1	36	42	13	11.2	6	105
BH-86LFA 30101	11	16	40	14	740	3.7	500	1	29	50	11	18.4	4	108
BH-86LFA 30201	10	13	40	34	1000	3.7	760	1	36	59	32	18	16	165
BH-86LFA 30301	11	20	60	30	1225	4.5	800	1	48	27	16	7.9	6	109
BH-86LFA 30401	18	12	80	24	740	3.2	230	2	40	42	11	20.0	4	97
BH-86LFA 50801	15	15	40	24	640	3.2	580	1	31	53	26	17.6	18	96
BH-86LFA 50901	13	11	42	24	540	3.4	590	1	36	58	38	17.6	14	148
BH-86LFA 51001	9	16	46	21	920	3.3	760	1	35	42	24	19.6	14	120
D-85LFA 17201	16	18	68	38	1040	6.0	1000	3	38	51	33	17.2	8	158
D-86LFA 21001	20	9	26	12	1050	2.2	310	2	22	23	3	1.5	4	28
D-85LFA 21901	15	21	73	44	1040	5.4	1040	3	47	38	24	17.5	6	130
D-85LFA 22001	8	20	84	38	700	5.6	800	2	52	28	17	3.8	4	120
D-86LFA 29101	8	24	72	43	900	3.8	780	1	55	29	15	9.9	14	119
D-86LFA 29201	40	21	64	42	940	4.4	720	1	57	32	12	10.4	6	107
D-86LFA 29301	40	28	70	68	940	4.8	820	2	53	55	26	18.0	20	154
D-86LFA 33001	68	24	66	42	980	3.4	1600	8	47	55	47	29.0	10	73
D-86LFA 33101	49	26	78	79	940	4.7	970	4	56	54	14	11.4	24	174
D-86LFA 33201	17	20	56	29	1100	3.9	1700	4	33	53	48	31.0	50	139
D-86LFA 33301	35	27	92	89	1375	4.3	950	4	51	71	16	17.5	10	106
D-86LFA 33401	68	34	78	80	1225	4.5	830	14	83	48	15	37.0	10	152
D-86LFA 33501	15	28	74	53	1100	4.2	910	4.0	51	36	17	17.2	6	109
D-86LFA 33601	8	25	74	33	800	4.0	710	4.0	45	31	20	7.4	8	94
D-86LFA 33701	23	25	72	42	900	4.0	610	4	47	41	20	17.6	14	121
D-86LFA 33801	9	22	74	38	830	4.3	440	3	51	32	11	6.9	24	114
D-86LFA 33901	6	17	72	28	830	3.7	670	2	44	41	15	5.2	4	94
D-86LFA 35701	60	27	58	104	1050	4.4	700	7	72	53	29	14.3	20	187
D-86LFA 41210	75	39	88	87	830	5.0	1000	7	103	38	22	15.4	16	127
D-86LFA 41301	79	25	52	80	830	4.3	720	6	60	51	32	27.0	16	95
D-86LFA 41401	80	19	64	45	530	4.0	480	6	37	45	29	12.6	16	99
D-86LFA 41501	104	41	94	66	1100	5.0	1200	62	122	54	38	12.6	16	136
D-86LFA 41601	91	33	82	76	700	3.3	950	12	52	36	27	35.0	24	85
D-86LFA 41701	60	24	76	48	90	3.9	820	4	57	42	34	15.2	24	138
D-86LFA 41801	128	21	52	79	1300	5.0	1800	2	59	34	37	25.0	24	141
D-86LFA 41901	72	15	72	44	740	4.6	600	6	52	51	41	16.4	12	178
D-86LFA 42001	72	18	56	34	1300	4.0	1100	8	35	49	300	41.0	80	104
D-86LFA 42101	21	14	44	34	940	4.0	650	4	35	43	40	14.4	24	164
D-86LFA 42401	42	17	104	45	390	4.7	530	4	52	50	14	3.1	8	118
D-86LFA 42501	150	33	70	106	980	4.1	1700	5	86	39	41	21.0	32	124
D-86LFA 42601	51	26	70	60	600	4.0	1000	6	51	43	37	19.0	24	101
D-86LFA 42701	116	6	58	25	450	4.2	360	6	20	36	30	13.0	100	66
D-86LFA 44301	21	18	70	33	620	4.1	340	3	46	30	11	6.5	8	99
D-86LFA 44401	11	17	66	33	1150	4.2	920	2	41	38	39	27.0	12	117
D-86LFA 44501	9	14	58	20	740	4.3	410	2	35	44	31	9.1	8	120
D-86LFA 44601	8	13	38	22	1050	3.4	980	2	25	50	66	36.0	24	122
D-86LFA 44701	7	20	54	35	920	4.1	800	1	37	44	31	22.0	6	122
D-86LFA 44801	7	18	78	26	1050	5.0	830	0	54	35	19	13.0	6	134
D-86LFA 44901	29	18	52	31	1275	4.0	780	1	36	40	31	20.0	18	118
D-86LFA 45001	11	19	68	30	700	2.9	800	1	32	24	17	10.0	4	81
D-86LFA 45101	7	9	56	12	280	3.8	260	1	21	31	16	6.4	1	57
D-86LFA 45201	8	17	58	17	670	4.2	760	1	36	35	25	8.4	6	107
D-86LFA 45301	7	16	60	34	890	4.2	900	0	39	40	29	18.4	6	128
D-86LFA 45401	9	5	36	10	361	2.3	310	2	11	29	19	18.4	8	63
D-86LFA 60702	110	39	60	157	1325	4.2	2000	3	73	28	42	21.0	30	147
TB-85LFA 13001	44	23	62	47	950	5.0	1000	3	54	39	12	7.8	12	150
TB-86LFA 22001	62	13	64	30	660	4.4	520	0	54	45	13	5.2	2	146
TB-86LFA 22101	39	17	54	42	820	3.8	920	2	53	66	20	13.2	8	152
TB-86LFA 22201	9	27	46	22	820	3.7	860	0	45	43	10	0.9	2	86
TB-86LFA 22301	196	15	59	113	853	3.8	803	3	48	84	21	14.0	9	323
TB-86LFA 22401	133	14	55	33	1175	3.4	630	4	49	72	15	8.1	9	130
TB-86LFA 22501	65	16	54	35	850	4.0	605	3	58	43	14	5.7	5	150

A. Clay fraction (<2 µm) – continued

Sample* No.	As (ppm)	Co (ppm)	Cr (ppm)	Cu (ppm)	F (ppm)	Fe (%)	Mn (ppm)	Mo (ppm)	Ni (ppm)	Pb (ppm)	Sn (ppm)	U (ppm)	W (ppm)	Zn (ppm)
TB-86LFA 22601	125	18	72	49	960	4.3	630	2	75	62	20	6.6	13	200
TB-86LFA 23701	56	22	76	74	538	5.2	870	1	73	22	4	1.5	2	120
TB-86LFA 26301	100	16	54	34	850	3.9	940	2	52	65	31	19.2	8	273
TB-86LFA 26302	175	17	56	74	1250	3.9	1000	3	48	90	37	35.0	14	420
TB-86LFA 26401	234	19	70	44	1000	4.3	1000	3	56	76	20	17.9	16	177
TB-86LFA 26501	131	17	68	58	1075	4.0	860	2	64	76	22	10.7	12	197
TB-86LFA 26601	213	16	76	68	1900	4.2	1400	5	50	56	45	90.0	14	660
TB-86LFA 26801	110	25	80	55	1000	4.1	820	2	79	41	14	4.2	14	130
TB-86LFA 26901	49	19	78	55	1250	5.2	920	1	78	31	10	2.2	6	143
TB-86LFA 27001	253	21	76	44	1250	4.1	600	3	77	42	17	5.7	12	328
TB-86LFA 27301	79	10	56	34	930	4.0	390	5	40	72	13	17.5	24	114
TB-86LFA 35101	53	25	76	2	0	5.5	920	2	64	37	2	2.2	7	153
TB-86LFA 35201	93	21	66	42	850	4.4	720	4	50	58	9	15.0	18	161
TB-86LFA 36201	22	5	94	44	155	3.9	230	7	22	19	3	6.5	4	34
TB-86LFA 36301	156	19	68	67	145	4.5	680	4	59	65	35	12.2	18	212
TB-86LFA 36401	23	6	30	13	380	4.5	390	5	13	44	16	7.5	8	90

*BH – Burnthill Pluton
D – Dungarvon Pluton
TB – Trout Brook Pluton

Appendix VI (cont.)

B. Clay plus silt fraction (<63mm)

Sample No.	As (ppm)	An (ppb)	Co (ppm)	Cr (ppm)	Fe (%)	Mo (ppm)	Ni (ppm)	Sb (ppm)	Th (ppm)	U (ppm)	W (ppm)	Zn (ppm)
BH-86LFA 24701	8.4	4	12	123	3.9	2	48	0.6	15.1	3.8	3	75
BH-86LFA 30001	0.6	3	10	130	3.7	2	32	0	16.0	4.9	0	50
BH-86LFA 30101	1.0	1	8	82	2.9	2	23	0	22.4	5.0	0	50
BH-86LFA 30201	2.3	3	13	110	3.9	3	44	0.2	16.0	3.8	0	50
BH-86LFA 30301	0.6	4	7	70	2.2	0	10	0	22.3	5.6	0	50
BH-86LFA 30401	0.8	5	6	65	2.0	1	10	0	29.6	6.9	0	50
BH-86LFA 50801	45.0	4	17	140	4.4	3	61	2.7	11.0	3.2	0	160
BH-86LFA 50901	6.3	1	2	10	2.0	13	10	0.4	61.5	21.2	10	120
BH-86LFA 51001	3.7	1	7	10	2.6	17	27	0.4	49.6	15.0	7	50
D-86LFA 21001	6.0	1	9	31	2.9	2	10	0.3	66.6	16.0	8	170
D-85LFA 22001	7.5	2	15	115	4.3	1	47	3.3	19.0	5.1	3	100
D-86LFA 29101	1.7	4	10	90	3.2	1	22	0.2	14.0	3.6	0	50
D-86LFA 29201	2.3	4	9	84	2.9	2	10	0.2	14.0	3.8	1	50
D-86LFA 29301	2.2	5	5	49	2.5	0	10	0.1	13.0	3.5	1	50
D-86LFA 33001	1.2	4	6	64	2.3	2	10	0	19.0	3.9	0	50
D-86LFA 33101	0.7	1	6	53	2.1	2	10	0	17.0	4.0	0	50
D-86LFA 33201	1.6	3	11	89	3.2	1	26	0.1	10.0	2.6	0	50
D-86LFA 33301	1.7	1	12	72	3.6	0	22	0	10.0	3.0	0	50
D-86LFA 33401	3.6	3	5	59	2.8	0	10	0.1	20.0	5.0	0	50
D-86LFA 33501	2.1	1	8	78	2.9	2	10	0	17.0	5.4	1	50
D-86LFA 33601	0.5	3	7	62	2.6	2	10	0	20.0	4.1	0	50
D-86LFA 33701	0.7	4	7	69	2.7	0	10	0	21.2	4.4	0	50
D-86LFA 33801	1.3	4	8	76	2.8	0	10	0.1	13.0	3.1	0	50
D-86LFA 33901	0.6	1	6	53	2.0	1	10	0	17.0	4.4	0	50
D-86LFA 35701	40.0	1	24	83	4.7	4	43	0.9	45.5	16.0	14	50
D-86LFA 41210	23.0	1	14	110	4.9	3	24	2.5	12.0	3.8	2	190
D-86LFA 41301	25.0	5	15	79	4.6	3	24	2.1	12.0	3.4	2	140
D-86LFA 41401	29.0	3	19	97	5.7	4	31	2.5	14.0	4.0	2	160
D-86LFA 41501	28.0	1	16	94	4.7	3	40	2.1	14.0	3.9	3	170
D-86LFA 41601	33.0	3	31	120	4.7	3	81	3.1	12.0	3.8	2	100
D-86LFA 41701	40.0	1	18	130	4.5	3	66	4.2	12.0	3.2	3	140
D-86LFA 41801	44.0	4	9	74	3.8	4	27	2.9	15.0	3.8	3	190
D-86LFA 41901	35.0	6	14	100	5.1	4	35	4.0	15.0	4.2	3	50
D-86LFA 42001	35.0	1	16	110	5.4	2	40	1.9	11.0	3.0	3	150
D-86LFA 42101	25.0	5	18	96	5.2	3	35	2.1	11.0	3.1	3	140
D-86LFA 42401	43.0	1	16	88	5.1	2	38	3.1	14.0	3.7	4	50
D-86LFA 42501	20.0	3	16	120	4.4	2	45	1.4	12.0	2.6	2	150
D-86LFA 42601	19.0	3	15	120	4.0	2	30	1.3	11.0	2.7	1	120
D-86LFA 42701	23.0	1	17	140	5.1	2	55	1.5	12.0	2.8	2	170
D-86LFA 44301	20.0	7	11	120	4.1	2	40	1.2	15.0	3.7	1	120
D-86LFA 44401	16.0	1	14	140	4.1	2	37	1.0	13.0	3.6	1	160
D-86LFA 44501	48.0	1	21	140	5.0	3	65	2.9	12.0	3.6	3	150
D-86LFA 44601	24.0	6	23	140	5.1	4	52	3.6	12.0	3.5	2	230
D-86LFA 44701	57.7	24	19	140	5.1	3	58	6.8	12.0	3.8	2	170
D-86LFA 44801	24.0	3	20	130	4.5	2	54	3.5	11.0	3.3	2	130
D-86LFA 44901	55.6	4	19	140	4.6	3	51	2.1	13.0	3.6	3	150
D-86LFA 45001	81.9	1	17	120	4.9	4	49	2.5	12.0	4.4	3	190
D-86LFA 45101	105.0	6	20	120	5.4	4	70	2.9	13.0	4.9	4	210
D-86LFA 45201	47.0	1	13	120	4.4	2	57	2.3	12.0	3.1	3	200
D-86LFA 45301	15.0	1	12	110	3.8	2	33	1.2	11.0	2.7	2	120
D-86LFA 45401	23.0	1	11	120	3.8	3	40	1.5	12.0	3.4	2	140
D-86LFA 60702	50.3	6	33	67	4.1	5	33	0.9	49.2	17.0	17	130
TB-85LFA 13001	12.0	2	11	80	3.0	3	25	0.6	27.0	7.3	6	100
TB-86LFA 22001	18.5	2	14	110	3.9	1	50	1.2	15.1	4.2	4	140
TB-86LFA 22101	21.5	2	9	83	3.4	4	28	4.6	21.1	7.2	5	165
TB-86LFA 22201	15.0	2	16	108	4.1	2	32	1.1	19.1	5.6	4	115
TB-86LFA 22301	65.0	2	11	101	3.6	3	18	0.8	21.2	8.7	8	250
TB-86LFA 22401	104.2	2	10	102	3.3	2	30	2.0	20.1	6.7	7	105
TB-86LFA 22501	25.5	3	7	103	3.4	2	28	0.9	21.6	6.2	6	135
TB-86LFA 22601	106.0	2	14	114	4.4	2	60	0.7	18.6	6.6	10	205
TB-86LFA 23701	35.3	5	20	75	5.0	2	45	3.0	12.7	3.1	3	75
TB-86LFA 26301	3.0	6	10	87	3.6	2	10	0.1	12.0	3.5	0	50
TB-86LFA 26302	6.6	5	7	62	2.9	2	10	0.2	14.0	3.3	0	50

B. Clay plus silt fraction (<63mm) – continued

Sample No.	As (ppm)	An (ppb)	Co (ppm)	Cr (ppm)	Fe (%)	Mo (ppm)	Ni (ppm)	Sb (ppm)	Th (ppm)	U (ppm)	W (ppm)	Zn (ppm)
TB-86LFA 26401	1.6	24	2	56	1.6	2	10	0	19.0	5.2	1	50
TB-86LFA 26501	1.1	1	2	69	1.8	0	10	0.2	20.0	3.7	0	50
TB-86LFA 26601	0.8	7	9	77	2.6	3	30	0.2	13.0	4.0	0	50
TB-86LFA 26801	1.3	48	7	75	2.3	2	10	0.1	20.8	5.2	0	50
TB-86LFA 26901	1.0	8	6	79	2.1	2	10	0	18.0	4.5	0	50
TB-86LFA 27001	8.8	7	13	110	3.6	1	27	0.2	12.0	3.9	1	110
TB-86LFA 27301	15.0	8	15	110	4.4	2	32	0.2	14.0	3.8	1	50
TB-86LFA 35101	33.0	1	19	91	4.4	1.0	21	1.2	19.0	4.2	7	50
TB-86LFA 35201	41.0	1	18	71	3.7	1.0	26	0.9	28.5	12.0	7	50
TB-86LFA 36201	33.0	1	17	160	6.0	6	42	0.5	17.0	6.1	10	50
TB-86LFA 36301	88.5	1	11	95	4.9	2	34	1.1	34.2	13.0	17	50
TB-86LFA 36401	16.0	1	7	73	3.5	4	10	0.5	36.5	11.0	12	50

C. Till samples location

Sample No.	Latitude °	′	″	Longitude °	′	″	Sample No.	Latitude °	′	″	Longitude °	′	″
BH-86LFA 24701	46	36	43	66	55	20	D-86LFA 42701	46	40	15	66	33	55
BH-86LFA 30001	46	41	26	66	48	40	D-86LFA 44301	46	42	21	66	32	17
BH-86LFA 30101	46	42	32	66	49	57	D-86LFA 44401	46	42	35	66	33	10
BH-86LFA 30201	46	37	55	66	50	30	D-86LFA 44501	46	42	55	66	33	56
BH-86LFA 30301	46	39	54	66	51	55	D-86LFA 44601	46	42	45	66	34	47
BH-86LFA 30401	46	42	03	66	51	47	D-86LFA 44701	46	43	20	66	35	11
BH-86LFA 50801	46	39	11	66	45	31	D-86LFA 44801	46	43	50	66	35	09
BH-86LFA 50901	46	39	21	66	45	47	D-86LFA 44901	46	41	30	66	35	22
BH-86LFA 51001	46	39	47	66	45	48	D-86LFA 45001	46	44	49	66	35	20
D-85LFA 17201	46	41	48	66	34	25	D-86LFA 45101	46	44	22	66	35	00
D-86LFA 21001	46	42	49	66	32	32	D-86LFA 45201	46	43	37	66	36	05
D-85LFA 21901	46	42	33	66	37	30	D-86LFA 45301	46	43	50	66	36	15
D-85LFA 22001	46	44	02	66	38	47	D-86FA 45401	46	41	39	66	33	30
D-86LFA 29101	46	44	07	66	40	53	D-86FA 60702	46	40	00	66	34	38
D-86LFA 29201	46	42	08	66	38	10	TB-85LFA 13001	46	33	30	66	42	02
D-86LFA 29301	46	41	00	66	36	25	TB-86LFA 22001	46	33	43	66	43	36
D-86LFA 33001	46	40	30	66	36	10	TB-86LFA 22101	46	34	23	66	43	20
D-86LFA 33101	46	41	09	66	36	50	TB-86LFA 22201	46	34	07	66	41	06
D-86LFA 33201	46	41	30	66	37	30	TB-86LFA 22301	46	34	22	66	40	03
D-86LFA 33301	46	41	30	66	38	09	TB-86LFA 22401	46	34	52	66	40	40
D-86LFA 33401	46	40	55	66	37	41	TB-86LFA 22501	46	34	55	66	38	58
D-86LFA 33501	46	43	23	66	39	30	TB-86LFA 22601	46	35	26	66	39	11
D-86LFA 33601	46	43	42	66	40	05	TB-86LFA 23701	46	36	12	66	39	08
D-86LFA 33701	46	42	57	66	38	15	TB-86LFA 26301	46	35	16	66	37	39
D-86LFA 33801	46	43	42	66	38	42	TB-86LFA 26302	46	35	16	66	37	39
D-86LFA 33901	46	44	40	66	38	52	TB-86LFA 26301	46	35	16	66	37	39
D-86LFA 35701	46	39	20	66	36	10	TB-86LFA 26302	46	35	16	66	37	39
D-86LFA 41210	46	40	00	66	36	35	TB-86LFA 26401	46	34	43	66	40	42
D-86LFA 41301	46	39	05	66	37	19	TB-86LFA 26501	46	34	39	66	39	27
D-86LFA 41401	46	39	01	66	37	05	TB-86LFA 26601	46	35	25	66	38	02
D-86LFA 41501	46	39	50	66	36	50	TB-86LFA 26801	46	34	20	66	43	43
D-86LFA 41601	46	39	53	66	36	30	TB-86LFA 26901	46	33	23	66	43	21
D-86LFA 41701	46	39	50	66	35	05	TB-86LFA 27001	46	34	13	66	40	52
D-86LFA 41801	46	40	03	66	34	20	TB-86LFA 27301	46	34	49	66	40	15
D-86LFA 41901	46	40	34	66	35	18	TB-86LFA 35101	46	33	40	66	44	45
D-86LFA 42001	46	40	41	66	34	29	TB-86LFA 35201	46	34	02	66	44	05
D-86LFA 42101	46	41	18	66	34	04	TB-86LFA 36201	46	35	21	66	40	40
D-86LFA 42401	46	42	49	66	32	30	TB-86LFA 36301	46	35	10	66	40	30
D-86LFA 42501	46	39	52	66	34	12	TB-86LFA 36401	46	34	31	66	41	38
D-86LFA 42601	46	40	20	66	34	27							

Appendix VII

Locations and in situ determinations of uranium, thorium, and potassium contents of the granitic rocks of Burnthill (BH), Dungarvon (D), Trout Brook (TB), and Rocky Brook (RB) plutons.

Sample No.	Latitude °	'	"	Longitude °	'	"	eU (ppm)	eTh (ppm)	K (%)	ROCK DESCRIPTION
BH-1A	46	40	39	66	47	13	9.7	31.5	5.0	Pink, coarse grained, porphyritic granite.
BH-1B	46	40	41	66	47	15	10.2	23.0	4.6	Pink, coarse grained, porphyritic granite (slightly weathered).
BH-1C	46	40	43	66	47	11	3.6	8.4	3.0	Pink, coarse grained, porphyritic granite (slightly weathered).
BH-2	46	40	37	66	48	15	2.4	7.0	1.2	Mafic dyke intrudes coarse grained, porphyritic granite.
BH-3A	46	40	12	66	47	14	15.5	41.4	6.0	Pink, coarse grained, porphyritic biotite granite (moderately weathered).
BH-3B	46	40	11	66	47	12	15.5	38.5	5.8	Pink, coarse grained, porphyritic, biotite granite with alkali-feldspar phenocrysts (moderately weathered).
BH-3C	46	40	13	66	47	13	14.4	47.7	5.7	Pink, coarse grained, porphyritic, biotite granite with alkali-feldspar phenocrysts (slightly weathered).
BH-4A	46	40	13	66	47	55	11.8	31.3	4.9	Coarse grained, porphyritic, biotite granite (partially limonitized).
BH-4B	46	40	12	66	47	56	10.8	30.0	4.8	Coarse grained, porphyritic, biotite granite (limonitized).
BH-5A	46	40	13	66	48	13	16.3	40.3	5.8	Coarse grained, porphyritic, biotite granite, with alkali-feldspar phenocrysts.
BH-5B	46	40	15	66	48	11	15.9	40.9	5.7	Coarse grained, porphyritic, biotite granite, with alkali-feldspar phenocrysts.
BH-5C	46	40	14	66	48	15	15.9	35.2	5.8	Coarse grained, porphyritic, biotite granite, with alkali-feldspar phenocrysts.
BH-6A	46	40	13	66	48	13	13.6	35.5	5.9	Pink, coarse grained, porphyritic, biotite granite (strongly weathered).
BH-6B	46	40	12	66	48	11	13.0	35.5	5.3	Pink, seriate biotite granite (strongly limonitized).
BH-7	46	40	13	66	48	28	14.5	39.0	5.9	Pink, seriate biotite granite (strongly fractured and weathered).
BH-8	46	40	13	66	48	56	13.9	38.1	5.6	Pink, coarse grained, porphyritic biotite granite, with alkali-feldspar phenocrysts.
BH-9A	46	40	14	66	49	11	13.6	40.5	5.3	Pink, coarse grained, porphyritic biotite granite.
BH-9B	46	40	13	66	49	13	31.2	94.1	7.1	Biotite-enriched pod (30 cm in diameter) embedded in coarse grained, porphyritic granite.
BH-10	46	40	12	66	49	15	25.4	31.6	6.6	Red, porphyritic biotite granite with alkali-feldspar phenocrysts.
BH-11A	46	40	09	66	49	16	25.1	31.8	6.6	Red, fine grained, porphyritic biotite granite.
BH-11B	46	40	10	66	49	14	16.9	30.3	5.7	Red, fine grained, porphyritic biotite granite.
BH-12A	46	40	30	66	49	45	25.0	64.9	7.6	Red to pink, fine grained, porphyritic biotite granite with quartz and alkali-feldspar phenocrysts.
BH-12B	46	40	28	66	49	43	29.2	75.1	7.8	Pink, fine grained, porphyritic biotite granite with quartz and alkali-feldspar phenocrysts.
BH-13A	46	42	15	66	48	28	10.0	27.7	5.0	Coarse grained, porphyritic granite with alkali-feldspar phenocrysts.
BH-13B	46	42	13	66	48	30	8.2	24.0	4.8	Pink, coarse grained, porphyritic granite with alkali-feldspar phenocrysts (moderately weathered).
BH-13C	46	42	14	66	48	29	8.6	25.5	5.9	Pink, coarse grained, porphyritic granite.
BH-13D	46	42	16	66	48	30	9.3	29.2	5.7	Aplite dyke crosscutting coarse grained, porphyritic granite.
BH-14A	46	42	12	66	48	28	11.9	36.7	6.1	Pink, coarse grained, biotite granite exhibits rapakivi texture.
BH-14B	46	42	11	66	48	30	12.1	36.2	5.8	Pink, coarse grained, biotite granite exhibits rapakivi texture.
BH-15	46	42	09	66	48	29	16.9	31.9	6.1	Pink, fine grained granite with quartz phenocrysts.

Appendix VII (cont.)

Sample No.	Latitude °	'	"	Longitude °	'	"	eU (ppm)	eTh (ppm)	K (%)	ROCK DESCRIPTION
BH-16A	46	42	08	66	48	19	13.4	39.1	6.1	Pink, coarse grained, porphyritic granite with alkali-feldspar phenocrysts. The rock contains northwest-trending vertical joints.
BH-16B	46	41	06	66	48	21	17.1	51.6	6.2	Pink, coarse grained, porphyritic granite with alkali-feldspar phenocrysts. The rock contains northwest-trending joints, dipping 75° SW.
BH-16C	46	41	07	66	48	18	15.8	58.9	6.4	Pegmatite pod (40 cm in diameter) embedded pink, coarse grained, porphyritic granite.
BH-16D	46	41	08	66	48	21	13.1	35.1	6.9	Pegmatite pod (20 cm in diameter) embedded pink, coarse grained, porphyritic granite.
BH-16E	46	41	10	66	49	20	13.4	36.5	6.1	Pink, medium grained, porphyritic granite. The rock intersected by two sets of northeast- and northwest-trending joints.
BH-17A	46	42	02	66	48	20	13.4	38.3	6.2	Aplite dyke (15 cm wide), with quartz phenocrysts intersecting medium grained, porphyritic granite. The dykes strike northeast (065°) and dip steeply southeast.
BH-17B	46	42	01	66	48	22	12.6	37.4	6.0	Coarse grained, porphyritic granite exhibiting rapakivi texture.
BH-18	46	42	03	66	48	21	13.6	33.3	5.8	Aplite dyke intersecting coarse grained, porphyritic granite and trending northeast.
BH-19	46	42	05	66	48	25	14.4	34.6	5.0	Porphyritic biotite granite. The rock contains joints, trends northeast (065°), and is steeply dipping.
BH-20A	46	42	10	66	48	20	10.0	30.7	5.6	Coarse grained, porphyritic granite (hematitized and slightly mineralized).
BH-20B	46	42	12	66	48	21	12.1	38.0	5.9	Coarse grained, granite (altered and slightly mineralized).
BH-20C	46	42	11	66	48	19	12.6	37.9	5.6	Coarse grained granite (altered and moderately mineralized).
BH-20D	46	42	12	66	48	20	10.5	30.2	4.5	Quartz pod (15 cm in diameter) embedded in coarse grained granite.
BH-20E	46	42	13	66	48	22	6.8	20.2	4.2	Pegmatite pod (50 cm in diameter) embedded in coarse grained granite.
BH-21	46	40	32	66	50	42	17.7	56.2	6.4	Pink, coarse grained granite (strongly weathered).
BH-22	46	40	33	66	50	50	17.6	50.5	6.8	Pink, coarse grained granite (strongly weathered).
BH-23	46	40	38	66	50	46	13.2	44.5	6.0	Light pink, coarse grained granite.
BH-24	46	40	38	66	51	03	11.2	35.2	5.8	Light pink, coarse grained granite.
BH-25A	46	41	34	66	53	07	16.3	50.2	6.7	Coarse grained granite exhibits rapakivi texture. The rock is exfoliated and strongly weathered.
BH-25B	46	41	36	66	53	05	14.0	40.9	5.7	Coarse grained granite exhibits rapakivi texture. The rock is exfoliated and strongly weathered.
BH-25C	46	41	38	66	53	04	15.4	44.1	6.8	Fine grained, biotite granite with quartz and alkali-feldspar phenocrysts.
BH-25D	46	41	39	66	53	03	16.1	46.6	6.5	Coarse grained, porphyritic granite with quartz and alkali-feldspar phenocrysts. The rock exhibits rapakivi texture.
BH-26A	46	41	33	66	53	07	12.8	36.1	5.9	Pink, coarse grained, porphyritic granite with quartz and alkali-feldspar phenocrysts.
BH-26B	46	41	34	66	53	08	12.3	39.9	5.7	Pink, coarse grained, porphyritic granite with quartz and alkali-feldspar phenocrysts.
BH-26C	46	41	36	66	53	10	11.9	39.3	6.0	Pink, coarse grained, porphyritic granite with quartz and alkali-feldspar phenocrysts.
BH-26D	46	41	37	66	53	11	12.4	37.8	5.6	Pink, coarse grained, porphyritic granite with quartz and alkali-feldspar phenocrysts.
BH-26E	46	41	37	66	53	09	12.2	38.6	5.7	Pink, coarse grained, porphyritic granite with quartz and alkali-feldspar phenocrysts.
BH-26F	46	41	38	66	53	10	11.9	37.0	5.8	Pink, coarse grained, porphyritic granite with quartz and alkali-feldspar phenocrysts.

Appendix VII (cont.)

Sample No.	Latitude °	'	"	Longitude °	'	"	eU (ppm)	eTh (ppm)	K (%)	ROCK DESCRIPTION
BH-26G	46	41	37	66	53	13	11.7	38.7	6.1	Pink, coarse grained, porphyritic granite with quartz and alkali-feldspar phenocrysts.
BH-27A	46	41	33	66	53	06	11.5	36.1	6.0	Pink, coarse grained, porphyritic granite with quartz and alkali-feldspar phenocrysts.
BH-27B	46	41	34	66	53	05	11.2	40.4	6.2	Pink, coarse grained, porphyritic granite with quartz and alkali-feldspar phenocrysts.
BH-27C	46	41	32	66	53	06	13.8	39.4	5.7	Pegmatite pod (tabular, 1 m long and 25 cm wide) embedded in coarse grained porphyritic granite.
BH-27D	46	41	33	66	53	06	13.9	42.7	2.9	Pink, coarse grained, porphyritic biotite granite with quartz and alkali-feldspar phenocrysts.
BH-27E	46	41	35	66	53	05	11.7	38.6	5.8	Coarse grained, biotite granite (altered).
BH-28A	46	41	43	66	53	56	11.9	21.2	5.9	Pegmatite pod embedded in medium grained porphyritic biotite granite.
BH-28B	46	41	44	66	53	55	13.3	35.9	6.1	Aplite dyke trending northwest intersects medium grained porphyritic biotite granite.
BH-29A	46	41	45	66	53	56	12.4	35.0	5.7	Porphyritic biotite granite with feldspar phenocrysts.
BH-29B	46	41	46	66	53	57	12.2	38.9	2.6	Medium grained, porphyritic biotite granite.
BH-29C	46	41	48	66	53	56	13.0	34.8	5.6	Medium grained, porphyritic biotite granite.
BH-29D	46	41	45	66	53	56	8.9	28.9	5.5	Medium grained, porphyritic biotite granite.
BH-29E	46	41	47	66	53	55	11.0	37.2	5.7	Medium grained, porphyritic biotite granite with feldspar phenocrysts.
BH-30A	46	40	07	66	53	59	7.4	23.7	5.3	Medium grained, porphyritic biotite granite with feldspar phenocrysts.
BH-30B	46	42	08	66	53	58	12.3	36.4	6.0	Aplite dyke intersects medium grained porphyritic biotite granite.
BH-30C	46	42	08	66	54	00	8.1	26.1	5.6	Medium grained, porphyritic biotite granite.
BH-31A	46	42	07	66	54	03	7.6	25.3	5.2	Pink, medium grained, porphyritic granite with feldspar phenocrysts.
BH-31B	46	42	09	66	54	02	9.9	28.2	5.4	Pink, medium grained, porphyritic granite.
BH-32A	46	42	05	66	53	58	9.3	30.5	5.8	Porphyritic biotite granite with feldspar phenocrysts.
BH-32B	46	42	04	66	53	57	7.3	27.1	5.0	Porphyritic biotite granite with feldspar phenocrysts.
BH-33A	46	34	34	66	54	40	5.5	10.7	3.3	Medium grained, mafic dyke (weathered).
BH-33B	46	34	35	66	54	41	4.8	12.9	3.7	Fine grained, mafic dyke.
BH-34	46	35	00	66	55	28	6.5	14.9	5.2	Fine grained, mafic dyke.
BH-35A	46	34	53	66	55	37	15.2	41.3	5.9	Medium grained, equigranular biotite granite.
BH-35B	46	34	54	66	55	38	12.2	31.3	5.1	Medium grained, equigranular biotite granite.
BH-35C	46	34	55	66	55	38	14.4	35.7	5.6	Medium grained, equigranular biotite granite, contains randomly oriented aplitic veinlets (<10 cm wide).
BH-35D	46	34	56	66	55	37	16.9	41.2	6.0	Medium grained, biotite granite, contains aplitic veinlets.
BH-35E	46	34	56	66	55	36	15.0	42.2	5.6	Medium grained, biotite granite, contains aplitic veinlets.
BH-36A	46	34	50	66	55	40	13.5	34.9	5.4	Medium grained, biotite granite (weathered), contains swarm of quartz veinlets (<5 cm wide).
BH-36B	46	34	51	66	55	37	18.5	39.4	6.3	Medium grained, biotite granite, contains quartz veinlets.
BH-36C	46	34	49	66	55	38	15.5	38.7	5.8	Medium grained, biotite granite, contains quartz veinlets.
BH-36D	46	34	49	66	55	37	16.7	37.6	6.0	Medium grained, biotite granite, contains quartz veinlets.
BH-37A	46	34	56	66	54	16	18.7	35.2	5.3	Pink, medium grained equigranular biotite granite.

Appendix VII (cont.)

Sample No.	Latitude °	'	"	Longitude °	'	"	eU (ppm)	eTh (ppm)	K (%)	ROCK DESCRIPTION
BH-37B	46	34	57	66	54	18	17.6	34.6	5.9	Pink, medium grained porphyritic biotite granite with quartz and alkali-feldspar phenocrysts.
BH-37C	46	34	56	66	54	19	16.5	25.2	5.6	Medium grained, equigranular biotite granite.
BH-37D	46	34	56	66	54	18	19.0	26.9	5.9	Medium grained, equigranular biotite granite.
BH-38A	46	34	59	66	54	16	23.1	31.5	7.2	Medium grained, equigranular biotite granite. The rock contains two sets of northeast- and northwest-trending vertical joints.
BH-38B	46	34	58	66	54	14	19.8	34.9	6.3	Medium grained, equigranular biotite granite. The rock intersected by two sets of joints trending 010° and 110°.
BH-39A	46	35	04	66	54	14	20.8	34.5	6.8	Coarse grained, equigranular biotite granite. The rock intersected by one set of joints trending northwest (110°) and filled with quartz. The rock is altered along the joints (hematitization and chloritization).
BH-39B	46	35	06	66	54	15	18.9	30.9	6.6	Coarse grained, equigranular biotite granite. The rock contains northwest-trending quartz veins and altered (hematitization and chloritization).
BH-39C	46	35	07	66	54	13	19.0	33.5	6.4	Coarse grained, equigranular biotite granite (jointed and altered).
BH-40A	46	35	13	66	54	35	9.4	21.9	3.5	Coarse grained, equigranular biotite granite with two sets of joints partially filled with quartz.
BH-40B	46	35	14	66	54	37	17.6	36.2	6.5	Coarse grained, equigranular biotite granite with two sets of joints partially filled with quartz.
BH-40C	46	35	15	66	54	35	18.1	31.2	7.0	Coarse grained, equigranular biotite granite with two sets of joints filled with quartz. The rock is chloritized.
BH-41A	46	35	11	66	54	33	16.1	35.8	6.5	Light pink, coarse grained equigranular biotite granite. The rock contains two sets of joints (015° and 110°) and is chloritized.
BH-41B	46	35	12	66	54	34	18.8	34.2	6.9	Light pink, coarse grained porphyritic biotite granite. The rock contains two sets of joints (015° and 110°) and is chloritized.
BH-42	46	38	53	66	52	00	10.8	31.5	4.7	Pink, coarse grained, porphyritic granite with alkali-feldspar phenocrysts.
BH-43	46	38	52	66	52	03	11.4	34.1	5.0	Pink, porphyritic biotite granite with alkali-feldspar phenocrysts.
BH-44	46	38	19	66	50	20	12.9	30.8	5.2	Pink, porphyritic granite with alkali-feldspar phenocrysts.
BH-45A	46	38	21	66	50	18	16.0	37.5	6.2	Pink, porphyritic biotite granite with alkali-feldspar phenocrysts.
BH-45B	46	38	23	66	50	17	13.0	23.6	5.4	Aplite dyke with quartz phenocrysts.
BH-46	46	38	13	66	53	25	17.2	23.0	5.5	Light pink, coarse grained, equigranular biotite granite.
BH-47	46	38	07	66	53	54	13.1	26.2	4.9	Light grey, coarse grained porphyritic granite with quartz and alkali-feldspar phenocrysts.
BH-48	46	38	14	66	53	29	14.9	34.1	5.5	Light pink, coarse grained, porphyritic granite with quartz and alkali-feldspar phenocrysts.
BH-49A	46	38	56	66	53	57	5.7	10.7	3.2	Light grey, coarse grained biotite granite.
BH-49B	46	38	54	66	53	56	6.1	13.6	3.1	Light grey, coarse grained biotite granite.
BH-50	46	38	54	66	53	54	10.4	28.5	5.4	Light pink, coarse grained, porphyritic granite with quartz and alkali-feldspar phenocrysts. The rock contains rapakivi and miarolitic textures.
BH-51A	46	39	15	66	54	05	20.1	40.5	8.7	Coarse grained, biotite granite.
BH-51B	46	39	16	66	54	06	16.5	40.9	5.7	Coarse grained, biotite granite.
BH-51C	46	39	14	66	54	03	10.7	26.5	5.2	Coarse grained, biotite granite with quartz and alkali-feldspar phenocrysts. The rock contains rapakivi and miarolitic textures.
BH-52	46	40	37	66	55	06	8.6	22.8	3.9	Coarse grained, porphyritic granite with alkali-feldspar phenocrysts.
BH-53	46	40	35	66	55	06	5.6	10.1	3.9	Coarse grained, porphyritic granite.
BH-54A	46	40	34	66	55	01	8.2	25.7	4.7	Coarse grained, porphyritic granite with alkali-feldspar phenocrysts.

Appendix VII (cont.)

Sample No.	Latitude °	'	"	Longitude °	'	"	eU (ppm)	eTh (ppm)	K (%)	ROCK DESCRIPTION
BH-54B	46	40	36	66	55	03	11.2	38.1	5.5	Coarse grained, porphyritic biotite granite with alkali-feldspar phenocrysts.
BH-54C	46	40	32	66	55	04	8.3	27.4	4.9	Coarse grained, porphyritic granite with alkali-feldspar phenocrysts.
BH-54D	46	40	31	66	55	01	11.0	31.9	4.9	Coarse grained, porphyritic granite with alkali-feldspar phenocrysts.
BH-54E	46	40	32	66	55	03	8.9	31.9	4.9	Pink, coarse grained, porphyritic granite with alkali-feldspar phenocrysts exhibiting rapakivi texture.
BH-54F	46	40	33	66	55	01	9.3	30.9	5.2	Pink, coarse grained, porphyritic granite exhibits rapakivi texture.
BH-55A	46	40	03	66	54	25	10.8	32.9	6.1	Aplite dyke emplaced in coarse grained, porphyritic biotite granite.
BH-55B	46	40	01	66	54	29	11.8	33.6	5.2	Light pink, coarse grained, porphyritic granite.
BH-55C	46	40	04	66	54	27	12.3	35.3	5.1	Aplite dyke emplaced in coarse grained, porphyritic granite.
Bh-55D	46	40	03	66	54	26	9.2	33.7	4.8	Light pink, coarse grained, porphyritic granite with quartz and alkali-feldspar phenocrysts.
BH-56A	46	36	15	66	50	08	22.1	44.2	6.5	Light pink, coarse grained, porphyritic biotite granite with quartz and alkali-feldspar phenocrysts.
BH-56B	46	36	14	66	50	07	22.1	46.3	6.9	Light pink, coarse grained, porphyritic granite with quartz and alkali-feldspar phenocrysts.
BH-56C	46	36	16	66	50	10	20.5	37.8	6.2	Light pink, coarse grained, porphyritic granite with quartz and alkali-feldspar phenocrysts.
BH-57	46	37	46	66	47	57	17.2	30.1	5.5	Aplite with quartz phenocrysts (weathered).
BH-58A	46	38	04	66	47	27	18.3	35.4	5.9	Pink, coarse grained biotite granite with alkali-feldspar phenocrysts.
BH-58B	46	38	05	66	47	29	23.1	35.9	6.9	Pink, coarse grained biotite granite with alkali-feldspar phenocrysts.
BH-59A	46	38	53	66	47	18	31.8	38.8	8.0	Pink, coarse grained biotite granite. The rock has undergone muscovitization, alteration, and mineralization.
BH-59B	46	38	54	66	47	20	27.8	40.0	7.6	Biotite aplite with quartz phenocrysts.
BH-59C	46	38	55	66	47	19	56.9	37.2	10.5	Red, aplite with quartz phenocrysts.
BH-59D	46	38	57	66	47	18	35.3	41.4	5.4	Biotite aplite with quartz phenocrysts.
BH-60A	46	39	13	66	46	22	15.6	36.5	6.0	Light pink, coarse grained biotite granite.
BH-60B	46	39	14	66	46	21	18.3	36.4	6.1	Pink, coarse grained biotite granite.
BH-60C	46	39	16	66	46	22	18.8	36.1	6.2	Pink, coarse grained biotite granite.
BH-60D	46	39	15	66	46	20	17.8	43.9	6.3	Pink, coarse grained biotite granite with quartz and alkali-feldspar phenocrysts. The rock exhibits rapakivi texture.
BH-60E	46	39	12	66	46	21	18.4	41.4	6.2	Pink, coarse grained biotite granite with quartz and alkali-feldspar phenocrysts.
BH-61A	46	39	44	66	46	00	14.7	39.5	6.4	Light pink, coarse grained biotite granite with alkali-feldspar phenocrysts.
BH-61B	46	39	45	66	46	01	17.6	33.1	5.5	Aplite dyke (25 cm wide) crosscutting coarse grained biotite granite.
BH-61C	46	39	47	66	46	45	11.8	30.0	5.5	Pink, coarse grained, porphyritic biotite granite with alkali-feldspar phenocrysts.
BH-61D	46	39	45	66	46	43	10.7	36.9	5.3	Pink, coarse grained, porphyritic, biotite granite with alkali-feldspar phenocrysts.
BH-61E	46	39	43	66	46	45	10.7	28.7	4.8	Aplite dyke (50 cm wide) crosscutting porphyritic biotite granite.
BH-62A	46	39	52	66	46	04	17.9	44.8	5.9	Pink, coarse grained, porphyritic biotite granite with quartz and alkali-feldspar phenocrysts. The rock is strongly exfoliated and exhibits two sets of joints (040° and 110°).
BH-62B	46	39	53	66	46	03	15.1	45.9	6.0	Pink, coarse grained, porphyritic biotite granite with quartz and alkali-feldspar phenocrysts. The rock is exfoliated and exhibits two sets of joints (040° and 110°).

Appendix VII (cont.)

Sample No.	Latitude °	'	"	Longitude °	'	"	eU (ppm)	eTh (ppm)	K (%)	ROCK DESCRIPTION
BH-62C	46	39	52	66	46	03	14.7	38.4	5.7	Pink, coarse grained, porphyritic biotite granite contains quartz veinlets (1 cm wide) trending northwest (110°).
BH-62D	46	39	53	66	46	02	25.0	46.9	7.4	Pink, fine grained, porphyritic biotite granite with quartz and alkali-feldspar phenocrysts. The rock is mineralized (cassiterite).
BH-62E	46	39	52	66	46	02	18.1	39.2	6.3	Pink, fine grained, porphyritic biotite granite with quartz and alkali-feldspar phenocrysts.
BH-62F	46	39	54	66	46	03	17.2	40.1	6.1	Pink, fine grained, porphyritic biotite granite with quartz and alkali-feldspar phenocrysts.
BH-62G	46	39	54	66	46	05	15.8	42.1	5.9	Pink, coarse grained, equigranular granite contains quartz veinlets.
BH-63A	46	40	07	66	46	07	19.1	32.5	5.9	Pink, coarse grained, porphyritic biotite granite with alkali-feldspar phenocrysts.
BH-63B	46	40	09	66	46	04	14.7	40.1	6.1	Pink, coarse grained, porphyritic biotite granite with alkali-feldspar phenocrysts.
BH-63C	46	40	08	66	46	06	22.0	40.3	6.6	Pink, coarse grained, porphyritic biotite granite with alkali-feldspar phenocrysts.
BH-64A	46	40	19	66	46	05	12.1	21.5	4.5	Pink, aplite pod with quartz phenocrysts.
BH-64B	46	40	17	66	46	06	18.0	35.2	6.2	Biotite aplite pod with miarolitic cavities.
BH-64C	46	40	18	66	46	04	14.6	30.8	5.6	Biotite aplite pod with miarolitic cavities.
BH-64D	46	40	20	66	46	05	20.7	37.0	6.2	Red, aplite pod with quartz phenocrysts.
BH-64E	46	40	21	66	46	03	16.6	43.6	6.6	Red, aplite with quartz phenocrysts.
BH-64F	46	40	22	66	46	04	22.7	34.9	6.5	Aplite pod.
BH-65A	46	40	31	66	46	01	26.2	50.0	7.9	Coarse grained, equigranular biotite granite. The rock is fractured.
BH-65B	46	40	32	66	46	03	20.4	43.2	6.5	Coarse grained, equigranular biotite granite.
BH-65C	46	40	34	66	46	04	21.5	40.3	6.8	Pink, coarse grained, porphyritic biotite granite with alkali-feldspar phenocrysts.
BH-65D	46	40	33	66	46	04	16.9	36.9	6.6	Pink, fine grained, porphyritic granite with quartz phenocrysts (slightly altered).
BH-65E	46	40	35	66	46	02	17.6	22.5	6.3	Aplite dyke crosscutting coarse grained, porphyritic granite.
BH-65F	46	40	33	66	46	02	18.1	39.4	6.3	Pink, coarse grained seriate biotite granite with alkali-feldspar phenocrysts.
BH-66A	46	40	45	66	45	48	25.0	38.5	7.3	Red, coarse grained, equigranular biotite granite at the contact with older (Ordovician) granite.
BH-66B	46	40	46	66	45	46	27.1	39.0	7.5	Red, coarse grained, equigranular biotite granite at the contact with older (Ordovician) granite.
D-1	46	44	41	66	33	17	11.9	20.9	5.5	Pink, coarse grained, subporphyritic granite.
D-2	46	44	43	66	33	10	12.6	26.0	5.4	Deep red, coarse grained, subporphyritic granite.
D-3	46	44	47	66	33	07	13.8	24.2	5.2	Pink to red, coarse grained subporphyritic biotite granite.
D-4	46	44	50	66	33	00	11.9	24.7	5.0	Light pink to red, subporphyritic biotite granite. The rock contains northeast-trending (055°) joints.
D-5	46	44	54	66	32	55	14.0	26.2	5.1	Pink, coarse grained, subporphyritic biotite granite.
D-6	46	45	00	66	32	42	13.3	23.7	5.2	Pink, coarse grained, subporphyritic biotite granite.
D-7	46	45	03	66	32	35	13.6	20.2	4.6	Pink, subporphyritic biotite granite.
D-8	46	45	07	66	32	17	9.4	18.5	4.1	Aplite dyke crosscutting coarse grained biotite granite.
D-9	46	45	19	66	32	18	8.7	19.9	4.7	Coarse grained granite, strongly altered, at the contact with the metasedimentary (country) rocks.

Appendix VII (cont.)

Sample No.	Latitude °	'	"	Longitude °	'	"	eU (ppm)	eTh (ppm)	K (%)	ROCK DESCRIPTION
D-10A	46	42	46	66	33	57	14.5	29.9	5.5	Light pink, fine grained, porphyritic biotite granite with alkali-feldspar phenocrysts. The rock contains rapakivi texture.
D-10B	46	42	49	66	33	58	11.2	23.5	5.1	Fine grained, porphyritic biotite granite with alkali-feldspar phenocrysts. The rock is chloritized.
D-11	46	42	43	66	33	52	13.3	27.3	5.5	Light pink, coarse grained, porphyritic biotite granite with alkali-feldspar phenocrysts. The rock exhibits rapakivi texture.
D-12A	46	42	33	66	33	30	11.9	29.7	5.1	Pink, coarse grained, porphyritic granite contains two sets of joints.
D-12B	46	42	35	66	33	31	11.6	30.8	5.3	Pink, coarse grained, subporphyritic granite contains two sets of joints.
D-13	46	42	24	66	33	13	12.3	23.9	4.9	Light pink, coarse grained, subporphyritic biotite granite.
D-14A	46	42	32	66	32	48	7.7	21.8	4.2	Pink, medium grained equigranular biotite granite.
D-14B	46	42	34	66	32	49	8.7	23.5	4.2	Pink, medium grained equigranular biotite granite.
D-15A	46	42	39	66	32	43	11.2	25.2	5.2	Coarse grained, porphyritic biotite granite. Hematitized along fractures.
D-15B	46	42	41	66	32	42	13.1	24.6	4.7	Coarse grained, porphyritic biotite granite. Hematitized along fractures.
D-16	46	42	50	66	32	43	11.2	19.7	4.1	Medium grained, equigranular granite (altered).
D-17	46	42	51	66	32	34	12.2	21.0	4.3	Medium grained, equigranular granite (altered).
D-18A	46	42	27	66	32	33	9.1	23.2	4.0	Grey, porphyritic melanocratic biotite granite.
D-18B	46	42	29	66	32	34	6.5	15.9	3.6	Grey, porphyritic melanocratic biotite granite.
D-18C	46	42	26	66	32	32	8.5	13.4	3.6	Grey, porphyritic melanocratic biotite granite.
D-18D	46	42	27	66	32	35	7.1	15.8	3.6	Dark grey, porphyritic melanocratic biotite granite with alkali-feldspar phenocrysts.
D-19	46	42	30	66	32	17	16.1	30.8	5.9	Light pink, medium grained equigranular biotite granite. The rock contains two sets of joints.
D-20	46	42	18	66	32	20	5.4	13.4	4.1	Feldspar vein crosscutting medium grained equigranular granite. Mineralized (cassiterite).
D-21	46	42	22	66	32	16	13.8	25.2	5.1	Coarse grained, porphyritic granite with alkali-feldspar phenocrysts (altered).
D-22	46	42	57	66	39	30	7.9	26.2	4.3	Light pink seriate biotite granite with alkali-feldspar phenocrysts.
D-23	46	42	56	66	39	29	12.1	28.3	4.8	Light pink porphyritic biotite granite with alkali-feldspar phenocrysts.
D-24A	46	42	53	66	39	28	10.5	27.0	4.8	Pink, coarse grained porphyritic biotite granite containing aplitic veinlets. The rock exhibits rapakivi texture.
D-24B	46	42	55	66	39	30	11.3	26.2	4.6	Pink, coarse grained porphyritic biotite granite containing aplitic veinlets. The rock exhibits rapakivi texture.
D-25A	46	42	43	66	39	23	10.0	20.5	4.1	Pink, coarse grained, porphyritic granite with alkali-feldspar phenocrysts.
D-25B	46	42	45	66	39	26	13.0	23.9	4.5	Grey, porphyritic biotite granite.
D-26	46	42	36	66	39	18	16.3	31.6	5.8	Light pink, aplite dyke trending northeast.
D-27	46	42	32	66	39	20	12.9	31.0	4.9	Pink, coarse grained, equigranular biotite granite.
D-28A	46	42	10	66	38	12	12.4	33.2	5.4	Pink, medium grained, porphyritic granite.
D-28B	46	42	12	66	38	11	12.6	28.8	5.0	Pink, medium grained, porphyritic granite.
D-29A	46	42	04	66	38	04	13.4	34.6	5.5	Pink, medium grained, porphyritic biotite granite with alkali-feldspar phenocrysts.
D-29B	46	42	06	66	38	02	15.3	35.7	5.8	Pink, medium grained, porphyritic biotite granite with alkali-feldspar phenocrysts. The rock exhibits rapakivi texture.

Appendix VII (cont.)

Sample No.	Latitude °	'	"	Longitude °	'	"	eU (ppm)	eTh (ppm)	K (%)	ROCK DESCRIPTION
D-29C	46	42	07	66	38	05	11.6	32.3	3.2	Pink, medium grained, porphyritic biotite granite with alkali-feldspar phenocrysts. The rock exhibits rapakivi texture.
D-29D	46	42	08	66	38	04	16.0	34.3	5.6	Coarse grained, medium grained, porphyritic biotite granite with a3kali-feldspar phenocrysts (altered).
D-30A	46	41	53	66	38	22	12.5	23.8	5.4	Pink, coarse grained subporphyritic biotite granite.
D-30B	46	41	54	66	38	23	11.8	28.0	5.1	Pink, coarse grained, subporphyritic biotite granite (weathered).
D-31	46	41	37	66	37	41	12.6	22.9	5.9	Grey, medium grained, melanocratic biotite granite with quartz phenocrysts.
D-32	46	41	33	66	37	09	17.9	32.2	6.0	Pink, aplite dyke trending northeast.
D-33A	46	41	20	66	37	24	12.2	22.8	5.9	Grey, medium grained melanocratic biotite granite with quartz and alkali-feldspar phenocrysts.
D-33B	46	41	22	66	37	22	15.3	25.2	6.0	Grey, medium grained, porphyritic molanocratic biotite granite with quartz and alkali-feldspar phenocrysts.
D-33C	46	41	21	66	37	23	11.8	24.9	6.0	Grey, medium grained, porphyritic melanocratic biotite granite with quartz and alkali-feldspar phenocrysts. The rock is fractured and slightly hematitized.
D-33D	46	41	23	66	37	22	11.8	25.4	6.1	Grey, medium grained, porphyritic melanocratic biotite granite with quartz and alkali-feldspar phenocrysts. The rock is strongly fractured.
D-33E	46	41	25	66	37	24	12.5	25.9	5.6	Grey, fine grained, porphyritic melanocratic biotite granite with quartz and alkali-feldspar phenocrysts.
D-34	46	40	27	66	36	30	15.0	28.6	5.7	Grey, coarse grained, porphyritic melanocratic biotite granite. The rock contains aplitic dykes (3 cm wide).
D-35	46	40	17	66	36	27	19.0	33.4	5.8	Pink, fine grained, porphyritic biotite granite with quartz and alkali-feldspar phenocrysts. The rock contains miarolitic cavities.
D-36A	46	40	15	66	36	30	17.1	32.5	5.8	Pink, coarse grained, porphyritic biotite granite with quartz and alkali-feldspar phenocrysts.
D-36B	46	40	17	66	36	29	17.9	30.7	6.0	Dark, porphyritic melanocratic biotite granite with quartz and alkali-feldspar phenocrysts.
D-36C	46	40	16	66	36	31	18.9	29.0	6.0	Grey, porphyritic melanocratic biotite granite with alkali-feldspar phenocrysts.
D-36D	46	40	18	66	36	30	15.1	24.7	5.6	Grey, porphyritic, melanocratic biotite granite with alkali-feldspar phenocrysts.
D-36E	46	40	19	66	36	31	15.0	27.5	5.6	Grey, porphyritic, melanocratic biotite granite with alkali-feldspar phenocrysts.
D-37A	46	42	50	66	36	44	12.1	23.0	5.4	Medium grained, porphyritic granite with quartz and alkali-feldspar phenocrysts (weathered).
D-37B	46	42	52	66	36	42	5.8	12.5	3.3	Pink, medium grained, equigranular biotite granite.
D-38	46	42	51	66	36	43	9.0	21.5	4.1	Light pink, equigranular granite (weathered).
D-39A	46	42	57	66	32	34	14.7	26.5	4.8	Pink, medium grained, equigranular granite.
D-39B	46	42	58	66	32	33	14.2	30.0	4.9	Pink, medium grained, equigranular granite.
D-39C	46	42	56	66	32	33	14.0	26.7	5.0	Pink, medium grained, equigranular granite.
D-39D	46	42	57	66	32	35	19.0	35.9	6.4	Pink, medium grained, equigranular granite. The rock exhibits joints trending (110°).
D-40A	46	43	02	66	32	37	12.2	26.3	4.8	Pink, coarse grained, porphyritic biotite granite with quartz phenocrysts. The rock is vertically jointed along 110° direction.
D-40B	46	43	03	66	32	38	17.3	28.2	5.1	Pink, coarse grained, porphyritic biotite granite. The rock is jointed in the 110° direction.
D-40C	46	43	05	66	32	37	14.9	27.6	5.4	Pink, coarse grained, porphyritic biotite granite. The rock is jointed in the 110° direction.
D-40D	46	43	04	66	32	36	13.6	30.5	5.4	Pink, coarse grained, porphyritic biotite granite.

Appendix VII (cont.)

Sample No.	Latitude °	'	"	Longitude °	'	"	eU (ppm)	eTh (ppm)	K (%)	ROCK DESCRIPTION
D-40E	46	43	05	66	32	35	15.8	30.9	5.8	Pink, coarse grained, porphyritic biotite granite with quartz and alkali-feldspar phenocrysts. The rock exhibits rapakivi texture.
D-40F	46	43	04	66	32	35	18.2	30.4	5.6	Light pink, porphyritic biotite granite with quartz and alkali-feldspar phenocrysts.
D-40G	46	43	05	66	32	36	16.7	29.9	5.6	Light pink, porphyritic biotite granite with quartz and alkali-feldspar phenocrysts.
D-41A	46	43	00	66	32	36	13.5	27.9	4.8	Pink, coarse grained, porphyritic biotite granite with quartz and alkali-feldspar phenocrysts.
D-41B	46	43	02	66	32	37	14.7	30.1	5.5	Pink, coarse grained, porphyritic biotite granite with quartz and alkali-feldspar phenocrysts.
D-41C	46	43	01	66	32	35	13.3	27.7	5.0	Pink, coarse grained, porphyritic biotite granite (slightly mineralized).
TB-1A	46	34	50	66	38	18	13.8	17.4	5.3	Pink, fine grained, equigranular muscovite-biotite granite (altered).
TB-1B	46	34	49	66	38	17	15.8	18.3	4.8	Pink to red, fine grained, muscovite-biotite granite (greisenized and contains molybdenite).
TB-2A	46	34	52	66	38	17	18.3	21.9	6.3	Light pink, fine grained, muscovite-biotite granite (greisenized and mineralized).
TB-2B	46	34	52	66	38	18	21.1	18.3	4.7	Light pink, fine grained, muscovite-biotite granite (strongly altered and mineralized).
TB-2C	46	34	53	66	38	19	20.6	24.5	6.1	Fine grained, equigranular, muscovite-biotite granite (greisenized and slightly mineralized).
TB-3A	46	34	53	66	38	15	20.1	22.4	6.6	Pink, fine grained, equigranular, muscovite-biotite granite (greisenized and mineralized). The rock contains two sets of joints in the 020° and 120° directions.
TB-3B	46	34	52	66	38	14	20.6	31.4	6.2	Fine grained, equigranular, muscovite-biotite granite (greisenized and mineralized). The rock contains two sets of joints in the 020° and 120° directions.
TB-3C	46	34	52	66	38	13	24.3	22.8	7.1	Pink, fine grained, equigranular granite (altered and mineralized).
TB-3D	46	34	51	66	38	13	14.3	20.2	5.6	Medium grained, equigranular granite (altered and mineralized).
TB-3E	46	34	51	66	38	12	23.6	26.5	6.9	Medium grained, equigranular, muscovite-biotite granite (altered and mineralized).
TB-4A	46	34	53	66	38	03	22.4	20.2	6.2	Medium grained, equigranular, muscovite-biotite granite (altered and mineralized).
TB-4B	46	34	53	66	38	05	25.0	24.2	6.9	Medium grained, equigranular, muscovite-biotite granite (greisenized and contains cassiterite).
TB-4C	46	34	55	66	38	04	20.9	24.1	6.3	Fine grained, equigranular granite. The rock is strongly greisenized and mineralized (Mo).
TB-4D	46	34	54	66	38	03	22.7	23.2	7.4	Feldspar dyke. Strongly altered and mineralized.
TB-4E	46	35	56	66	38	04	22.0	22.0	7.9	Medium grained, equigranular granite. The rock is strongly greisenized and mineralized.
TB-4F	46	34	56	66	38	03	23.0	25.7	5.5	Medium grained, equigranular biotite granite (weathered).
TB-4G	46	34	57	66	38	03	19.8	18.9	6.0	Medium grained, equigranular granite. Slightly greisenized.
TB-4H	46	34	56	66	38	05	24.8	22.8	6.7	Medium grained, equigranular biotite granite. Moderately greisenized.
TB-4I	46	34	58	66	38	05	26.2	26.9	6.7	Medium grained, equigranular biotite granite (greisenized).
TB-4J	46	34	55	66	38	14	19.5	22.6	4.8	Feldspar dyke crosscutting the equigranular biotite granite (greisenized).
TB-4K	46	34	55	66	38	16	26.4	24.6	6.8	Light grey, fine grained, equigranular granite.
TB-5A	46	34	57	66	38	07	23.6	25.1	6.8	Light grey, fine grained, equigranular granite, contains miarolitic cavities.

Appendix VII (cont.)

Sample No.	Latitude °	'	"	Longitude °	'	"	eU (ppm)	eTh (ppm)	K (%)	ROCK DESCRIPTION
TB-5B	46	34	56	66	38	05	26.2	23.0	7.2	Light grey, fine grained, equigranular granite, contains miarolitic cavities.
TB-5C	46	34	58	66	38	08	17.3	24.8	5.9	Grey, fine grained, equigranular granite.
TB-5D	46	34	58	66	38	10	21.9	24.2	6.7	Light grey, medium grained, equigranular granite.
TB-5E	46	34	56	66	38	09	24.6	25.6	6.9	Light grey, medium grained, equigranular granite.
TB-5F	46	35	00	66	38	09	18.2	21.0	5.3	Light pink, coarse grained, equigranular biotite granite.
TB-5G	46	35	01	66	38	10	24.8	26.8	5.0	Light pink, coarse grained, equigranular granite.
TB-5H	46	35	03	66	38	11	25.5	23.2	5.1	Pink, coarse grained, equigranular granite.
TB-5I	46	35	05	66	38	12	16.1	22.1	6.1	Light grey, fine grained, equigranular granite (slightly altered).
TB-6A	46	35	22	66	37	44	5.8	11.7	3.2	Medium grained, porphyritic granite with quartz and alkali-feldspar phenocrysts.
TB-6B	46	35	23	66	37	45	19.8	26.1	6.1	Coarse grained, porphyritic biotite granite (fractured northwesterly and sericitized).
TB-6C	46	35	23	66	37	46	16.1	23.6	6.0	Medium grained, equigranular quartz-rich biotite granite (mineralized).
TB-6D	46	35	23	66	37	47	25.5	27.1	7.4	Pink, medium grained, equigranular quartz-rich biotite granite. The rock contains quartz veinlets and is mineralized.
TB-6E	46	35	24	66	37	48	27.5	28.8	7.9	Quartz-rich, biotite granite. Slightly mineralized and contains two sets of joints in the 010° and 110° directions.
TB-6F	46	35	24	66	37	50	26.8	31.0	8.4	Light pink, quartz-rich biotite granite (limonitized).
TB-6G	46	35	25	66	37	52	25.4	28.9	7.4	Pink, quartz-rich, equigranular muscovite-biotite granite (contains molybdenite and cassiterite).
TB-6H	46	35	25	66	37	53	25.3	27.2	7.4	Pink, medium grained, equigranular, quartz-rich granite.
TB-6I	46	35	26	66	37	56	28.8	31.0	7.8	Medium grained, equigranular, quartz-rich granite. Strongly altered and mineralized.
TB-6J	46	35	26	66	37	57	25.0	29.2	7.7	Medium grained, equigranular, quartz-rich granite. Strongly altered and mineralized.
TB-7A	46	35	26	66	38	02	21.9	25.3	7.6	Pink, medium grained, equigranular quartz-rich granite.
TB-7B	46	35	26	66	38	03	18.6	23.2	6.3	Coarse grained, quartz-rich granite. Strongly altered and mineralized (cassiterite and molybdenite).
TB-7C	46	35	26	66	38	04	21.0	22.5	7.8	Coarse grained, quartz-rich, muscovite-biotite granite. Slightly mineralized.
TB-7D	46	35	26	66	38	05	20.6	28.5	7.1	Light pink, coarse grained, quartz-rich granite.
TB-7E	46	35	26	66	38	06	20.3	26.1	6.9	Quartz-rich, biotite granite. The rock is slightly altered and jointed toward 060°.
TB-7F	46	35	26	66	38	07	19.2	22.6	5.4	Quartz-rich, muscovite-biotite granite. Mineralized with cassiterite and molybdenite.
TB-7G	46	35	26	66	38	08	21.2	22.2	6.5	Quartz-rich, muscovite granite. Strongly altered (greisenized)and mineralized.
TB-7H	46	35	24	66	38	08	23.3	22.5	6.3	Medium grained, porphyritic biotite granite with quartz phenocrysts.
TB-7I	46	35	24	66	38	09	17.2	18.9	5.4	Medium grained, porphyritic biotite granite with quartz phenocrysts.
TB-7J	46	35	24	66	38	09	17.4	15.2	4.8	Fine grained, quartz-rich, granite. The rock is slightly altered and mineralized and jointed along 070° direction.
TB-7K	46	35	24	66	38	10	20.4	17.4	5.6	Grey, fine grained, porphyritic granite with quartz phenocrysts. The rock is slightly mineralized.
TB-7L	46	35	24	66	38	11	21.1	18.9	5.4	Grey, fine grained, quartz-rich granite (altered).
TB-7M	46	35	24	66	38	12	24.3	17.9	6.4	Grey, fine grained, equigranular, quartz-rich granite.

Appendix VII (cont.)

Sample No.	Latitude			Longitude			eU (ppm)	eTh (ppm)	K (%)	ROCK DESCRIPTION
TB-7N	46	35	24	66	38	12	31.3	21.6	7.1	Fine grained, equigranular granite. The rock is altered and mineralized.
TB-8A	46	35	20	66	38	22	13.2	18.5	5.1	Coarse grained, porphyritic biotite granite with quartz phenocrysts.
TB-8B	46	35	18	66	38	21	14.3	25.2	5.7	Grey, coarse grained, porphyritic biotite granite with quartz phenocrysts.
RB-1A	46	37	13	66	37	05	9.7	20.6	5.3	Coarse grained, biotite granite (weathered).
RB-1B	46	37	15	66	37	06	8.5	17.4	4.7	Pink, medium grained, equigranular granite. The rock contains quartz veinlets.
RB-1C	46	37	14	66	37	04	10.5	24.8	4.9	Pink, medium grained, equigranular granite.
RB-2	46	37	14	66	37	05	9.4	22.3	4.7	Pink, fine grained, porphyritic granite with quartz phenocrysts. The rock exhibits joints trending in the 110° direction.
RB-3A	46	37	45	66	37	14	12.0	28.6	5.2	Light pink, fine grained granite (weathered).
RB-3B	46	37	46	66	37	13	11.6	27.1	5.4	Light pink, fine grained, porphyritic granite with quartz and alkali-feldspar phenocrysts.
RB-4A	46	37	54	66	37	16	15.8	22.6	5.4	Fine grained, biotite granite. Hematitized along 110° trending joints.
RB-4B	46	37	56	66	37	14	11.5	28.7	5.3	Light pink, fine grained biotite granite.
RB-4C	46	37	58	66	37	15	11.9	33.7	5.5	Light pink, fine grained biotite granite.
RB-4D	46	37	57	66	37	13	14.0	30.1	6.2	Light pink, fine grained, porphyritic granite with quartz and alkali-feldspar phenocrysts. The rock contains two sets of joints trending along 020° and 110° directions.
RB-5A	46	36	54	66	37	09	12.3	31.7	5.4	Coarse grained, porphyritic biotite granite with alkali-feldspar phenocrysts.
RB-5B	46	36	56	66	37	11	10.5	25.4	5.0	Aplite dyke crosscutting, coarse grained, porphyritic granite.
RB-5C	46	36	57	66	37	12	14.0	29.9	5.6	Grey, fine grained, porphyritic granite with quartz phenocrysts.
RB-5D	46	36	56	66	37	13	13.3	26.3	5.5	Light pink, medium grained granite. The rock is slightly greisenized.
RB-5E	46	36	57	66	37	13	15.9	33.7	5.3	Light pink, fine grained granite. The granite contains 5 cm wide quartz vein with greisen at its border.
RB-5F	46	36	54	66	37	14	19.1	33.7	6.7	Fine grained, equigranular granite. Fractured and hematitized.
RB-6A	46	36	57	66	37	14	14.2	31.6	5.5	Light pink, medium grained, equigranular granite with red stains.
RB-6B	46	36	58	66	37	14	16.4	32.3	6.3	Medium grained, equigranular biotite granite. The rock is hematitized and contains northwest-trending (dipping 80° SE) joints. The joints contain quartz veins bordered with greisenization.
RB-6C	46	36	56	66	37	15	20.0	32.1	6.2	Medium grained, equigranular biotite granite. The rock is hematitized, fractured northwesterly and contains quartz veins bordered with greisenization.
RB-6D	46	36	57	66	37	16	15.9	29.6	5.7	Medium grained, porphyritic granite with quartz phenocrysts. The rock is hematitized.
RB-7A	46	37	00	66	37	41	11.3	27.2	5.1	Light pink, coarse grained biotite granite.
RB-7B	46	37	02	66	37	45	11.8	32.9	5.4	Light pink, coarse grained biotite granite.
RB-8	46	37	00	66	37	30	7.6	19.3	2.9	Quartz vein intersecting coarse grained granite.
RB-9A	46	36	58	66	37	23	12.9	25.7	5.0	Light grey, medium grained, equigranular granite.
RB-9B	46	36	56	66	37	25	16.7	29.5	5.6	Light grey, medium grained, equigranular granite.
RB-9C	46	36	59	66	37	22	10.7	27.1	5.2	Medium grained, equigranular biotite granite (weathered).
RB-10A	46	37	02	66	37	17	12.1	29.9	5.7	Light pink, medium grained, equigranular biotite granite. The rock contains two sets of joints.
RB-10B	46	37	03	66	37	19	12.4	33.1	5.6	Light pink, medium grained, equigranular biotite granite. The rock contains two sets of joints.
RB-10C	46	37	05	66	37	21	12.5	31.5	5.4	Light pink, medium grained, equigranular granite.

Appendix VII (cont.)

Sample No.	Latitude °	'	"	Longitude °	'	"	eU (ppm)	eTh (ppm)	K (%)	ROCK DESCRIPTION
RB-10D	46	37	08	66	37	22	12.9	31.2	5.7	Light pink, medium grained, equigranular biotite granite.
RB-10E	46	37	11	66	37	23	12.8	25.9	3.5	Quartz vein emplaced along 110° trending joints crosscutting medium grained, equigranular biotite granite.
RB-11A	46	37	13	66	37	25	12.1	30.1	5.3	Light grey, coarse grained, porphyritic biotite granite with quartz and alkali-feldspar phenocrysts. The rock intersected with northwest-trending vertical joints.
RB-11B	46	37	15	66	37	27	12.0	30.9	5.5	Light pink, medium grained, porphyritic granite with quartz and alkali-feldspar phenocrysts.
RB-11C	46	37	16	66	37	30	11.2	35.9	5.0	Light pink, medium grained, equigranular biotite granite.
RB-12A	46	37	56	66	37	27	10.6	30.4	5.9	Light pink, coarse grained, porphyritic granite with quartz and alkali-feldspar phenocrysts. The rock contains two sets of joints trending toward 020° and 110° directions.
RB-12B	46	37	57	66	37	29	10.6	32.5	5.0	Light pink, medium grained, equigranular biotite granite. The rock contains quartz veinlets.
RB-12C	46	37	58	66	37	26	9.2	26.8	5.5	Medium grained, porphyritic biotite granite with quartz and alkali-feldspar phenocrysts (weathered).
RB-13A	46	37	36	66	37	28	14.6	38.9	6.1	Light pink, medium grained, equigranular biotite granite exhibiting two sets of joints trending toward 030° and 110° direction. The rock contains molybdenite.
RB-13B	46	37	38	66	37	30	9.1	19.0	2.2	Quartz vein intersecting coarse grained, equigranular biotite granite. The vein trending along 110° direction.
RB-14A	46	37	25	66	37	28	14.8	33.2	5.8	Pink, coarse grained, equigranular biotite granite intersected by northwest- and northeast-trending joints with vertical dips.
RB-14B	46	37	27	66	37	30	20.2	46.4	8.3	Coarse grained, equigranular biotite granite. Greisenzed along 110° strike fractures.
RB-15A	46	37	24	66	37	26	18.3	39.8	6.7	Medium grained, porphyritic granite with quartz and alkali-feldspar phenocrysts. The rock also contains secondary muscovite. Two sets of joints in the 050° and 110° direction are observed in the rock. The rock is also mineralized (cassiterite and molybdenite).
RB-15B	46	37	26	66	37	24	17.5	32.6	6.5	Medium grained, porphyritic granite with quartz and alkali-feldspar phenocrysts. The rock contains two sets of joints and is mineralized.
RB-15C	46	37	25	66	37	25	13.2	28.9	5.2	Medium grained, equigranular biotite granite. The rock is limonitized and contains quartz veins.
RB-15D	46	37	27	66	37	26	17.4	32.9	5.6	Medium grained, porphyritic biotite granite with quartz and alkali-feldspar phenocrysts. The rock is hematitized.
RB-15C	46	37	27	66	37	26	13.2	28.9	5.2	Medium grained, biotite granite. The rock contains quartz veins and is limonitized.
RB-15D	46	37	30	66	37	25	17.4	32.9	5.6	Pink, medium grained, porphyritic biotite granite with quartz and alkali-feldspar phenocrysts. The rock is coated with Mn- and Fe-staining.
RB-15E	46	37	32	66	37	27	12.9	29.8	5.3	Pink, medium grained biotite granite.
RB-15F	46	37	34	66	37	28	13.7	31.5	5.5	Pink, medium grained biotite granite. The rock contains randomly oriented quartz veinlets.
RB-15G	46	37	36	66	37	30	13.9	27.5	4.6	Quartz vein (30 cm wide) trending along 010° direction and dips vertically. The vein emplaced in hematitized biotite granite.
RB-15H	46	37	38	66	37	32	20.4	35.5	6.5	Medium grained, equigranular biotite granite. The rock is coated with red stains and is mineralized.
RB-15I	46	37	37	66	37	35	21.4	34.6	6.7	Medium grained, equigranular biotite granite. The rock is mineralized with cassiterite and molybdenite.
RB-15J	46	37	39	66	37	34	16.5	33.7	6.1	Light pink, medium grained, porphyritic biotite granite.

Appendix VII (concl.)

Sample No.	Latitude			Longitude			eU (ppm)	eTh (ppm)	K (%)	ROCK DESCRIPTION
RB-15K	46	37	40	66	37	30	14.8	31.8	5.9	Medium grained, porphyritic biotite granite with quartz and alkali-feldspar phenocrysts. The rock is coated with limonite.
RB-15L	46	37	41	66	37	31	15.6	31.6	6.2	Light pink, medium grained, porphyritic biotite granite with quartz phenocrysts.
RB-15M	46	37	41	66	37	35	19.3	28.4	6.4	Medium grained, equigranular biotite granite coated with red stains.

Appendix VIII

Chemical analyses, norms, and locations of the granitic rocks of the North Pole Pluton (data compiled from Fyffe and Pronk, 1985).

A. Chemical analysis and norms

	17	15C	16C	15B	16A	16B	20	21	18	19	10	11	12A	14A	12B	12C	13	14B	15A
SiO_2 (%)	76.45	76.53	76.80	77.60	77.02	75.92	74.28	73.47	86.47	80.72	71.10	71.79	71.96	70.00	73.06	72.32	74.42	68.88	74.69
TiO_2 (%)	0.15	0.09	0.15	0.09	0.13	0.20	0.02	0.27	0.08	0.20	0.38	0.43	0.35	0.60	0.28	0.28	0.50	0.43	0.47
Al_2O_3 (%)	13.32	12.99	13.76	12.55	13.08	23.84	14.32	14.17	6.48	10.91	14.04	14.97	14.98	15.15	13.89	14.24	12.57	14.75	14.76
Fe_2O_3 (%)	0.70	0.69	1.04	2.83	1.68	1.05	0.46	0.63	0.83	0.50	0.53	0.92	0.34	0.31	1.37	1.35	1.46	1.60	2.38
FeO (%)	0.64	0.74	0.24	0.54	2.02	3.17	1.13	0.98	0.20	0.47	0.51	1.75	1.72	2.94	3.22	4.05	2.63	4.62	0.91
MnO (%)	0.05	0.02	0.04	0.03	0.34	0.34	0.03	0.04	0.02	0.01	0.07	0.06	0.06	0.08	0.16	0.22	0.12	0.15	0.02
MgO (%)	0.30	0.20	0.29	0.13	0.19	0.39	0.43	0.44	0.17	0.19	0.60	0.71	0.70	1.00	0.54	0.58	0.84	1.00	0.51
CaO (%)	0.28	0.08	0.10	0.12	0.08	0.09	0.88	0.59	0.10	0.11	1.14	0.91	1.32	1.79	0.09	0.00	0.21	0.19	0.10
K_2O (%)	4.91	5.17	5.14	4.07	3.87	3.60	4.84	4.96	2.66	4.62	4.24	4.07	4.33	3.92	4.09	4.02	3.67	3.66	4.66
Na_2O (%)	3.35	1.64	0.09	0.19	0.17	0.11	3.44	3.24	0.17	0.21	3.58	3.57	3.55	3.16	0.17	0.15	0.26	0.13	0.20
H_2O+ (%)	0.81	1.66	2.37	1.00	2.04	2.20	0.93	1.30	1.56	2.00	1.21	1.36	1.29	1.73	2.25	2.83	2.10	3.20	1.79
H_2O- (%)	0.09	0.23	0.28	0.00	0.00	0.00	0.00	0.07	0.11	0.11	0.00	0.32	0.24	0.10	0.16	0.13	0.18	0.10	0.10
P_2O_5 (%)	0.04	0.01	0.04	0.06	0.08	0.04	0.10	0.08	0.04	0.08	0.08	0.10	0.08	0.16	0.08	0.06	0.05	0.16	0.08
CO_2 (%)	0.18	0.107	0.05	0.05	0.03	0.05	0.10	0.07	0.05	0.03	0.00	0.10	0.02	0.10	0.03	0.02	0.02	0.02	0.10
TOTAL	101.27	100.12	100.39	99.26	100.73	100.00	100.96	100.31	98.96	100.17	98.48	101.66	100.94	101.04	99.39	100.25	99.03	99.89	100.77
Be (ppm)	6.8	11.0	5.5	7.1	6.0	4.1	5.4	6.6	10.0	4.3	5.4	6.4	6.5	5.7	5.5	6.5	1.8	4.5	5.6
Ba (ppm)	300	170	180	125	200.0	180	400	470	150	290	430	440	440	720	180	260	265	415	235
Cu (ppm)	3	66	9	105	99	77	4	17	2	10	4	15	10	21	86	31	120	60	70
F (ppm)	600	300	600	640	600	780	290	320	410	360	290	340	400	420	690	750	640	780	1120
Mo (ppm)	1	2	4	7	6	7	1	0.5	8	6	1	2	2	2	7	6	5	25	4
Pb (ppm)	18	13	246	2	360	22	22	28	10	140	36	20	28	12	100	282	24	82	10
Rb (ppm)	201	300	261	420	345	347	204	234	186	271	136	163	197	159	386	341	210	308	440
B (ppm)	–	9	12	16	9	9	4	2	57	48	7	5	3	3	21	65	16	11	25
Sn (ppm)	4.6	8.0	8.0	86.0	72.0	68.0	76	6.0	6.0	8.1	6.9	7.0	7	6.0	97.0	124.0	90.0	102.0	86.0
Sr (ppm)	99	19	8	–	7	7	52	85	15	14	120	150	108	90	7	–	–	5	5
Zn (ppm)	96	260	145	29	1160	2750	54	51	45	75	312	98	82	230	780	135	1000	128	52
U (ppm)	4.9	8.5	26.8	5.0	18.5	11.1	4.2	4.2	5.4	9.1	3.3	6.7	6.5	3.9	5.6	6.3	3.2	5.0	6.6
W (ppm)	–	4	–	4	–	8	–	–	–	–	–	–	4	–	16	16	12	20.0	8
Li (ppm)	6	9	10	18	17	22	23	25	52	140	13	11	10	17	17	25	18	28	31
Bi (ppm)	–	0.08	–	3.20	1.60	1.80	0.06	0.06	0.07	0.05	0.06	0.08	0.05	0.06	2.70	1.70	2.20	4.20	6.00
Zr (ppm)	75	75	45	105	60	70	100	75	30	115	240	85	75	155	220	410	180	215	340
S (ppm)	120	40	40	13300	1900	2520	20	20	400	340	60	100	50	40	200	100	2260	2500	60
Q (%)	36.97	47.30	57.38	61.39	60.78	60.18	32.73	33.90	77.06	62.73	30.95	32.11	30.18	30.04	55.41	53.93	58.18	51.41	55.62
C (%)	2.07	4.66	8.15	7.85	8.76	8.88	2.06	2.62	3.32	5.66	1.72	3.30	2.26	2.86	9.49	10.02	8.16	10.98	9.51
Or (%)	28.99	31.15	31.12	24.38	23.18	21.76	28.65	29.67	16.18	27.88	25.78	24.25	25.77	23.40	24.94	24.44	22.42	22.40	27.91
Ab (%)	28.29	14.14	0.98	1.63	1.46	0.95	29.13	27.73	1.48	1.81	31.14	30.42	30.22	26.98	1.48	1.30	2.27	1.14	1.71
An (%)	1.13	0.34	0.24	0.21	–	0.19	3.71	2.43	0.24	0.02	5.28	3.89	6.06	7.90	–	–	0.74	–	–
En (%)	0.75	0.51	0.74	0.33	0.48	0.99	1.07	1.11	0.44	0.48	1.54	1.78	1.75	2.51	1.39	1.49	2.16	2.58	1.29
Fs (%)	0.40	0.69	–	–	2.11	4.32	1.72	0.92	–	0.02	1.85	1.83	2.39	4.34	4.25	6.40	2.14	6.76	–
Mt (%)	1.01	1.02	0.48	–	2.39	1.56	0.67	0.92	0.19	0.74	0.79	1.34	0.50	0.45	2.05	2.01	2.19	2.90	2.79
Il (%)	0.28	0.17	0.29	–	0.25	0.39	0.04	0.52	0.16	0.39	0.74	0.82	0.67	1.15	0.55	0.55	0.98	0.85	0.90
Hm (%)	–	–	0.73	1.61	–	–	–	–	0.72	–	–	–	–	–	–	–	–	–	0.07
Ap (%)	0.09	0.24	0.10	0.14	0.19	0.10	0.23	0.19	0.10	0.19	0.19	0.23	0.19	0.37	0.19	0.14	0.12	0.38	0.19

B. Sample locations and descriptions

Sample	Latitude			Longitude			ROCK DESCRIPTION
	°	'	"	°	'	"	
10	47	02	20	66	51	19	Biotite granite (unaltered)
11	47	02	18	66	51	12	Biotite granite (unaltered)
12A	47	02	20	66	51	03	Biotite granite (unaltered)
12B	47	02	20	66	51	00	Biotite granite (altered, containing visible sulphides)
12C	47	02	20	66	50	58	Biotite granite (altered, containing visible sulphides)
13	47	02	50	66	50	21	Biotite granite (altered, containing visible sulphides)
14A	47	01	35	66	51	19	Biotite granite (unaltered)
14B	47	01	34	66	51	20	Biotite granite (altered, containing visible sulphides)
15A	47	01	55	66	51	41	Biotite granite (altered, containing visible sulphides)
15B	47	01	54	66	51	41	Quartz feldspar porphyry (intensely altered)
15C	47	01	53	66	51	40	Quartz feldspar porphyry (mildly altered)
16A	47	01	20	66	50	41	Quartz feldspar porphyry (intensely altered)
16B	47	01	20	66	50	39	Quartz feldspar porphyry (intensely altered)
16C	47	01	20	66	50	37	Quartz feldspar porphyry (mildly altered)
17	47	00	38	66	49	37	Quartz feldspar porphyry (unaltered)
18	47	00	35	66	50	30	Biotite-muscovite granite (silicified and brecciated)
19	47	00	44	66	51	57	Biotite-muscovite granite (silicified and brecciated)
20	47	01	15	66	54	51	Biotite-muscovite granite (unaltered)
21	47	01	08	66	54	35	Biotite-muscovite granite (unaltered)

Appendix IX

Chemical analyses, norms, locations and descriptions of the granitic rocks of the central Miramichi Anticlinorium plutons (data compiled from Fyffe and MacLellan, 1988 and MacLellan and Taylor, 1989).

A. Burnthill Pluton (fresh and altered rock samples).

	85.45	85-498	85.61	85.195	85-201	85.266	2A-85	12-261	12-373	12-397	85-22	1A-156	85-155	85-40C	3-470	85-175	5-125	85-21
SiO_2 (%)	76.55	77.28	75.56	73.82	71.44	67.69	76.75	77.02	77.12	77.10	76.82	73.95	65.58	76.15	76.81	76.56	77.11	77.92
TiO_2 (%)	0.18	0.18	0.15	0.33	0.33	0.25	0.16	0.05	0.06	0.05	0.18	0.23	0.21	0.21	0.14	0.08	0.07	0.03
Al_2O_3 (%)	12.98	12.42	12.76	13.47	14.89	18.24	12.51	12.65	12.84	12.67	12.62	13.42	16.71	12.80	12.68	12.50	12.74	12.80
CaO (%)	0.74	0.75	0.67	1.03	2.08	0.24	0.81	0.47	0.52	0.49	0.59	1.17	0.05	0.61	0.68	0.39	0.49	0.24
MgO (%)	0.32	0.34	0.16	0.56	0.83	0.36	0.24	0.20	0.22	0.19	0.34	0.40	0.26	0.34	0.24	0.15	0.14	0.09
Na_2O (%)	3.50	3.15	3.57	3.47	3.57	9.01	4.00	3.50	3.88	4.03	3.31	3.36	0.98	3.35	3.44	3.41	3.81	4.03
K_2O (%)	4.69	4.28	4.64	4.28	4.03	2.03	4.51	4.60	4.51	4.26	4.59	4.49	11.83	4.68	4.92	4.49	4.60	4.29
Fe_2O_3(%)	0.56	0.79	0.46	0.64	0.09	1.21	0.50	0.61	0.46	0.24	0.45	0.37	0.59	0.39	0.11	1.43	0.18	0.12
FeO (%)	0.84	0.58	0.84	1.43	2.09	0.53	0.69	0.50	0.51	0.60	0.93	1.16	2.05	1.07	1.01	–	0.56	0.42
MnO (%)	0.06	0.05	0.06	0.06	0.10	0.04	0.06	0.09	0.07	0.10	0.06	0.06	0.10	0.07	0.05	0.09	0.04	0.02
P_2O_5 (%)	0.06	0.05	0.01	0.11	0.08	0.08	0.02	0.01	0.02	0.02	0.05	0.07	0.06	0.005	0.00	0.01	0.00	0.01
Rb (ppm)	404	369	410	307	295	87	379	540	470	497	421	354	920	398	413	581	455	564
Sr (ppm)	45	69	35	95	319	232	34	1	20	15	44	99	91	67	34	9	16	4
Cs (ppm)	7.4	9.9	9.4	13.6	14.2	2.3	15.1	7.5	8.2	9.3	8.1	9.0	22.0	12.2	6.3	8.5	5.6	8.6
Ba (ppm)	103	208	84	168	514	153	131	58	53	84	135	262	622	191	110	47	100	77
Y (ppm)	57	58	74	38	29	55	46	82	95	91	60	47	66	60	59	82	101	74
Zr (ppm)	116	117	124	177	150	142	102	64	63	61	122	131	147	135	99	67	78	53
Nb (ppm)	13	18	24	19	8	12	42	39	40	37	18	20	15	22	21	32	33	51
Hf (ppm)	4.3	4.6	5.1	4.9	4.3	4.7	4.0	4.3	4.2	3.9	4.8	4.5	5.1	4.5	4.1	3.6	3.9	4.7
Ta (ppm)	3.6	6.1	5.9	4.9	1.5	3.2	7.2	11.9	13.7	18.6	6.3	4.3	3.8	5.3	5.9	8.1	9.5	15.4
La (ppm)	23.0	30.0	35.0	41.0	32.0	110.0	15.4	14.6	16.5	18.2	30.0	34.3	42.0	29.2	23.1	16.0	13.5	10.7
Lu (ppm)	0.65	0.75	0.84	0.34	0.19	0.56	0.55	1.1	1.2	1.1	0.90	0.75	0.79	0.84	0.86	1.3	1.7	1.2
Zn (ppm)	12	41	46	45	66	45	53	231	36	22	14	36	62	54	nd	65	16	126
W (ppm)	1.5	1.5	1.4	0.7	33.0	4.9	1.2	7.7	4.6	7.4	1.5	0.21	3.3	1.3	1.5	3.6	2.1	15.4
Sn (ppm)	13	13	11	9	31	6	10	36	17	24	15	14	25	15	8	27	14	17
Sc (ppm)	4.6	4.2	6.7	5.8	4.2	4.2	3.7	5.1	5.1	5.4	6.0	5.7	4.5	5.5	4.7	5.4	5.4	5.2
Tb (ppm)	1.3	1.5	2.2	1.3	0.6	1.8	1.5	2.1	2.2	2.4	1.4	1.4	1.8	1.4	1.4	1.7	2.2	1.2
Yb (ppm)	5.3	6.0	7.7	3.5	1.9	4.8	5.9	9.6	10.7	9.8	5.7	5.1	6.9	5.6	5.5	9.0	10.9	8.3
F (ppm)	430	630	765	705	2430	100	655	1810	1070	1115	510	1085	1420	510	640	1530	470	80
U (ppm)	13.1	7.6	17.2	8.7	7.3	4.2	29.0	26.0	26.0	24.0	13.1	13.1	10.2	7.7	19.5	15.4	22.1	26.1
Th (ppm)	39.0	31.0	46.0	46.0	20.0	27.0	35.0	28.0	30.0	29.0	42.7	35.8	27.0	38.0	45.9	25.2	28.9	8.9
Q (%)	36.10	40.61	35.33	34.05	28.43	6.69	33.99	37.74	35.63	36.15	37.89	34.06	13.04	36.54	35.35	38.87	35.80	37.16
C (%)	0.94	1.38	0.67	1.53	0.88	0.98	0.00	1.11	0.68	0.59	1.26	1.09	2.38	1.25	0.45	1.36	0.61	1.11
Or (%)	27.60	25.29	27.72	25.47	23.99	12.06	26.59	27.24	26.59	25.23	27.13	26.89	71.04	27.72	29.08	26.77	27.24	24.35
Ab (%)	29.45	26.65	30.55	29.62	30.38	76.49	33.76	29.62	32.75	34.19	28.01	28.77	8.46	28.43	29.11	29.11	32.32	34.10
An (%)	3.28	3.39	3.31	4.44	9.85	0.67	2.85	2.27	2.45	2.30	2.60	5.45	0.00	2.70	3.37	1.87	2.43	1.13
Hy (%)	0.95	1.05	1.43	3.07	5.51	0.90	0.87	1.00	1.00	0.52	2.00	2.61	3.81	2.27	2.22	0.37	1.19	0.86
Mt (%)	1.22	1.15	0.68	0.94	0.13	1.11	0.72	0.88	0.74	0.87	0.65	0.54	0.87	0.54	0.16	–	0.26	0.17
Il (%)	0.34	0.34	0.28	0.63	0.63	0.47	0.30	0.09	0.11	0.09	0.34	0.44	0.40	0.40	0.27	0.15	0.13	0.06
Ap (%)	0.14	0.12	0.02	0.25	0.19	0.19	0.05	0.02	0.05	0.05	0.12	0.16	0.14	0.12	0.00	0.02	–	0.02

Appendix IX (cont.)

B. Burnthill Pluton (mineralized rock samples):

	85-129B	85-129C	85-131	85-132C	85-133B	85-285A	85-155B	TH-0	TH-1	TH-3
SiO_2 (%)	68.8	82.3	81.0	76.5	77.3	81.8	55.9	63.3	43.5	40.1
TiO_2 (%)	0.02	0.10	0.14	0.05	0.16	0.09	0.97	0.23	0.14	0.76
Al_2O_3 (%)	16.9	5.36	10.0	0.12	10.4	8.87	13.1	17.5	22.8	25.0
CaO (%)	0.07	0.57	0.05	0.35	0.02	0.09	0.27	0.71	0.18	0.04
MgO (%)	0.02	0.09	0.19	0.04	0.24	0.10	1.40	0.22	0.53	0.52
Na_2O (%)	0.95	0.68	0.26	0.04	0.10	0.40	0.07	0.14	0.12	0.18
K_2O (%)	12.0	2.11	3.33	0.03	3.77	3.65	5.44	5.66	7.50	8.12
Fe_2O_3 (%)	0.98	0.95	2.46	2.04	4.19	2.52	18.6	8.40	4.52	12.7
MnO (%)	--	0.16	--	0.92	--	0.08	0.62	0.20	0.22	0.17
P_2O_5 (%)	0.02	0.03	0.04	0.02	0.04	0.06	0.27	0.09	0.03	0.10
Li (ppm)	<10	<10	70	10	110	30	960	130	160	470
Be (ppm)	<5	<5	<5	<5	5	5	5	10	15	15
Rb (ppm)	934	205	476	<10	586	598	1260	848	947	992
Sr (ppm)	97	14	22	<10	99	<10	73	66	25	18
Cs (ppm)	16	<1	10	<1	13	11	98	30	55	36
Ba (ppm)	361	122	122	127	117	169	273	427	298	329
B (ppm)	10	20	20	20	20	20	<10	20	30	10
S (ppm)	<100	720	660	480	120	<100	<100	<100	240	80
As (ppm)	11	1	1800	<1	22	24	22	6	18	<1
Sb (ppm)	0.6	0.6	<0.2	1.0	0.9	0.2	0.2	0.4	0.4	<0.2
Y (ppm)	<10	77	60	30	63	17	84	<10	<10	<10
Zr (ppm)	<10	23	77	<10	100	56	344	155	69	226
Nb (ppm)	<10	68	17	377	35	69	90	<10	33	18
V (ppm)	<10	10	<10	<10	<10	<10	70	10	20	30
Cr (ppm)	<2	2	<2	<2	<2	<2	4	6	6	6
Mn (ppm)	150	--	230	--	210	--	--	--	--	--
Co (ppm)	<1	<1	<1	<1	<1	1	15	7	3	2
Ni (ppm)	4	5	5	6	8	9	14	2	2	1
Cu (ppm)	31.0	26.0	160.0	17.0	130.0	140.0	4.0	230.0	130.0	100.0
Zn (ppm)	10.0	14.0	77.0	12.0	13.0	95.0	260.0	69.0	830.0	94.0
Pb (ppm)	150	42	280	4	2	66	<2	10	140	4
Hf (ppm)	<1	2	4	<1	6	3	8	4	2	5
Ta (ppm)	<1	<1	4	<1	5	6	13	3	<1	3
Ga (ppm)	14	14	18	2	33	15	45	43	39	68
Mo (ppm)	95	61	14	538	26	19	34	11	43	5
Ag (ppm)	2.0	<0.5	6.5	1.0	<0.5	1.5	<0.5	1.0	4.0	<0.5
Cd (ppm)	<1	<1	2	<1	<1	<1	<1	<1	6	<1
In (ppm)	<1	<1	<1	1	1	2	<1	3	3	4
Sn (ppm)	<10	<10	22	<10	61	198	40	72	9400	6090
W (ppm)	1700	1520	59	217	489	889	582	32	43	566
Au (ppb)	3	2	8	94	4	<1	<1	<1	<1	<1
Tl (ppm)	3	<1	2	<1	3	3	12	7	10	9
Bi (ppm)	125.0	74.5	33.5	182.0	75.0	15.6	1.0	19.0	13.8	1.3
La (ppm)	<2	17	22	8	34	15	77	24	36	37
Ce (ppm)	4	46	44	18	78	32	165	45	72	74
Nd (ppm)	2.5	26.4	19.6	8.6	35.6	13.6	75.4	22.6	35.1	36.0
Sm (ppm)	0.7	7.9	4.5	2.3	7.6	2.9	15.0	4.5	6.4	6.9
Eu (ppm)	0.5	0.3	0.1	<0.1	0.1	0.2	0.4	0.4	0.6	0.7
Gd (ppm)	<0.5	6.5	3.7	2.1	4.2	2.4	11.9	3.3	4.3	4.2
Dy (ppm)	0.7	6.9	4.4	5.9	2.3	2.6	7.2	3.0	2.1	2.7
Er (ppm)	<0.5	3.6	2.2	6.8	0.8	1.3	2.4	1.3	0.6	0.9
Lu (ppm)	<0.1	0.7	0.3	3.4	0.2	0.2	0.3	0.2	0.1	0.2
U (ppm)	8.1	12.6	18.8	6.2	5.1	12.2	28.9	9.6	1.8	7.3
Th (ppm)	<1	17	31	5	44	20	34	24	23	22

C. Dungarvon Pluton (mineralized rock samples):

	86-131B	86-149	86-189	86-213	86-240	86-242D	86-242E	86-243	86-245B	86-248	86-263	86-264B	86-572B	DC-1	SO-18-1	SO-19-1	DROO4
(%)																	
SiO_2	91.1	90.1	92.2	79.5	58.3	69.7	88.8	44.2	90.4	80.8	55.3	70.1	75.6	81.6	59.8	52.2	61.6
TiO_2	0.05	0.06	0.06	0.12	0.31	0.17	0.09	0.01	0.06	0.08	0.43	0.06	0.14	0.07	0.06	0.09	0.18
Al_2O_3	2.06	4.97	3.57	11.2	16.0	16.0	4.94	1.50	2.47	9.88	19.0	13.1	12.7	6.17	9.95	8.96	19.2
CaO	1.38	0.08	0.11	0.18	0.30	1.15	0.09	44.3	1.28	0.10	3.54	0.10	0.48	0.10	4.96	0.49	2.20
K_2O	0.31	1.12	0.54	4.10	4.83	8.30	1.69	0.85	0.68	2.38	7.34	8.68	5.33	0.55	6.28	3.57	5.98
Fe_2O_3	1.52	0.22	0.96	0.78	9.41	0.11	1.97	0.35	1.87	2.14	5.45	3.39	0.94	0.32	0.85	0.77	2.11
MnO	--	--	--	--	--	--	--	--	--	0.21	0.10	--	--	--	--	--	0.09
P_2O_5	0.03	0.01	0.02	0.03	0.09	0.03	0.03	0.02	0.02	0.02	0.40	0.03	0.05	0.02	0.04	0.03	0.05
(ppm)																	
Li	210	420	460	10	90	20	210	30	210	210	610	70	50	20	10	80	10
Be	5	5	5	5	10	<5	5	<5	<5	180	5	25	10	<5	40	15	5
Rb	<10	141	50	293	<10	633	<10	50	65	639	1040	707	347	<10	<10	<10	422
Sr	27	104	53	65	93	89	53	55	54	61	176	53	23	28	59	50	420
Cs	5	9	9	3	8	10	11	2	2	18	69	14	7	2	14	8	6
Ba	185	99	140	126	380	617	135	60	127	107	300	423	85	120	505	245	202
B	20	20	30	20	<10	20	20	<10	20	20	<10	20	20	20	10	20	20
S	2000	<100	1960	<100	10000	<100	4400	80	1500	<100	<100	1200	1100	<100	<100	<100	480
As	190	4	93	<1	10	<1	17	14	10	20	<1	11	<1	<1	9	4	22
Sb	10.0	0.8	2.9	0.3	0.3	0.2	7.0	0.4	0.3	<0.2	0.2	0.5	<0.2	<0.2	<0.2	0.2	0.7
Y	<10	17	13	31	<10	94	12	25	<10	82	65	16	78	<10	<10	<10	58
Zr	16	16	<10	74	152	66	32	<10	<10	60	274	<10	73	21	<10	<10	91
Nb	<10	22	<10	29	14	11	<10	20	24	59	<10	<10	29	19	13	108	27
V	20	20	<10	<10	30	<10	120	10	<10	<10	50	20	10	<10	20	20	30
Cr	4	4	6	4	4	4	4	4	<2	6	2	4	4	4	4	4	6
Mn	34	150	230	150	190	82	44	42	220	--	--	100	210	84	290	430	--
Co	<1	<1	2	2	28	<1	<1	2	2	<1	6	<1	1	<1	2	2	4
Ni	2	2	3	4	5	2	<1	3	2	<1	7	<1	2	1	3	3	5
Cu	3.0	2.0	2.0	27.0	1200.0	5.0	13.0	1.0	5.5	33.0	1.5	6.0	36.0	10.0	8.0	6.5	18.0
Zn	16.0	15.0	16.0	22.0	22.0	17.0	10.0	12.0	36.0	92.0	36.0	23.0	44.0	47.0	37.0	44.0	23.0
Pb	60	10	12	16	16	12	8	10	10	180	8	90	32	16	12	12	46
Hf	<1	2	<1	5	4	3	2	<1	<1	4	8	<1	4	1	<1	2	6
Ta	<1	3	<1	7	4	3	2	<1	<1	7	7	1	7	<1	<1	1	7
Ga	5	9	6	13	24	27	11	3	6	23	40	17	18	15	8	14	32
Mo	33	43	259	3	8	<2	3	3	8	195	<2	49	4	<2	<2	<2	2
Ag	<0.5	<0.5	<0.5	<0.5	<0.5	<0.5	<0.5	<0.5	<0.5	1.0	<0.5	1.0	<0.5	<0.5	<0.5	<0.5	5.0
Cd	<1	<1	<1	<1	<1	<1	<1	<1	<1	<1	<1	<1	<1	<1	<1	<1	<1
In	<1	<1	<1	<1	<1	<1	<1	<1	<1	2	<1	<1	<1	<1	<1	<1	<1
Sn	<10	<10	<10	<10	<10	<10	<10	388	21	30	21	43	18	6850	7300	12700	12
W	11	5	6	<3	27	<3	7	<3	<3	460	9	<3	4	8	6	5	10
Au*	5	<1	10	1	<1	1	1	<1	<1	<1	3	6	<1	<1	<1	<1	<1
Tl	1	<1	3	2	3	3	2	<1	<1	3	5	7	3	<1	4	2	4
Bi	6.0	19.3	2.3	1.6	4.8	2.8	1.0	2.7	6.1	101.0	23.6	15.0	2.7	1.1	3.4	1.7	99.0
La	3	2	5	8	22	10	5	<2	7	16	17	4	20	5	2	3	20
Ce	7	7	16	23	46	20	10	2	6	39	22	7	46	6	4	10	57
Nd	3.3	3.2	4.7	9.4	19.6	15.7	4.4	1.2	5.2	19.6	22.9	4.7	22.7	4.6	3.1	3.6	23.0
Sm	0.7	1.0	0.8	3.0	3.6	4.1	1.4	0.7	0.9	5.3	8.3	0.8	4.5	0.9	2.1	0.7	6.0
Eu	0.2	<0.1	0.1	<0.1	0.4	0.2	0.3	<0.1	<0.1	<0.1	0.5	<0.1	<0.1	0.2	0.3	<0.1	0.2
Gd	0.8	0.9	0.8	2.8	2.9	4.7	2.0	1.1	0.9	3.4	10.0	0.8	4.0	1.0	2.9	<0.5	5.3
Dy	1.8	2.4	1.4	3.8	2.8	5.9	5.4	2.7	1.0	3.3	8.9	1.2	3.4	1.8	4.5	1.1	7.5
Er	1.2	1.1	0.8	2.3	1.5	3.9	4.7	1.9	0.7	2.1	4.5	1.0	2.2	0.9	2.6	0.5	5.0
Lu	0.2	0.2	<0.1	0.5	0.3	0.7	0.7	0.4	0.2	0.4	0.7	0.3	0.3	0.2	0.5	0.1	0.9
U	207.0	4.0	3.0	22.6	8.6	8.6	9.3	1.0	5.5	15.2	13.8	2.6	29.6	2.4	4.8	4.2	36.1
Th	3	14	3	41	30	17	12	<1	3	27	61	4	30	3	1	14	49

*ppb

Appendix IX (cont.)

D. Trout Brook Pluton (mineralized rock samples):

	86-329	86-369B	86-439B	86-447
SiO_2 (%)	78.1	77.9	78.5	60.1
TiO_2 (%)	0.11	0.06	0.19	0.07
Al_2O_3 (%)	12.1	13.2	9.36	20.2
CaO (%)	0.48	0.16	0.71	0.13
MgO (%)	0.15	0.16	0.03	0.06
Na_2O (%)	0.19	1.00	0.29	4.57
K_2O (%)	3.83	4.22	7.60	8.80
Fe_2O_3 (%)	3.10	1.98	1.85	3.16
MnO (%)	0.22	0.07	--	0.11
P_2O_5 (%)	0.03	0.07	0.07	0.10
Li (ppm)	240	230	30	170
Be (ppm)	5	25	5	5
Rb (ppm)	716	676	554	1030
Sr (ppm)	43	49	116	<10
Cs (ppm)	48	23	7	26
Ba (ppm)	112	158	977	83
B (ppm)	40	30	20	20
S (ppm)	<100	<100	3500	<100
As (ppm)	1	7	2	14
Sb (ppm)	<0.2	<0.2	0.2	0.2
Y (ppm)	58	24	20	28
Zr (ppm)	62	19	157	52
Nb (ppm)	11	28	29	<10
V (ppm)	<10	<10	<10	<10
Cr (ppm)	4	4	2	2
Mn (ppm)	--	--	100	--
Co (ppm)	1	1	1	2
Ni (ppm)	2	3	1	<1
Cu (ppm)	90.0	3.5	2.5	1.5
Zn (ppm)	290.0	34.0	42.0	26.0
Pb (ppm)	<2	4	40	22
Hf (ppm)	4	3	5	4
Ta (ppm)	3	11	6	12
Ga (ppm)	29	33	9	36
Mo (ppm)	11	22	14	33
Ag (ppm)	0.5	<0.5	<0.5	<0.5
Cd (ppm)	<1	<1	<1	<1
In (ppm)	2	1	<1	<1
Sn (ppm)	384	38	<10	18
W (ppm)	20	71	<3	8
Au (ppb)	<1	<1	<1	<1
Tl (ppm)	4	3	6	6
Bi (ppm)	4.8	343.0	8.0	<5.0
La (ppm)	19	5	22	8
Ce (ppm)	43	10	45	19
Nd (ppm)	19.5	5.8	21.7	8.9
Sm (ppm)	4.6	1.7	4.3	2.6
Eu (ppm)	<0.1	<0.1	0.4	<0.1
Gd (ppm)	2.4	1.1	3.2	1.6
Dy (ppm)	1.6	1.1	4.1	2.3
Er (ppm)	0.9	<0.5	2.8	1.3
Lu (ppm)	0.2	0.2	0.5	0.3
U (ppm)	5.2	11.0	7.3	22.9
Th (ppm)	22	12	22	17

E. Rocky Brook Pluton (mineralized rock samples):

	86-298	86-610	86-615	86-647
SiO_2 (%)	59.1	61.4	68.7	15.5
TiO_2 (%)	0.82	0.13	0.18	<0.01
Al_2O_3 (%)	13.7	15.6	16.0	0.62
CaO (%)	9.13	1.22	0.33	85.3
MgO (%)	4.26	0.37	0.14	0.07
Na_2O (%)	1.79	2.11	4.34	<0.01
K_2O (%)	2.85	8.90	6.23	0.17
Fe_2O_3 (%)	6.63	7.41	1.31	0.18
MnO (%)	0.13	0.33	--	--
P_2O_5 (%)	0.12	0.07	0.05	0.02
Li (ppm)	100	40	70	50
Be (ppm)	10	25	5	<5
Rb (ppm)	295	712	505	<10
Sr (ppm)	344	85	73	70
Cs (ppm)	11	13	29	2
Ba (ppm)	282	517	267	<10
B (ppm)	<10	<10	20	<10
S (ppm)	130	8200	1600	180
As (ppm)	3	50	49	14
Sb (ppm)	0.8	<0.2	0.7	<0.2
Y (ppm)	31	14	12	25
Zr (ppm)	120	96	74	<10
Nb (ppm)	<10	16	<10	17
V (ppm)	130	20	10	<10
Cr (ppm)	--	4	4	4
Mn (ppm)	--	--	110	12
Co (ppm)	18	7	<1	2
Ni (ppm)	77	1	2	2
Cu (ppm)	44.0	9.5	2.0	<0.5
Zn (ppm)	90.0	220.0	17.0	8.0
Pb (ppm)	<2	38	14	<2
Hf (ppm)	3	4	4	<1
Ta (ppm)	2	3	4	<1
Ga (ppm)	19	26	22	3
Mo (ppm)	6	<2	20	14
Ag (ppm)	0.5	1.0	0.5	<0.5
Cd (ppm)	<1	<1	<1	<1
In (ppm)	<1	2	<1	<1
Sn (ppm)	20	39	29	<10
W (ppm)	10	<3	<3	<3
Au (ppb)	<1	2	<1	<1
Tl (ppm)	3	6	4	<1
Bi (ppm)	185.0	8.3	2.5	0.6
La (ppm)	26	18	7	3
Ce (ppm)	54	41	14	3
Nd (ppm)	26.5	19.9	9.0	2.4
Sm (ppm)	5.5	4.6	2.0	1.1
Eu (ppm)	0.9	0.4	<0.1	0.1
Gd (ppm)	4.3	4.3	1.7	1.5
Dy (ppm)	4.3	3.0	2.5	2.9
Er (ppm)	2.4	1.6	1.7	2.4
Lu (ppm)	0.4	0.3	0.3	0.4
U (ppm)	2.7	10.0	16.0	0.8
Th (ppm)	11	29	26	1

F. Locations and descriptions of chemically analyzed rock samples.

Appendix IX (concl.)

Sample No.	Latitude °	'	"	Longitude °	'	"	ROCK DESCRIPTION
85-45	46	39	03	66	50	54	Fine grained granite porphyry dyke cutting subporphyritic biotite granite.
85-49B	46	39	18	66	51	00	Coarse grained, subporphyritic biotite granite.
85-61	46	40	43	66	46	57	Coarse grained, porphyritic biotite granite.
85-195	46	37	15	66	54	33	Medium grained granite porphyry.
85-201	46	37	41	66	51	24	Medium grained, melanocratic biotite granite.
85-266	46	40	46	66	55	30	Coarse grained biotite granite altered to an assemblage of secondary albite and chlorite.
2A-85	46	37	48	66	49	25	Garnet-muscovite-bearing aplite dyke cutting subporphyritic biotite-granite. From core (at adepth of 85 m).
12-261	46	34	07	66	34	07	Greisenized equigranular biotite granite. From core (at a depth of 261 m).
12-373	46	34	07	66	48	37	Fine grained, equigranular biotite granite. From core (at a depthof 373 m)
12-397	46	34	10	66	48	40	Fine- to medium-grained equigranular biotite granite. From core (at a depthof 397 m).
85-22	46	37	14	66	48	45	Coarse grained subporphyritic biotite granite.
1A-156	46	39	48	66	48	10	Coarse grained subporphyritic granite. From core (at a depth of 156m).
85-155	46	35	42	66	47	29	Coarse grained biotite granite altered to an assemblage of secondary biotite, K-feldspar and quartz.
85-40C	46	37	40	66	50	12	Medium grained equigranular biotite granite.
3-470	46	35	11	66	54	39	Medium grained equigranular biotite granite. From core (at a depth of 143 m).
85-175	46	34	38	66	49	12	Fine grained equigranular biotite granite.
5-125	46	34	36	66	55	07	Fine grained equigranular biotite. From core (at a depth of 38 m).
85-21	46	37	45	66	48	03	Biotite aplite dyke cutting equigranular biotite granite.
85-129B,C	46	35	16	66	54	42	Silicified granite breccia with narrow quartz-filled fractures containing minor pyrite, wolframite, and arsenopyrite (McLean Brook North).
85-131	46	34	34	66	54	19	Silicified granite breccia with pyrite and arsenopyrite (McLean Brook North).
85-132C	46	34	34	66	54	45	Quartz vein with very coarse wolframite (McLean Brook North).
85-133B	46	34	35	66	54	48	Greisenized granite (McLean Brook North).
85-285A	46	34	40	66	52	25	Fine grained, altered or greisenized biotite granite rubble cut by quartz-cassiterite veins.
85-155B	46	35	43	66	47	30	Coarse biotite-rich border zone of quartz vein in altered coarse grained porphyritic granite (Tin Hill).
TH-0	46	35	27	66	47	27	Sericitic greisen at Tin Hill.
TH-1	46	35	27	66	47	27	Quartz, cassiterite, wolframite vein in greisenized granite (Tin Hill).
TH-3	46	35	27	66	47	27	Coarse greisen with large cassiterite crystals (Tin Hill).
85-131B	46	42	59	66	32	40	Silicified vuggy granite breccia with high radiometric response (500-600 cps); Harris Lake Uranium.
86-149	46	43	25	66	33	45	Brecciated and silicified, fine grained, equigranular granite.
86-189	46	42	37	66	32	40	Silicified breccia with fine grained, pyritized granite fragments and wolframite cluster (Harris Lake).
86-213	46	40	28	66	36	18	Sparse quartz stockwork in fine grained, equigranular granite.
86-240	46	39	45	66	36	56	Coarse grained, biotite granite containing fractures filled with massive pyrite and minor chalcopyrite (Dungarvon, Vein 7).
86-242D	46	39	50	66	36	58	Narrow feldspathic vein centered by quartz-filled fracture within coarse grained miarolitic granite (Dungarvon, Vein 7).
86-242E	46	39	50	66	36	58	Silicified breccia containing altered granite fragments and massive pyrite (Dungarvon, Vein 7).
86-243	46	39	53	66	36	51	Coarse quartz and fluorite breccia (Dungarvon, Vein 7).
86-245B	46	40	36	66	36	20	Silicified breccia containing pyritized granite fragments.
86-248	46	40	18	66	35	40	Quartz stockwork in medium grained, equigranular granite fragments.
86-263	46	38	56	66	37	08	Biotite-rich miarolitic feldspathic granite boulder.
86-264B	46	38	55	66	37	47	Silicified breccia containing minor sulphides (Four Mile Brook).
86-572B	46	39	58	66	38	30	Fine grained, equigranular biotite granite (Young's Dam A, B).
DC-1	46	40	05	66	36	10	Quartz vein with disseminated cassiterite (Dungarvon, Veins 2, 4, 6, 11, 14).
S0-18-1 and SO-19-1	46	38	55	66	37	47	Cassiterite-bearing quartz vein in brecciated and feldspathized granite (Four Mile Brook, Vein 1).
DR004	46	43	44	66	36	00	Red miarolitic feldspathic vein.
86-329	46	35	15	66	37	42	Coarse grained greisen (Trout Lake Pluton, East).
86-469B	46	33	24	66	44		Medium grained greisen on margin of leucogranitic dyke (Deadman Brook).
86-439B	46	35	58	66	40	57	Narrow quartz veins containing pyrite and fluorite in medium grained granite (Gilman Brook).
86-447	46	35	18	66	40	30	Red miarolitic feldspathic vein.
86-298	46	36	30	66	37	32	Greisenized medium grained granite.
86-610	46	37	45	66	37	44	Feldspathic vein with abundant pyrite and fluorite.
86-615	46	37	58	66	37	50	Quartz-feldspar vein containing pyrite.
86-647	46	36	48	66	37	30	Coarse quartz-fluorite breccia (Rocky Brook).

APPENDIX X

Chemical analyses of Au, Th, U, Cu, Pb, Zn, Mo, and Ag in outcrop, float, and trench samples in the Long Lake area (data compiled from Hauseux, 1980a,b, 1981).

A. Outcrop Samples:

Sample No.	Au [ppb]	Th [ppm]	U [ppm]	Cu [ppm]	Pb [ppm]	Zn [ppm]	Mo [ppm]	Ag [ppm]	Rock Type	Latitude	Longitude
80/26	ND	14	5.8	15	470	2030	ND*	ND	Silicified and mineralized granite	47° 02' 21"	66° 52' 31"
80/28	–	16	6.7	10	16	87	ND	ND	Quartz-feldspar porphyry	47° 02' 10"	66° 52' 02"
80/29	–	22	3.7	11	16	57	ND	ND	Quartz-feldspar porphyry	47° 02' 10"	66° 52' 02"
80/44	ND	22	14.7	120	48	3720	44	2	Altered and mineralized quartz-feldspar porphyry	47° 01' 23"	66° 50' 52"
80/45	ND	14	8.7	66	28	8500	8	1	Altered and mineralized quartz-feldspar porphyry	47° 01' 18"	66° 50' 30"
80/48	–	9	18.8	100	140	120	12	8	Sericitized biotite granite	47° 01' 30"	66° 51' 05"
80/49	200	21	7.7	53	32	180	8	1	Mineralized biotite granite	47° 01' 25"	66° 51' 04"
80/51	–	7	5.1	97	8	63	12	ND	Silicified mineralized and brecciated biotite granite	47° 01' 34"	66° 51' 05"
80/53	–	14	6.4	130	4	41	ND	1	Altered and mineralized biotite granite	47° 01' 43"	66° 51' 34"
80/54	–	24	12	140	12	43	4	ND	Mineralized quartz-feldspar porphyry	47° 01' 53"	66° 51' 34"
80/55	–	12	6.3	42	8	18	4	ND	Silicified and limonitized quartz-feldspar porphyry	47° 01' 53"	66° 51' 34"
80/58	–	9	5.4	6	150	6700	18	1	Mineralized quartz-feldspar porphyry	47° 01' 18"	66° 50' 41"
80/91	–	81	1.1	21	13	160	6	0.5	Biotite granite	47° 02' 49"	66° 52' 31"
80/95A	–	27	1.6	91	17	14	8	0.6	Altered quartz-feldspar porphyry	47° 02' 08"	66° 51' 09"
80/95B	–	32	3.6	93	156	72	6	1.4	Altered and mineralized quartz-feldspar porphyry	47° 02' 08"	66° 51' 09"
80/97	–	25	2.3	22	28	63	6	0.7	Quartz-feldspar porphyry	47° 01' 53"	66° 49' 33"
80/100	–	25	ND	34	920	1240	15	1.8	Altered and mineralized biotite granite	47° 01' 53"	66° 49' 32"
80/101	–	29	0.9	101	88	31	8	1.0	Altered and mineralized biotite granite	47° 02' 08"	66° 50' 48"
80/102	–	13	2.1	30	34	440	6	0.5	Quartz-feldspar porphyry	47° 01' 18"	66° 50' 56"

*ND = not detected

B. Float Samples:

Sample No.	Au [ppb]	Th [ppm]	U [ppm]	Cu [ppm]	Pb [ppm]	Zn [ppm]	Mo [ppm]	Ag [ppm]	Rock Type	Latitude	Longitude
80/11A	–	3	420	19	126	210	16	ND	Altered two-mica granite	47° 00' 30"	66° 50' 10"
80/11B	–	12	130	17	40	70	20	1	Altered and mineralized two-mica granite	47° 00' 30"	66° 50' 10"
80/12A	–	11	18	120	900	1100	8	3	Mineralized biotite granite	47° 01' 03"	66° 50' 33"
80/12B	–	15	59	83	60	620	ND	1	Altered, and mineralized biotite granite	47° 01' 03"	66° 50' 33"
80/16	–	5	63	14	130	48	ND	ND	Altered and mineralized two-mica granite	47° 00' 56"	66° 51' 30"
80/19A	31	1	310	11	96	17	190	1	Brecciated and altered biotite granite	47° 00' 33"	66° 50' 03"
80/19C	ND	17	5	25	36	550	ND	ND	Brecciated and altered biotite granite	47° 00' 33"	66° 50' 03"
80/19E	12	1	70	16	96	10	25	ND	Brecciated, altered, and mineralized biotite granite	47° 00' 33"	66° 50' 03"
80/19F	12	2	39	5	240	4	140	ND	Altered and mineralized biotite granite	47° 00' 33"	66° 50' 03"
80/27	–	6	6.1	1110	480	18400	4	4	Altered and mineralized biotite granite	47° 02' 19"	66° 51' 04"
80/36	–	ND	41	5	100	13	4	ND	Mineralized and altered biotite granite	47° 00' 55"	66° 50' 53"
80/37A	–	11	8.3	30	1100	210	4	ND	Altered and mineralized quartz-feldspar porphyry	47° 00' 54"	66° 50' 53"
80/37B	–	16	23	94	2000	820	14	ND	Altered and mineralized biotite granite	47° 00' 54"	66° 50' 52"
80/37C	–	22	3.7	2	28	1260	4	ND	Altered quartz-feldspar porphyry	47° 00' 54"	66° 50' 52"
80/37D	–	ND	570	9	140	36	24	ND	Brecciated, altered, and mineralized quartz-feldspar porphyry	47° 00' 54"	66° 50' 52"
80/37F	–	16	17	2	32	18	2	ND	Altered quartz-feldspar porphyry	47° 00' 54"	66° 50' 52"
80/37G	–	7	7.2	2	100	17	ND	ND	Altered quartz-feldspar porphyry	47° 00' 54"	66° 50' 52"
80/37K	–	8	14	5	88	8	8	ND	Altered and mineralized quartz-feldspar porphyry	47° 00' 54"	66° 50' 52"
80/38	23	2	37	9	250	16	1060	ND	Brecciated and silicified biotite granite	47° 00' 39"	66° 49' 49"
80/46	–	ND	18	12	12	23	120000	ND	Mineralized two-mica granite	47° 00' 39"	66° 50' 39"
80/47A	ND	ND	1560	360	68	42	100	17	Brecciated autunite-torbernite-bearing two-mica granite	47° 00' 43"	66° 50' 56"
80/47B	ND	ND	3300	170	36	12	20	7	Brecciated two-mica granite	47° 00' 43"	66° 50' 56"
80/56	1	15	26.4	110	400	740	ND	1	Altered and mineralized biotite granite	47° 01' 07"	66° 50' 26"
80/59	–	4	1360	4	250	84	78	1	Brecciated, altered, and mineralized two-mica granite	47° 01' 07"	66° 50' 26"
80/64A	–	9	298	54	204	64	106	1.2	Altered and mineralized two-mica granite	47° 01' 00"	66° 50' 30"
80/82	–	14	1.6	20	190	80	4	0.5	Weathered biotite granite	47° 00' 42"	66° 50' 45"
80/98A	–	20	2.2	110	13	36	10	1.4	Silicified and mineralized biotite granite (weathered)	47° 01' 55"	66° 49' 34"

C. Trench Samples:

Sample No.	Au (ppb)	Th (ppm)	U (ppm)	Cu (ppm)	Pb (ppm)	Zn (ppm)	Mo (ppm)	Ag (ppm)	Sn* (ppm)	Rock Type	Latitude	Longitude
80/41	–	15	19.8	24	540	180	4	1		Altered and mineralized biotite granite	47° 02' 24"	66° 51' 55"
80/42	–	11	17.3	96	180	600	8	1		Altered and mineralized biotite granite	47° 02' 24"	66° 51' 55"
80/43	–	16	14.7	75	3120	2270	8	2		Altered and mineralized biotite granite	47° 02' 24"	66° 51' 55"
80/50	–	27	23.5	55	12	160	4	ND		Altered biotite granite	47° 01' 35"	66° 51' 55"
80/52	–	18	4.5	36	ND	80	4	ND		Altered biotite granite	47° 01' 42"	66° 51' 20"
80/57	–	13	8.3	11	260	33800	4	3		Altered and mineralized biotite granite	47° 02' 29"	66° 51' 25"
80/60A	–	315	2.3	30800	407	312	23	292		Mineralized biotite granite	47° 01' 18"	66° 50' 25"
80/60B	–	173	2.3	31200	128	260	19	70		Mineralized biotite granite	47° 01' 18"	66° 50' 25"
80/62	–	33	7.4	192	840	660	52	5.2		Mineralized biotite granite	47° 01' 18"	66° 50' 30"
80/63	–	18	0.6	80	81	2720	25	1.8		Mineralized quartz–feldspar porphyry	47° 01' 18"	66° 50' 30"
80/64B	–	28	2.6	45	1360	296	40	1.6		Altered and mineralized biotite granite	47° 01' 20"	66° 50' 30"
80/65A	ND	ND	845	117	620	580	420	3.2		Altered and mineralized [Mo,U] quartz–feldspar porphyry	47° 02' 21"	66° 50' 42"
80/65B	ND	38	273	92	2880	1000	11	3.4		Altered and mineralized [U, base metal sulphides] quartz–feldspar porphyry	47° 01' 21"	66° 50' 42"
80/65C	ND	ND	26	60	100	48	290	2		Altered quartz–feldspar porphyry	47° 01' 21"	66° 50' 42"
81/15071	3000	349	2.2	17000	120	269	13	72	439			
81/15072	2600	590	4.5	1800	1800	800	23	54	976	Mineralized [base–metal sulphides] biotite granite	47° 01' 18"	66° 50' 25"
81/15078	40	138	2.6	640	3160	720	134	6	34	Mineralized [base–metal sulphides] biotite granite	47° 01' 21"	66° 50' 26"
81/15074	–	133	4.3	760	2880	3840	8	4.8	169	Mineralized [base–metal sulphides] biotite granite	47° 01' 21"	66° 50' 26"
81/15075	–	480	3.4	196	17600	3880	18	6.8	55	Altered and mineralized [base–metal sulphides] biotite granite	47° 01' 21"	66° 50' 26"
81/15076	–	48	5.4	256	800	1360	400	9.2	119	Mineralized [base–metal sulphides] quartz–feldspar granite	47° 01' 19"	66° 50' 37"
81/15077	–	13	6.4	200	60	3080	10	1.4	67	Altered and mineralized [base–metal sulphides] quartz–feldspar porphyry	47° 01' 19"	66° 50' 37"
81/15078	–	43	90	2780	760	16000	2000	9.8	ND	Altered and mineralized [base–metal sulphides] quartz–feldspar porphyry	47° 01' 19"	66° 50' 37"
81/15079	–	6	35	158	70	1640	28	3.4	7	Mineralized [base–metal sulphides] quartz–feldspar porphyry	47° 01' 18"	66° 50' 41"
81/15080	–	57	10.7	91	640	11200	16	5.5	134	Silicified quartz–feldspar porphyry	47° 01' 18"	66° 50' 41"
81/15081	–	24	390	37	332	1040	9	1.0	8	Altered and mineralized [base–metal sulphides] biotite granites	47° 01' 18"	66° 50' 41"
81/15082	–	33	8.6	35	800	480	4	1.0	58	Moderately altered and mineralized [base–metal sulphides] quartz–feldspar porphyry	47° 01' 18"	66° 50' 41"
81/15083	–	17	5.6	21	69	188	6	0.4	55	Altered and mineralized [base–metal sulphides] quartz–feldspar porphyry	47° 01' 18"	66° 50' 41"
81/15084	–	24	7.4	61	180	324	4	1.3	130	Strongly altered biotite granite		
81/15085	10	3	6.6	46	77	540	2	0.6	ND	Strongly altered biotite granite		
81/15086	–	13	1.5	16	10	220	2	0.2	9	Altered biotite granite		
81/15087	–	75	50	352	1760	1200	4	5.4	2	Mildly altered biotite granite	47° 01' 16"	66° 50' 48"
81/15110	–	27	6.3	128	2640	10800	50	4.0	–	Mineralized [base–metal sulphides] quartz–feldspar porphyry	47° 01' 21"	66° 50' 42"
81/15111	–	26	13.5	680	2400	36000	44	9.7	–	Altered and mineralized [base–metal sulphides] quartz–feldspar porphyry	47° 01' 19"	66° 50' 37"
81/15112	–	ND	3036	117	800	4080	18	8.0	–	Altered and mineralized [base–metal sulphides] quartz–feldspar porphyry	47° 01' 19"	66° 50' 37"
										Mineralized [U, base–metal sulphides] quartz–feldspar porphyry	47° 01' 21"	66° 50' 42"

* Sn analysis not available for 1980 series of samples.